Technical University of Denmark

DTU

Design of Low Power Algorithms for Automatic Embedded Analysis of Patch ECG Signals

Saadi, Dorthe Bodholt; Sørensen, Helge Bjarup Dissing; Egstrup, Kenneth

Publication date:
2015

Document Version
Publisher's PDF, also known as Version of record

[Link back to DTU Orbit](#)

DTU Library
Technical Information Center of Denmark

Technical University of Denmark

DTU

Dorthe Bodholt Saadi

Design of Low Power Algorithms for Automatic Embedded Analysis of Patch ECG Signals

PhD thesis, January 2015

DTU Electrical Engineering
Department of Electrical Engineering

Region of Southern Denmark

DELTA

Technical University of Denmark
Department of Electrical Engineering
DK-2800 Kgs. Lyngby
Denmark

Submitted in partial fulfillment of the requirements for the degree of Doctor of Philosophy at the Technical University of Denmark.

Preface

The research described in this Ph.D. dissertation has been conducted as a partial fulfillment of the requirements for the degree of Doctor of Philosophy in Engineering. The work has been carried out in a very close corporation between the Biomedical Engineering group at the Department of Electrical Engineering, Technical University of Denmark (DTU), the Body Sensors group at the Danish company DELTA, and the Department of Medical Research at Svendborg Hospital.

The presented research has been carried out between May 2011 and January 2015 together with other activities, e.g. teaching biomedical signal processing, supervising master students, participation in international conferences, and periods of regular engineering work conducted in DELTA. The research has resulted in two journal papers, one white paper, three conference papers, one conference abstract, and this summary report. The seven research papers are included as appendixes to this thesis.

The Ph.D. project has been fully financed by DELTA through the DELTA Performance Contract 2010-2012: Intelligent Welfare Technologies and Single Use Devices. In practice, the project has therefore been conducted similarly to an industrial Ph.D. project.

Dorthe Bodholt Saadi
Lyngby, January 2015

Acknowledgments

First of all, I would like to express my deepest appreciation to my supervisors Associate Professor Helge B. D. Sørensen from the Technical University of Denmark, Professor Kenneth Egstrup from the Department of Medical Research at Svendborg Hospital as well as Key Account Manager Jens Branebjerg, Development Manager Gunnar B. Andersen, and Research Manager Karsten Hoppe from DELTA for the constant support and guidance throughout the project and for helping me find new ways to proceed in a continuously changing environment. Furthermore, Associate Professor Alberto Nannarelli from the Department of Applied Mathematics and Computer Science at the Technical University of Denmark deserves thanks for providing me with his knowledge within the field of hardware implementation of signal processing algorithms.

My fellow Ph.D. students from the Department of Medical Research at Svendborg Hospital, especially Armin Osmanagic and Hussam Sheta, deserve my greatest appreciation for welcoming me in their group and, most of all, for introducing me to the clinical world. Furthermore, very special thanks go to Kenneth Egstrup, ECG Technician Inge Fauerskov, Armin Osmanagic, Hussam Sheta, and Cardiologist Jørgen L. Jeppesen from the Department of Medicine at Glostrup Hospital for patiently teaching me about the clinical interpretation of ECGs.

A very special appreciation also goes to all of my colleagues at DELTA, especially my fellow Ph.D. student Shadi Chreiteh and my Supervisor Karsten Hoppe, for always helping me keep up the good spirit, participating in valuable discussions, and always letting me draw on their extensive knowledge in each of their fields of expertise. I would furthermore like to thank all of my colleagues at DELTA for always taking the time to help me.

I would also like to thank my fellow Ph.D. students from the Biomedical Signal Processing group, especially my office mates Julie A. E. Christensen and Lykke Kempfner, for always keeping a positive working environment and participating in rewarding discussions.

Finally, I would like to thank my friends and family, especially my husband Essie Saadi, my sister Tine Nielsen, and Poul Dige, for always being there to support and encourage me. Poul Dige furthermore deserves special thanks for proofreading parts of this dissertation.

Abstract

The diagnosis of cardiac arrhythmias often depends on information from long-term ambulatory electrocardiographic (ECG) monitoring. For several decades, these recordings have been obtained by wired Holter recorders. However, to overcome some of the known disadvantages of the old technologies, several different cable-free wireless patch-type ECG recorders have recently reached the market. One of these recorders is the ePatch designed by the Danish company DELTA. The extended monitoring period available with the patch recorders has demonstrated to increase the diagnostic yield of outpatient ECG monitoring. Furthermore, the patch recorders facilitate the possibility of outpatient ECG monitoring in new clinically relevant areas, e.g. telemedicine monitoring of cardiac patients in their homes. Some of these new applications could benefit from real-time embedded interpretation of the recorded ECGs. Such algorithms could allow the real-time transmission of clinically relevant information to a central monitoring station. The first step in embedded ECG interpretation is the automatic detection of each individual heartbeat. An important part of this project was therefore to design a novel algorithm that was optimized for heartbeat detection in ePatch ECGs and embed the algorithm in the ePatch sensor for real-time analysis. We designed the algorithm based on a novel cascade of computational efficient filters and adaptive thresholds. We evaluated the algorithm on both standard databases and three different manually annotated ePatch databases. We found a very high detection performance with respect to both normal and abnormal beats as well as different types of artifacts arising from different daily life activities (average detection performance on 952,632 manually annotated beats obtained from 198 different patients: Se = 99.86% and P^+ = 99.74%). This shows the possibilities for the embedded analysis of the ePatch ECGs, and the designed algorithm thus provides a platform for further research in this area.

The expected advantages of the patch recorders are, however, unconditionally limited by their ability to record high-quality diagnostic ECGs throughout the recording period. Another main focus of this thesis was therefore to investigate different important clinical aspects of the novel ePatch recorder. To achieve this, we designed two pilot studies that were intended to provide information about the clinical usability of the ePatch ECGs for heart rhythm analysis. In the first pilot study, two medical doctors were asked to provide an individual assessment of the usefulness of 200 ePatch ECG segments for heart rhythm analysis. They found that more than 98% of the segments were useful. The second pilot study was designed as a high level comparison between the diagnostic information that could be extracted from simultaneous recordings obtained with the ePatch recorder and the traditional telemetry equipment. This comparison was conducted by a cardiologist on 11 admitted patients. He found no clinically relevant differences between the information extracted from the two systems. Both pilot studies thus indicate a high potential for the clinical application of ECGs recorded with the ePatch system. To further investigate the general signal quality obtained by the ePatch, we designed a novel algorithm for the automatic estimation of the overall percentage of analyzable time (PAT) in ECGs. The algorithm obtained very high classification performance and is therefore expected to provide a reliable estimation of the overall PAT. We then applied the algorithm to investigate the PAT in 250 different ePatch recordings. We found that 10% of the recordings obtained less than 10% analyzable time, and they were considered as incorrect measurements. For the remaining 90% of the recordings, we found a very high PAT (median: 100% (interquartile range: 97.9% to 100%); mean: (92.4 ± 18.8)%). We therefore didn't find indications of problems related to the general signal quality obtained by the ePatch recorder. Overall, we thus find a high potential for the application of the ePatch recorder in many different clinical settings in the future.

Resumé

Diagnosticering af patienter med hjerterytmeforstyrrelser er ofte baseret på ambulante målinger af patientens elektrokardiografi (EKG). Disse målinger er i flere årtier blevet opsamlet ved hjælp af de såkaldte Holter optagere. Det er dog kendt, at denne teknologi har en del begrænsninger i form af høj patientbyrde og relativ lav indvilligelse i at bære optageren i længere tidsperioder. I de senere år er der derfor blevet udviklet forskellige "plaster"-løsninger til ambulant måling af EKG. Én af disse løsninger af DELTA's ePatch. Videnskabelige studier har vist, at muligheden for en forlænget monitoreringsperiode kan øge det diagnostiske udbytte af målingerne. Den nye teknologi giver desuden muligheder for at anvende ambulant EKG i mange klinisk relevante sammenhænge, hvor det endnu ikke er udbredt i dag. Dette kunne fx være telemedicinsk monitorering af hjertepatienter i deres eget hjem. Der er mange af disse nye anvendelsesmuligheder, der vil kunne drage stor nytte af automatisk real-time-analyse af de målte signaler. Sådanne algoritmer kunne fx give mulighed for trådløst at sende relevante, kliniske markører til en central overvågningsenhed. Det første skridt i automatisk analyse af EKG signaler er detektion af hvert enkelt hjerteslag. Det har derfor været en vigtig del af dette projekt at designe en ny algoritme, der er optimeret til indlejret detektion af hjerteslag i ePatch-sensoren. Vi besluttede at designe algoritmen ud fra et sæt af nye beregningseffektive filtre og adaptive tærskelværdier. Vi validerede algoritmens performance på EKG fra to standarddatabaser og tre forskellige manuelt annoterede ePatch-databaser. Vi opnåede en meget høj detektionsrate i forhold til både detektion af normale og unormale hjerteslag og i forhold til forskellige former for artefakter forårsaget af normale dagligdagsaktiviteter (gennemsnitlig performance på 952,632 manuelt annoterede hjerteslag fra 198 forskellige patienter: Se = 99,86% og P^+ = 99,74%). Den høje performance viser potentialet for fremtidig indlejret real-time-analyse af EKG signaler i ePatch-sensoren. Den designede algoritme danner desuden en platform for videre forskning i nye algoritmer, der kan anvendes til automatisk at ekstrahere klinisk relevant information under målingerne.

De mange forventede fordele ved den nye teknologi er dog stærkt betinget af teknologiens evne til at optage diagnostisk EKG af høj kvalitet igennem hele måleperioden. Der har derfor også været stor fokus på at undersøge vigtige, kliniske aspekter af den nye ePatch-teknologi i dette projekt. For at kunne gøre dette, designede vi to forskellige pilotstudier, der havde til formål at undersøge den kliniske anvendelighed af EKG optaget med ePatch. I det første pilotstudie fik vi to læger til uafhængigt af hinanden at vurdere den kliniske anvendelighed af 200 forskellige ePatch EKG segmenter. Resultatet var, at flere end 98% af segmenterne var brugbare til hjerterytmeanalyse. Det andet pilotstudie var designet med henblik på at opnå en overordnet sammenligning af det diagnostiske indhold i samtidige målinger med ePatch-systemet og traditionelt telemetriudstyr. Sammenligningen blev udført af en kardiolog på data fra 11 indlagte patienter. Kardiologen fandt ingen klinisk relevant forskel imellem de tilgængelige informationer fra de to systemer. Resultaterne fra begge disse pilotstudier indikerer således et højt potentiale for klinisk anvendelse af EKG optaget med ePatch-sensoren. Vi ønskede yderligere at undersøge den generelle signalkvalitet, der kan opnås med ePatch-sensoren. For at kunne undersøge denne, designede vi en ny algoritme til automatisk estimering af den procentvise andel af en EKG måling, der er klinisk analyserbar. Vores algoritme opnåede en høj klassifikationsperformance i forhold til genkendelse af analyserbare og ikke-analyserbare EKG segmenter. Vi mener derfor, at den kan give et pålideligt estimat af den overordnede, analyserbare procentandel af en given måling. Vi anvendte algoritmen til undersøgelse af 250 ePatch-målinger. Vi fandt, at 10% af målingerne havde mindre end 10% analyserbar tid. Disse målinger betragtede vi som fejl-målinger. For de resterende 90% af målingerne fandt vi, at de havde en meget høj analyserbar tid (median: 100% (kvartil range: 97,9% til 100%), gennemsnit: (92,4 ± 18,8)%). Baseret på vores studier, har vi derfor ikke fundet problemer i forhold til den signalkvalitet, ePatch-sensoren opnår. Vores overordnede konklusion er derfor, at ePatch systemet har et højt potentiale indenfor mange forskellige, kliniske anvendelser i fremtiden.

Abbreviations

Acc	Accuracy
ADC	Analog-to-digital conversion
AF	Atrial fibrillation
AFL	Atrial flutter
ASIC	Applications specific integrated circuit
AV	Atrioventricular
B	Ventricular bigeminy
BP	Bandpass
BPM	Beat per minute
bxb	Function from the WFDB Toolbox for beat-by-beat comparison of QRS detection performance
CE	Conformité Européenne
CRMDB	Cardio-respiratory-monitoring database
CVD	Cardiovascular disease
DSP	Digital signal processor
ECG	Electrocardiography
EDB	European ST-T database
EKG	Elektrokardiografi (Danish for electrocardiography)
EPJ	Electronic patient journal
eTDB	ePatch training database
eVDB	ePatch validation database
FD	False detection
FDA	Food and Drug Administration
FDB	Fitness database
FIR	Finite impulse response
FP	False positive
FN	False negative
Fs	Sampling frequency
GUI	Graphical user interface
HP	Highpass
HR	Heart rate
IEC	International Electrotechnical Commission
LP	Lowpass
MITDB	MIT-BIH arrhythmia database
NSR	Normal sinus rhythm
P^-	Negative predictivity
P^+	Positive predictivity
PAT	Percentage of analyzable time
PeDB	Preliminary ePatch database
PR	Time interval from beginning of P-wave to beginning of QRS complex
RR	Time interval between two subsequent QRS complexes
SA	Sinoatrial
Sb	Search back
Se	Sensitivity
SNR	Signal to noise ratio

Sp	Specificity
sqrs	Function for automatic QRS detection from the WFDB Toolbox
STRDB	Stroke database
SVEB	Supraventricular ectopic beat
SVM	Support vector machine
SVT	Supraventricular tachycardia
T	Ventricular trigeminy
TDB	Telemetry database
TN	True negative
TP	True positive
VEB	Ventricular ectopic beat
VF	Ventricular fibrillation
VT	Ventricular tachycardia
WFDB	Waveform datadase
WHO	World Health Organization
xform	Function from the WFDB Toolbox for simultaneous resampling of data and reference annotations

Table of Contents

1   Introduction

Cardiovascular diseases (CVDs) are not only lethal, they are also associated with a high economic burden on the healthcare facilities, and they can significantly decrease the quality of life for the affected patients and their families. Early diagnosis and treatment is furthermore essential to decrease the risk of dangerous complications. The diagnosis of cardiac arrhythmias often depends on information from long-term ambulatory electrocardiographic (ECG) monitoring [1]. However, many of the older technologies applied for outpatient heart rhythm assessment today suffer from significant issues related to patient comfort and consequently reduced compliance with wearing the systems for extended periods of time. This might be problematic since an extended monitoring period has shown to increase the diagnostic yield of outpatient ECG monitoring [2]. To overcome some of these difficulties, the novel ePatch recorder was designed by the Danish company DELTA. The novel technology has a high number of advantages compared to the traditional Holter recorders, but the clinical applicability and acceptance of the new technology is inextricably conditioned by the recorder's ability to obtained high-quality diagnostic ECGs throughout the monitoring period. This ability has been questioned in the literature [1], [3], [4]. One of the main goals in this project was therefore to explore different aspects of the clinical applicability of ECGs recorded with the ePatch system. This investigation is two-fold and includes both an investigation of the clinical usefulness and recognisability of ePatch ECGs for heart rhythm analysis and an investigation of the obtained signal quality. These investigations are described in the first two main objectives listed below. As long as the ECG quality is ensured, the new technology is not only imagined to be able to substitute the currently applied Holter or telemetry recorders. This technology also reveals opportunities for monitoring in completely new clinically relevant patient populations. This could for instance include real-time monitoring of cardiac patients in their own homes. Many of these new applications could highly benefit from automatic real-time embedded interpretation of the recorded ECGs. The system could, for instance, automatically transmit heart rate (HR) trend curves, potential arrhythmia events, signal quality indices, and patient activity levels to a central monitoring station. Another main goal in this project was therefore to initiate the design of new low-power signal processing algorithms for the automatic embedded analysis of the recorded ePatch ECGs. The first step in this analysis is the reliable detection of each individual heartbeat. This was therefore the primary focus of the low-power algorithm research conducted in this part of the project. The requirements regarding high clinical performance as well as low computational burden are obvious when the purpose is embedded analysis. However, it might be less trivial to define the exact limits for the acceptable algorithm power consumption. Furthermore, the power consumption required for a given algorithm depends on the specific implementation and realization of the algorithm in the ePatch sensor (e.g. general purpose microprocessor, digital signal processor (DSP), or application specific integrated circuit (ASIC)). From a practical point of view and to keep the required flexibility of the ePatch platform in mind, we decided to define the acceptable power consumption as the ability to perform real-time embedded analysis in the currently CE-market ePatch sensor without significantly reducing the total recording time of the system. This leads to the third project objective stated below:

Objectives:	• *To conduct a preliminary investigation of the clinical usability of ECGs recorded with the novel ePatch technology*
	• *To conduct a preliminary investigation of the ability to obtain sufficient diagnostic quality of ECG recordings obtained with the ePatch technology*
	• *To design and validate a novel embedded QRS complex detection algorithm with high clinical performance in real-life ePatch ECGs and low computational load*

1.1 Scientific Contributions

The scientific contributions obtained throughout this project are mainly presented in two journal papers, one white paper, three conference papers, and one conference abstract. These contributions are listed below. The author of this thesis is cited as Dorthe Bodholt Nielsen until October 2012 and Dorthe Bodholt Saadi hereafter. Each contribution is provided at the end of this thesis, and the paper number refers to the order in which they are included.

Journal papers

- D.B. Saadi, G. Tanev, M. Flintrup, A. Osmanagic, K. Egstrup, K. Hoppe, P. Jennum, J. Jeppesen, H.K. Iversen, and H.B.D. Sorensen, *"Automatic Real-time Embedded QRS Complex Detection for a Novel Patch-Type Electrocardiogram Recorder"*, Submitted to IEEE Translational Engineering in Health and Medicine. (Paper V)

- D.B. Saadi, A. Osmanagic, H.M Sheta, K. Egstrup, L. Bay, K. Hoppe, J.L. Jeppesen, H.K. Iversen, P. Jennum, and H.B.D. Sorensen, *"Investigation of Analyzable Time in 24-hour Patch Electrocardiogram Recordings"*, Submitted to IEEE Transactions on Biomedical Engineering. (Paper VII)

White paper

- D.B. Saadi, H.B.D. Sorensen, I.H. Hansen, K. Egstrup, P. Jennum, and K. Hoppe, *"ePatch® - A Clinical Overview"*, available online: http://orbit.dtu.dk/en/publications/epatch--a-clinical-overview(5a3e37a2-76a8-4240-aae6-781269a8ca2a).html, 2014. (Paper I)

Conference papers

- D.B. Nielsen, K. Egstrup, J. Branebjerg, G.B. Andersen, and H.B.D. Sorensen, *" Automatic QRS complex detection algorithm designed for a novel wearable, wireless electrocardiogram recording device"*, 34th Annual International Conference of the IEEE Engineering in Medicine and Biology Society (EMBC), IEEE, pp. 2913-6, 2012. (Paper IV)

- D.B. Saadi, I. Fauerskov, A. Osmanagic, H.M. Sheta, H.B.D. Sorensen, K. Egstrup, and K. Hoppe, *"Heart rhythm analysis using ECG recorded with a novel sternum based patch technology"*, CARDIOTECHNIX 2013: Proceedings of the International Congress on Cardiovascular Technologies, SciTePress, pp. 15-21, 2013. (Paper II)

- D.B. Saadi, K. Hoppe, K. Egstrup, P. Jennum, H. K. Iversen, J. L. Jeppesen, and H.B.D. Sorensen, *"Automatic quality classification of entire electrocardiographic recordings obtained with a novel patch type recorder"*, 36th Annual International Conference of the IEEE Engineering in Medicine and Biology Society (EMBC), IEEE, pp. 5639-42, 2014. (Paper VI)

Conference abstract

- D.B. Saadi, K. Egstrup, K. Hoppe, and H.B.D. Sorensen, *"Comparison of diagnostic information from regular telemetry equipment and a novel patch type electrocardiogram recorder"*, 36th Annual International Conference of the IEEE Engineering in Medicine and Biology Society (EMBC), 2014. (Paper III)

1.2 Thesis Outline

This thesis is organized in three main research chapters together with a preliminary chapter and an overall conclusion. The preliminary chapter is included to provide some basic knowledge needed to understand and appreciate the impact of the research described later. The three main chapters cover the three different research topics defined on page 1. The three chapters are therefore naturally related, but they can be read individually. Since each chapter covers quite different aspects of our research, each chapter is initiated with its own brief background section, including the motivation, the hypothesis, and an overview of the relevant literature. Furthermore, each of the three main chapters contains its own conclusion on the investigations described in the relevant chapters. As summarized in section 1.1, the research is also presented in a number of papers. In some cases, the relevant methodology and results described in the papers are reproduced in the thesis. In other cases, this thesis contains either a brief summary of the findings in the paper, or it might contain more details and illustrations than the original paper. Furthermore, some sections contain additional previously unpublished results. Throughout this summary report, it is clearly stated when only a brief description is included. It is therefore recommended to read this summary report first and only refer to the papers if additional information is desired on these topics. A brief overview of the content in each chapter is provided below.

Chapter 2 provides a brief description of the origin of the ECG, a brief description of a few selected arrhythmias, and an overview of currently applied ambulatory ECG recorders.

Chapter 3 presents the results of two different pilot studies that we conducted to investigate the clinical usefulness of ECG recorded with the ePatch placed at the sternum. This chapter thus creates the foundation for the clinical real-life applicability of the ePatch system and, hereby, the applicability of the remaining research described in this thesis. This content is related to Papers I – III.

Chapter 4 presents the results of our investigations of the possibilities for the real-time embedded detection of individual heartbeats in the ePatch sensor. This content is also addressed in Paper IV and Paper V.

Chapter 5 contains an investigation and discussion of the signal quality obtained with the ePatch ECG recorder. This research is also addressed in Paper VI and Paper VII.

Chapter 6 summarizes the main conclusions of the research described in the other chapters.

2 Preliminaries

This chapter is intended to provide a quick fundamental introduction to a few areas that might ease the understanding of the research discussed in later chapters. The chapter thus contains a brief description of the origin of the ECG signal, illustrations of a few relevant arrhythmias, and a brief overview of currently applied ambulatory ECG recording techniques. The descriptions in this chapter are not intended to be exhaustive. Instead, they are intended to provide a brief overview and an understanding of the clinical "World" that the ePatch technology is a part of.

2.1 The Electrocardiogram

The repeated contraction and relaxation of the heart during each heartbeat is caused by organized depolarization and repolarization of the muscle cells in the heart. The ECG provides a visualization of this electrical activity. Each of the characteristic waveforms in the ECG signal represents different periods of the normal heart cycle. Generally, the functionality of the heart and its electrical system is altered in different ways during arrhythmias. These abnormalities naturally change the characteristic appearance of the electrical activity, and hereby the morphology of the recorded ECGs. Therefore, the standardized 12-lead ECG has served as the "gold standard" for diagnosis of different heart conditions, including arrhythmias, for more than hundred years [1]. To allow the reader a fundamental understanding of this, a very brief description of the origin of the ECG is provided below.

2.1.1 The Origin of the ECG

The important parts of the electrical conduction system of the heart are illustrated in Figure 2.1. Each normal heart beat is initiated by spontaneous depolarization in the *sinus node* (SA). This depolarization is spread to the atria that hereby contract. This depolarization results in the P-wave in the surface ECG (see Figure 2.2). The propagation of the depolarization wave is delayed in the *atrioventricular (AV) node*. This is observed as the brief isoelectric line between the P-wave and the QRS complex. In the normal heart, the AV node provides the only conduction path from the atria to the ventricles. After the AV node, the depolarization propagates through the *Bundle of His* to the *bundle branches* and continues to the *purkinje fibers.* This causes depolarization and hereby contraction of the ventricles. This results in the QRS complex in the ECG signal. After the contraction, the ventricles are repolarized, and this is observed as the T-wave. [5]
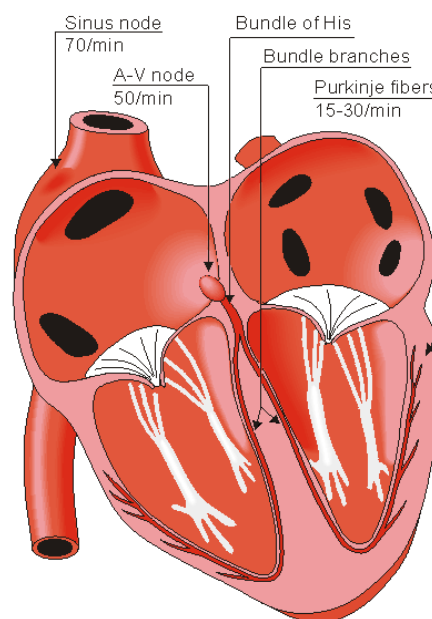
Figure 2.1: Illustration of the conduction system of the heart. The numbers indicate the intrinsic pacemaker frequency of each part in the conduction system. [5]
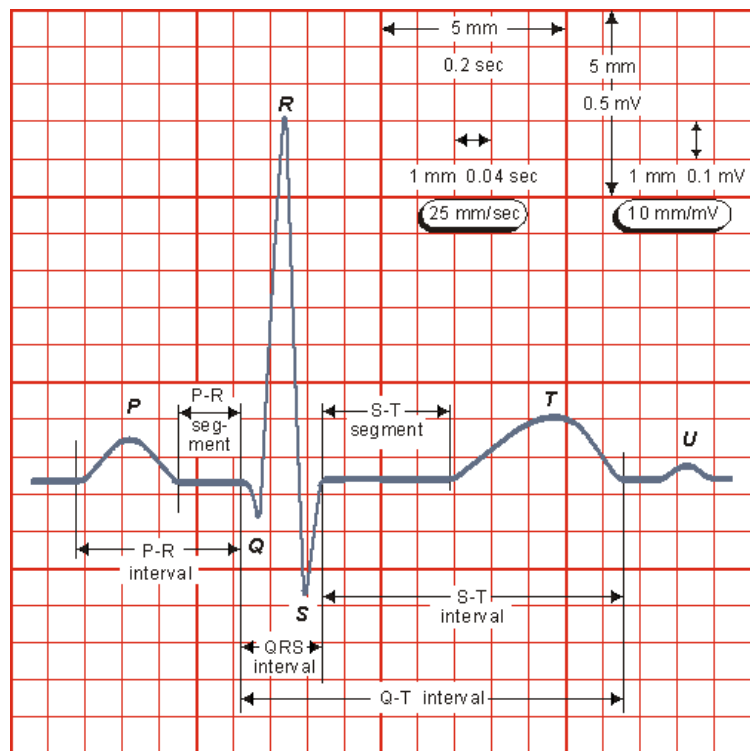
Figure 2.2: Illustration of the characteristic points in a normal ECG signal. [5]

2.1.2   Cardiac Arrhythmias

Based on the above description of the origin of the ECG, it becomes clear that diseases that alter the normal order of events in the heart can cause specific changes in the electrical activity and hereby cause changes in the recorded ECG. Cardiac rhythm disorders can basically be divided into two main categories: The supraventricular arrhythmias and the ventricular arrhythmias. The supraventricular arrhythmias originate from a location in the atria or the AV junction, whereas ventricular arrhythmias originate from a location within the ventricles [5]. One example of the latter is a ventricular ectopic beat (VEB). This is illustrated in Figure 2.3. When the depolarization is initiated in the ventricles, it will not follow the normal conduction pathway. This implies that it takes longer time for the activation front to proceed throughout the ventricles. This causes the wide QRS complex observed in Figure 2.3. Furthermore, no P-wave is observed. [5]

Figure 2.3: Illustration of a premature ventricular contract. [5]

Figure 2.4 contains an example of a supraventricular rhythm where the origin of the atrial contraction varies. This example illustrates how different origins in the atria affect the appearance of the P-wave. It is observed that if the atrial activation is originated close to the AV node, the depolarization occurs in the opposite direction and hereby produces a negative P-wave. It is furthermore observed that the appearance of the QRS complexes is unaffected since the depolarization is lead through the AV node to the ventricles using the normal conduction pathway. [5]
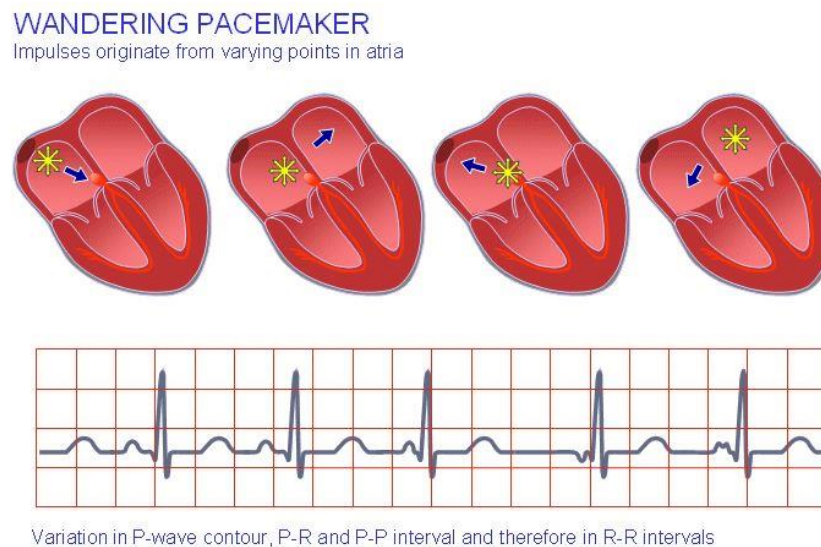
Figure 2.4: Illustration of wandering pacemaker. [5]

Another clinically very interesting supraventricular arrhythmia is atrial fibrillation (AF). This arrhythmia is characterized by irregular and rapid beating of the two atria. This causes the surface ECG to display a fibrillating baseline and irregular QRS complexes. An ECG snippet illustrating this is provided in Figure 2.5.
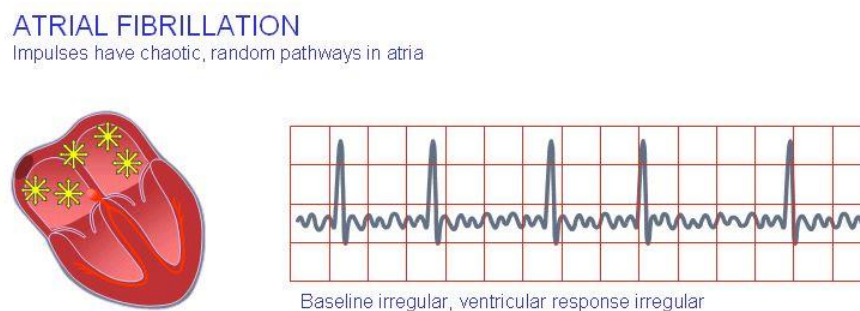
Figure 2.5: Illustration of atrial fibrillation (AF). [5]

AF occurs in 1-2% of the general population, and the prevalence is expected to be at least doubled within the next 50 years due to the aging population [6]. Some patients might present symptoms including palpitations, dizziness, dyspnoea, syncope or fatigue, but about one-third of the patients are asymptomatic [6]. This makes AF a "silent killer" meaning that many patients suffer from AF without knowing it. This is highly problematic due to the increased risk of other serious clinical events (see Table 2.1). Early recognition of AF is thus very important to initiate correct treatment to avoid both progression of the disease and decrease the risk of related clinical consequences. However, the often "silent" nature of the arrhythmia impedes the chance of early detection [6]. Furthermore, AF can be paroxysmal meaning that episodes of AF alternate with episodes of normal sinus rhythm. This makes prolonged monitoring important to ensure that potential paroxysmal AF events are correctly identified [7]. It might therefore be beneficial to conduct large-scale screening programs to identify patients with AF

before the development of for instance injurious episodes of stroke. As described below, dangerous arrhythmias like AF might therefore not be sufficiently managed by the earlier accepted monitoring techniques. This draws the attention to the benefits of new recording techniques that facilitate prolonged comfortable ambulatory ECG recordings. This was one of the main motives for designing the novel ePatch ECG recorder.

Table 2.1: Clinical events (outcomes) affected by AF [6].

Outcome parameter	Relative change in AF patients
1. Death	Death rate doubled
2. Stroke (including hemorrhagic stroke and cerebral bleeds)	Stroke risk increased (5-fold) and AF is associated with more severe stroke.
3. Hospitalization	Hospitalizations are frequent in AF patients and may contribute to reduced quality of life.
4. Quality of life and exercise capacity	Wide variation, from no effect to major reduction. AF can cause marked distress through palpitations and other AF-related symptoms.
5. Left ventricular function	Wide variation, from no change to tachycardiomyopathy with acute heart failure.

2.2   Overview of Ambulatory ECG Monitoring Devices

Since the first Holter recorders were invented in the 1940s there has been a tremendous development in the capabilities for ambulatory ECG monitoring [1]. A detailed overview of the different monitoring techniques is provided in [8] and [1], whereas a brief overview of three selected monitoring devices is presented in Table 2.2. It should be noted that different variations of the three selected devices exists, e.g. not all event and loop recorders require patient participation in transmission of the recorded events. The events can also be stored locally for analysis after the recording. However, it is generally observed that many of the older technologies induce significant issues related to patient comfort, the duration of the monitoring period, and the integrity of the recorded data. The event and loop recorders only store ECG data when either a patient trigger system or an automatic event detection system is activated. This prevents full disclosure and investigation of potential dangerous but asymptomatic events which were not correctly detected by the automatic algorithms. Furthermore, the auto-trigger algorithms are not designed to detect the offset of an arrhythmia. This implies that it is impossible to assess for instance the AF burden [1]. This situation is overcome by the continuous Holter and telemetry systems. However, the nature of these systems induces issues related to patient comfort and compliance with wearing the systems for extended periods of time. As mentioned, this might be problematic since recent research have demonstrated how a prolonged monitoring period using patch devices can result in an increased diagnostic yield, e.g. in patients with AF [2], [7], [9]. A variation of the loop recorders is the implantable loop recorder. These are implanted subcutaneously, and they are triggered automatically or by patient activation. Their battery life time is more than 24 months and they can therefore be applied for very prolonged monitoring [8]. However, they require surgical insertion. The selection of monitoring technique in each situation can thus be characterized as a compromise between sufficient diagnostic information from adequate continuous monitoring on one hand, and patient comfort and compliance on the other. To overcome this, a new generation of long-term ECG monitoring techniques has reached the market during the last couple of years. The patch type recorders were created to fit right in the middle of this compromise: The patches were designed to provide reliable high quality continuous ECG monitoring for long periods of time without any patient discomfort or impairment of normal daily life activities. One of them is the ePatch recorder investigated in this project.

Table 2.2: Comparison of different types of important currently applied ambulatory ECG monitors [1] [8].

Device type	Holter monitor	Event monitor	Loop recorder
Illustration of device	[1]	[1]	[1]
Data flow	Patient wears monitor contiuously → Patient keeps diary of symptoms → Patient returns monitor to technician → Technician creates final report for reffering physician	Patient carries monitor → Patient places monitor on chest during symptoms → Patient transmit data via telephone line to monitoring station → Monitoring station sends data to physician	Patient wears monitor → Patient activate monitor during symptoms (auto-trigger possibility) → Patient transmit data via telephone line to monitoring station → Monitoring station sends data to physician
Typical duration	24-48 hours	Up to 30 days	Up to 30days
Complete data storage?	Yes	No	No
Remote monitoring?	No	Yes	Yes
Advantages	- Continous ECG recording and analysis of all data - No patient participation in data transmission	- The patient is not constantly "wired up" - Relatively long monitoring duration	- The combination of auto-trigger and manual activation allows detection of both asymptomatic and symptomatic events - Storage of the pattern initiating the cardiac event - Relatively long monitoring duration
Disadvantages	- Relative short duration - Patient incompliance to keep diary of symptoms and constantly wear the device - Real-time analysis is impossible - Time consuming manual analysis	- No information about asymptomatic events - No information about the pattern initiating a symptomatic event - Issues with patient incompliance to apply device and immedialetly transmit signals	- Risk of missing asymptomatic events if the auto-trigger function fails - Patient incompliance with constantly wearing the device or immediately transmit data

2.2.1 The ePatch Technology

Based on knowledge about the disadvantages of the older ambulatory monitoring technologies, the ePatch heart monitoring platform was designed according to a "wear and forget" principle. Thus, the device is designed to be reliable, comfortable and easy to use for both the patient and the healthcare professionals. This was accomplished by the novel patch design illustrated in Figure 2.6. The ePatch system consists of two parts: 1) A bio-compatible, single-use adhesive electrode with multiple skin contact points that is attached directly to the skin surface (this part is termed the ePatch electrode) and 2) A reusable device that contains a rechargeable battery, electronic parts, data storage module, equipment for wireless data transmission, and a signal processing module (this part is termed the ePatch sensor). The ePatch sensor is attached directly on the ePatch electrode. This makes the system completely free of cables. This is designed to increase patient comfort and compliance and ensure the possibility of full participation in normal daily life activities during the recording. This patch design also facilitates a very small and light weight construction that minimizes the awareness of the system while wearing it. The ePatch version applied in most of this dissertation is CE approved for 24-hour ambulatory ECG recordings, and the ECG signals are stored locally on an internal memory. This ePatch version records two bipolar ECG channels with a resolution of

12 bits and a sampling frequency of 512 Hz. Furthermore, in compliance with IEC 60601-2-47, the ePatch front end had an analog bandpass (BP) filter between 0.67 and 40 Hz [10]. The ePatch is designed as a technology platform that can be customized to account for the needs in a high variety of situations. This is accomplished by a modular design that for instance allows addition of additional sensors for other recording modalities. Further details about the clinical application of the ePatch and results obtained from different clinical studies applying the ePatch are presented in Papers I - III.
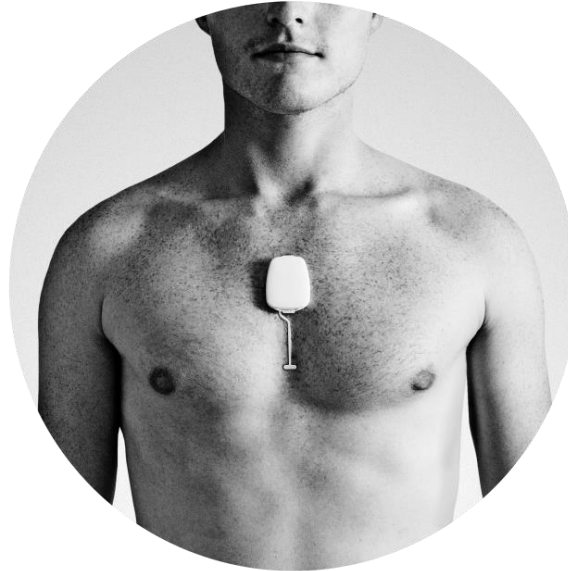

Figure 2.6: Illustration of the ePatch electrode and sensor correctly placed on the sternum.

Some of the expected advantages of the ePatch technology compared to the traditional Holter or event recorders thus include increased patient comfort and compliance, the possibility of real-time data transmission of clinically relevant cardiac events (enabled through embedded signal processing), and prolonged continuous monitoring. Furthermore, the patch design is expected to decrease the burden on the hospital staff to handle issues with loose or disconnected electrodes, a high number of cables attached to the patient, and difficulties with personal care, e.g. patient showering. However, the placement of the ePatch electrode results in a shorter distance between the bipolar recording electrodes. Furthermore, the placement of the electrodes is not similar to the electrode placements in the traditional Holter recordings. This causes the recorded electrical activity to be slightly different. Based on the brief description of the origin of the ECG, it can be appreciated that the different electrode positions might therefore slightly change the appearance and/or quality of the recorded ECGs. This might induce difficulties regarding the medical professional's ability to recognize different heart rhythms and hereby reduce the practicability of the system. The reservation towards the quality of ECG signals recorded using patch technologies with closely spaced bipolar recording electrodes was furthermore stated by [1]. On the other hand, the advantages of the cable-free design and the placement on the sternum are expected to include the benefits of reduced artifacts from large muscles and large movements of electrodes and wires. To summarize, some of the important concerns related to this new technology include uncertainties about the ability to record high-quality diagnostic ECGs throughout the monitoring period. However, a number of other competitive patch-type ECG recorders have also reached the market. Two of the other players in the market are designed by Corventis [11]–[14] and IRhythm [2], [7], [9], [15], respectively. The high activity in the patch recorder market illustrates the interesting potentials with this technology and indicates that it is expected that the potential difficulties described above can be handled. Furthermore, it is observed how the important players in the patch recorder market has documented and validated their clinical performance through published clinical studies. In the beginning of this project, no publications regarding the clinical performance of the ePatch were available. We thus found it important to conduct investigations regarding the ability to record diagnostic meaningful high-quality ECG using the ePatch recorder placed at the sternum. As mentioned earlier, this topic is therefore the focus in chapter 3 and chapter 5. If the quality of the recorded signals can be assured, the potential for future application of the ePatch recorder as a substitute for

current recorders in areas were outpatient ECG monitoring is routinely applied today seem obvious. However, the new technologies also open for completely new areas were outpatient ECG monitoring is not possible or feasible today due to the limitations of the current devices. Examples of this might include:

- Prolonged monitoring to improve diagnosis and management of dangerous paroxysmal arrhythmias that might be difficult to diagnose using traditional devices (e.g. AF)
- Large-scale cardiac screening programs
- Tele-monitoring of known cardiac patients in their own homes
- Improved monitoring and guidance in exercise and rehabilitation programs
- Monitoring of high risk patients (e.g. patients with diabetes)
- Improved monitoring of post-operative patients

Many of these new application areas might benefit from the possibilities of real-time embedded interpretation of the recorded ECGs. As mentioned earlier, the first step in this analysis is reliable detection of each heartbeat. The design of an algorithm for embedded detection of QRS complexes in the ePatch sensor is thus the main focus in chapter 4. Overall, the application areas of the novel ePatch technology are very wide, and it is therefore worth spending some time and effort on investigations related to the practical applicability of this novel technology in real-life clinical settings.

3 Clinical Usability of ECGs Obtained with the ePatch Recorder

Objectives: The general advantages of the novel patch-type ECG recorders should be obvious. However, the primary requirement for the successful diagnosis and treatment of the patients remains to be the possibility for reliable interpretation of the recorded ECGs. This requires that the long-term patch ECG recordings obtain sufficient diagnostic quality for the analysis of specific ECG patterns. The aim of this part of the project was therefore to investigate the usability of two-channel sternal ECG recorded with the ePatch technology for heart rhythm analysis. This investigation thus forms the basis for the relevance of applying the ePatch ECG sensor in real-life clinical applications and, hereby, also the relevance of the remaining research described in this thesis. The clinical work described in this chapter is a summary and discussion of the work presented in Papers I – III.
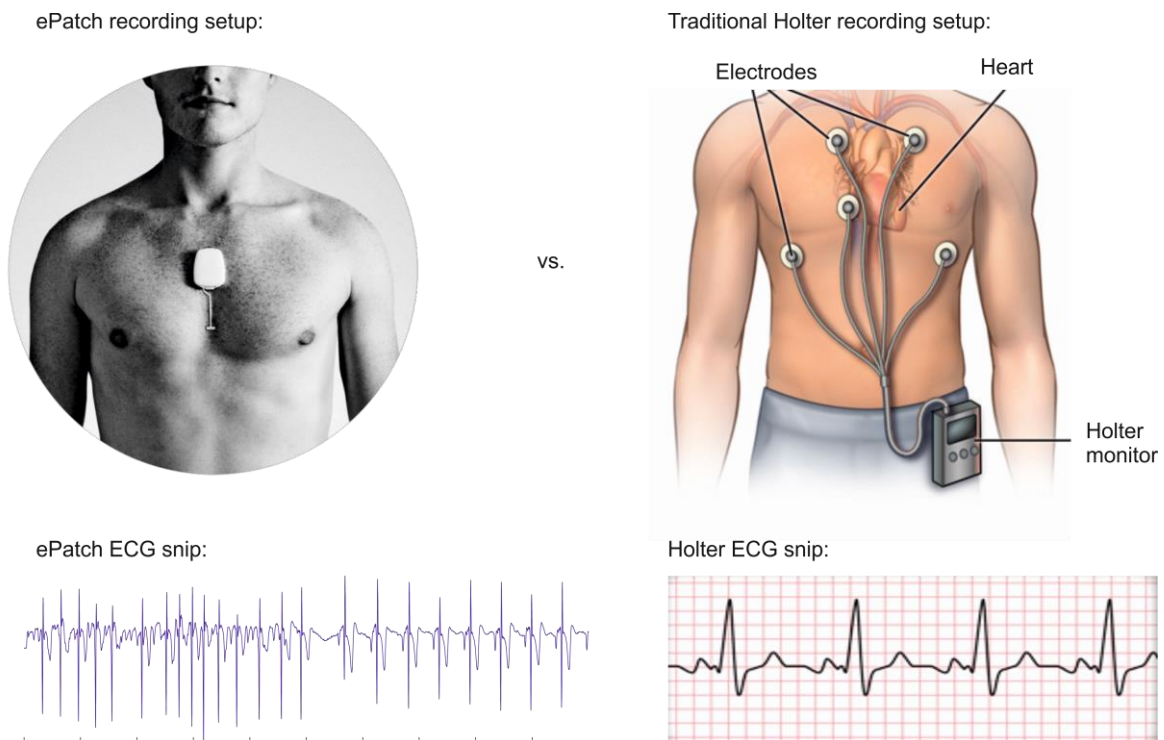
Figure 3.1: The advantages of the patch-type ECG recorders include increased patient comfort and compliance with wearing the system for extended periods of time, decreased artifacts from movements of cables, and the possibility of recording during most everyday activities, e.g. showering. However, it is important to investigate whether the recorded ECGs possess the same diagnostic information as ECGs recorded with traditional ECG equipment. This investigation is the main focus of this chapter. Modified from [16].

3.1   Background

In the beginning of this project, the ePatch technology was very new, and it was therefore not well understood whether the analysis of ePatch ECGs could provide satisfactory clinical information. This concern was highly related to the necessary short inter-electrode distances and the placement of the ePatch on the sternum. As can be imagined, these design choices were crucial to achieve the wear-and-forget goals, but they also imply that the projection of the cardiac vector is different from the projection applied in traditional ECG equipment. The information obtained from the recorded ECG channels does therefore not necessarily correspond to the information obtained from any of the known leads in the traditional Holter or telemetry systems. This could induce a risk of misinterpretation and difficulties during the analysis of the recorded ECGs. It was therefore an important part of this project to investigate the clinical usefulness of two-channel ECGs recorded on the sternum with the novel ePatch technology. This investigation is clearly important to validate the clinical usefulness of the ePatch technology and hereby create the foundation for the real-life clinical applicability of the remaining parts of this thesis.

3.1.1   Research Hypothesis

The above described concerns led to the formulation of two research questions that will be investigated and discussed throughout this chapter:

1. Is two-channel ECG recorded with the novel ePatch ECG recorder placed at the sternum useful for heart rhythm analysis? The usefulness for heart rhythm analysis implies that the relevant ECG fiducial points are visible (e.g. the presence/absence of P-waves, the regularity of the QRS complexes, and the width of the QRS complexes).
2. Is the clinically relevant information obtained from the ePatch system comparable to the diagnostic information obtained from simultaneous recordings obtained with traditional ECG equipment?

3.1.2   Literature Overview

A few studies in the literature have addressed similar questions related to other patch-type devices. Some of the most interesting findings from the literature are summarized below:

- In [3], the use of a prototype patch ECG recorder designed by Phillips Healthcare was investigated and compared to traditional Holter recordings. They extracted seven-second ECG segments from simultaneous recordings obtained with the prototype device and a traditional Holter recorder. They compared each pair of simultaneously extracted ECG segments from the two devices with respect to the ability to correctly capture episodes of ventricular ectopy. They found a 100% agreement for the recognition of ventricular fibrillation (VF) and a very high accuracy for the correct detection of the total number of VEBs and the number of different VEB configurations in each ECG snippet.
- In [4], the same prototype patch ECG recorder designed by Phillips Healthcare was investigated again. They investigated four different placements of the experimental patch recorder. One of the investigated positions was at the sternum. Again, they extracted seven-second ECG segments from simultaneous recordings obtained with the experimental device and a traditional Holter recorder and compared the segments with respect to the presence of important diagnostic ECG fiducial markers. In this study, they found a very accurate assessment of atrial activity (presence/absence of P-waves and PR interval) and overall rhythm diagnosis at the midsternal position and a good assessment of the QRS width in all four investigated locations. In both [3] and [4], segments were excluded if the interpretation was obscured by noise in either one of the two different recording modalities.
- In [9], recordings of up to 14 days with the one-channel Zio Patch recorder (iRhythm Technologies) placed over the left pectoral region were compared to three-channel 24-hour traditional Holter recordings obtained from 146 patients. They found that, during the initial 24-hour period where both devices were worn, the Holter recorder found a few cases of clinically significant arrhythmias that went undetected by the patch recorder. However,

comparing the total wear time of the two devices (Holter: median = 1.0 day; patch: median = 11.1 days), the patch recorder detected significantly more arrhythmia events than the traditional Holter device.

- In [7], the Zio Patch was used on 74 patients referred for evaluation of paroxysmal AF. They found an excellent agreement between the detection of AF episodes and estimation of the overall AF burden using the Zio Patch and the traditional Holter recorder during the initial 24 hours where both devices were applied.

A review of the literature thus indicates a strong potential for the recording of clinically relevant ECG signals on the sternum using a patch-type ECG recorder. However, the described systems are not completely comparable to the ePatch system, and it was therefore also important to investigate the clinical usefulness of ECGs recorded with the novel ePatch recorder.

3.1.3   Chapter Overview

To allow the investigation of the formulated research questions, we conducted two clinical pilot studies. These studies were designed with inspiration from the above described literature review as well as considerations for the practical circumstances and the practical possibilities at the time of the investigations. This chapter contains a description and discussion of the findings in each individual pilot study, followed by a common discussion of the study limitations and the overall conclusions gained from both studies.

3.2   Pilot Study I: Usability of ePatch ECG Segments for Heart Rhythm Analysis

One of the expected ePatch applications is a substitution of today's traditional Holter recorders. The first pilot study was therefore designed to investigate whether ECGs recorded with the ePatch sensor placed on the sternum are useful for heart rhythm analysis in a setting fairly similar to that of the traditional and well-known Holter analysis. In the traditional setting, a medical technician with speciality in Holter or telemetry analysis extracts relevant ECG segments that are provided to the referring medical doctor together with an overall description of the findings in the recording. The referring medical doctor applies this information as input to the diagnosis together with other relevant clinical tests and the medical history. To obtain a realistic impression of the usefulness of the ePatch ECGs, we applied a methodology that is fairly similar to this approach: An experienced nurse (ECG technician) was asked to extract ECG segments from each patient, and two medical doctors were then asked to individually judge the usefulness of each of the extracted segment for heart rhythm analysis. The data extraction procedure and the medical evaluation of each segment were conducted in two different Graphical User Interfaces (GUIs) that we designed in MATLAB R2012B. The next sections contain a summary of the findings in this pilot study, whereas a detailed description is provided in Paper II.

3.2.1   Description of Database

To facilitate a meaningful investigation, it was important to ensure the representation of realistic amounts of different abnormal beat morphologies. We therefore decided to include hospitalized patients that were already selected for regular telemetry monitoring. We included ECG data from 25 randomly selected admitted patients. Each patient was monitored simultaneously with the CE-marked ePatch ECG recorder and the traditional telemetry equipment for approximately 24 hours. The recorded data were stored locally on the ePatch sensor for offline analysis. The ECG segments were provided to both the nurse and the medical doctors without any form of pre-processing.

3.2.2 Extraction of the ECG segments

In line with [4] and [3], the duration of each segment was seven seconds. A total of eight ECG segments were extracted from each patient by an experienced ECG technician. The segments were extracted according to the procedure described below and illustrated in Figure 3.2:

1. If the current seven-second data segment was considered noise free, it was selected for the study, and a new seven-second segment was investigated five minutes later.
2. If the current seven-second data segment was not considered noise free, it was excluded from the study, and a new seven-second data segment was investigated one minute later.
3. If it was not possible to extract eight segments of sufficient signal quality within the three investigated hours of data (indicated by red squares in the top plot of Figure 3.2), the patient was excluded from the study.
4. This procedure was continued until a total of 200 ECG segments were extracted from 25 different patients.
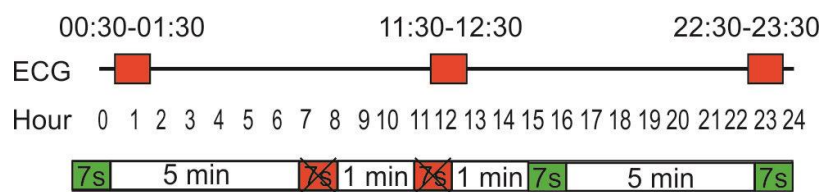

Figure 3.2: Illustration of the procedure for ECG segment selection. For each patient, only three hours of data was considered. These three hours are indicated by red marks in the top panel for a recording of exactly 24 hours. This prevents the very time-consuming process of going through a long-term recording of very poor quality minute by minute and, at the same time, ensures that the patient is only excluded if the quality remains poor throughout the entire recording period. The bottom panel illustrates the process of extracting the seven-second ECG segments. Green segments were selected for the study, whereas red segments were excluded due to insufficient recording quality.

3.2.3 Results

The results are provided in Table 3.1. It is observed that the first and the second medical doctor found 197 and 199 of the 200 segments useful, respectively.

Table 3.1: Results from the medical evaluation of each of the 200 ECG segments.

Segments marked as "useful"	Number	Percentage
Medical doctor 1	197	98.5%
Medical doctor 2	199	99.5%
Both medical doctors	196	98.0%
At least one medical doctor	200	100%

3.2.4 Discussion

Both medical doctors indicated that more than 98% of the selected ECG segments were diagnostically meaningful to them. This implies that the ECG segment could help toward heart rhythm analysis and, hereby, the diagnosis of the patient. It should, of course, be stated that the diagnosis would include results from other relevant clinical tests, medical history, review of the entire long-term ECG recording, and general comments from the nurse preparing the ECG analysis report. The diagnosis is not imagined to be based solely on the seven-second ECG segments investigated in this study. It should furthermore be noted that this study was focused on the clinical interpretability of the recorded ECGs, and we were therefore not concerned about the obtained signal quality. This is in line with the investigations described in [3] and [4]. The signal quality of patch ECG recorders is further discussed in chapter 5. Furthermore, it was observed that the two doctors did not agree on which segments that were not useful for rhythm analysis. This could indicate a certain degree of inter-reader variability. The number of doctors could be increased in a future study to investigate the true inter-reader variability. For the purpose of this pilot study, it was, however, considered sufficient with the evaluation by two medical doctors. It should also

be stated that, even using the "worst case" still results in 98% of the segments being useful. Furthermore, in a real-life situation, cases of doubt are expected to be solved by discussion and consensus with other doctors. It is therefore important to note that the "best case" indicates that all 200 segments were useful. The results from this pilot study are therefore very promising and strongly indicate the potential for ambulatory cardiac monitoring using the ePatch ECG recorder. This finding corresponds well with other findings in the literature for different types of patch ECG recorders [2]–[4], [7], [9]

3.3   Pilot Study II: Comparison with Traditional Telemetry Equipment

To investigate the second research question, we designed this pilot study to allow a high level comparison of the clinically relevant information obtained from simultaneous recordings obtained with the ePatch ECG recorder and the traditional telemetry equipment. The study includes both an overall comparison of the clinically relevant information from both techniques and a "spot check" of the ability to correctly reproduce specific interesting arrhythmia events in the ePatch recordings. The next sections contain a detailed description of the comparison, whereas a short abstract is presented in Paper III.

3.3.1   Description of Database

The database was generated from the database described in section 3.2.1. However, the investigations in this pilot study were more time consuming, and therefore, only 11 of the 25 patients were included. The 11 patients were randomly selected among all patients with a recording time of at least 24 hours and 10 minutes (the first 10 minutes of each recording was discarded due to the risk of pronounced artifacts caused by the mounting of the device).

3.3.2   Methodology

The available information was extracted from the two monitoring systems, and the clinical interpretation obtained from each system was compared by a cardiologist. This procedure is described in detail below.

3.3.2.1   Extraction of Information from the Telemetry Equipment

After each ePatch recording, information from the telemetry reports was extracted from the automatic analysis software. The extracted information included ECG segments of automatically generated alarms indicating potential arrhythmia events, automatically generated overviews of arrhythmia events, and HR trend curves for each patient. In some cases, no alarms were automatically generated. Therefore, it was also investigated whether any significant findings, diagnosis, or conclusions from the telemetry monitoring system were added to the electronic patient journal (EPJ).

3.3.2.2   Extraction of Information from the ePatch Equipment

For the ePatch system, a full disclosure of the 24-hour digital ECG recording was available for visual inspection by the cardiologist. The automatic telemetry software applies pre-processing, e.g. filtering, before the recorded ECG data are visualized. To allow a fair comparison, the ePatch recordings were therefore also pre-processed. During this step, it is important to attenuate the influence of different types of artifacts without deteriorating clinically relevant ECG characteristics. The pre-processing is described in detail in Appendix A. The ePatch ECG data were visualized using LabChart 7 Pro from ADInstruments. A third channel with the instantaneous HR was added in LabChart. This provides an overview of the recording that can be compared to the HR trend curves from the telemetry recordings. Furthermore, it provides an overview of the variation in the RR intervals and hereby clearly indicates heart rhythms like AF as well as episodes of VEBs and supraventricular ectopic beats (SVEBs). Episodes of poor data quality will also often be highlighted from the instantaneous HR curve due to incorrect heartbeat detections.

3.3.2.3   Comparison of Diagnostically Relevant Information

The comparison of the clinically relevant information for each patient was conducted as described below:

1. The cardiologist selected relevant alarm events from the telemetry system. It was then investigated whether the same event(s) could be visually identified and correctly diagnosed at the same time instance in the ePatch recording. This provides a "spot check" of the diagnostic quality of two-channel ECG recorded with the ePatch placed at the sternum.
2. The cardiologist looked through the entire 24-hour ePatch recording and hereby obtained an assessment of the heart rhythm, any abnormal beats, the HR trend curve, and the general signal quality obtained in the ePatch recording.
3. The general heart rhythm observed from the telemetry alarms or written in the EPJ was compared to the general heart rhythm found in the ePatch recording. The same procedure was conducted for the HR trend curves.
4. The cardiologist was asked to provide an overall judgment of the signal quality obtained in the ePatch recordings.
5. The cardiologist was finally asked if there were any clinically relevant differences in the findings and diagnosis that could be made based on the 24-hour ePatch recording and the available information from the traditional telemetry monitoring system.

3.3.3   Results

One of the important comparisons was the "spot checks" of the diagnostic quality of the ePatch ECG recordings. These "spot checks" served to ensure the correct reproduction of relevant arrhythmia events in the ePatch recordings. The following figures therefore contain a few examples of these "spot checks." Figure 3.3 illustrates an example of an alarm from patient 4 indicating asystole. The asystole is observed from both the telemetry printout and the ePatch ECG snip. The general heart rhythm for this patient is AF. This is also observed from both the telemetry system and the ePatch recording. Figure 3.4 contains an example from patient 10. The general heart rhythm is normal sinus rhythm (NSR) with a sudden onset of tachycardia. This is observed from both the ePatch recording and the telemetry alarm printout. The telemetry printout furthermore shows a flat line in channel II. Figure 3.5 illustrates an example of a comparison for patient 11. The general heart rhythm for this patient is NSR. The alarm is an episode of AF with aberration. This is also observed from the ePatch recording. An overview of the comparisons for all 11 patients is provided in Table 3.2 on page 20. Finally, the cardiologist found that there were no clinically relevant differences between the information that could be extracted from each of the 24-hour ePatch recordings and the available information from the traditional telemetry monitoring system.
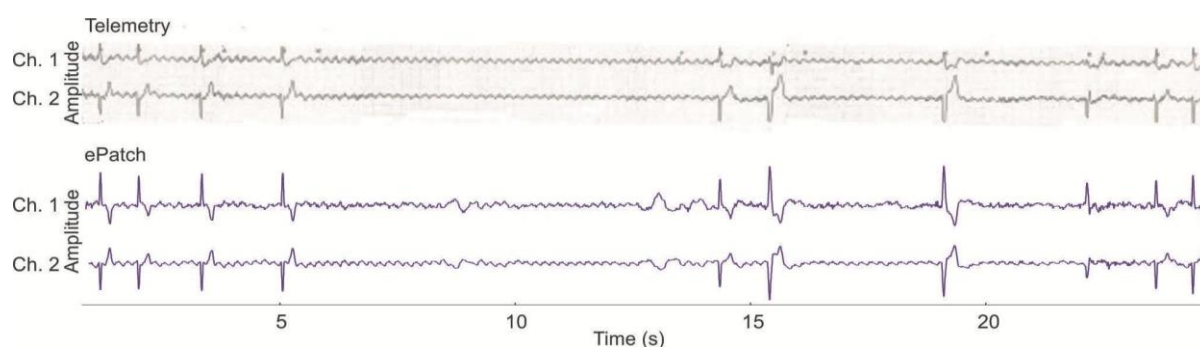

Figure 3.3: Example of comparison between telemetry and ePatch for patient 4: Episode of approximately nine-second asystole is correctly recorded by the ePatch system. Note that the general heart rhythm is AF.
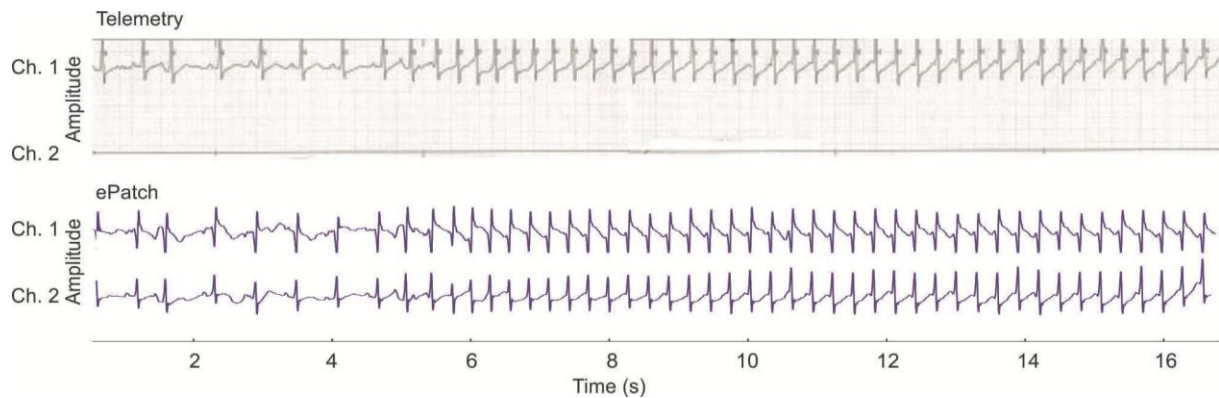
Figure 3.4: Example of comparison between telemetry and ePatch for patient 10: Episode of sudden onset of tachycardia is correctly recorded by the ePatch system. Note that channel II of the telemetry recording is only a flat line.
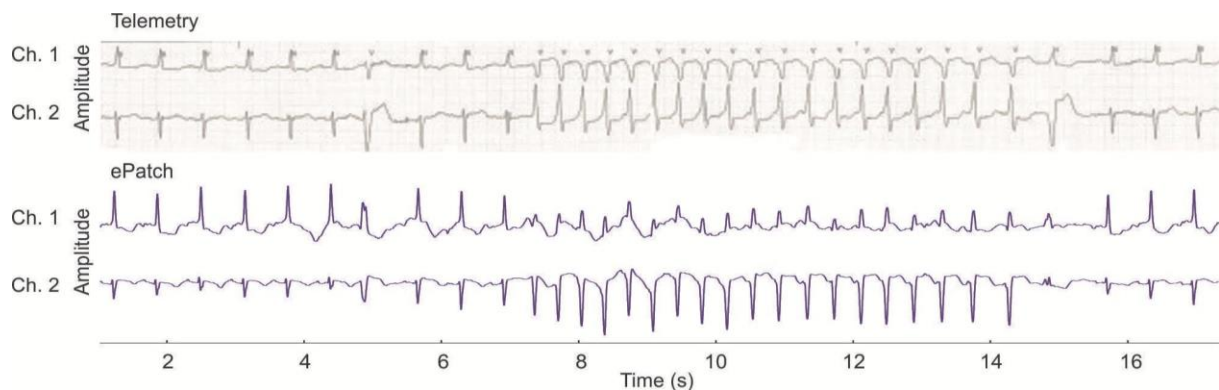
Figure 3.5: Example of comparison between telemetry and ePatch for patient 11: Episode of AF with aberration is correctly recorded by the ePatch system.

3.3.4   Discussion

In this pilot study, it was investigated whether the same clinically relevant information could be extracted from the 24-hour simultaneous recording obtained with the ePatch ECG recorder and the traditional telemetry equipment. For all patients, the HR trend curves could be reproduced using the ePatch technology. Furthermore, episodes of ventricular frequencies of up to 150 BPM and bradycardia episodes with low ventricular frequencies were correctly reproduced by the ePatch recordings. This indicates the usefulness of the ePatch technology in a large portion of the clinically relevant HR range. Different clinically relevant heart rhythms and beat morphologies (NSR, AF, sinus tachycardia, VEBs, run of VEBs, SVEBs, and asystole) were furthermore correctly recorded by the ePatch technology. This indicates the clinical usefulness of two ECG channels recorded on the sternum with this novel patch technology. Furthermore, the fact that no clinically relevant differences between the available information from the two technologies were noted by the cardiologist is very promising for the future application of the ePatch technology in this setting. In addition, ten of the investigated ePatch recordings were judged to obtain a very high signal quality. This is extremely important for the reliability of the system. One recording was noted to contain a high number of very noisy segments. The visual appearance of the artifacts indicates that they were caused either by many movements or by bad electrode contact. However, for the same patient, the automatic telemetry system generated a number of false alarms due to noisy data segments. This could indicate that the general quality of the ePatch recording was not necessarily lower than the quality of the traditional telemetry recording. The impression of the findings in this pilot study is thus that ePatch recordings could be imagined as a substitute to the traditional telemetry monitoring of admitted as well as ambulant patients requiring real-time cardiac surveillance. As for the first pilot study, the findings correspond well with other findings in the literature [3], [4], [7], [9]

Table 3.2: Summary of comparison between information extracted from the telemetry monitoring versus the ePatch recording (AF = atrial fibrillation, NSR = normal sinus rhythm, EPJ = electronic patient journal, HR = heart rate, BPM = beats per minute, VEB = ventricular ectopic beat, and SVEB = supraventricular ectopic beat).

Patient	Telemetry	ePatch
1	General rhythm: AF. HR: around 50 BPM. Selected telemetry alarm episodes include run of wide QRS complexes, cases of VEBs, and bradycardia during the night.	General rhythm: AF. HR: around 50 BPM. All selected alarm episodes from the telemetry software were correctly found in the ePatch recording.
2	No alarms from the telemetry, and no comments in EPJ. This indicates NSR during the entire recording. HR: around 100 BPM. No drop in HR during the night.	General rhythm: NSR/sinus tachycardia with frequency around 100 BPM. No drop in HR during the night.
3	General rhythm: NSR. HR: around 100 BPM without decrease during the night. Telemetry overview indicates several VEBs in the recording. Selected telemetry alarm examples include run of wide QRS complexes and VEB.	General rhythm: NSR. HR: around 100 BPM without nightly decrease. Many episodes of VEBs found in the ePatch recording. Selected telemetry alarms with run of wide QRS complexes and VEB correctly located in ePatch recording.
4	General rhythm: AF. HR: around 75 BPM but with several episodes of very high ventricular frequency of up to 150 BPM. Selected telemetry alarm with asystole of approximately nine seconds.	General rhythm: AF. HR: around 75 BPM. Episodes of ventricular frequency up to 150 BPM are also observed in the ePatch recording. Episode of asystole correctly found; see Figure 3.3.
5	EPJ states NSR with run of SVEBs with aberration. Telemetry episodes of SVEB with compensatory pause. HR: 60-70 BPM with many brief episodes of higher HR.	General rhythm: NSR. HR shows the same pattern as the telemetry trend curve. Example of episode of SVEB with compensatory pause was correctly found in the ePatch recording.
6	The telemetry overview indicates NSR with a few abnormal beats. HR: 60-70 BPM with small decrease during the night.	NSR with examples of isolated SVEBs. The HR trend curve is comparable to the telemetry HR trend curve.
7	EPJ indicates AF with high ventricular frequency. HR from telemetry trend curve is approximately 75-100 BPM.	AF during the entire recording without other significant arrhythmias. HR curve has the same trend as telemetry HR curve.
8	General rhythm: NSR. Several false alarms due to noisy data segments.	General rhythm: NSR. Several episodes of very noisy data.
9	EPJ indicates paroxysmal AF. No alarms from the telemetry system. However, the first two hours are indicted to contain a relatively high number of arrhythmia events.	Paroxysmal AF with episodes of clear change between NSR and AF. Episodes of SVEBs are observed.
10	EPJ indicates NSR. Selected example of telemetry alarm shows episode of tachycardia.	General rhythm: NSR. Example of episode of tachycardia from telemetry correctly identified; see Figure 3.4.
11	EPJ indicates NSR with brief episodes of AF with aberration. Examples of this are also found in the telemetry alarms.	General rhythm: NSR. Selected example of brief episode of AF with aberration correctly found in the ePatch recording; see Figure 3.5.

3.4   Study Limitations and Suggestions for Future Work

Both pilot studies serve to gain preliminary knowledge about the clinical applicability of ECGs recorded with the novel ePatch heart monitor. It should, of course, be mentioned that these preliminary studies have a high number of limitations. Some of these limitations are listed below together with suggestions for further clinical studies that might be conducted to establish a more solid knowledge about this novel technology:

1. Both pilot studies were conducted on a very limited number of patients. They should be performed on much larger patient populations to confirm the findings in the general population. It might also be interesting to conduct detailed investigations of the usefulness in specific patient populations.
2. In the first pilot study, we applied a procedure similar to the traditional Holter analysis. However, simultaneous Holter recordings were not available, and a direct comparison with the gold-standard Holter recorder was therefore not possible. This direct comparison might be interesting in future clinical studies.
3. In the second pilot study, we conducted a high level comparison of the clinically relevant information obtained from the ePatch technology and the traditional telemetry equipment. It might be interesting to conduct a direct comparison on a beat-by-beat basis between telemetry/Holter recordings and the ePatch recordings. This could, for instance, include an investigation of the ability to correctly detect specific ECG features, e.g. the presence/absence of P-waves [3] [4]. This investigation was not practically possible because the extraction of digital full-disclosure 24-hour ECG data files was not possible with the available telemetry software. The issue was therefore somehow addressed using the carefully selected "spot checks," but this comparison might be conducted more thoroughly. Furthermore, it should be mentioned that the comparison was not conducted using statistical methods. A thorough statistical analysis was not feasible due to the relatively small number of data points and the limited available time. This analysis might therefore also be conducted in future studies.
4. However, a more interesting and clinically relevant comparison could include an analysis of potential differences in the final analysis reports obtained from simultaneous recordings obtained with the ePatch technology and traditional Holter or telemetry systems. This would somehow be similar to the investigations described in [7] and [9]. However, this was not possible due to the previous lack of commercial automatic software approved for the analysis of the ePatch ECGs. Today, these software systems exist [17][18], and this analysis might therefore be both very interesting and practically possible in future studies.
5. In the described pilot studies, only two medical doctors and one cardiologist were asked to assess the usability of the recorded ECGs. It might be interesting to conduct investigations with more physicians to ensure the general acceptance of the appearance/morphology of the recorded ePatch ECGs.
6. Preliminary studies (not further described in this thesis) have also suggested that the ePatch placed in different chest locations might have certain degrees of similarity with some of the traditional leads from the standard 12-lead resting ECG. It might also be interesting to explore this topic further in future research projects.
7. Finally, one of the major areas that have not been satisfactorily covered for patch-type ECG recorders in general is the long-term stability and quality of the recorded ECGs. As mentioned, this topic will be further discussed in chapter 5.

3.5   Conclusions

In spite of the above discussed limitations, these pilot studies clearly indicate the clinical usefulness and relevance of ECG recorded with the ePatch placed at the sternum. In the first pilot study, it was found that more than 98% of the extracted ECG segments were useful for heart rhythm analysis. This implies that the important ECG fiducial points necessary for heart rhythm analysis were visible in the extracted ECG snippets (e.g. absence/presence of P-waves, QRS regularity, and QRS width). We therefore conclude that two-channel ECG recorded with the ePatch ECG recorder placed at the sternum is useful for heart rhythm analysis. The recorded ECGs can therefore be applied as input to patient diagnosis together with other relevant clinical tests and the medical history. The main finding in the second pilot study was that the cardiologist found no clinically relevant differences in the information that could be extracted from the ePatch recordings and the traditional

telemetry equipment for all 11 investigated patients. This indicates that the ePatch recordings could be applied on equal terms as recordings obtained with traditional telemetry equipment. The clinical relevance of ECG recorded with the ePatch placed on the sternum is thus clearly indicated, and it is expected that the new patch technologies might completely substitute the currently applied Holter and telemetry systems in the future. The future possibilities for this type of long-term ambulatory ECG recorders furthermore seem to be very high in areas like home monitoring, screenings, and follow-up consultations. However, the knowledge about the practical application of the new patch technologies is still relatively limited due to the lack of large-scale applications of the technology in everyday clinical situations [1]. These pilot studies thus contribute to the currently limited knowledge about the usability of this novel patch-type ECG recorder. The overall conclusion from this chapter is thus that ECG recorded with the ePatch system placed at the sternum is clinically meaningful. This creates the foundation for the real-life clinical applicability of the remaining research described in this thesis. It should, however, be noted that the research described in this chapter was only focused on the clinical interpretation of the recorded ECG morphology in artifact-free ECG segments.

4 Automatic Real-Time Embedded Heartbeat Detection

Objectives *Many of the new interesting clinical fields that could benefit from future application of outpatient ECG monitoring using the novel patch recorders could also benefit from the possibilities of performing embedded real-time interpretation of the recorded ECGs. This embedded analysis would for instance allow real-time wireless transmission of HR trend curves, arrhythmia events, patient activity levels, and estimation of the general signal quality. The first important step in automatic ECG analysis is the reliable automatic detection of each individual heartbeat represented by the QRS complexes. The aim of this part of the project was therefore to explore the design of algorithms for automatic real-time embedded detection of QRS complexes in ECGs recorded with the ePatch system. The essential algorithm requirements are thus exceptional clinical performance with minimal computational costs. The work described in this chapter is an extension and discussion of the work presented in Paper IV and Paper V.*
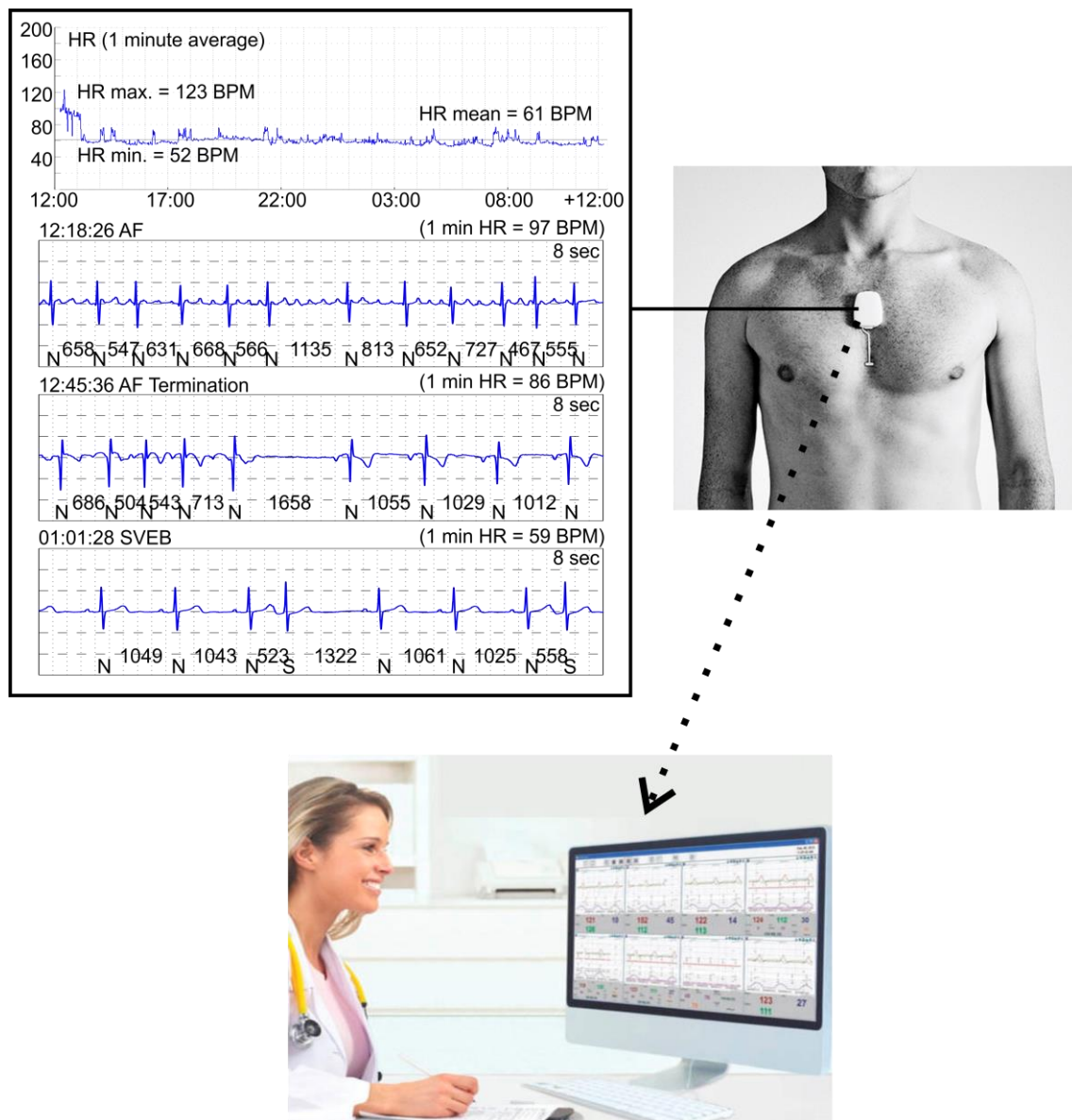
Figure 4.1: In many applications it is desirable to perform real-time embedded processing of the recorded signals and for instance transmit pre-selected clinically relevant information to a central monitoring station. The first essential step in embedded ECG processing is reliable automatic detection of each individual heartbeat. The focus of this chapter is therefore to explore the design of automatic algorithms for real-time embedded detection of QRS complexes in ECGs recorded with the ePatch system. Modified from [19].

4.1 Background

The field of automatic QRS complex detection has been subject to extensive research efforts for at least 30 years [20]. This has partly been facilitated by the design of a number of publicly available standard ECG databases extracted from traditional Holter recordings [21]–[23]. These databases have achieved to optimize the research effort by providing a possibility for reproducible and simple evaluation of algorithm performance and consequently easy comparison between different published algorithms. A high number of algorithms obtaining high detection performance on these standard databases have thus been presented in the literature. This research field might therefore seem adequately covered in the literature already. However, most of the algorithms achieving clinically high detection performance are not optimized for embedded functionality. Furthermore, there is a huge difference between obtaining high clinical detection performance on carefully extracted standard databases and real-life ECG recordings with realistic amounts of artifacts arising from normal daily life activities. This issue was also addressed by the design of the Noise Stress Test database (NSTDB [20]). The performance of this databases must be stated to comply with [24]. However, this database is usually not applied for performance evaluation in the literature. Furthermore, this database is artificially created by adding noise to clean ECG recordings. It is therefore not well investigated in the literature how different algorithms perform on real-life ECG data recorded during normal daily life activities. Furthermore, the influence of the slightly different morphology of the ePatch ECGs was not well understood in relation to automatic ECG interpretation. Since our goal was to design and validate an algorithm to be applied embedded in real-life recordings obtained with the ePatch sensor, we therefore found it very relevant to conduct new research in this field. This ensures that we end up with an algorithm with high clinical performance on ePatch ECGs and with a computational load that can be handled by the resources available in the ePatch sensor.

4.1.1 Research Hypothesis

The chapter objectives and the above described considerations led to the formulation of a number of research questions that will be investigated and discussed throughout this chapter:

1. How pronounced is the similarity between ECG recorded with the ePatch technology and traditional equipment from an automatic algorithm point-of-view: Is it possible to design algorithms that can achieve high clinical performance on both types of ECGs?
2. Will the inclusion of information from the second ECG channel improve the clinical detection performance in long-term real-life ePatch ECG recordings or is the information from the two simultaneously recorded ePatch ECG channels redundant with respect to automatic QRS complex detection?
3. Can we design novel biomedical signal processing methods that can enhance the current detection performances stated in the literature?
4. Can the computational load be decreased to a level that allows embedded real-time heartbeat detection in the ePatch sensor with a satisfactory clinical performance and without significantly decreasing the total recording time with the current version of the ePatch sensor?
5. Is it possible to achieve a satisfying compromise between high sensitivity for detection of abnormal beat morphologies and a high tolerance to different types of inevitable artifacts arising from normal daily life activities in real-life ePatch recordings?

4.1.2 Literature Overview

Naturally, no literature was available regarding the first two research questions. For the remaining three questions, it was natural to take a close look at the existing literature describing different automatic methods for QRS complex detection. An extensive literature review of this area can be found in [25]. Generally, the automatic QRS complex detection algorithms can be divided into two steps: 1) The feature extraction step, where the QRS complexes are enhanced and different types of artifacts are attenuated, and 2) the detection step, where the position of the QRS complexes are found based on the feature signal and a classification procedure. Two of the commonly applied techniques for feature extraction include different

variations of digital BP filtering [26] and the wavelet decomposition scheme [27]–[33], but several other techniques have also been proposed, e.g. morphological operators [34], application of the phase-space portrait of the ECG [35], or the phasor transform method [36]. Especially, the wavelet decomposition has obtained high performance on most standard databases in many different studies. For the detection step, a well-known and accepted method is different variations of adaptive thresholding [26]–[29], [32]–[34]. Furthermore, some algorithms include an additional confirmation block to decrease the number of false positive detections due to noisy episodes crossing the relevant thresholds. In the literature, most algorithms are furthermore designed to process only a single ECG channel [26]–[31], [34], [36]. These algorithms are thus not designed to take advantage of the available multi-channel information. However, some studies have also proposed methods for automatic two or three channel QRS detection [33], [37], [38]. An overview of the obtained performances of different published studies is provided in Table 4.9 on page 53.

4.1.3   Description of Project Workflow

As discussed in the previous chapters, the short distance between the recording sites and the placement of the ePatch sensor implies that the projection of the cardiac vector is slightly different in ePatch recordings compared to traditional telemetry or Holter recorders. In the beginning of this project, the level of similarity between the ePatch ECGs and traditionally recorded ECGs was therefore not well understood. This is also reflected in the research effort discussed in the previous chapter. In the beginning of the project, it was therefore not clear whether it would be possible to analyze traditionally recorded ECGs and ePatch ECGs using the same automatic algorithms with satisfactory performance. To obtain an understanding of these issues and gain experience with the potential difficulties in automatic QRS complex detection in ePatch ECGs, we visually looked through a high number of long-term ePatch recordings. We hereby observed some characteristic challenges in the ePatch recordings. Many of these challenges are expected to be caused by the short distance between the recording sites and the sternal placement of the ePatch sensor. Some of the challenges include cases of "double" R-peaks (in healthy subjects), cases of very pronounced P-, Q- and/or S-waves, recording of profound atrial activity during episodes of AF, and relatively large changes in signal amplitude (including changes in QRS polarity). The amplitude changes were pronounced both between patients and sometimes also within the same recording. These changes might originate from high sensitivity to changes in patient posture. In addition, the comfortable design of the ePatch is expected to result in an increased activity level during the recording. This is expected to result in an increased number of artifacts and hereby more ECG segments characterized by a potentially low signal to noise ratio (SNR). Some of these challenges are illustrated in Figure 4.2. Based on this, we formulated some essential algorithm requirements:

1. The algorithm should, of course, obtain high detection performance on both normal and abnormal beats. This ensures high applicability in a clinical environment.
2. The algorithm should be able to handle sudden amplitude changes.
3. The algorithm should be able to handle high/pronounced T-waves.
4. The algorithm should be able to handle different QRS morphologies, including morphologies with very pronounced Q- or S-waves (sometimes even more pronounced than the R-peak). This includes QRS complexes with "negative" polarity.
5. The algorithm should be able to handle relatively high amounts of artifacts arising from normal daily life activities.
6. The algorithm should be able to handle very pronounced recording of atrial activity.
7. The above requirements should be fulfilled by an algorithm with low power consumption. As described earlier, we defined an acceptable low power consumption based on the ability to perform real-time embedded analysis within the ePatch sensor without unacceptable reduction in the total recording time.
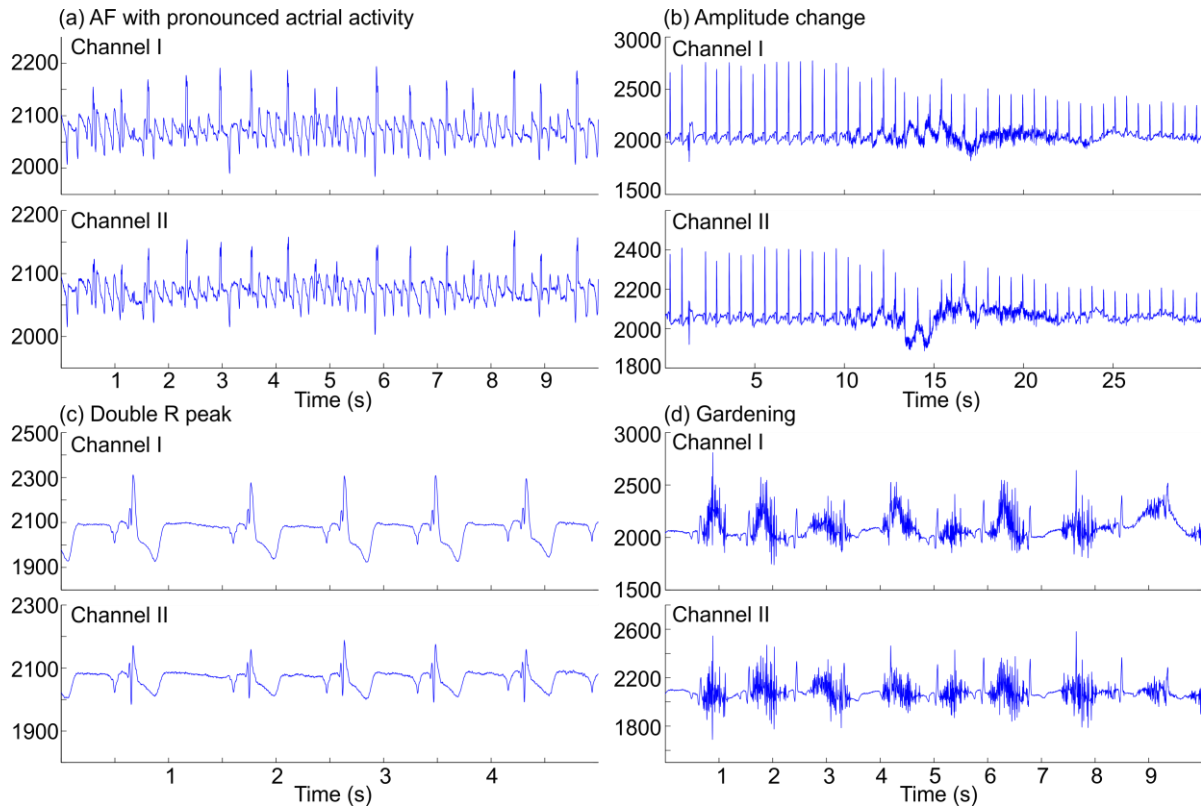
Figure 4.2: Illustration of some of the challenges experienced in automatic QRS complex detection in ePatch ECGs. (a) ECG segment displaying an episode of AF with very pronounced atrial activity between the QRS complexes. This ECG appearance has some visual similarity with ECG recorded from esophagus and is sometimes observed in the ePatch recordings. This is probably due to the electrode placement. (b) ECG segment with a sudden change in amplitude, probably due to patient movements. (c) ECG segment displaying a "double" R peak. This morphology is sometimes observed from healthy test subjects. This is probably caused by the sternal placement of the ePatch sensor. (d) Illustration of an ECG segment recorded with the ePatch sensor during gardening. It is expected to observe more of these types of artifacts in ePatch ECGs due to the expected increase in the general activity level compared to patients who are wired up with traditional equipment.

Furthermore, the projections of the cardiac vector obtained from the two ePatch channels describe approximately the same electrical axis. It was therefore not clear whether the information provided from the second ePatch ECG channel was redundant. Again, we initiated this investigation by visual inspection of ePatch ECGs. As indicated in Figure 4.2, the similarity between the two channels was often found to be high. However, it was also observed that the quality obtained in the two channels sometimes differs. A few clinical examples of this are illustrated in Figure 4.3. It is furthermore observed that abnormal beats sometimes display quite different morphologies in the two channels. It was therefore not clear in the beginning of the project whether information from the second ePatch ECG channel would be redundant with respect to automatic QRS complex detection. Looking at the literature overview, it was observed that most algorithms apply only a single ECG channel. The primary assumption for including additional channels is that the quality of one channel might occasionally or permanently decrease during a long-term recording without deterioration in quality of the remaining channels. For many of the recordings obtained from the standard databases, the quality of channel II is significantly lower than the quality of channel I – the opposite is rarely the case. It is therefore natural that the inclusion of information from channel II will not significantly improve the detection performance on these databases. This was also observed by [26] back in 1985. They state that the orthogonal placement of the electrodes in the traditional Holter leads applied in these databases implies that a high-quality signal in one channel often leads to a low-quality signal with low amplitude in the other channel. It is therefore natural that most algorithms described in the literature based on these standard databases only apply one channel. Opposite to the available standard databases, it might be difficult to foresee which channel that will achieve to obtain the most stable high-quality signal throughout the entire recording period in real life long-term recordings. For the real-life ePatch recordings, the inclusion of clean ECG from the additionally recorded channel might therefore be expected to improve the detection performance. Furthermore, we expected that information from both channels might increase the

likelihood of correct detection of abnormal beat morphologies. We therefore started by designing an algorithm that applies information from both simultaneously recorded ePatch channels. However, as we proceeded and continuously learned more about the characteristics of the ePatch ECGs, we began to believe that one ePatch channel would be sufficient in most cases. Furthermore, with the desired embedded implementation in mind, it is important to note that the computational load associated with the feature extraction and allocation of memory (RAM) is doubled when both channels are processed simultaneously. We therefore decided to design a second algorithm that only applies information from one of the available channels and investigate whether this would decrease the detection performance. A schematic overview of the two proposed algorithms is provided in Figure 4.4. Both algorithms are described and discussed in details later in this chapter. It is furthermore observed that we decided to implement different algorithm "building" blocks in the two proposed algorithms. This allows a better investigation of the exact functionality and influence of different algorithm steps, and hereby provides an understanding of the best future approach for real-time embedded QRS detection in patch ECG devices. The selection of building blocks in the second proposed algorithm was highly influenced by the knowledge gained from analysis of the performance of the first proposed algorithm in different challenging ECG snippets. This is further illustrated and discussed in section 4.5.
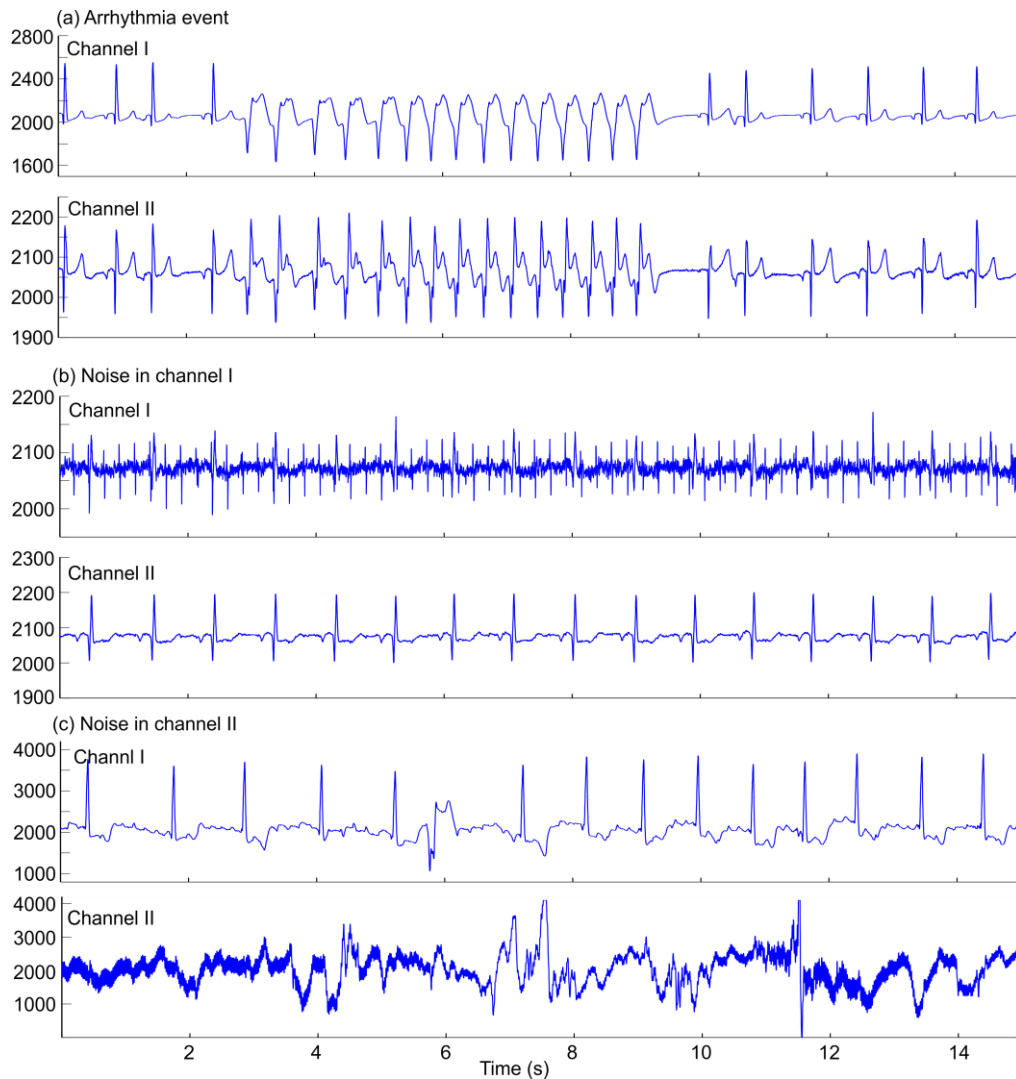

Figure 4.3: (a) Illustration of arrhythmia event with different morphology in the two channels. (b) Illustration of poor quality of channel I and high quality of channel II. (b) Illustration of high quality in channel I and poor quality in channel II. The rhythm is observed to be AF with a single VEB beat.
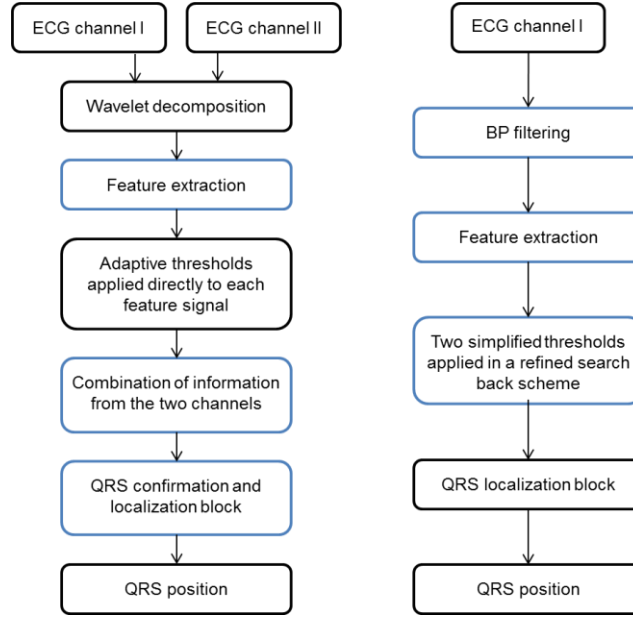
Figure 4.4: Schematic overview of the two proposed algorithms. The blue squares indicate blocks that were invented or significantly modified in the current work compared to the literature. (a) The first proposed algorithm applies simultaneous information from both available channels, the feature signals are extracted using the well-known wavelet decomposition, a single adaptive threshold is applied for QRS detection, and a confirmation block is included to decrease the number of false detections. (b) The second proposed algorithm is based on a single-channel approach, the feature extraction is based on a novel cascade of BP filters, the QRS detection block was implemented using two simplified adaptive thresholds in a refined search back scheme, and a localization block estimates the R peak position.

The proposed multi-channel algorithm was based on the well-known wavelet decomposition scheme. This was chosen based on the high performance obtained by this method in many studies in the literature. Some of the novel contributions of the multi-channel wavelet based algorithm are the scheme for combination of information from the two channels and the designed QRS confirmation block. However, as discussed later, the wavelet decomposition was found to possess some limitations, and the wavelet filtering scheme was therefore refined using a novel cascade of simple finite impulse response (FIR) BP filters in our second proposed single-channel algorithm.

Due to the high performance of adaptive thresholding in the literature, we decided that this was a sensible starting point, and therefore a variation of adaptive thresholding was implemented in the first algorithm. The adaptive thresholds can be applied according to different paradigms. One approach is the application of two different adaptive thresholds in a search back scheme [26]. Another scheme is to apply only a single adaptive threshold to each feature signal [29]. The search back mechanism induces an unavoidable, but small, delay in the detection of the QRS complexes. The search back scheme might therefore be more complex than a single threshold approach when the goal is real-time embedded QRS complex detection. We therefore decided to investigate the single adaptive threshold approach in our first proposed algorithm. We therefore implemented a threshold with inspiration from [29]. However, as discussed later, we found that the single threshold approach requires the threshold to be relatively low to allow acceptable detection of abnormal beats. This has the disadvantage of also increasing the vulnerability to different types of artifacts. Based on these considerations and experience from the first algorithm, we therefore found it feasible to investigation the possibilities with the search back scheme in the second algorithm. As mentioned, the search back methodology is a well-known procedure [26]. However, we have simplified the calculation of the adaptive thresholds to decrease the computational load, and we have refined the adaptation of the search back procedure in cases of irregular heart rhythms. This is described in detail later. To ensure sufficiently low power consumption, we embedded the second proposed algorithm in the ePatch sensor and evaluated both the energy consumption and the detection performance of the embedded algorithm. It is revived that we defined the acceptable power consumption as the ability to perform real-time embedded analysis without significantly reducing the total recording time of the current CE-market ePatch sensor.

4.1.4   Chapter Overview

Section 4.2 contains a detailed description of the selection of databases. Then a detailed description of the first proposed algorithm is presented in section 4.3. In section 4.4, the second proposed algorithm is described in detail. This section also contains the evaluation of the embedded implementation of this algorithm. Section 4.5 contains a discussion and comparison of the two algorithms. This also includes a comparison with the performances obtained by other published works, and this section is concluded with a set of recommendations for future embedded QRS complex detection in the ePatch sensor.

4.2   Description of Databases

To allow a careful investigation of the first research question related to the similarity between ePatch ECGs and ECGs recorded with traditional equipment, we found it essential to obtain throughout validation of the proposed algorithms on both ECGs recorded with the ePatch system and ECGs recorded with traditional equipment. It was furthermore very important to obtain databases with a high representation of normal beats with different ventricular frequencies, many different types of abnormal beats, and a high number of different artifacts. It was therefore of high importance to select relevant databases. For the standard databases, it was natural to select the two most popular databases in the literature. This allows both evaluation of detection performance on a high number of manually annotated abnormal beats and it allows easy comparison with the performance obtained by other published algorithms. It was furthermore important to obtain a representation of ePatch ECG recorded during different conditions. We therefore decided to apply the five databases defined below:

1. The MIT-BIH Arrhythmia Database (MITDB) [21]
2. The European ST-T Database (EDB) [22]
3. The Preliminary ePatch Database (PeDB)
4. The ePatch Training Database (eTDB)
5. The ePatch Validation Database (eVDB)

A summary of the recordings from the five databases is provided in Table 4.1 and a detailed description of each database is provided in section 4.2.1 - 4.2.4. It is important to note that a considerable amount of effort was put into the design of a suitable protocol for the extraction of the ePatch databases as well as the design of a relevant protocol for the manual annotations of the extracted databases. These steps were highly relevant to ensure proper validation in different aspects of the ePatch ECGs. It is furthermore important to note that the different databases were obtained throughout the course of the project. This implies that the EDB, the eTDB, and the eVDB were not available during the design of the first proposed algorithm. The application of the five databases is therefore slightly different for the two algorithms. This is summarized in Table 4.2. The first proposed algorithm was thus designed and optimized for automatic QRS complex detection based on the PeDB and the MITDB, whereas the second proposed algorithm was designed and optimized based on the MITDB and the eTDB. The PeDB was extracted from an existing database of recordings that were obtained with an early version of the ePatch sensor. This implies that the original sampling frequency of this database is 500 Hz and the channel configuration is slightly different from the configuration applied for the eTDB and the eVDB. The first proposed algorithm was therefore designed to function at a sampling frequency of 500 Hz. The recordings in the eTDB and the eVDB were extracted from three existing databases that were obtained using the currently newest CE-market ePatch sensor. As stated in Table 4.1 and Table 4.2, this implies that their sampling frequencies were 512 Hz. The second proposed algorithm was thus designed to function at a sampling frequency of 512 Hz. During the design and validation of each of the two algorithms, the relevant databases were therefore resampled to 500 Hz and 512 Hz, respectively. In compliance with [24], the resampling was performed using the "xform" function from the WFDB Toolbox [23]. As observed from Table 4.2, the multi-channel wavelet based algorithm was not embedded, and embedded evaluation was therefore not conducted for this algorithm.

Table 4.1: Comparison of the five different databases applied for design, optimization, and validation of the two proposed algorithms.

Database	Bit resolution	Fs (Hz)[a]	Records[b]	Length (min)[c]	Total beats[d]	VEB beats[e]	SVEB beats[f]
MITDB	11	360	48	30	91,285	6,101	2,745
EDB	12	250	90	120	759,878	4,375	1,075
PeDB	13	500	11	30	22,080	361	420
eTDB	12	512	120	10	45,248	*	*
eVDB	12	512	61	15	38,429	*	*
Total	-	-	330	14,685	956,920	10,837	4,240

[a] The original database sampling frequency.

[b] The total number of recordings in the database.

[c] The length of each record in the database. Note that the first five minutes are not used for evaluation.

[d] The total number of beats in the database during the evaluation period.

[e] The total number of VEB beats in the database during the evaluation period.

[f] The total number of SVEB beats in the database during the evaluation period.

* Not stated (all beats were labelled as normal during the manual annotation).

Table 4.2: Application of the five databases for the design, optimization, and validation phases of both proposed algorithms.

	Programming language	Multi-channel wavelet based	Single-channel BP filter based
Sampling frequency	-	500 Hz	512 Hz
Design and Optimization	MATLAB	MITDB PeDB	MITDB eTDB
Offline validation	MATLAB	EDB eTDB eVDB	EDB PeDB
Real-time embedded validation	ANSI C	-	eVDB

4.2.1 The Standard Databases

The MITDB [21] and the EDB [22] were both downloaded from Physionet [23], and they were converted to mat-files using the WFDB Toolbox for MATLAB [23]. All beats in both databases are manually labelled according to the beat type. This allows evaluation of the detection performance with respect to VEB and SVEB beats. This is especially important if the designed automatic QRS complex detection algorithm is intended to function as an initiator of an event detection or beat classification algorithm.

4.2.2 The Preliminary ePatch Database

The PeDB consists of ECG data extracted from recordings on 11 different admitted patients. This choice ensures a realistic amount of abnormal beat morphologies. One segment with 30 minutes of data was extracted from each recording. For all patients, the 30 minutes were extracted one hour after the beginning of the recording. The patients were allowed to move around in the monitoring unit during the recordings. This ensures a fair amount of realistic in-hospital artifacts. The manual reference annotation files were created in several steps: 1) Automatic pre-annotation using the automatic QRS complex detection algorithm "sqrs" available from [23], 2) automatic QRS position correction using a maximum algorithm in MATLAB, 3) manual correction by a biomedical engineer (using the "WAVE" program – available from [23]), and finally 4) manual correction by a cardiologist using "WAVE". During the first three steps of the annotation protocol, all beats were labelled as normal. During the final manual annotation conducted by the cardiologist, each beat was manually classified into different beat types: Normal, pause (RR > 2s), SVEB, VEB, or unclassifiable beat.

4.2.3   The ePatch Training Database

The eTDB was generated by extracting 10 minute ECG segments from two large existing ePatch databases. The first original database contains recordings from patients admitted to the stroke unit at Glostrup Hospital. The second original database contains ECG recordings from patients undergoing ambulatory diagnosis for obstructive sleep apnea at Glostrup Hospital. Each ECG recording in the two databases was associated with an ECG analysis report (similar to a traditional Holter analysis report). It was important to include ECG recordings from many different patients. We therefore selected 30 patients from the stroke unit database and 30 patients from the ambulatory database. It was furthermore important to ensure representation of many different abnormal beat morphologies as well as normal sinus rhythm with different ventricular frequencies. To ensure this, we selected the 60 patients based on the summaries in the associated ECG analysis reports. From the selected patients, we extracted a total of 120 ECG segments of which 40% were selected randomly and the remaining 60% were selected based on markings of interesting data segments in the analysis reports. This segment extraction ensures a database with realistic amounts of artifacts as well as representation of many different types of abnormal beat morphologies. Some examples of included arrhythmia events are: Atrial fibrillation (AF), episodes of supraventricular tachycardia (SVT) with different frequencies, SVEBs, runs of SVEBs, VEBs, ventricular bigeminy (B), ventricular trigemini (T), bradycardia, and AV blocks. The reference annotations for both the eTDB and the eVDB were created based on manual corrections of the output from the "sqrs" function from the WFDB Toolbox [23]. The manual corrections were conducted by a biomedical engineer with experience in ECG interpretation. All beats were labelled as normal. To validate the annotation performance of the biomedical engineer, 12 randomly selected records from the eTDB (10%) were also annotated by a medical doctor. The medical doctor did not find any errors in the manual annotations conducted by the biomedical engineer. The manual corrections were conducted using the WAVE program from the WFDB Toolbox [23].

4.2.4   The ePatch Validation Database

The eVDB was generated from three ECG recordings obtained from three different healthy volunteers. The volunteers continued normal daily life activities throughout the recordings. The embedded algorithm output was calculated in real-time during the recordings, and saved in a special channel in the data file. The algorithm output was not investigated before the manual annotation of the eVDB. For each subject, a 15 minute segment was automatically extracted from minute 30 to 45 in each hour of the recording. The mean recording time was 21.0 hours, yielding a total of 20-21 segments for each subject. This ensures representation of realistic amounts of normal daily life activities and provides an overview of a potential change in performance during the recording period.

4.2.5   Performance Evaluation

For both proposed algorithms, the beat detection accuracy was evaluated using the QRS sensitivity (*Se*), and positive predictivity (*P+*) defined by 4.1 and 4.2, where TP is the number of true positive detections, FP is the number of false positive detections, and FN is the number of false negative detections.

$$Se = \frac{TP}{TP+FN} \qquad\qquad\qquad\qquad (4.1)$$

$$P^+ = \frac{TP}{TP+FP} \qquad\qquad\qquad\qquad (4.2)$$

In compliance with [24], TP, FP, and FN for each record, were calculated using the default settings of the "bxb" function from the WFDB toolbox (five minute training period and episodes of ventricular flutter or fibrillation (VF) were excluded) [23] [24]. The average performances for each database are stated as gross statistics [24], meaning that Se and P+ are calculated based on the overall TP, FP, and FN from all records from each database. Unless otherwise mentioned, no records were excluded from the database average performances. Furthermore, when possible, the sensitivities with respect to detection of VEB and SVEB beats were also calculated.

4.3   Multi-Channel Wavelet Based Approach

This section contains a detailed description of the methodology and the obtained results for the multi-channel wavelet based algorithm. The algorithm is also described and discussed in Paper IV. As mentioned, the motivation for including an additional channel arises from the assumption that the signal quality of one channel might occasionally or permanently decrease during a long-term ambulatory recording. The contaminating noise is maybe only present in one of the channels. Therefore, the inclusion of information from an additional clean channel is expected to improve the detection performance. The information from the two channels can be combined in a high number of different ways. In [33], information from three different ECG channels is constantly simultaneously applied. This approach may have some limitations: Episodes of extreme amounts of noise in one channel might deteriorate otherwise good performance obtained from analysis of the other channels. A different approach was introduced by [38]. In [38], the QRS detection is generally based on channel I of the MITDB, and then a combination of the two channels is applied only if the current RR interval exceeds a predefined interval. However, this approach probably benefits from the fact that channel I of the MITDB generally obtains higher signal quality than channel II. It might therefore be difficult to transfer their results to real life recordings where the channel with the highest quality might not be known beforehand. To overcome these issues, we decided to propose an algorithm that can function in two different modes: Single-channel mode and multi-channel mode. The multi-channel mode applies information from both available channels simultaneously. The single-channel mode is derived from the multi-channel mode, but with the exclusion of information from a noisy channel. The algorithm can automatically switch between the two modes when predefined artifacts are present in one or both channels. If the predefined artifacts are present in both channels, a complete shutdown occurs. The idea of generally applying both channels and then exclude a potentially noisy channel was also investigated by the authors of [37].

4.3.1   Algorithm Description

An overview of the proposed multi-channel wavelet based algorithm is provided in Figure 4.5. The channel exclusion block marks the point of separation between the single-channel and the multi-channel mode. This implies that the exclusion of one or even both channels does not significantly reduce the computational load. The BP filtering, wavelet decomposition, and feature extraction is performed even when a channel is excluded. This is necessary to avoid errors from for instance filter delays when the channel is considered useful again. However, the adaptive maximum removal procedure and calculation of the adaptive thresholds is not updated when a channel is excluded. This prevents adaptive fitting to extremely noisy events. The channel exclusion, high maximum removal, adaptive threshold calculation, and decision fusion blocks were executed in one second non-overlapping analysis windows [29]. Each of the algorithm building blocks are described in details in the following sections.

4.3.1.1   Channel Exclusion Criteria

The purpose of the channel exclusion block is to automatically capture episodes of extremely noisy data and exclude these episodes from disturbing the analysis. Several different types of noise can be accounted for in such an exclusion paradigm. The different types of noise might require different measures/features for automatic detection. For this algorithm, we only accounted for saturation of the raw ECG signals. Saturation is not intended and it can produce false detections and disturb the adaptive algorithm parameters. The ECG channel was therefore excluded if the raw ADC count of 15 consecutive samples in the current analysis window obtained the maximum or minimum possible analog-to-digital count (ADC) value. The threshold of 15 samples was found by visual and experimental analysis of challenging ECG examples. It is thus selected as a compromise between correctly distinguishing problematic cases of saturation and cases where the "saturation" is only caused by very pronounced R peaks that sometimes reached the maximum possible ADC value in the PeDB recorded with the first version of the ePatch sensor. The minimum and maximum possible ADC values depend on the recording equipment and they were therefore set individually for each database. Furthermore, it was expected that the feature signals might be disturbed immediately after an episode of pronounced saturation. The channel was therefore also

considered in shutdown in the first "clean" analysis window after a case of problematic saturation. An example of the effect of the designed shutdown paradigm is provided and discussed in Figure 4.19 on page 56.
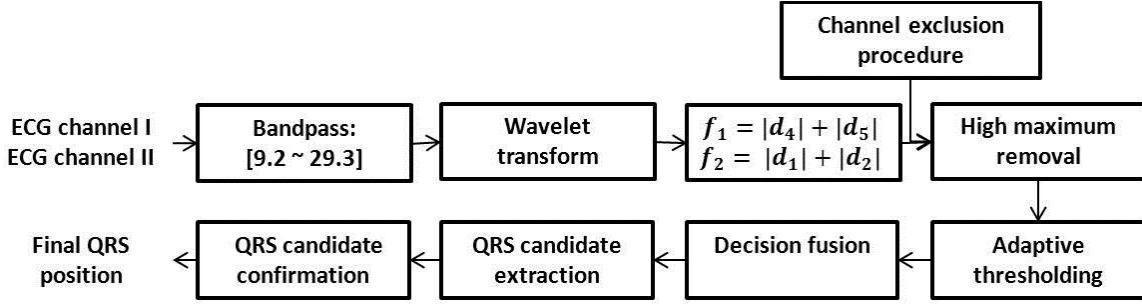

Figure 4.5: Schematic overview of the proposed automatic multi-channel wavelet based QRS complex detection algorithm. The algorithm input is two raw ECG channels and the output is a vector with indication of the detected QRS positions

4.3.1.2 Bandpass Filtering

The purpose of the BP filtering step is to increase the influence of the QRS complexes and decrease the influence of different types of artifacts as well as pronounced P- and T-waves. As illustrated later, the wavelet decomposition is in itself a type of BP filter. In many algorithms from the literature, the wavelet decomposition is therefore applied directly without a preceding BP filter. However, some of the best results are obtained by the authors of [33] who applied a FIR BP filter with passband from 0.40-40 Hz before the wavelet decomposition. We therefore decided to include this step. Keeping the desired embedded implementation in mind, we decided to apply a simple FIR filter with impulse response h_{BP} defined by (4.3) [35]. The amplitude characteristic of the BP filter is provided in Figure 4.6. After correction for the filter delay, the BP filtered signal will ideally obtain a zero-crossing at the R peak position in the raw ECG signal.

$$h_{BP}[k] = \left\{ \begin{array}{l} \delta[k+10] + \delta[k+9] + \delta[k+8] + \delta[k+7] + \delta[k+6] \ldots \\ +\delta[k+5] + \delta[k+4] + \delta[k+3] + \delta[k+2] + \delta[k+1] \ldots \\ -\delta[k] - \delta[k-1] - \delta[k-2] - \delta[k-3] - \delta[k-4] \ldots \\ -\delta[k-5] - \delta[k-6] - \delta[k-7] - \delta[k-8] - \delta[k-9] \end{array} \right\} \qquad (4.3)$$
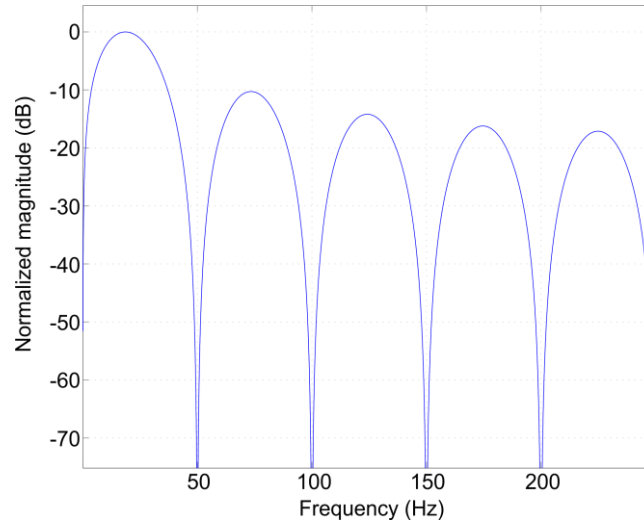

Figure 4.6: Illustration of the amplitude characteristic of the applied BP filter using a sampling frequency of 500 Hz.

4.3.1.3   Wavelet Transform

The purpose of the wavelet decomposition is to divide the ECG signal into different frequency sub-bands and hereby further enhance the influence of the QRS complexes. Some of the known advantages of the wavelet transform are a good balance between detection performance and computational load [29], and the possibility of dividing the ECG signals into defined frequency sub-bands that might also help detection and delineation of P- and T-waves [27]. The non-downsampling *a trous algorithm* is the most popular for wavelet decomposition of ECG signals in the literature [29] [33]. This decomposition consists of a cascade of simple FIR lowpass (LP) and highpass (HP) filters as illustrated in Figure 4.7.
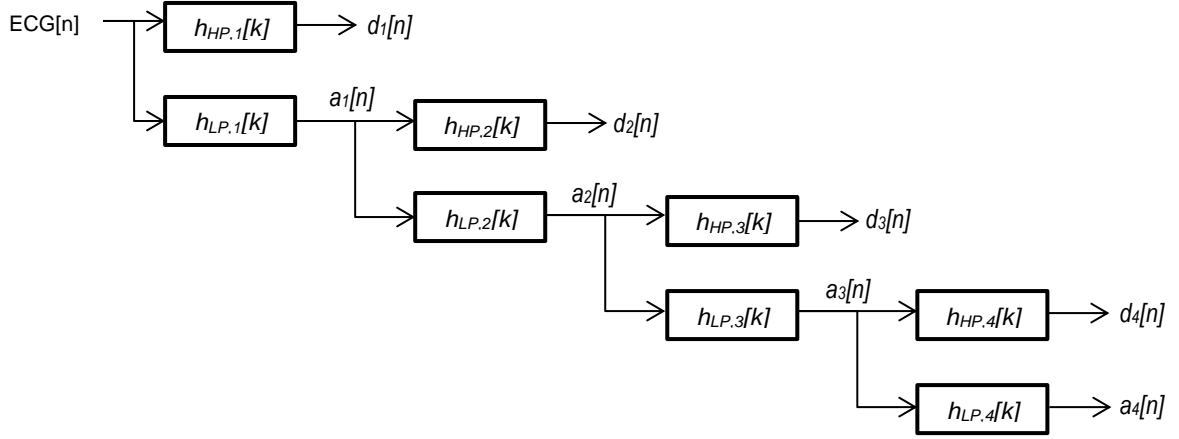

Figure 4.7: Schematic overview of the wavelet transform. The output from each LP filter step is termed approximation coefficients (a_q) and the output from each HP filter step is termed the detail coefficients (d_q). Note that there is no down sampling using the *a trous* wavelet decomposition scheme. The decomposition can be continued until any desired level.

The output of the wavelet decomposition at level $q > 1$ was implemented by (4.4) and (4.5), where a_q is the LP filter output (approximation coefficients) and d_q is the HP filter output (detail coefficients) [29]. For level $q = 1$, the input to the filtering scheme is the BP filtered ECG signal. The impulse responses, $h_{LP,1}$ and $h_{HP,1}$, were implemented by (4.6) and (4.7), respectively [29]. For scale $q > 1$, $h_{LP,q}$ and $h_{HP,q}$ were obtained by inserting ($2^{q-1} - 1$) zeros between each of the coefficients of $h_{LP,1}$ and $h_{HP,1}$ [29].

$$a_q[n] = \sum_k h_{LP,q}[k] \cdot a_{q-1}[n-k] \tag{4.4}$$

$$d_q[n] = \sum_k h_{HP,q}[k] \cdot a_{q-1}[n-k] \tag{4.5}$$

$$h_{LP,1}[k] = \frac{1}{8} \cdot \{\delta[k+2] + 3 \cdot \delta[k+1] + 3 \cdot \delta[k] + \delta[k-1]\} \tag{4.6}$$

$$h_{HP,1}[k] = 2 \cdot \{\delta[k+1] - \delta[k]\} \tag{4.7}$$

An illustration of the filter characteristics for each wavelet detail-band is provided in Figure 4.8. It is observed that the bandwidth of each individual detail-band is relatively wide. It is generally accepted in the literature that the frequency content of the QRS complex is around 5-22 Hz [26], [28], [33], [34]. With a sampling frequency of 500 Hz, this corresponds approximately to the wavelet detail-bands d_4 and d_5. However, due to the wideness of each detail-band, it is difficult to avoid the influence of the lower frequency P- and T-waves as well as some amounts of high frequency noise using d_4 and d_5 directly. Figure 4.9 contains an illustration of the BP filtering and the wavelet decomposition on a brief ECG snippet from record 106 from the MITDB.
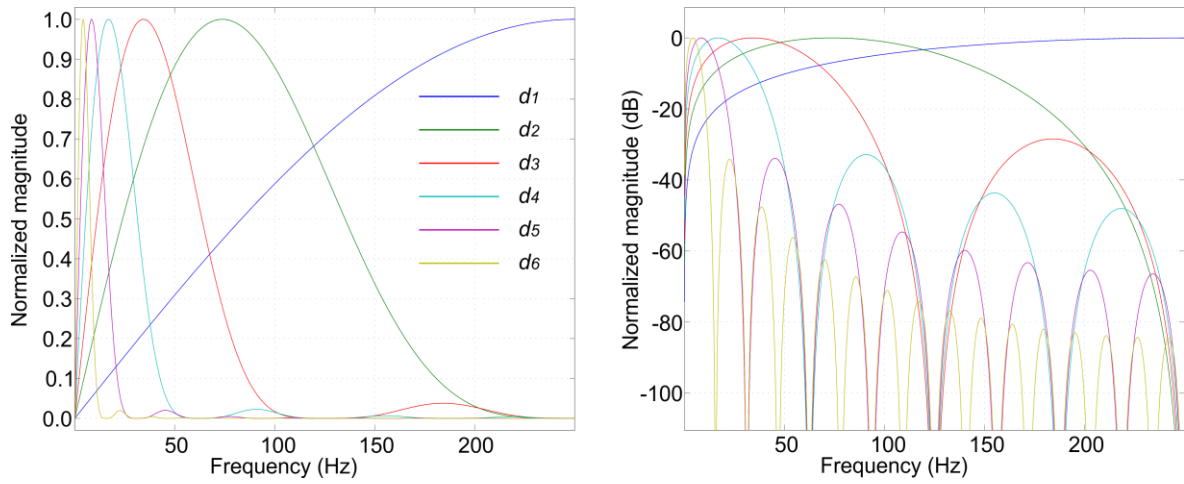
Figure 4.8: Amplitude characteristic of each individual wavelet detail-band using a sampling frequency of 500 Hz.
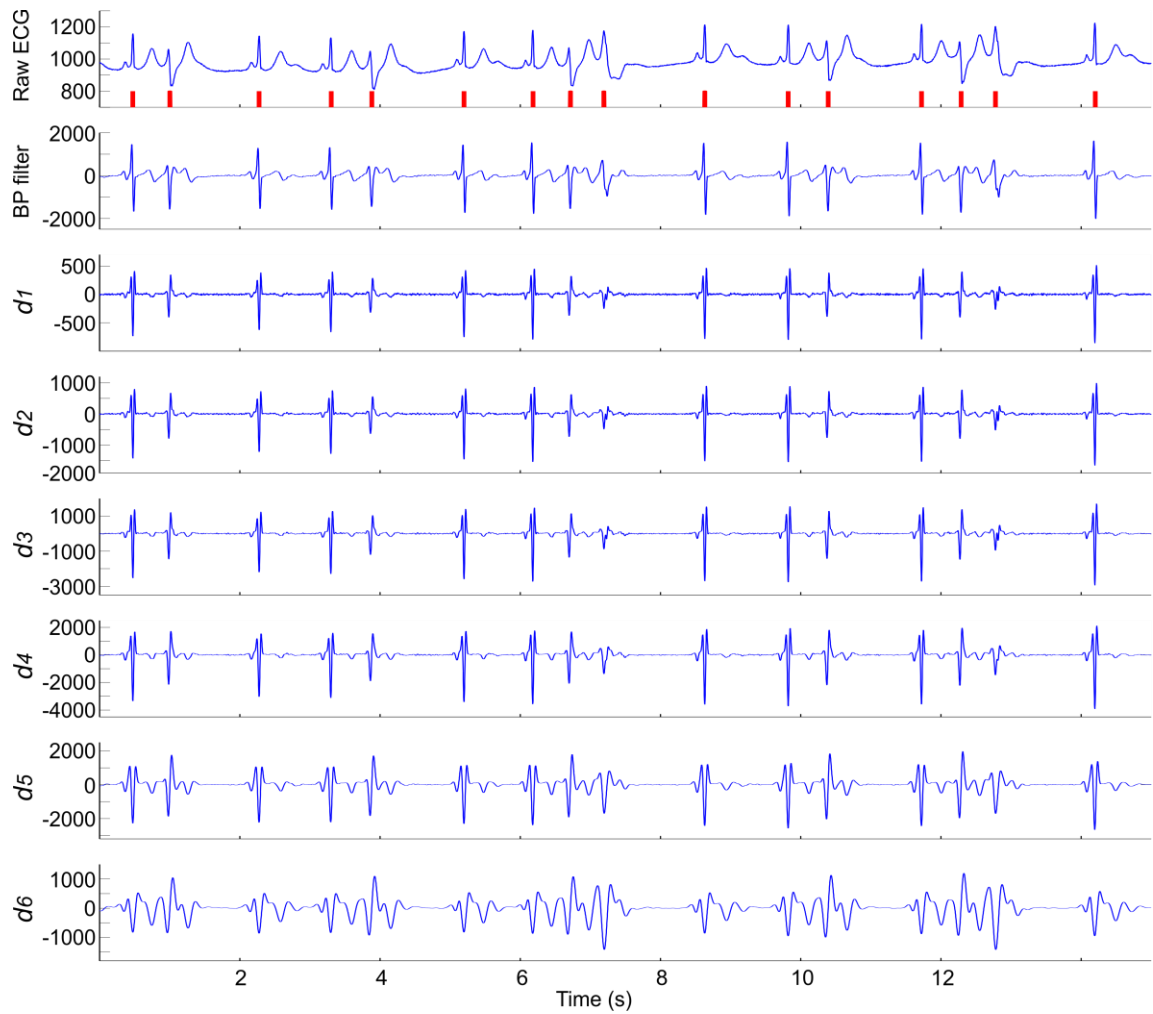
Figure 4.9: Illustration of the BP filtering and wavelet decomposition of record 106 from the MITDB. The top plot contains the raw channel I ECG (blue line) and the QRS positions obtained from the reference annotation (red lines), the second plot contains the BP filtered ECG signal, and the third to eighth plot contain the wavelet detail-bands from $d_1 - d_6$. It is observed that the QRS complexes are visible in all detail-bands. As expected, it is observed that the influence of the VEB beats is highest in the detail-bands containing the lower frequencies. It is furthermore observed that the influence of the P- and T-waves also is increased in these sub-bands. However, this issue is more pronounced in recordings with higher P- and/or T-waves.

4.3.1.4 Feature Extraction

As mentioned, the energy of the QRS complexes is expected to be most pronounced in d_4 and d_5. The first feature, $F_{1,j}$, was therefore calculated according to (4.8). The feature signal was calculated for each channel j individually. The absolute value is applied to ensure equal detection of QRS complexes with positive and negative polarity. This was one of the algorithm requirements formulated in section 4.1.3. In some cases it was observed that pronounced P- and/or T-waves could disturb these detail bands even after the BP filtering step. It was furthermore observed that the QRS complex was also clearly present in the higher frequency detail-bands (see Figure 4.9). Therefore, and additional feature signal, $F_{2,j}$, representing the higher frequencies were calculated according to (4.9). Again, the feature signal was calculated for each channel individually.

$$F_{1,j} = \left| d_{4,j} \right| + \left| d_{5,j} \right| \tag{4.8}$$

$$F_{2,j} = \left| d_{1,j} \right| + \left| d_{2,j} \right| \tag{4.9}$$

It is thus expected that F_{1j} obtains high values during QRS complexes as well as during episodes of pronounced P- and/or T-waves, whereas F_{2j} is expected to obtain high values during QRS complexes and high frequency noise. Periods where all four feature signals obtain high values are thus expected to correspond to the location of the QRS complexes. Figure 4.10 contains an illustration of the feature extraction for the data segment illustrated in Figure 4.9. The adaptive thresholds (red lines) and the extracted QRS candidates (F_{final}) are also illustrated together with the final locations of the detected QRS positions. The latter algorithm steps are described in the next sections.

4.3.1.5 Adaptive Thresholding

We decided to apply an adaptive threshold to each of the four feature signals individually. These four thresholds were applied to calculate four binary feature signals defined by (4.10), where $z \in [1,2]$ indicates the two feature signals obtained from each channel $j \in [1,2]$ and $T_{z,j}$ is the corresponding adaptive threshold.

$$F_{bin,z,j}[n] = \begin{cases} 1, & F_{z,j}[n] > T_{z,j}[n] \\ 0, & F_{z,j}[n] \leq T_{z,j}[n] \end{cases} \tag{4.10}$$

The purpose of adaptive thresholding is to ensure smooth adaptation of the thresholds to changes in the feature signals. It was decided to update the four adaptive thresholds in non-overlapping one second analysis windows [29]. The thresholds were calculated according to (4.11), where $0 < \lambda < 1$ is a forgetting factor, c is a scaling parameter, $T_{m,z,j}$ is the final threshold value in the current window, m, $T_{m-1,z,j}$ is the threshold value in the previous window, and $\mu_{m,z,j}$ and $\sigma_{m,z,j}$ are the mean and standard deviation of feature number $z \in [1,2]$ from channel $j \in [1,2]$ in the current analysis window. Based on simulations on the PeDB, the parameters were chosen to $\lambda = 0.4$ and $c = 0.8$. The adaptive thresholds $T_{1,1}$ and $T_{2,1}$ for the segment illustrated in Figure 4.10 are indicated by red lines together with the respective feature signals. It should be mentioned that this threshold calculation implies a delay in the QRS detection of one second in addition to the filter delays.

$$T_{m,z,j} = \lambda \cdot T_{m-1,z,j} + (1 - \lambda) \cdot (\mu_{m,z,j} + c \cdot \sigma_{m,z,j}) \tag{4.11}$$

In cases with abnormal beat morphologies or high amount of artifacts with high amplitudes, the adaptive threshold might be increased to a level that can prevent detection of subsequent normal QRS complexes. To avoid this, a high maximum removal was applied before the adaptive threshold calculation. This block contains information about the maximum feature value in the eight previous one second analysis windows. Any sample in the current analysis window exceeding the median value of this maximum register was set to the median value before the threshold calculation. The adaptive threshold and the maximum register were not updated for channel j when it was excluded from the analysis. This precaution was included to ensure that the adaptive parameters where not updated during very noisy episodes.
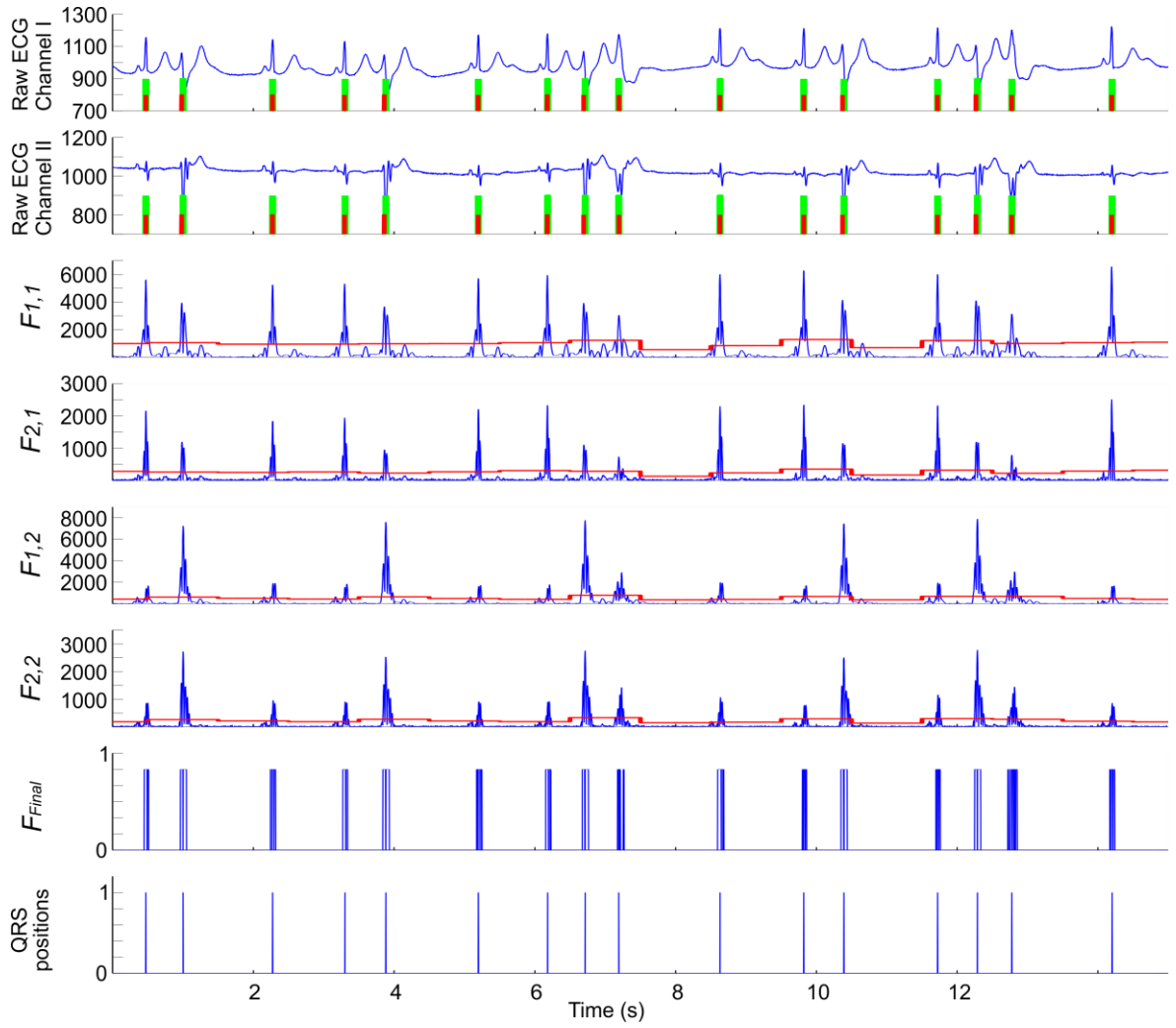
Figure 4.10: Illustration of the feature extraction, the creation of the final feature, F_{final}, that contains the QRS candidates, and the detected QRS positions. This segment illustrates the processing of record 106 from the MITDB (the same segment as illustrated in Figure 4.9). The vertical green lines illustrate the positions where the algorithm has detected QRS complexes. The red vertical lines illustrate the QRS positions obtained from the reference annotation. It is observed that all beats are correctly detected. It is furthermore observed that the appearance and quality of the two channels is quite different.

4.3.1.6   Extraction of QRS Candidates

The purpose of this algorithm block is to extract QRS candidates that can be provided to the QRS confirmation block for the final QRS detection step. This block is based on a decision fusion scheme that combines information from all four binary feature signals defined in (4.10). The information is combined according to the following scheme:

1. If both channels were selected for analysis during the channel exclusion procedure, at least three of the four binary features should be asserted to indicate a QRS candidate.
2. If one channel was excluded from the analysis, both binary feature signals from the other channel should be asserted.
3. If both channels were excluded from the analysis, a complete shutdown occurs and no QRS complexes could be detected in the current window.

The new binary feature signal is denoted F_{final}. The QRS candidates are then indicated when F_{final} is asserted. This final feature signal is illustrated in Figure 4.10. To the best knowledge of the authors, this combination of wavelet based features from two different ECG channels is novel.

4.3.1.7 QRS Localization and Confirmation Block

The purpose of this block is two-fold: The first functionality is to investigate whether a QRS candidate is in fact a QRS complex and the second functionality is to provide a reliable estimate of the actual R peak position of the confirmed QRS candidates. As observed from Figure 4.10, F_{final} is asserted for a period of time around the location of each QRS complex. The temporary duration of the QRS complex was defined from the rising edge of F_{final} and 100ms forward. The BP filtered signal was investigated for zero-crossings during this time interval. The QRS candidate was temporarily confirmed if at least one active channel possessed at least one zero-crossing during this period. Theoretically, this zero-crossing corresponds to a peak in the raw ECG signal. The first zero-crossing in this interval might correspond to the location of a pronounced Q peak. It was therefore decided to apply the location of the second zero-crossing if more than one zero-crossing occurred in the BP filtered signal during this time interval. The position of the selected zero-crossing was extracted for each active channel. In the multi-channel mode, the final QRS position was estimated as the minimum sample number suggested by the two active channels. This location was saved as the new position of the QRS candidate. To further decrease the number of false detections, an additional QRS confirmation step was implemented. The block was initiated if the current RR interval was less than half the median of the eight previous RR intervals. If the RR interval was larger than this, the QRS candidate was immediately confirmed as a new QRS complex. The assumption in this block was that the feature values of two closely located QRS complexes should not vary significantly. This was measured with the maximum amplitude value in all active feature signals. For each of the active feature signals, the maximum value was calculated in a 100ms window around the position of the previously detected QRS complex (F_{old}) and the current QRS candidate (F_{new}). The decision rule depends on the algorithm mode, see Table 4.3, where *case 1 – 3* refers to the following possible outcomes:

- Case 1: Accept both the previously detected QRS complex and the current QRS candidate
- Case 2: Delete the previously detected QRS complex and accept the current QRS candidate
- Case 3: Accept the previously detected QRS complex and reject the current QRS candidate

Table 4.3: Decision rule in the final QRS confirmation block.

Case	Multi-channel Mode	Single-channel Mode
1	At least three of four maximum values should satisfy the requirement: $$\frac{F_{old}}{2} < F_{new} < 2 \cdot F_{old}$$	Both maximum values should satisfy the requirement: $$\frac{F_{old}}{2} < F_{new} < 2 \cdot F_{old}$$
2	At least three of four maximum values should satisfy the requirement: $$F_{new} \geq 2 \cdot F_{old}$$	Both maximum values should satisfy the requirement: $$F_{new} \geq 2 \cdot F_{old}$$
3	Otherwise	Otherwise

This novel QRS confirmation block was designed based on experiments and visual inspection of different challenging ECG snippets. After the confirmation of the QRS candidate, a refractory period of 200ms was implemented in line with [26]. The functionality of the confirmation block is illustrated in Figure 4.11. The ECG segment is extracted from record 233 from the MITDB. The vertical black lines indicate samples where F_{final} is asserted, the vertical green lines indicate detected QRS positions, and the vertical red lines indicate the QRS positions in the reference annotations. It is observed that F_{final} has two false QRS candidates. It is furthermore observed how the algorithm correctly deletes these candidates and obtains perfect QRS detection throughout this ECG segment. In both cases, the confirmation block is initiated since the distance to the previously detected QRS complex is less than half the median of the eight previously detected RR intervals. The first false QRS candidate is never detected because the amplitude of the feature signals are too small compared to the amplitude of the feature signals for the previously detected QRS complex. Therefore, this QRS candidate falls in case 3 described above, and it is thus immediately deleted. The second false QRS candidate is initially detected as a QRS complex. But then a new QRS candidate (the true QRS complex) is detected within the predefined interval. The amplitude of the feature signals for the two QRS complexes are therefore compared, and this situation falls in case 2. The amplitude of the feature signals for

the new QRS candidate is significantly higher than the falsely detected QRS complex. Therefore the false QRS complex is deleted and the true QRS complex is accepted. This confirmation methodology implies that any QRS candidate that will be detected before the expected RR interval (estimated as the median of the eight previously detected RR intervals) will be compared to either the previous or the next QRS complex. It should be mentioned that this confirmation block implies that already detected QRS detections can be deleted from the final QRS detection. This methodology will, of course, impose an additional delay before the detection of each QRS complex can be confirmed. To our best knowledge, this design of the QRS confirmation block is novel.
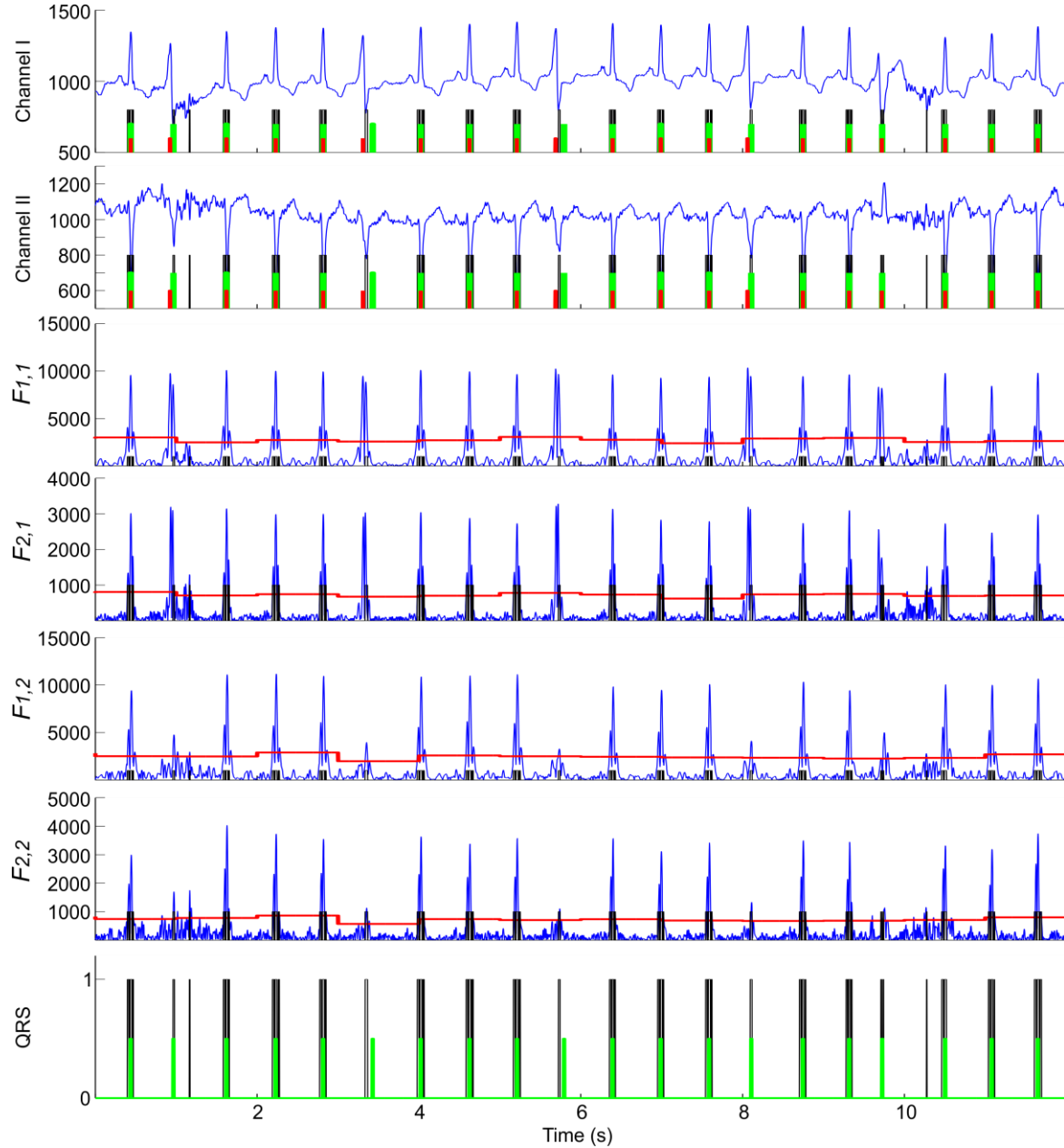
Figure 4.11: Illustration of the functionality of the confirmation block. The ECG segment is extracted from record 233 from the MITDB. The vertical black lines indicate samples where F_{final} is asserted, the vertical green lines indicate detected QRS positions, and the vertical red lines indicate the QRS positions in the reference annotations. It is observed that F_{final} has two false QRS candidates. It is furthermore observed how the algorithm correctly deletes these candidates and obtains perfect QRS detection in this ECG segment. The first candidate is deleted using case 3, whereas the second false QRS candidate is deleted based on case 2. Furthermore, a minor misalignment between the green and red lines is observed. However, these differences are within the match window of 150ms defined by [24] for all beats.

4.3.2 Results

The performance of the proposed multi-channel wavelet based algorithm on each record from the PeDB is provided in Table 4.4 and the average QRS detection performances of the multi-channel wavelet based algorithm on all five databases are provided in Table 4.5. Furthermore, the sensitivity with respect to detection of SVEB and VEB beats are stated for the MITDB, the EDB, and the PeDB. As mentioned, it is important to note that only the PeDB and the MITDB were accessible during the design and optimization phase of this algorithm. The performance of the algorithm is discussed and compared with results from the literature and the second proposed algorithm in section 4.5 on page 52. However, before this comparison, a detailed description of the second proposed algorithm is provided in the next section.

Table 4.4: Performance of the proposed multi-channel wavelet based algorithm on the PeDB.

Patient	Number of beats	Se (%)	P^+ (%)	Se VEB (%)	Se SVEB (%)
1	1,450	99.93	99.52	100.0	100.0
2	1,617	100.0	100.0	100.0	-
3	1,594	99.87	100.0	100.0	100.0
4	1,727	100.0	100.0	100.0	100.0
5	1,465	99.86	99.80	-	100.0
6	3,049	100.0	100.0	100.0	100.0
7	1,762	100.0	100.0	100.0	100.0
8	1,984	99.95	100.0	100.0	100.0
9	2,562	99.88	96.75	100.0	-
10	1,651	99.94	99.94	100.0	100.0
11	3,219	95.84	99.26	100.0	-
Total	22,080	99.35	99.46	100.0	100.0

Table 4.5: Overview of the proposed multi-channel wavelet based algorithm on the five different databases.

Database	Se (%)	P^+ (%)	Se VEB (%)	Se SVEB (%)
MITDB	99.65	99.63	98.71	98.80
EDB	99.75	99.79	92.27	99.63
eTDB	99.70	97.76	-	-
eVDB	99.80	98.20	-	-
PeDB	99.35	99.46	100	100
Total	99.73	99.61	96.15	99.13

4.4 Single-Channel Bandpass Filter Based Approach

During the design of the wavelet-based algorithm, it was noted that the width of each detail-band was relatively wide. From the literature, it was furthermore observed that different combinations of information from several wavelet sub-bands is usually required when applying the wavelet technique [27]–[33]. This was also necessary in our proposed wavelet based algorithm. This combination of information requires additional computations. Furthermore, the application of the wavelet transform often requires additional algorithm blocks after the wavelet decomposition to obtain satisfactory enhancement of the QRS complexes or to confirm a QRS candidate. This includes for instance calculation of maximum-minimum-difference [27], multiplication of detail coefficients from selected scales [28] [29], denoising of wavelet output [29], detection of

modulus-maxima exceeding pre-defined thresholds in several detail bands [30], [31], calculation of area-curve length [32][33], normalization using standard deviation [33], non-linear exponential amplification of the feature signal [33], or the QRS confirmation block designed for the first proposed algorithm described in the previous section. These additional algorithm steps decrease the computational efficiency. For the second proposed algorithm we therefore aimed at creating a novel filtering scheme that was able to directly output a single feature signal that would be smooth enough for immediate QRS complex detection without further enhancement, combination of different features, or additional blocks to confirm the presence of the QRS complexes. Furthermore, we aimed at avoiding any non-linear processing, e.g. squaring. This was avoided both in order to decrease the computational load and in order to avoid the risk of decreasing the influence of abnormal beat morphologies. We achieved this by designing a novel cascade of simple FIR filters that obtain both efficient enhancement of the QRS complexes and strong artifact attenuation. The cascading of filters was inspired by the wavelet decomposition, but we designed a filter cascade that accurately and directly extract the frequency content of interest in a single feature signal. As mentioned earlier and further discussed in section 4.5, we also decided to upgrade the adaptive threshold approach with a search back mechanism. The proposed single-channel algorithm is described in details in this section. The work described here is also presented in Paper V.

4.4.1   Algorithm Description

An overview of the second proposed algorithm is provided in Figure 4.12. The dashed green square illustrates the feature extraction block and the dashed blue square illustrates the detection block.
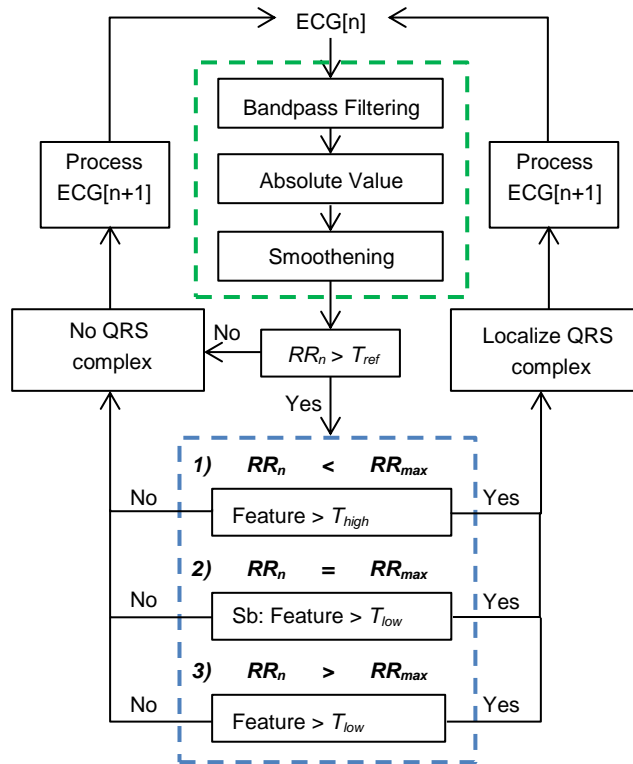

Figure 4.12: Schematic overview of the second proposed QRS complex detection algorithm. The algorithm processes the ECG signal sample by sample. The input to the algorithm is one channel raw ECG. The feature extraction is indicated by the dashed green square. It consists of BP filtering, removal of signs, and smoothening. RR_n indicates the current RR interval, if a QRS complex is detected at the current sample, n. If the refractory period (T_{ref}) is exceeded, the algorithm is allowed to continue to the detection block that is indicated by the dashed blue square. This block can operate in three different modes dependent on the distance to the previously detected QRS complex (RR_n). This implies that only one of the three modes is applied for each sample. The second mode includes the search back (Sb) procedure. The expected maximum distance between two subsequent QRS complexes is termed RR_{max}. If the relevant threshold is exceeded, a QRS complex is detected, and the localization block is initiated.

As observed from the dashed blue square, the QRS detection block can function in three different modes. The first mode applies the high threshold, T_{high}, and is active when the distance from the previously detected QRS complex is within the expected maximum RR interval (RR_{max}). If RR_{max} is exceeded, a search back is performed using the low threshold value, T_{low}. This search back procedure is the second mode. If no QRS complex is detected during the search back, T_{low} is applied until a new QRS complex is detected. This is the third mode. When a QRS complex is detected, a delineation procedure is applied to locate the QRS complex at the correct position, and the detection block switches back to the first mode. The algorithm is designed to analyze the ECGs in a sample by sample manner. This enables real-time embedded detection with only minor insignificant delays in the detection of each QRS complex. The following sections contain a detailed description of each part of the algorithm.

4.4.1.1 Bandpass Filtering

As mentioned earlier, the purpose of the BP filtering step is two-fold: 1) Increase the influence of the QRS complexes, and 2) attenuate the influence of different types of artifacts, as well as pronounced P- and T-waves. However, it is also important to keep in mind that BP filtering might unintentional decrease the influence of abnormal beat morphologies, especially VEBs. The performance of the BP filtering step is thus a major determinant of the necessary complexity of the remaining parts of the algorithm. As mentioned, it is generally accepted that the frequency components of the QRS complex primarily is between 5 to 22 Hz [26], [28], [33], [34]. We therefore designed a novel cascade of simple FIR filters that obtain a favorable passband in this frequency region. The cascade of filters consists of two BP filters followed by one LP filter. The impulse responses for the two successive BP filters are defined by (4.12) and (4.13), respectively.

$$h_{BP1}[k] = \begin{Bmatrix} -\delta[k+10] - \delta[k+9] + \delta[k+2] + \delta[k+1] \, ... \\ +\delta[k] + \delta[k-1] - \delta[k-8] - \delta[k-9] \end{Bmatrix} \qquad (4.12)$$

$$h_{BP2}[k] = \begin{Bmatrix} -\delta[k+14] - \delta[k+13] + \delta[k+2] + \delta[k+1] \, ... \\ +\delta[k] + \delta[k-1] - \delta[k-12] - \delta[k-13] \end{Bmatrix} \qquad (4.13)$$

The LP filter, with impulse response defined by h_{LP}, is an average filter with 16 points. This cascade of filters corresponds to an equivalent BP filter with impulse response, h, defined by (4.14), where $*$ is the convolution operation. The amplitude characteristics of the three individual filters, and the equivalent BP filter is provided in Figure 4.13.

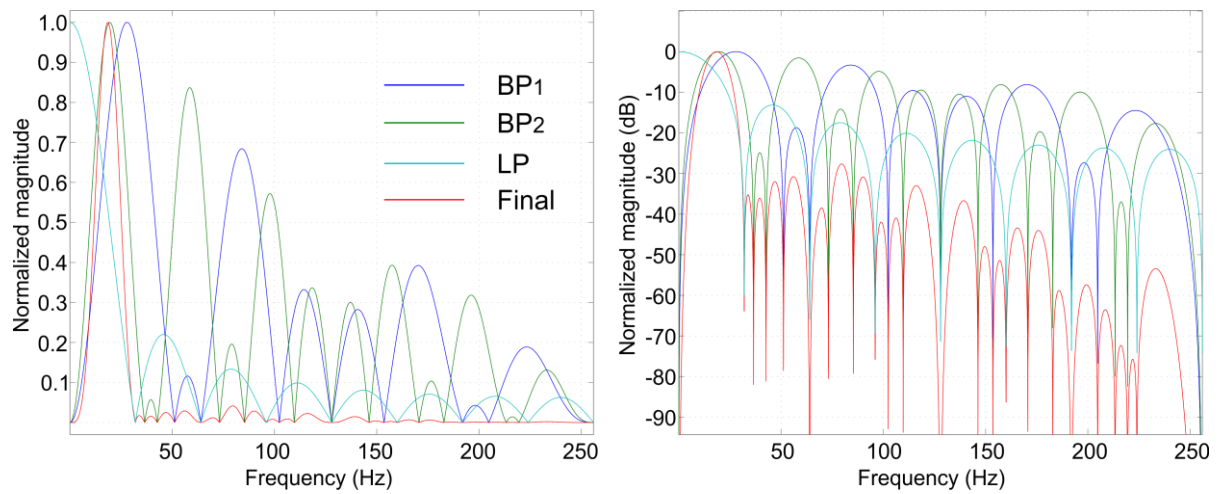$$h[k] = h_{BP1}[k] * h_{BP2}[k] * h_{LP}[k] \qquad (4.14)$$

Figure 4.13: The amplitude characteristics of the three individual filters (dark blue line represents BP$_1$, green line represents PB$_2$, and light blue line represents LP), and the resulting equivalent BP filter (red line) using a sampling frequency of 512 Hz.

4.4.1.2   Final Feature Extraction

The final feature signal is obtained by smoothening the absolute value of the output from the novel filtering scheme using an 8 point FIR average filter. As for the proposed multi-channel wavelet based algorithm, the absolute value is applied to ensure equal detection of QRS complexes with positive and negative polarity. An illustration of the feature extraction is provided in Figure 4.14. It is observed how muscle artifacts, electrode motion artifacts, and P- and T-waves are attenuated. The total delay of all four cascaded filters is 34 samples. Using a sampling frequency of 512 Hz, this corresponds to 66.4ms, which we considered to be within the acceptable limit for clinical applications.
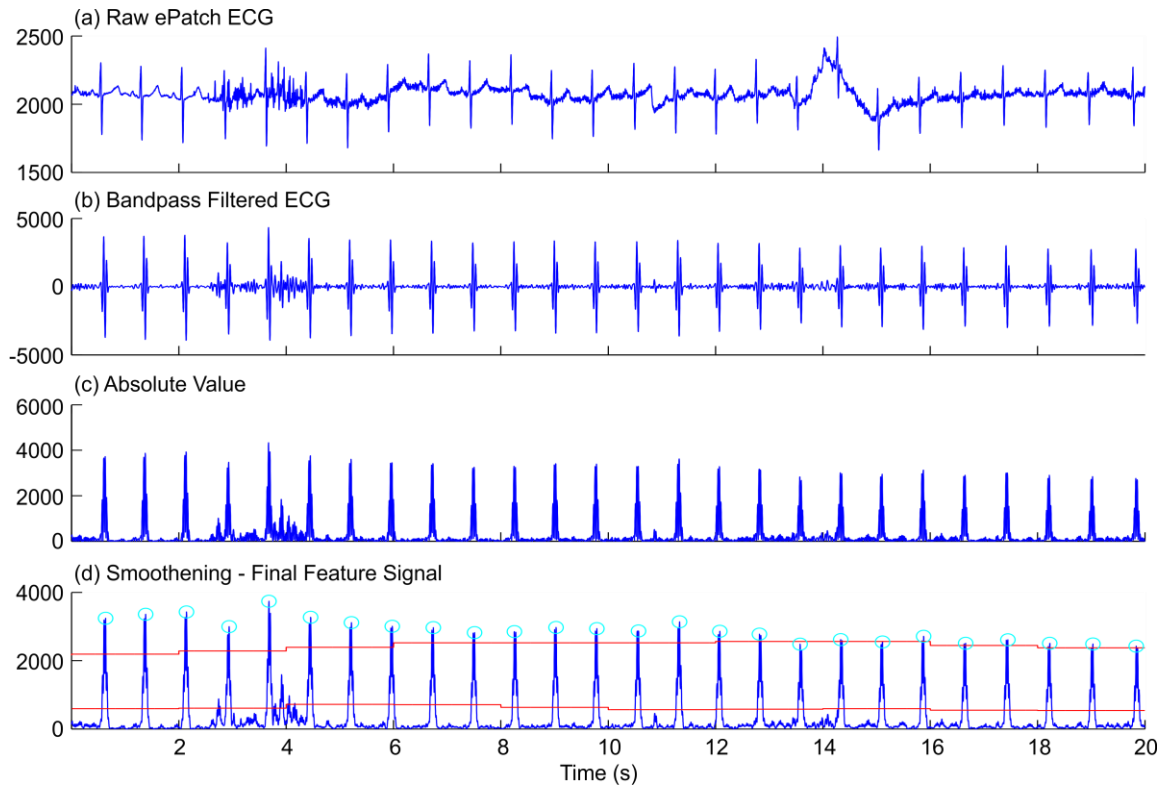

Figure 4.14: Illustration of each of the pre-processing steps: (a) Example of raw ECG signal recorded with the ePatch sensor. The amplitude is illustrated in analog-to-digital count (ADC) values for all plots. Note the presence of both muscle artifacts and electrode motion artifacts. (b) The ECG signal after BP filtering using the novel cascade of simple FIR filters. (c) Absolute value of the BP filtered ECG signal. (d) Smoothening of the feature signal. The red lines indicate T_{high} and T_{low}. The light blue circles indicate the detected positions of QRS complexes.

4.4.1.3   The QRS Detection Block

The purpose of the detection block is to localize the preliminary positions of the QRS complexes based on the feature signal and the adaptive thresholds. One of the important components in such an algorithm is timely initiation of the search back procedure. This initiation is decided by the maximum expected RR interval between two subsequent QRS complexes, RR_{max}. The assumption in this study was that RR_{max} should vary with the general variation of the RR intervals. The timely initiation of the search back procedure is especially important in the presence of many abnormal beats that might be missed by T_{high}. In many cases, it is therefore advantageous to initiate the search back procedure earlier in a recording with high variability in the RR intervals. The algorithm was therefore designed to function in two different variability modes described below.

To estimate the optimal variability mode and RR_{max}, three different set of previous RR intervals are saved:

1. RR_{long}: This contains the 34 previously detected RR intervals, disregarding the detection mode used for detection. The number of RR intervals is chosen to obtain enough RR intervals to provide a reliable estimate of the variability, but without losing the adaptive capability if the heart rhythm suddenly changes.

2. RR_{short}: This contains the 8 previously detected RR intervals, disregarding the detection mode. This can be derived directly from RR_{long}, but it contains a shorter history, and is thus faster adapted to changes in the heart rhythm.

3. $RR_{searchback}$: This contains the 8 previously detected RR intervals that were detected during search back. This implies that information about the general RR intervals during previous episodes of search back is saved, even though the search back procedure might not have been initiated during the previous 34 RR intervals.

The current variability parameter, θ, is then estimated as:

1. Calculate the median of RR_{long}.
2. Calculate the absolute deviation between each RR interval in RR_{long} and the median. The deviation vector is termed ε.
3. Remove the two largest values from ε.
4. θ is then defined as the mean value of the remaining 32 entries in ε.

The third step is included to prevent a single ectopic beat detection, a single missed detection, or a single false positive from pushing the algorithm into the high variability mode. This mode is only intended to be activated in recordings with many ectopic beats or generally high variation in the RR intervals. In these records, it is expected that the risk of missing a beat is increased, and to prevent this, the "sensitivity" of the search back procedure is increased. The high and low variability modes are defined based on θ being above or below a threshold, T_{θ}. The threshold was set by visual inspection of figures similar to Figure 4.15. In Figure 4.15, the RR intervals obtained from the reference annotations in the MITDB were used to calculate θ throughout the entire duration of each recording. The time course of θ was then compared to the types of heart rhythms that are intended to activate the high variability mode. By visual inspection of these figures, T_{θ} was set to 35 samples. It is observed from Figure 4.15 that record 212 with normal sinus rhythm is in the low variability mode during the entire recording. This is as intended. The general rhythm in recording 203 is AF. This recording is in the high variability mode during the entire recording. This is also as intended. The general rhythm in recording 223 is normal sinus rhythm. However, this recording has episodes of bigeminy (B), trigeminy (T), and ventricular tachycardia (VT). As expected, the algorithm jumps to the high variability mode during many of these episodes.
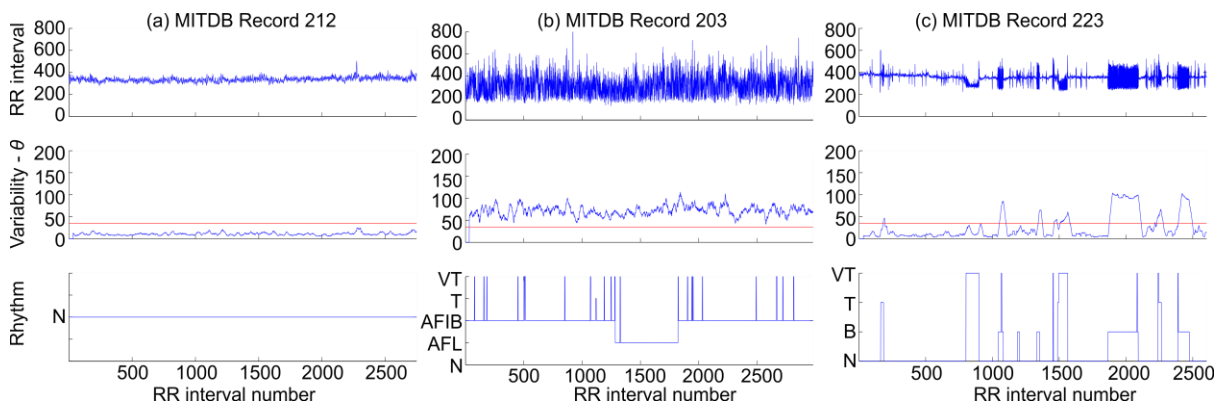
Figure 4.15: Example of visual inspection of θ on three different records from the MITDB: (a) Record 212 with normal sinus rhythm (N) during the entire recording, (b) Record 203 with atrial flutter (AFL), atrial fibrillation (AF), ventricular trigeminy (T) and ventricular tachycardia (VT), and (c) Record 223 with normal sinus rhythm (NSR), ventricular bigeminy (B), T and VT. The top plots illustrate the RR intervals from the reference annotations in samples. The middle plots illustrate θ (blue line) in samples, and the threshold T_{θ} = 35 (red line). The button plots indicate the heart rhythms obtained from the reference annotations

4.4.1.3.2   Estimation of the Maximum Expected RR Interval (RR_{max})

RR_{max} is calculated according to (4.15) and (4.16), where $\tilde{x}$ is the median value of the elements in x, $Min(x)$ is the minimum value of the elements in x, and RR_{scale} is a scaling parameter. The median value is applied to avoid high influence of a single false high or low RR interval. In the low variability mode, RR_{long} provides a good estimation of the expected RR interval. In the high variability mode, the minimum of the two more sensitive RR variables are used to increase the search back sensitivity. The adaptive parameters, RR_{max} and θ, are updated every two seconds together with the adaptive thresholds descried below.

$$RR_{temp} = \begin{cases} \widetilde{RR_{long}} & if \ \theta \leq T_{\theta} \\ Min(\widetilde{RR_{short}}, \widetilde{RR_{searchback}}) & if \ \theta > T_{\theta} \end{cases} \qquad (4.15)$$

$$RR_{max} = \ RR_{temp} \ \cdot \ RR_{scale} \qquad (4.16)$$

4.4.1.3.3   Adaptive Thresholding

The purpose of adaptive thresholding is to obtain thresholds that follow the changes in the signal. This is especially important for analysis of ePatch ECG signals. The goal is to obtain smooth adaptation to changes in both ECG signal amplitude and changes in the amount and types of artifacts. In this algorithm, we decided to update the threshold parameters in non-overlapping windows of two seconds. The high threshold, T_{high}, is based on the median value of the maximum feature value in the eight previous windows:

$$T_{high}[m] = \ (\widetilde{max_{F[m-8]}, \ ... \ max_{F[m-1]}}) \ \cdot \ \alpha \qquad (4.17)$$

In (4.17) m indicates the window number, $F[m]$ represents the final feature signal in window m, max_x is the maximum value of the elements in x, and α is a scaling factor slightly lower than 1. Using a window length of two seconds implies that we expect at least one QRS complex in each analysis window. It most cases, the maximum value in each analysis window is therefore expected to represent the amplitude of a QRS complex. T_{high} is thus designed to float right below the expected amplitude of the QRS complexes. This avoids adaptation to the level of the isoelectric line in cases of low HR. Furthermore, it is observed that this threshold calculation does not require any information from the current analysis window. Opposite to the proposed multi-channel wavelet based algorithm, this algorithm thus functions in a very close to real-time manner where the adaptive threshold is "ready" right from the beginning of each new analysis window.

The low threshold, T_{low}, is intended to adjust faster to rapid changes in the amount of artifacts. This threshold is therefore based on information about the mean value of the final feature signal in the two previous windows. It is known that an increase in heart rate induces an increase in the mean value of the feature signal. T_{low} is not intended to increase as a consequence of increased heart rate. Therefore, T_{low} is scaled according to the number of QRS detections obtained in the two successive windows applied for the threshold calculation. This modification is termed s_1. The s_1 parameter is furthermore bounded as follows:

- If no QRS complexes were detected, set s_1 = 1.
- If > 8 QRS complexes were detected, set s_1 = 8.

It is furthermore important to note that episodes of very noisy data might disturb the QRS detection and produce a number of false positive detections that might induce RR variability similar to e.g. episodes of AF, and hereby push the algorithm to activate the high variability mode. To prevent the increased sensitivity of the search back procedure from exacerbating the number of false positive detections in noisy data, a modification of T_{low} is therefore also needed in the high variability mode. This modification is defined as the s_2 parameter in (4.18). The values of s_2 were obtained by visual inspection of different

challenging ECG snippets from the training data (MITDB and eTDB). The temporary low threshold, $T_{low,temp}$, was thus calculated by (4.19), where μ_x is the mean value of the elements in x.

$$s_2 = \begin{cases} 10 & if \ \theta \le T_\theta \\ 12 & if \ \theta > T_\theta \end{cases} \tag{4.18}$$

$$T_{low,temp}[m] = \left(\widetilde{\mu_{F[m-2]}, \mu_{F[m-1]}} \right) \cdot \frac{s_2}{s_1} \tag{4.19}$$

Finally, T_{low} was furthermore bounded by a percentage, β, of T_{high}. This modification is defined in (4.20). This ensures a proper functionality of T_{low} to detect beats missed by T_{high}:

$$T_{low} = \begin{cases} T_{low,temp} & if \ T_{low,temp} \le T_{high} \cdot \beta \\ T_{high} \cdot \beta & if \ T_{low,temp} > T_{high} \cdot \beta \end{cases} \tag{4.20}$$

For the low threshold, it is again observed that the calculation only depends on data from previous analysis windows, and therefore no additional detection delay is introduced.

4.4.1.3.4   QRS Localization and Refractory Blanking

The purpose of the localization block is to provide a reliable estimate of the R peak position. The preliminary QRS location is selected as the first sample where the feature signal exceeds the relevant threshold. However, this point is probably not the location of the R peak. To allow better delineation, a search is performed for the maximum point in the feature signal for a period of time after the exceedance of the threshold. The sample point that obtains the maximum feature value during this time interval was selected as the QRS position. The search period was chosen to be equal to the refractory period (T_{ref}), in which detection of a new QRS complex was not allowed. It should be mentioned that only one QRS complex was detected in each search back. If several samples exceeded T_{low} during the search back period, the sample with the highest feature value was selected as the preliminary QRS position.

4.4.2   Results

4.4.2.1   Algorithm Parameter Optimization

Four of the algorithm parameters were chosen based on a parameter grid search on the training databases (MITDB and eTDB). The four parameters were the refractory blanking period (T_{ref} = 0.2ms, 0.25m, or 0.3ms), the scaling of the expected RR interval (RR_{scale} = 1, 1.2, or 1.3), the boundary for T_{low} (β = 0.4, 0.5, or 0.6), and the scaling parameter for T_{high} (α = 0.8, 0.9, or 0.99). The investigated values were selected based on clinical relevance, theoretical sense, and experience from the literature. The parameters are mutually dependent on each other. Therefore, the performances of all 81 different combinations of parameter values were investigated. The relationship between Se and P^+ for all 81 combinations is provided in Figure 4.16. Figure 4.16(a) illustrates the performance on the MITDB. The blue marks indicate the performance on the entire database, the green marks indicate Se on SVEB beats only, and the red marks indicate Se of VEB beats only. The black circles indicate the parameter combination selected for further embedded implementation. Figure 4.16(b) illustrates the performance on the eTDB. The selected parameter combination was T_{ref} = 0.25ms, RR_{scale} = 1.2, α = 0.8, and β = 0.4. The parameter optimization was based on channel I from both training databases.
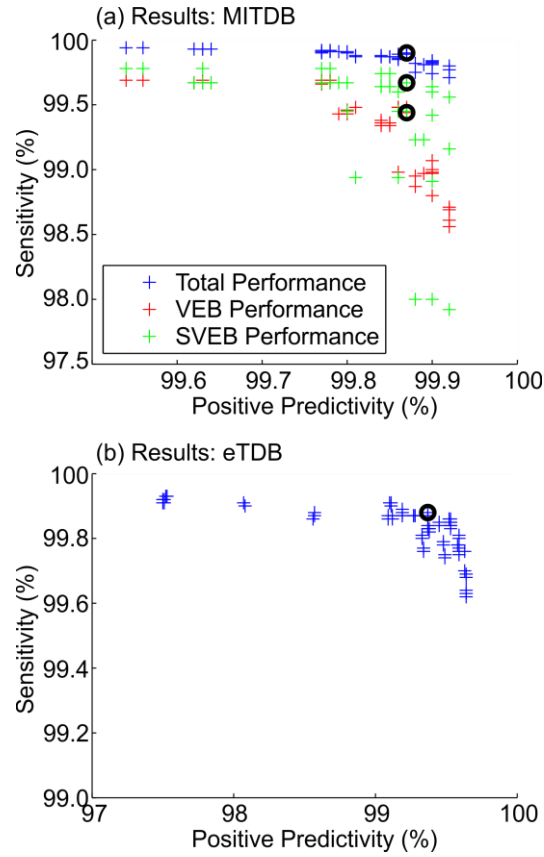
Figure 4.16: Relation between P^+ and Se for (a) the MITDB and (b) the eTDB. Each mark indicates the performance for one of the 81 investigated parameter combinations. In (a), the blue marks indicate the performance on the entire database, the green marks indicate the performance on SVEB beats only, and the red marks indicate the performance on VEB beats only. The black circles indicate the parameter combination that was selected for further embedded implementation. Note, that the axes are zoomed to allow a better view of each point.

4.4.2.2   QRS Detection Performance

Table 4.6 contains the QRS detection performances obtained on the five different databases. The performances are calculated for both channel I and channel II for each database. It should be noted that the algorithm was designed and optimized on channel I of the eTDB and the MITDB. The EDB, eVDB, and PeDB were only applied for validation purposes. The performance on the last three databases thus provides a reliable estimate of the performance on unseen data with a realistic amount of abnormal beat morphologies and different types of normal daily life activities.

Table 4.6: Performance of the proposed single-channel BP filter based algorithm on the five different databases.

Database	Channel I				Channel II			
	Se (%)	P^+ (%)	Se VEB (%)	Se SVEB (%)	Se (%)	P^+ (%)	Se VEB (%)	Se SVEB (%)
EDB	99.84	99.71	97.60	99.53	99.69	99.07	93.30	99.81
MITDB	99.90	99.87	99.44	99.67	99.11	97.64	98.41	98.72
PeDB	97.99	98.25	99.45	100	98.65	99.34	98.89	99.52
eTDB	99.88	99.37	-	-	99.67	98.99	-	-
eVDB	99.91	99.79	-	-	99.93	99.82	-	-
Total	99.80	99.67	98.70	99.67	99.62	98.96	96.36	99.08

4.4.2.3   QRS Detection Examples

Figure 4.17 illustrates the algorithm performance in different challenging clinically relevant ECG segments from the eTDB. The top plot of each subfigure illustrates one channel of raw ePatch ECG. The bottom plot illustrates the final feature signal (blue line) together with T_{low} and T_{high} (red lines). The green circles indicate QRS complexes detected using T_{high} (detection mode 1), the black circles indicate QRS complexes detected in search back (detection mode 2), and the magenta circles indicate QRS complexes detected using T_{low} (detection mode 3).
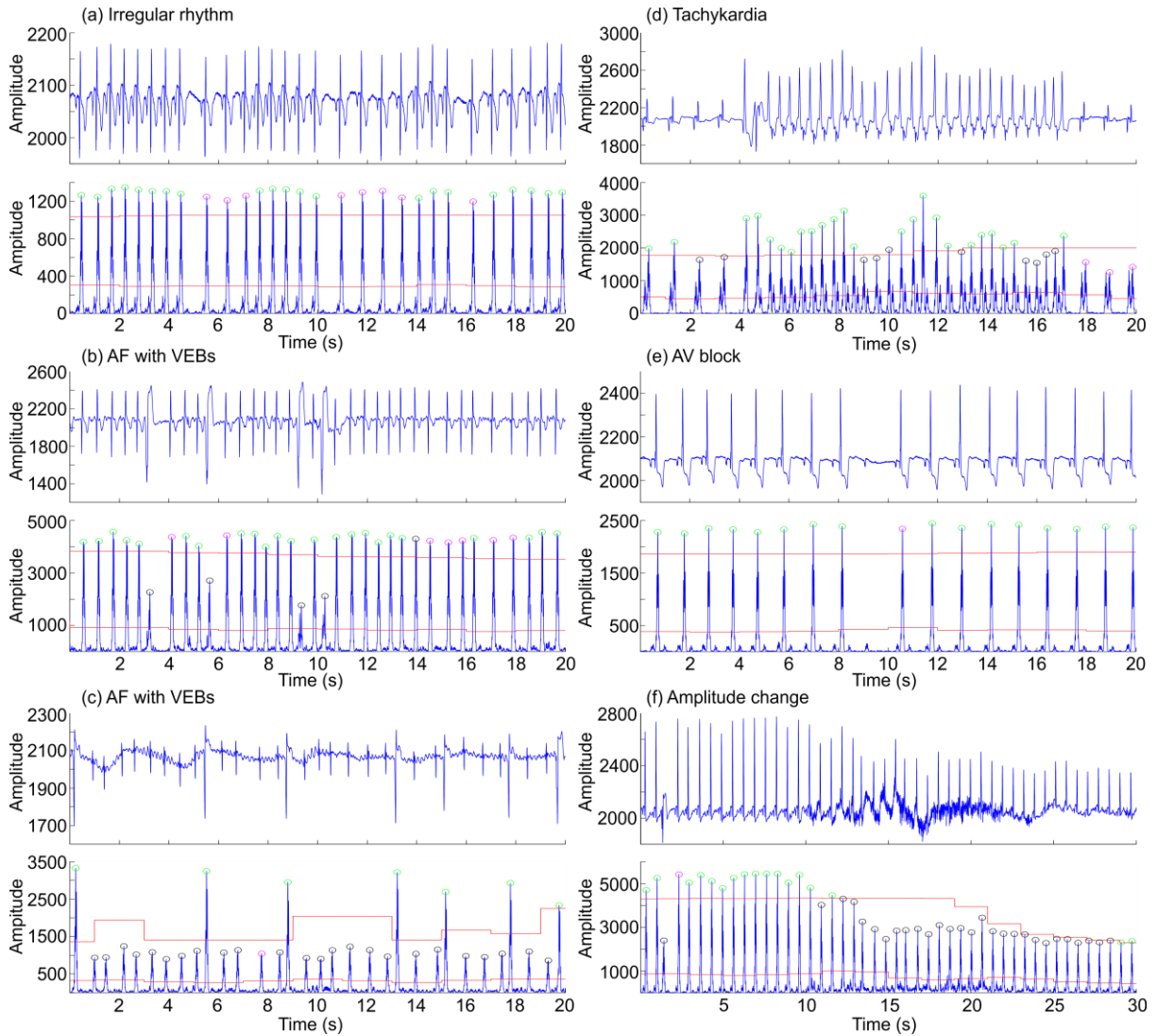

Figure 4.17: Illustration of performance on six challenging ECG segments from the eTDB: (a) Irregular heart rhythm, (b) AF with VEBs, (c) AF with VEBs, (d) Sudden onset of tachycardia, (e) 2nd degree AF block, and (c) sudden change in amplitude. The top plot in each subfigure is one channel of raw ECG. The amplitude is illustrated in ADC counts. The bottom plot in each subfigure illustrates the final feature signal (blue line) together with T_{high} and T_{low} (red lines). The green circles indicate QRS positions detected using T_{high} (detection mode 1), the black circles indicate QRS positions detected during search back (detection mode 2), and the magenta circles indicate QRS complexes detected using T_{low} (detection mode 3).

Figure 4.17(a) illustrates an example of perfect QRS detection in a segment with irregular heart rhythm. It is observed that beats with a prolonged RR interval are detected in the third detection mode (magenta circles). This implies that a search back has been correctly performed without detection of QRS complexes. This is due to the novel cascade of BP filters that succeed in a high attenuation of the pronounced P- and T-waves in this signal. Figure 4.17(b) and Figure 4.17(c) illustrates two different cases of AF with VEBs. In Figure 4.17(b) it is observed that the VEBs are wider than the normal beats, and therefore less pronounced in the final feature signal. This is observed not to be problematic due to timely initiation of the

search back procedure in the VEB positions (black circles). It is furthermore observed that the normal beats after two of the VEBs are detected in the third algorithm mode (magenta circles). In these two cases, the algorithm thus proves to function exactly as intended. At fourteen seconds, one QRS complex is detected using the search back mode even though the amplitude exceeds T_{high}. This is due to a very sensitive search back that is initiated on the rising slope of the QRS complex. The localization block is then initiated from the search back procedure and ensures correct localization of the QRS complex. The high search back sensitivity for this recording is caused by the characteristic irregularity of the RR intervals that is observed during episodes of AF. In Figure 4.17(c), the opposite case is illustrated. For this patient, the VEB beats are more pronounced than the normal beats and they have very large slopes. This implies that the VEB beats are more pronounced in the final feature signal. However, again, this is observed not to be problematic due to timely initiation of the search back procedure for each normal beat. It is furthermore observed that the search back procedure is also relatively sensitive for this segment. This is observed from the magenta circles that indicate that the beat was detected in the thrid algorithm detection mode. This increased sensitivity is also expected for a recording where the general heart rhythm is AF. Figure 4.17(d) illustrates two interesting issues: 1) Very pronounced P-waves with high slopes, and 2) a run of SVEBs/sudden tachycardia onset. It is observed that all QRS complexes are correctly detected by the algorithm. This is obtained through a timely initiation of the search back procedure for all QRS complexes in the SVEB run with amplitude lower than T_{high} (indicated by black circles). This illustrates the high adaptability of the search back initiation. It is furthermore observed that the QRS complexes after the SVEB run are detected using T_{low} in the third algorithm mode (magenta circles). This occurs because it requires some time to adapt to the lower RR variability by decreasing the sensitivity of the search back procedure again. The pronounced P-waves are also observed in the final feature signal. In cases using T_{high}, this is not a problem. In cases using the search back procedure and T_{low} this could induce false detections of the P-wave when they exceed T_{low}. However, the localization block is observed to correctly prevent false detections of the P-wave for all QRS complexes in this segment. Figure 4.17(e) illustrates the algorithm performance in case of a 2nd degree AF block. The general heart rhythm is observed to be regular, and therefore the search back is only initiated once at the location of the missed QRS complex. It is observed that the algorithm correctly detects that no QRS complex was present and stays in the third algorithm mode until the next QRS complex is detected (indicated by the magenta circle after the blocked P-wave). Finally, Figure 4.17(f) illustrates the performance during a sudden change in amplitude. This property is especially important for the ePatch data. As mentioned, the location on the sternum implies that the general amplitude can change rapidly due to changes in body position. It is observed how T_{high} is quickly adapted to the new level of the QRS complexes. Even in the meantime, no QRS complexes are missed due to the correct functionality of the search back procedure. This feature of the algorithm is very important in real-life clinical applications where patients would wear the ePatch during normal daily life activities for extended periods of time. Furthermore, it is observed that the minor muscle and motion artifacts present in Figure 4.17(f) does not disturb the automatic QRS detection.

4.4.2.4 Reflections on Algorithm Requirements

The algorithm performance is further discussed and compared to both results obtained from the literature and the proposed multi-channel wavelet based algorithm in section 4.5 on page 52. However, before we continue, it is worth taking a moment to reflect on the original algorithm requirements defined in section 4.1.3. These requirements were the motivation and guidance throughout the design of the algorithm. The first requirement was a high detection performance with respect to both normal and abnormal beat morphologies. This requirement was included to ensure high clinical applicability of the algorithm. Looking at Table 4.6 and Figure 4.17, this requirement is observed to be fulfilled. It is furthermore observed that the fulfillment of this requirement is highly related to the refined search back mechanism designed in this project. This search back procedure ensures high search back "sensitivity" in cases of irregular heart rhythms. The second algorithm requirement was related to proper handling of sudden amplitude changes in the recorded ECGs. This requirement was incorporated through the highly adaptive thresholds as well as the search back mechanism. As observed from Figure 4.17(f), this requirement also seems to be fulfilled by this algorithm. The third algorithm requirement was related to the ability to handle pronounced T-waves. This requirement was ensured by the design of the novel cascade of BP filters that provides high attenuation of the T-waves. Figure 4.17(a) and Figure 4.17(e) contains examples of relatively pronounced T-waves. It is observed that the T-waves are highly attenuated in the feature signal, and therefore do not impose difficulties by the

algorithm. The fourth requirement was related to the ability to handle QRS complexes with different morphologies (high Q- and/or S-waves), e.g. handling of QRS complexes with "negative" polarity. This feature was ensured by the application of the absolute value of the BP filtered ECGs. Figure 4.17(a)-(c) illustrates this functionality. The fifth and sixth requirements were related to the ability to handle different amounts of artifacts and very pronounced atrial activity, respectively. These requirements are only slightly touched in Figure 4.17. However, additional examples of these issues are provided in Figure 4.19, Figure 4.22, and Figure 4.23. These issues are also further discussed later, but we generally found an acceptable performance in the presence of pronounced atrial activity and a high detection performance in the presence of many different types of artifacts. Based on knowledge gained from the literature review, the experience gained from looking through a high number of ePatch ECGs, and the lessons learned during analysis of the performance of the first proposed algorithm, we thus succeeded in designing an algorithm that satisfactorily fulfill the first six selected algorithm requirements. It was therefore highly interesting to embed this algorithm in the ePatch sensor and investigate the last algorithm requirement related to the computational load. This investigation is described below.

4.4.3   Real-time Embedded Algorithm Validation

The algorithm was implemented in ANSI C, compiled and embedded in the ePatch sensor. This investigation was conducted to ensure that the designed algorithm could perform embedded QRS complex detection with high clinical performance without significantly decreasing the total recording time. A certain deviation in algorithm output is expected when the algorithm is implemented in a different programming language and consequently applied in a different environment. Some of these differences are expected to be related to rounding differences in the MATLAB version of the algorithm and the embedded version. These differences might be exacerbated over time due to the high adaptation of the algorithm. We therefore implemented several iterations where we compared the output from the MATLAB and the C implementation in long-term ePatch ECGs and hereby sought to minimize these differences. A minimal difference between the implementations is important to be able to apply the performances stated in Table 4.6 as a reliable estimate of the expected embedded performance. To investigation this further, we evaluated the performance of both the MATLAB implementation, the C implementation, and the embedded implementation on the eVDB. The embedded estimation of the QRS positions were calculated in real-time and saved in a special channel in the data file. This channel was compared to the manual annotations in a double-blinded validation scheme. The QRS detections obtained by the MATLAB and the C implementations were calculated offline after the recording (but still in a double-blinded scheme). The currently applied ePatch sensor has a 32 bit micro controller based on the ARM Cortex-M3 processor from Energy Micro (now acquired by Silicon Labs). The processing time for each sample will among other things depend on the algorithm detection mode applied for that specific sample and whether a QRS complex is detected or not. Furthermore, every two seconds the thresholds and the other adaptive parameters are updated. This will clearly require more processor time than processing a non-boundary ECG sample between two QRS complexes. We therefore decided to investigate the processing time using a histogram. The histogram was created with a clock cycle counter that counted how many clock cycles the algorithm spends on processing each sample in a real-life recording. The duration of the recording was approximately 2.3 hours, yielding a total of 4,271,185 samples. This is expected to provide a reliable estimate of the histogram.

4.4.3.1   Results and Discussions

The detection performances on the eVDB obtained by the MATLAB implementation, the offline C implementation, and the embedded implementation are provided in Table 4.7. The evaluation was conducted on channel I for all three implementations. Only minor performance differences are observed between the three implementations. These differences are considered insignificant, and they are not expected to cause issues with the extension of the results presented in Table 4.6. Furthermore, it should be noted that these performances were obtained throughout the duration of the three recordings. Based on this study, we thus find that the risk of exacerbating potential differences in long-term recordings (due to the high algorithm adaptability) is small. However, these findings should, of course, be validated on a larger database.

Table 4.7: Real-time embedded QRS detection performance of the proposed single-channel BP filter based algorithm on the eVDB.

Subject	Records	Beats	MATLAB		Offline C code		Embedded	
			Se (%)	P+ (%)	Se (%)	P+ (%)	Se (%)	P+ (%)
Subject1	20	11,510	99.83	99.72	99.83	99.72	99.83	99.72
Subject2	20	12,396	99.99	99.85	100	99.86	100	99.86
Subject3	21	14,523	99.92	99.80	99.91	99.79	99.89	99.80
Total	61	38,429	99.92	99.79	99.92	99.79	99.91	99.79

The histogram of the processing times for a real-life recording is provided in Figure 4.18. Two distinct peaks are observed from the histogram. The first peak represents samples with processing times between 30µs and 90µs. This peak corresponds to processing of a non-boundary sample. The smaller peak represents samples with processing times between 120µs and 240µs. This corresponds to samples lying on a two second boundary where all the adaptive parameters are updated. It is furthermore observed that no sample has a processing time of more than 240µs. Furthermore, 99.82% of the recorded samples where processed in less than 60µs. This implies that the algorithm is active in less than 3.1% of the time with a sampling frequency of 512Hz, and allows the processor to enter sleep mode or perform other activities approximately 97% of the time. The typical energy consumption of the processor is 5.62mA. Theoretically, the algorithm thus uses 0.1726mA. During normal operation (recording, sampling, storage etc.) the ePatch sensor uses 3.125mA. This implies that the algorithm causes a theoretic increase in the energy consumption compared to the normal ePatch sensor activity of 5.5%. This corresponds to a decrease from a maximum recording time of 80 hours to a maximum recording time of 75.8 hours using a standard 250mAh battery.
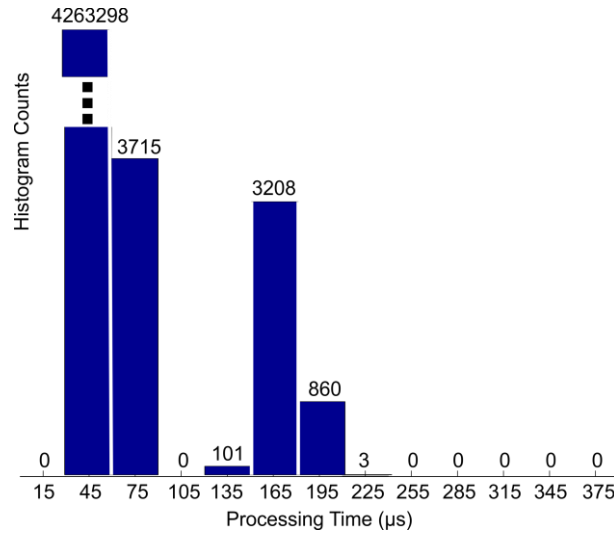

Figure 4.18: Histogram of the embedded algorithm processing time for each sample in a real-life recording of 2.3 hours. The x-axis indicates the mean value of each histogram bin. This implies that the first bin contains samples with a processing time of 0-30µs, the second bin contains samples with a processing time of 30-60µs etc. Note the two distinct peaks in the histogram.

Generally, it is observed that the embedded detection performance is considered to be very high. This performance is obtained on healthy young volunteers during normal active daily life activities. This performance therefore provides a reliable estimate of the performance in long-term ePatch recordings. However, it should, of course, be mentioned that these subjects were healthy, and it might therefore be interesting to conduct the same investigation on patients with a high number of abnormal beat morphologies. Furthermore, it is observed that the additional computational load required by the embedded algorithm is relatively low compared to the normal energy consumption in the ePatch sensor. We therefore consider the algorithm to be applicable in real-life situations. This implies that we also consider the algorithm to fulfill the last requirement related to the computational load.

4.5 Algorithm Comparison and Discussions

To summarize our results, Table 4.8 contains the detection performances obtained on the five different databases for the multi-channel wavelet based algorithm, the single-channel BP filter based algorithm applied to channel I, and the single-channel BP filter based algorithm applied to channel II. For the total average performance on all five databases, it is observed that the single-channel BP filter based algorithm applied to channel I obtains the best results. The second best results are obtained by the multi-channel wavelet based algorithm, and the worst result are obtained by only applying channel II of each database. Considering the increased quality of channel I in the standard databases, this result is not surprising. However, it is also observed that the performance with respect to detection of VEB beats is lowest for the multi-channel algorithm. This was not expected. This is therefore further discussed later. Before continuing, it is worth noting that both algorithms, and especially the second proposed algorithm applied to channel I, generally obtain very satisfactory performance on most of the databases and that the performances obtained on the five different databases are comparable. During the design and optimization of the two proposed algorithms, we emphasized the special characteristics of the ePatch ECGs, but these considerations did not result in a decreased detection performance on ECGs recorded with traditional equipment (represented by the MITDB and the EDB). This indicates that algorithms can be designed to obtain high performance on both ECGs recorded with traditional equipment and ECGs recorded with the ePatch recorder. This was one of the key research questions investigated in this part of the project. This finding is important because it might indicate that algorithms applied in commercial automatic Holter analysis software could be updated to also include possibilities of analysis of ePatch ECGs. This would highly decrease the difficulties that would otherwise be experienced during large-scale implementation of the ePatch recorder for clinical outpatient ECG monitoring in the future. However, this area should be further investigated for arrhythmia detection algorithms before a definitive conclusion can be made.

Table 4.8: Comparison of performance of the first proposed multi-channel wavelet based algorithm and the second proposed single-channel BP filter based algorithm. The performance of the BP filter based approach is stated for both channel I and channel II of each database.

| Database | Wavelet Transform Based Channel I & Channel II | | | | BP Filter Based Channel I | | | | BP Filter Based Channel II | | | |
	Se (%)	P+ (%)	VEB Se (%)	SVEB Se (%)	Se (%)	P+ (%)	VEB Se (%)	SVEB Se (%)	Se (%)	P+ (%)	VEB Se (%)	SVEB Se (%)
EDB	99.75	99.79	92.27	99.63	99.84	99.71	97.60	99.53	99.69	99.07	93.30	99.81
EDB[a]	99.76	99.80	94.33	99.63	99.84	99.71	98.56	99.53	99.72	99.09	98.17	99.81
MITDB	99.65	99.63	98.71	98.80	99.90	99.87	99.44	99.67	99.11	97.64	98.41	98.72
PeDB	99.35	99.46	100	100	97.99	98.25	99.45	100	98.65	99.34	98.89	99.52
PeDB[b]	99.95	99.49	100	100	99.94	99.66	99.44	100	99.79	99.53	98.89	99.52
eTDB	99.70	97.76	-	-	99.88	99.37	-	-	99.67	98.99	-	-
eTDB[c]	99.81	99.55	-	-	99.95	99.92	-	-	99.83	99.64	-	-
eVDB	99.80	98.20	-	-	99.91	99.79	-	-	99.93	99.82	-	-
Total	99.73	99.61	96.15	99.13	99.80	99.67	98.70	99.67	99.62	98.96	96.36	99.08
Total[d]	99.76	99.70	96.98	99.13	99.86	99.74	99.09	99.67	99.68	99.02	98.33	99.08

[a] Gross average performance with corrections for record e0614 from the EDB, see Appendix B.

[b] Gross average performance with exclusion of record 11 from the PeDB, see section 4.5.2.

[c] Gross average performance with exclusion of record 28 and 29 from the eTDB, see section 4.5.2.

[d] Total gross average performance on all five databases with the modifications described by [a], [b], and [c].

4.5.1 Comparison with literature

As discussed earlier, we believe that especially the second proposed algorithm obtains satisfactory fulfilment of the selected algorithm requirements. However, it is still important to compare the obtained performances with other performances stated in the literature. This is, of course, not possible for the ePatch databases. We therefore only conduct this comparison using the MITDB and the EDB. To allow comparison, Table 4.9 therefore contains the performances obtained by different studies from the literature on these databases. The algorithms were selected for comparison based on several criteria:

- It was prioritized to compare with some of the algorithms obtaining the best performance in the literature.
- It was prioritized to select literature that could allow comparison with different types of algorithms applying different methodologies, and hereby requiring different computation loads.
- It was prioritized to compare with algorithms that have been evaluated on both databases.
- Finally, it was prioritized to compare with algorithms based on both the single-channel paradigm and different multi-channel paradigms

As mentioned earlier, the single-channel based algorithms described in the literature are generally only evaluated on channel I of the MITDB and the EDB. We therefore only compare with the performance of our proposed single-channel algorithm applied to channel I. In spite of the high clinical relevance, the other studies did not publish their detection performances with respect to VEB and SVEB beats. A comparison with respect to detection of abnormal beats was therefore not possible. The next two sections contain a brief comparison of each of the proposed algorithm with the results stated in Table 4.9.

Table 4.9: Comparison with some of best results obtained from the literature.

Method	MITDB		EDB	
	P+	Se	P+	Se
Multi-channel wavelet based algorithm [e]	99.63	99.65	99.80	99.76
Single-channel BP filter based algorithm [a]	99.87	99.90	99.71	99.84
Di Marco and Chiari [27]	99.86	99.77	99.56	99.81
Ghaffari *et al.* [32]	99.88	99.91	99.55	99.63
Ghaffari *et al.* [33]	99.91	99.94	-	-
Boqiang *et al.* [38] [e]	99.93	99.91	-	-
Chiarugi *et al.* [37] [e]	99.81	99.76	-	-
Liu *et al.* [29] [b]	99.86	99.80	-	-
Li *et al.* [30] [d]	99.94	99.89	-	-
Martìnez *et al.* [36]	99.97	99.71	99.73	99.67
Martìnez *et al.* [31]	99.86	99.80	99.48	99.61
Zhang and Bae [34] [c]	99.82	99.76	-	-
Pan and Tompkins [26] [d][a]	99.54	99.75	-	-
Zidelmal *et al.* [28]	99.82	99.64	-	-

[-] Not stated in paper.

[a] Algorithm is implemented and tested in a microprocessor.

[b] Algorithm is implemented and tested on an ASIC.

[c] Algorithm is implemented and tested on a FPGA.

[d] A discrepancy was found between the stated total number of beats and the record-by-record total number of beats. In this table, the record-by-record numbers are applied.

[e] Algorithm is evaluated using a multi-channel paradigm.

4.5.1.1 Single-Channel BP Filter Based Algorithm

The performance of the single-channel BP filter based algorithm on the MITDB is definitely comparable to the best results obtained in the literature. These results [32], [33], [38] are, however, not obtained by embedded algorithms that have been tested in real-life situations. When compared to other embedded algorithms [26], [29], [34], the performance obtained by our novel algorithm is slightly superior. Furthermore, we consider our detection sensitivity with respect to VEBs and SVEBs to be very high for the single-channel algorithm applied to channel I. This is especially relevant when the algorithm is intended to be applied in a clinical setting. The performance on the EDB is also superior to other algorithms from the literature. It should furthermore be noted that this database was used only as a validation database. This implies that the algorithm design and parameter selection was not changed prior to the processing of this database. This result can thus provide a relatively realistic impression of the performance on unseen ECGs with different types of abnormal beat morphologies from a high number of different patients. The comparison with the literature thus strengthens our impression of this algorithm as highly clinically relevant in the future.

4.5.1.2 Multi-Channel Wavelet Based Algorithm

The performance of the multi-channel wavelet based algorithm on the MITDB is slightly lower than most of the studies selected for comparison. The lower performance might be caused by the optimization to the quite small PeDB or the choice of a multi-channel paradigm. As mentioned, the quality of channel II is often lower than channel I for this database. In our approach, we only tested the implementation of a very simple channel exclusion measure based on saturation. The detection performance on the MITDB might therefore be improved by implementation of more sophisticated channel exclusion measures. The overall performance on the EDB is considered very high compared to other published work. However, for the EDB, the sensitivity with respect to abnormal beats is considered to be relatively low compared to the proposed single-channel algorithm. This is discussed further in the next sections.

4.5.2 Comparison of Performance of the Two Proposed Algorithms

The previous section contains an overview comparison of each proposed algorithm relative to performances stated in the literature. This section, on the other hand, contains a detailed comparison and discussion of the performances obtained by the two proposed algorithms. During the comparison of the two algorithms it is important to keep in mind that the goal of the work described in this chapter was to design an automatic algorithm for embedded QRS complex detection in the ePatch sensor. Therefore, the detection performances obtained on the ePatch databases (especially the eTDB and the eVDB that were recorded with the newest CE-market ePatch) is generally prioritized over the performances obtained on the standard databases. This is especially relevant when discussing the potential benefits from applying information from both ePatch ECG channels. Looking at the performances obtained by the two algorithms on each ePatch record, a few interesting findings became clear:

- The difference in performance on the PeDB was primarily caused by differences in record 11. When this record is excluded from the overall statistics, the performances become quite similar (see Table 4.8). This record contains approximately 2.5 minutes of very poor data quality in both channels and several episodes of saturation. The increased performance obtained by the multi-channel algorithm for this record was found to originate primarily from the channel "shutdown" methodology implemented in this algorithm. This issue is further discussed in section 4.5.2.1.
- It was generally observed that the performances obtained by applying the single-channel algorithm to the two different ePatch channels were quite similar. This indicates that the two channels possess approximately equal amount of information for automatic embedded QRS complex detection. Furthermore, it is observed from the ePatch databases that the multi-channel algorithm obtains slightly lower performance than the single channel algorithm. This furthermore indicates that no additional information is provided by including both channels from the ePatch recordings. This is further discussed in section 4.5.2.2.

- It was observed that the difference in performances obtained on the eTDB primarily originates from record 28 and 29. These recordings were extracted from the same patient. This patient suffers from AF and the recorded atrial activity is very pronounced. It is revived that high performance in these cases was one of the algorithm requirements defined in section 4.1.3. If these records are excluded, the overall statistics from both algorithms become quite similar (see Table 4.8). We found that the increased performance obtained by the single-channel algorithm in this example is caused by the influence of proper functionality of the novel search back mechanism implemented in the second algorithm. This issue is further discussed in section 4.5.2.3.
- For the eVDB, the differences in performance originate from several different recordings. However, a common characteristic for these recordings is relatively high amounts of high frequency artifacts caused by muscle activations. It is revived that high performance in these cases was one of the algorithm requirements defined in section 4.1.3. The improved detection performance by the single-channel algorithm was, again, observed to be highly related to the search back mechanism. This issue is therefore also further addressed in section 4.5.2.3.

When comparing the performances with respect to detection of abnormal beat morphologies, the performances on the standard databases were the primary source of information (due to the lack of large-scale manual annotations of abnormal beat morphologies in the ePatch databases). Based on the standard databases, the following observation was clear with respect to detection of abnormal beats:

- It was observed that the multi-channel algorithm obtained the lowest detection performance with respect to abnormal beats, especially VEBs, on the EDB. One of the assumptions for including an additional channel was an increased chance of detecting abnormal beats. This finding was therefore not expected. This issue is therefore further discussed in section 4.5.2.2.

As mentioned above, each of these performance differences were found to be related to specific differences in the design of the two algorithms. Two of the important blocks implemented in the second algorithm were the novel BP filtering scheme and the refined search back methodology. These improvements were partly made based on experiences with the first algorithm. Furthermore, an important difference between the algorithms was the application of either one or both channels. Finally, the first proposed algorithm contains a "shutdown" block that is intended to "protect" the algorithm in cases of extremely noisy data segments. This block was not included in the single-channel algorithm. The influence of each of these four design choices are indicated in the above listed bullets. The next sections contain a number of illustrations that are intended to highlight the strengths and weaknesses of these design choices using clinically relevant ECG snippets. This investigation led to a set of recommendations for future embedded detection of QRS complexes in the ePatch sensor (see section 4.5.3).

4.5.2.1 Influence of the Channel "Shutdown" Methodology

In the first proposed algorithm, a channel "shutdown" procedure was implemented to exclude information from a potentially noisy channel. An example of the performance of both algorithms during an episode of pronounced saturation in record 11 from the PeDB is provided in Figure 4.19. It is observed that the improved detection performance is ensured by the channel exclusion measure: The multi-channel algorithm is in complete "shutdown" mode during the episodes of saturation. This ensures that no false detections are produced. It is furthermore observed how fast the multi-channel algorithm recovers after the artifact episode. This is achieved because the adaptive algorithm parameters are not updated during periods of "shutdown". This ensures that the thresholds are able to "catch" the QRS complexes immediately after this episode of saturation. This might suggest that the single-channel algorithm could be further improved by implementation of protective features similar to the "shutdown" approach implemented in the multi-channel algorithm. This could for instance ensure that the adaptive algorithm parameters would not be updated and hereby fitted to noise during "shutdown" or it might be implemented in the form of resetting the adaptive algorithm parameters if a noisy episode has been detected. It should

furthermore be mentioned that the "shutdown" approach might be improved by the implementation of more sophisticated channel exclusion measures. Therefore, this block is definitely worth more exploration in future studies.
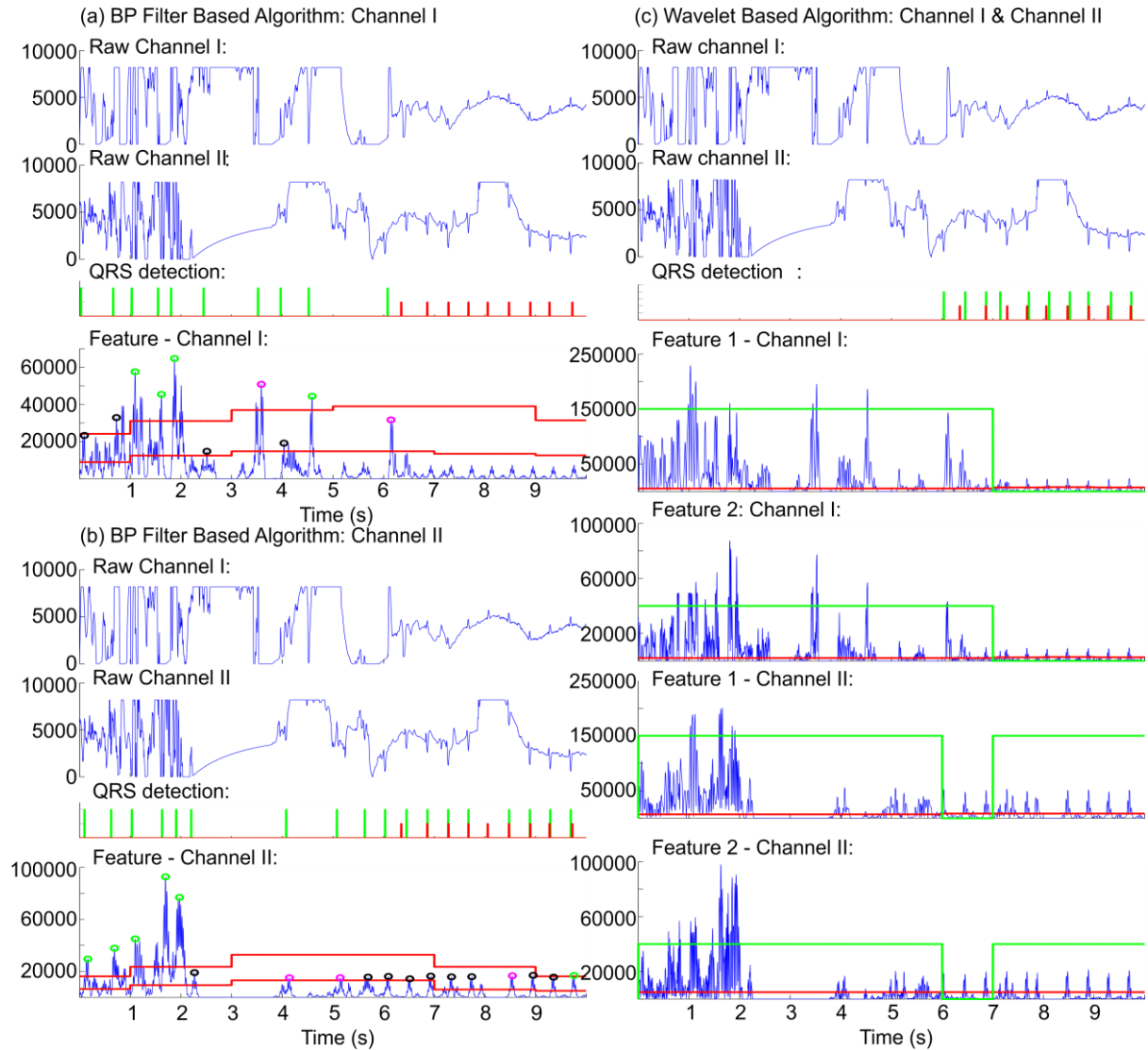

Figure 4.19: Illustration of detection performance on record 11 from the PeDB during an episode of saturation in both channels: (a) Performance of the single-channel algorithm applied to channel I, (b) Performance of the single-channel algorithm applied to channel II, and (c) Performance of the multi-channel wavelet based algorithm. The vertical red lines indicate the position of QRS complexes in the reference annotations. The vertical green lines indicate the QRS positions detected by the different algorithms. In (a) and (b), the green circles indicate QRS complexes detected using T_{high} (algorithm mode 1), the black circles indicate QRS complexes detected using T_{low} during search back (algorithm mode 2), and the magenta circles indicate QRS complexes detected using T_{low} after search back (mode 3). The horizontal red lines indicate the adaptive threshold values. The horizontal green lines indicate the channel exclusion measure (asserted = channel excluded). It is observed how both channels are excluded (complete algorithm shutdown) for the first six seconds, and hereafter one of the channels is constantly active.

4.5.2.2   Influence of Application of Information from Both ePatch Channels

It was important to investigate whether the two simultaneously recorded ePatch ECG channels provide non-redundant information with respect to the automatic detection of QRS complexes. In the beginning, we believed that there might be additional information in the second channel, especially during episodes of artifacts or abnormal beat morphologies. However, as observed from Table 4.8, this does not seem to be the case. Furthermore, it is also observed that the sensitivity with respect to detection of VEB beats is highly decreased for the multi-channel algorithm on the EDB. This was not expected. An example of this issue is illustrated in Figure 4.20.
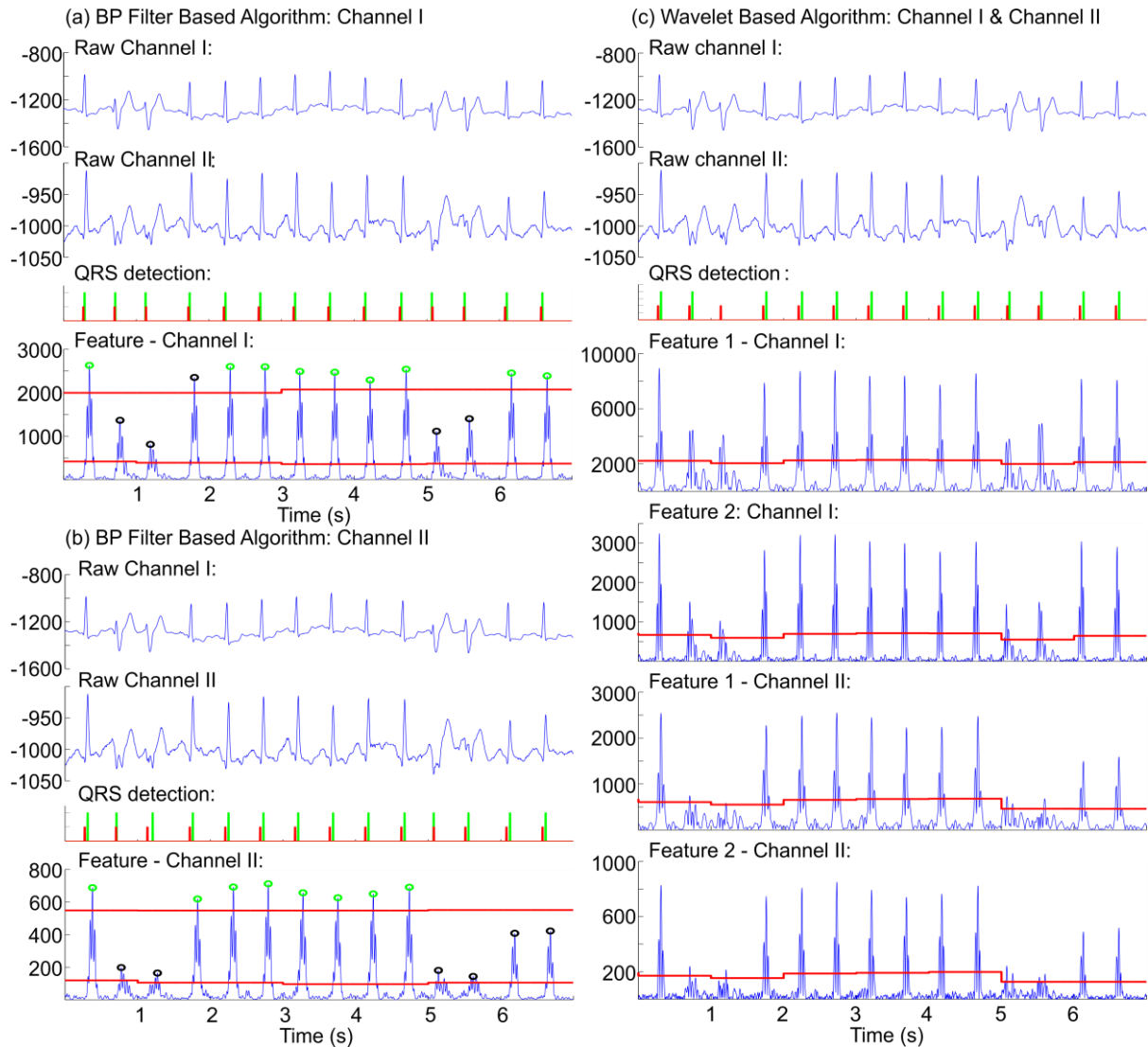
Figure 4.20: Illustration of detection performance on record e0605 from the EDB during an episode with several VEB beats: (a) Performance of the single-channel algorithm applied to channel I, (b) Performance of the single-channel algorithm applied to channel II, and (c) Performance of the multi-channel wavelet based algorithm. The horizontal red lines indicate the appropriate threshold values. The vertical red lines indicate the position of QRS complexes in the reference annotations. The vertical green lines indicate the QRS positions detected by the different algorithms. It is observed that all four VEB beats are correctly detected using the single-channel BP filter based algorithm applied to both channel I (a) and channel II (b), but one of the VEB beats is missed using the multi-channel wavelet based algorithm (c). In (a) and (b), the green circles indicate QRS complexes detected using T_{high} (algorithm mode 1) and the black circles indicate QRS complexes detected using T_{low} during search back (algorithm mode 2).

It is observed how the single-channel algorithm obtains perfect VEB detection in this ECG segment independent of the channel applied. It is furthermore observed how the multi-channel algorithm misses the second VEB beat. To investigate this issue further, a zoomed version of the first two seconds of the segment is provided in Figure 4.21.
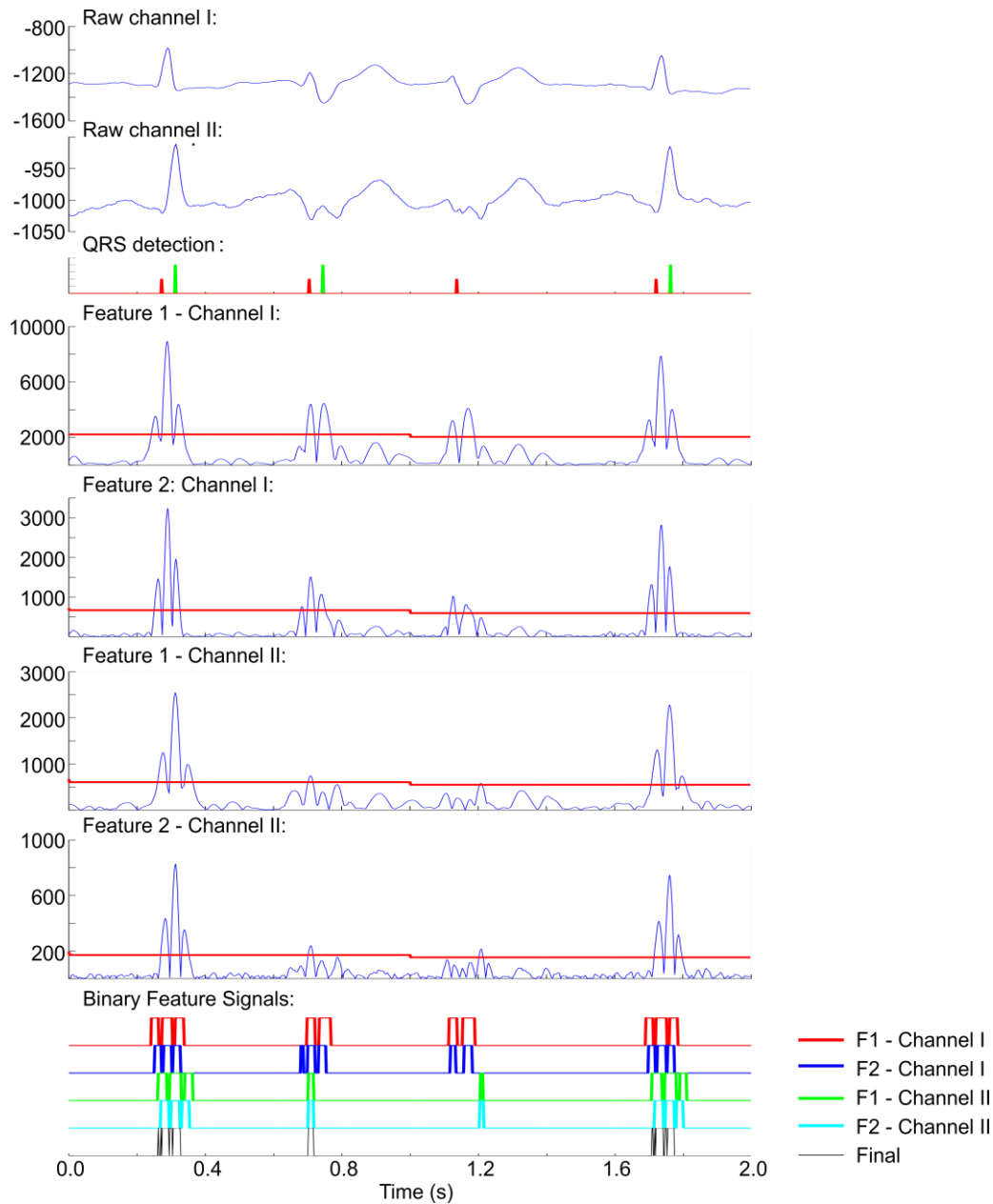

Figure 4.21: Illustration of a zoom on the first two seconds illustrated in Figure 4.20. It is observed that the second VEB beat is missed. As illustrated in the bottom plot, this is caused by a difference in the assertion of the binary feature signals for the two channels. It is furthermore observed how a very low threshold value is required to detect the first VEB beat.

It is observed that the missed VEB detection is caused by a misalignment between the locations where the two feature signals from the two channels cross the respective thresholds. This was generally observed to be the case for many of the VEB beats that where missed by the multi-channel algorithm. This might suggest that a different decision fusion scheme should be designed to combine information from the two channels. However, the feature signals from the two channels indicate that any simple combination of the information from the two channels might be difficult without also unintentionally increasing the risk of additional false positive detections during episodes of noisy data. It should, however, be noted that the decreased detection performance with respect to VEB beats might be caused by the BP filter applied before the wavelet

decomposition in the multi-channel algorithm. It is known that a BP filter might unintentionally decrease the influence of VEB beats that are generally recognized by lower frequency content than the normal beats. It should also be mentioned that in some cases the detection performance with respect to abnormal beats was increased in the multi-channel algorithm. But the overall impression is that the single-channel algorithm obtains higher performance with respect to detection of VEB beats. Furthermore, based on the available data, no significant difference between the performances obtained on the two different ePatch channels was observed. At the same time, the multi-channel algorithm obtains lower performance on the eTDB and the eVDB than both channel I and channel II individually. This might indicate that the information in the two ePatch channels is redundant with respect to automatic heart beat detection and that a single-channel approach therefore might be the best choice in ePatch ECGs. It should, of course, be mentioned that the multi-channel algorithm might be improved, and hereby obtain a higher performance. However, even if improvements were made, it is not considered likely that including both channels for analysis of the ePatch recordings will be able to significantly improve the high detection performance obtained by the proposed single-channel algorithm applied to either channel I or channel II. The computational load is furthermore significantly higher when two ECG channels are processed simultaneously. The designed multi-channel algorithm should therefore obtain significantly higher performance in order to serve as the first choice for real-time embedded QRS detection. We therefore recommend application of only one ePatch ECG channel for automatic embedded detection of QRS complexes in the ePatch sensor. However, as suggested in the previous section, the single-channel algorithm might be further improved by implementation of a "shutdown" procedure. This could ensure that the algorithm always applies the channel with the highest quality and hereby always provide the best environment for reliable detection of the QRS complexes.

4.5.2.3   Influence of the Search Back Mechanism

As described earlier, we applied two different variations of adaptive thresholding. In the first algorithm a single adaptive threshold was applied. However, it was found that this approach requires that the threshold is relatively low to ensure adequate detection of abnormal beat morphologies. An example of this is illustrated in Figure 4.20 and Figure 4.21. However, it was found that this low threshold has a high tendency to produce false detections. We therefore decided to investigate the application of two adaptive thresholds applied in a search back scheme in the second algorithm. An example of the influence of this detection methodology is provided in Figure 4.22. This ECG snippet is extracted from record 28 from the eTDB. The rhythm is AF, and the fibrillating "P-waves" are very pronounced compared to the QRS complexes. As mentioned, this is one of the characteristic challenges that are sometimes experienced during episodes of AF recorded with the ePatch. The accurate assessment of the atrial activity is expected to be caused by the location of the ePatch. It is observed how the multi-channel approach achieves very poor performance in this ECG snippet. It is also observed that the increased performance obtained by the single-channel algorithm is caused by the novel search beach mechanism. Several episodes from the atrial activity actually obtain peaks in the feature signal that are higher than the influence of the R peaks. This occurs for both algorithms. However, this is handled quite well by the search back mechanism. The idea of the search back mechanism is to increase the sensitivity of the algorithm when enough time has elapsed to confidently expect a new QRS complex, and this procedure is observed to increase the performance in this ECG snippet. However, it is expected that both algorithms can produce some FP detections during episodes of AF with this appearance. A single FP/FN pair is also observed using channel II in Figure 4.22. However, a few false detections during episodes of AF are not expected to disturb subsequent automatic rhythm analysis and automatic classification of AF versus other heart rhythms. The performance of the single-channel algorithm observed in Figure 4.22 is thus expected to be sufficient for subsequent automatic AF detection, whereas the performance of the multi-channel algorithm is considered too low for this segment. However, it is recommended to conduct further analysis to clarify the exact extend of this AF morphology in the ePatch recordings and conduct a proper performance evaluation on this specific arrhythmia morphology.
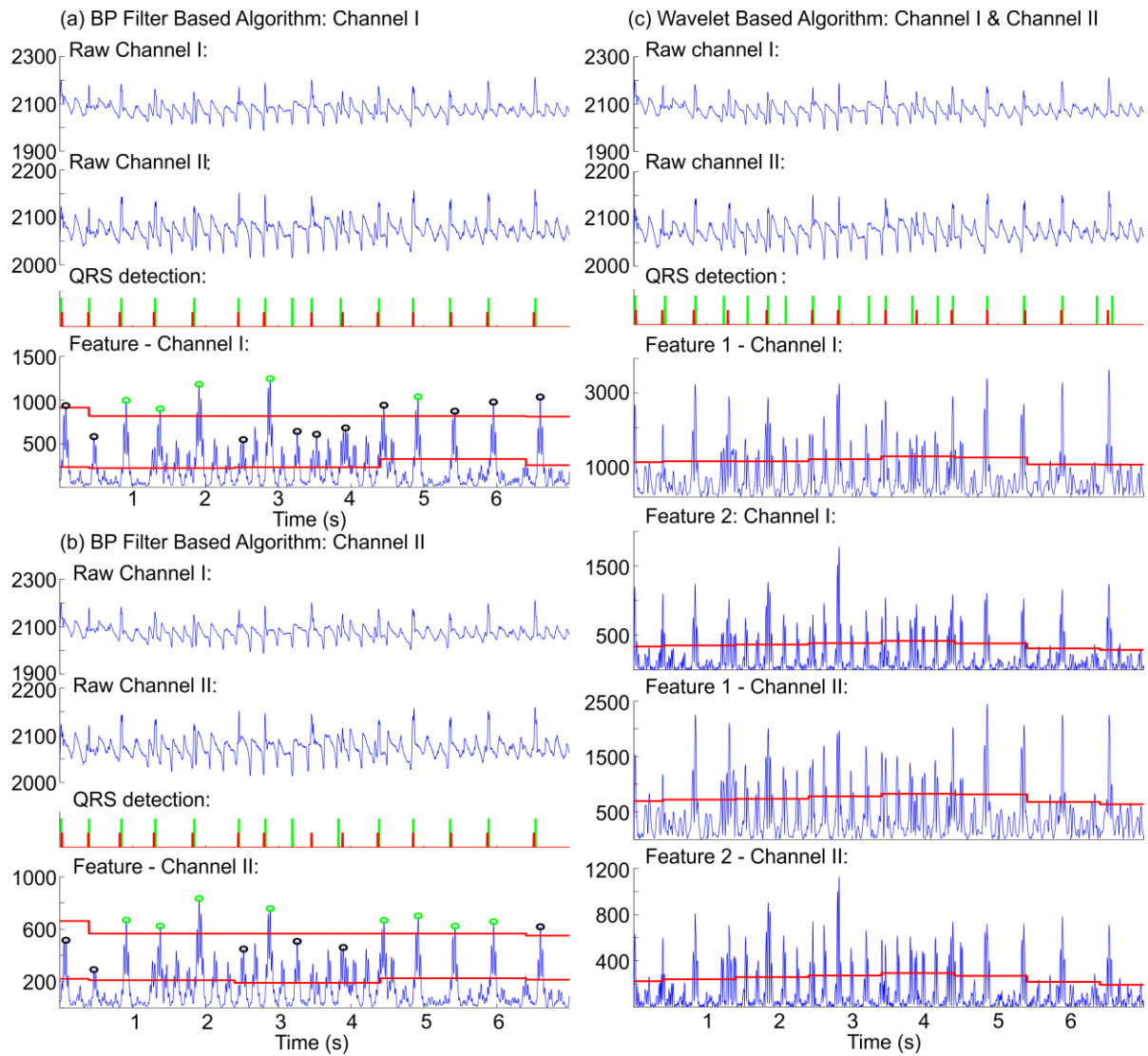
Figure 4.22: Illustration of detection performance on record 28 from the eTDB: (a) Performance of the single-channel algorithm applied to channel I, (b) Performance of the single-channel algorithm applied to channel II, and (c) Performance of the multi-channel wavelet based algorithm. The horizontal red lines indicate the appropriate threshold values. The vertical red lines indicate the position of QRS complexes in the reference annotations. The vertical green lines indicate the QRS positions detected by the different algorithms. In (a) and (b), the green circles indicate QRS complexes detected using T_{high} (algorithm mode 1) and the black circles indicate QRS complexes detected using T_{low} during search back (algorithm mode 2).

Another example of the influence of the detection methodology is provided in Figure 4.23. This illustrates the performance of both algorithms during gardening. It is clearly observed how the single-channel algorithm handles the high frequency muscle artifacts better than the multi-channel algorithm. It is observed that the feature signal obtained using the novel cascade of simple FIR filters in the single-channel algorithm is somehow smoother than the wavelet based features achieved in the multi-channel algorithm. However, many of the artifacts still cross the low threshold in the single-channel algorithm. This again illustrates the usefulness of timely initiation of a search back procedure. The search back allows a relatively high T_{high} that prevents erroneous detections of muscle artifacts without missing abnormal beats with lower amplitude. This is observed to increase the detection performance. However, it should be remembered that the training databases applied for the two algorithms were quite different (see section 4.2). The single adaptive threshold approach might therefore obtain slightly higher performance if the algorithm parameters were optimized using more ePatch data. However, after reviewing different challenging ECG snippets, we consider it unlikely that this optimization would be able to account for the higher performance obtained by the search back approach. Furthermore, we accomplished to implement the search back procedure using computationally simple adaptive thresholds. These thresholds can even be calculated without information

from data in the current analysis window. We therefore consider the search back procedure to be a good approach for embedded detection in long-term recordings with a high amount of real-life artifacts from normal daily life activities.
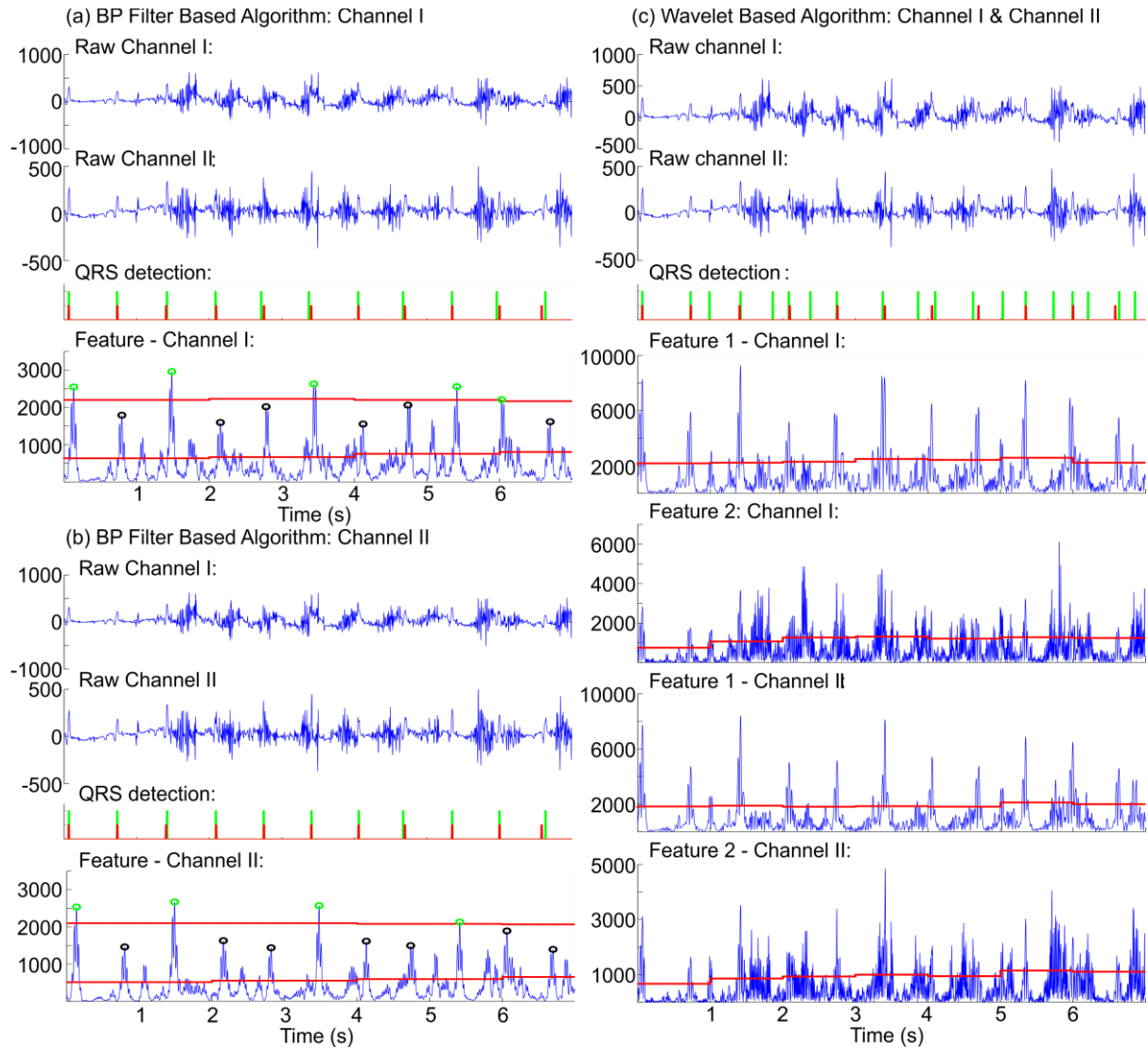

Figure 4.23: : Illustration of detection performance on record 14 from the eVDB during an episode of gardening: (a) Performance of the single-channel algorithm applied to channel I, (b) Performance of the single-channel algorithm applied to channel II, and (c) Performance of the multi-channel wavelet based algorithm. The horizontal red lines indicate the appropriate threshold values. The vertical red lines indicate the position of QRS complexes in the reference annotations. The vertical green lines indicate the QRS positions detected by the different algorithms. In (a) and (b), the green circles indicate QRS complexes detected using T_{high} (algorithm mode 1) and the black circles indicate QRS complexes detected using T_{low} during search back (algorithm mode 2).

When discussing the performance in noisy segments, it should be noted that future work could include specific noise stress tests of the algorithm. In our study, we include artifacts from normal daily life activities (especially in the eVDB), but the investigation of algorithm performance during specific types and amounts of artifacts could be further investigated. In noisy data segments there is always a risk of obtaining a high number of FP or FN detections. In these cases, this might disturb the adaptive parts of the algorithms. This might exacerbate poor performance. However, as mentioned earlier, this might be accounted for in future versions by implementation of sophisticated channel exclusion measures.

4.5.2.4   Discussion of the Feature Extraction Methodology

For the feature extraction step, we investigated the well-known and accepted wavelet decomposition and a novel designed cascade of simple FIR filters. One of the motivations for designing the novel filter system was to directly achieve an appropriate feature signal without the additional computations required to combine information from different wavelet sub-bands and without the requirement for further processing of the feature signal before the detection step. Both these purposes were achieved with the novel filter system. This can partly be explained by comparing the amplitude characteristics of the two filtering schemes (see Figure 4.24). It is observed that the novel resulting BP filter obtains a sharper passband for the relevant frequencies that any of the wavelet sub-bands.
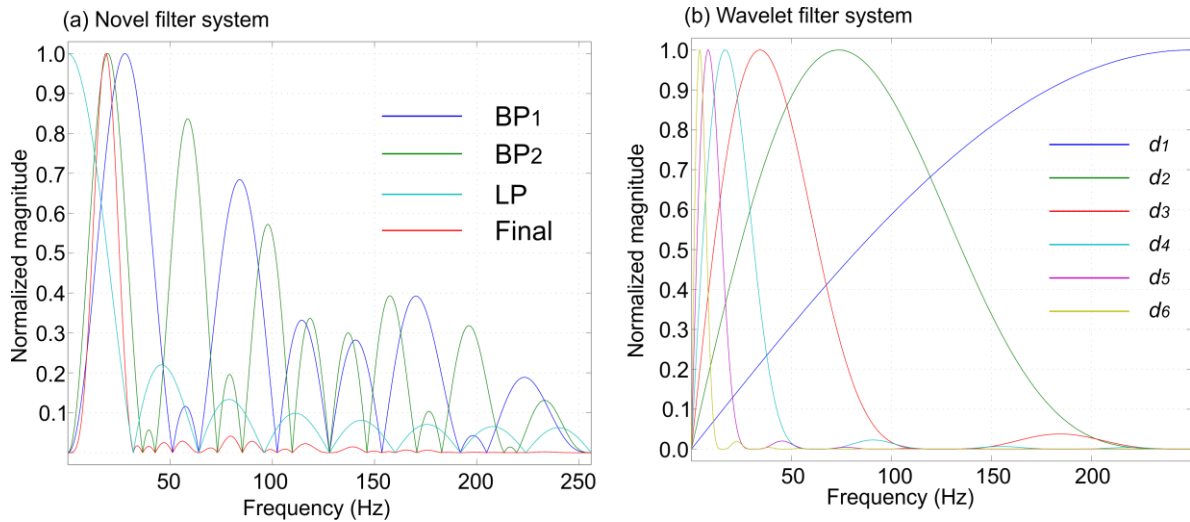
Figure 4.24: Comparison of the amplitude characteristics for the two filtering system. (a) The novel cascade of filters (sampling frequency: 512 Hz). (b) The wavelet decomposition system (sampling frequency: 500 Hz).

Table 4.10 contains a comparison of the computational load required for the two filtering schemes. To obtain an impression of the overall algorithm burden, we have also included the BP filter applied before the wavelet decomposition and the smoothening filter applied in the second proposed algorithm. The exact power consumption of each algorithm depends on the implementation and realization of the algorithm. However, it is observed that the computational profile is slightly different, but comparable, for the two systems. As mentioned earlier, the wavelet decomposition is generally characterized by a good compromise between high detection performance and possibilities of efficient hardware implementation [29]. We have thus designed a novel filter system with the same low computational burden, but our filter system has the advantage of providing a smooth feature signal that can be applied for QRS complex detection directly without any additional combination of information from different sub-bands, additional confirmation blocks, or other computationally demanding detection methodologies. This reduces the overall computational burden of the second proposed algorithm. Furthermore, we found that the embedded implementation of the second proposed algorithm was able to perform real-time QRS complex detection with high clinical performance without significantly reducing the total recording time of the ePatch sensor. This algorithm thus complies with our definition of acceptable power consumption. For an application that requires reliable embedded detection of heartbeats with low computational load, we therefore recommend applying this filter system. Furthermore, it should be noted that the single-channel algorithm based on the novel filter system actually obtains higher performance on the two standard databases than many of the wavelet based algorithms from the literature. However, in some situations it might still be advantageous to apply the wavelet decomposition. Several studies have obtained good delineation results with respect to detection of P- and T-wave fiducial points using the wavelet decomposition. If this is desired, it might therefore be considered to apply the wavelet decomposition in spite of the described advantages of the novel designed cascade of filters. As discussed earlier, the single-channel BP filter based algorithm generally obtains higher detection performance with respect to the detection of abnormal beat morphologies. However, it is difficult to decode how this result is influenced by the filtering scheme, the search back methodology, and the number of channels applied, respectively. Overall, our recommendation is to apply the novel cascade of FIR filters for embedded heart beat detection in the ePatch sensor.

However, it should be mentioned that further investigations should be conducted in order to update the novel filter system to handle different sampling frequencies if this is required.

Table 4.10: Comparison of the computational complexity of the two proposed algorithms. For the wavelet decomposition, we have included the requirements for calculation of the sub-band applied in the proposed wavelet based algorithm ($a_1 - a_4$, d_1, d_2, d_4, and d_5).

	Total filter coefficients	Memory requirements	Non-zero coefficients	Multiplications and divisions with 2^n	Other multiplications and divisions
BP filter system					
BP$_1$	20	20	8	0	0
BP$_2$	28	20	8	0	0
LP	16	16	16	1	0
Smoothening	8	8	8	1	0
Total	72	72	40	2	0
Wavelet system					
BP	20	20	20	0	0
Decomposition to d_5	80	66	24	8	8
Total	100	86	44	8	8

4.5.3 Recommendations for Real-Time Embedded Heart Beat Detection in ePatch ECGs

Based on the above discussions, it is recommended to apply a single-channel based algorithm for real-time embedded heart beat detection on ePatch ECGs. From the data investigated in this study, there is no apparent difference between detection on the two recorded ePatch ECG channels and the information obtained from the two different channels thus seem to be redundant with respect to automatic QRS complex detection. It is furthermore recommended to apply the computationally efficient BP filter approach where a suitable feature signal is obtained directly. For the detection block, it is recommended to apply two adaptive thresholds in a search back scheme. It is not considered necessary to implement additional confirmation blocks. However, it is recommended to explore the possibilities for improvements based on refined signal quality measures that might serve to avoid false detections during extreme episodes of artifacts and decrease the algorithm recovery time after such noisy events. New sensitive channel exclusion measures might be explored to further improve the performance of the shutdown mechanism. Furthermore, the exact delineation of the R peaks has not gained much attention in this thesis. For some applications, the exact position of the R peak is not important. In other applications it might be crucial. It is therefore recommended to continue with analysis of the delineation capabilities. The delineation performance of the algorithm might be improved by improving the delineation block. This should not necessarily affect the performance of the remaining parts of the algorithm. Finally, it is recommended to conduct controlled noise stress tests of the implemented algorithm to gain specific knowledge about the types and amounts of artifacts than can be handled satisfactorily. In this study, the noise tolerance has been investigated to some extend with the eVDB. It is expected that a high number of normal daily life activities are present in this database, but a specific noise stress test would be interesting.

4.6 Conclusions

In this chapter, we have investigated the possibilities of real-time embedded heartbeat detection in the ePatch sensor. Based on experience from the ePatch recordings, we defined a set of algorithm requirements that we sought to fulfill throughout the design phase. However, it was not only a priority to provide new knowledge about automatic signal processing in the ePatch ECGs. It was also a priority to provide new knowledge related to the similarity between ePatch ECGs and traditionally recorded ECGs, the potential redundancy of the second ePatch channel, and the general ability to obtain high clinical performance in a real-life environment.

One of our key findings was thus that it was possible to design automatic QRS complex detection algorithms that obtain high clinical performance on both ePatch ECGs and ECGs recorded with traditional equipment. This indicates some degree of similarity between the different ECGs from an algorithm point-of-view. However, it remains to be investigated whether algorithms designed and optimized for traditional ECGs also obtain high performance on ePatch ECGs. This discussion is highly relevant for the potential difficulties associated with the large-scale implementation of the ePatch recorder as a substitute for today's Holter devices in the future. Another key finding was that information provided from the two simultaneously recorded ePatch channels is redundant in most cases. This indicates that only one channel is required for reliable QRS complex detection in ePatch ECGs. This further indicates that for some applications it might be sufficient to record and store a single ePatch ECG channel in the future. This would significantly decrease the power consumption of the system.

During the project, we designed two novel algorithms and especially the second proposed algorithm obtained very high clinical performance (Se = 99.86% and P^+ = 99.74% on more than 950,000 manually annotated beats obtained from 198 different patients). This algorithm was based on a novel computationally efficient cascade of FIR filters that directly obtain a smooth feature signal that can be applied as input to the detection step. We furthermore refined the well-known search back mechanism and designed novel computationally simple methods for calculation of the adaptive thresholds. The detection performance with respect to abnormal beat morphologies is also considered very high. Furthermore, a high number of artifacts were included in the five different databases. Based on our databases, we thus find that it was possible to obtain a high tolerance to artifacts and still obtain high detection performance with respect to abnormal beats. This was partly obtained by the novel filter system and the refined search back procedure. We furthermore evaluated an embedded implementation of the algorithm to investigate the power consumption. We defined an acceptable computational load based on the algorithm's influence on the total recording time of the current version of the ePatch. We found that the theoretical maximum reduction in the recording time for the embedded implementation of the second proposed algorithm was approximately 5.5%. We found this within the acceptable limits. We thus conclude that it was possible to design a novel algorithm with high clinical performance and with low computational costs.

Overall, our impression is thus that the single-channel BP filter based approach obtains excellent results on both ePatch ECGs and standard databases. The high performance on both normal and abnormal beat morphologies as well as episodes of normal daily life activities, and the possibility of embedded implementation opens possibilities of real-time monitoring of clinically relevant parameters like HR curves, rhythm analysis, and detection of cardiac events on patients outside the hospital setting. This might help to improve the diagnosis and treatment of patients with varying life threatening diseases in the future.

5 Automatic ECG Quality Estimation

Objectives: The advantages of the novel patch-type ECG recorders are irresolvable conditioned by their ability to obtain high-quality diagnostic ECGs throughout the recording period. However, this ability might be decreased due to the short inter-electrode distance and the increased possibility of performing normal daily life activities that might produce a high number of artifacts. The purpose of this part of the study was thus to investigate whether the advantages of the novel ePatch recorder is counterbalanced by low signal quality.

(a) Sitting comely without movements
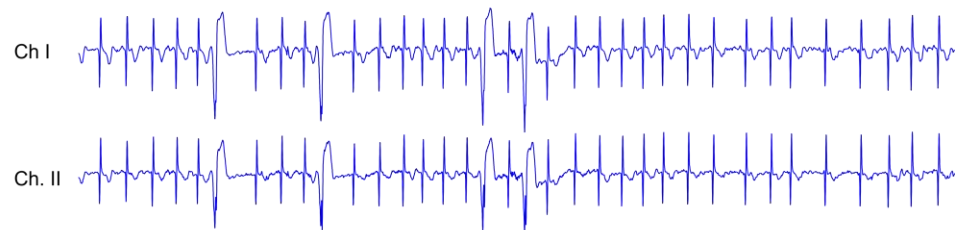
(b) Physical activity, e.g. gardening
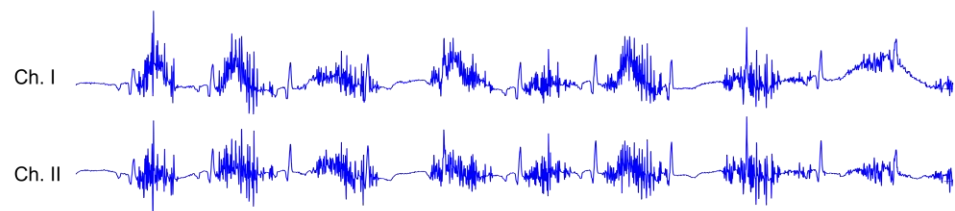
Figure 5.1: (a) Illustration of an artifact-free ECG segment of high quality. The rhythm is observed to be AF with scattered VEBs. In a traditional Holter recording, the patient is wired up and therefore naturally hindered in high intensity physical activity that might produce significant amounts of artifacts in the recorded ECG. (b) The increased patient comfort and possibility to perform normal daily life activities might increase the number of artifacts in the ePatch recordings. Modified from [39] and [40].

5.1 Background

The advantages obtained from the implementation of the novel patch-type ECG recorders are expected to highly increase the diagnostic possibilities in the future. However, outpatient ECG monitoring remains to be sensitive to artifacts arising from normal daily life activities that neither can nor shall be avoided during long-term recordings. The advantages of novel patch-type ECG recorders are thus irresolvable conditioned by the assurance of the ability to obtain high-quality diagnostic ECGs throughout the recording period. This ability has been questioned in the literature [1]. Furthermore, as mentioned earlier, the patch designs impose much less restrictions to normal daily life activities compared to the traditionally wired Holter recordings. This is, of course, an advantage for the patients, and this feature facilitates the possibility of prolonged continuous monitoring without the need for implantable devices. The diagnostic advantages of the prolonged monitoring have been investigated for the ZioPatch ECG recorder in a number of studies. They found that an extended monitoring period resulted in an overall higher diagnostic yield, the detection of more significant arrhythmias, and a higher degree of definitive diagnosis compared to the traditional Holter recordings [2], [7], [9]. However, the increased number of daily life activities also imposes an inevitable risk of an increased amount of artifacts that might interfere with the clinical interpretation of the recorded ECGs. It is therefore highly relevant to investigate the ePatch recorder's vulnerability to noise and the actual analyzable time obtained in ePatch ECG recordings. The research discussed in this chapter is also addressed in Paper VI and Paper VII.

5.1.1 Research Hypothesis

The above described discussions lead to the formulation of the following questions that will be investigated and discussed throughout this chapter:

1. How can we define ECG quality?
2. Is it possible to obtain sufficient signal quality for clinical applications of ECGs recorded with the ePatch system?
3. Is it possible to design novel biomedical signal processing algorithms for the automatic estimation of ECG quality?

5.1.2 Literature Overview

The literature review for this part of the project covers two different areas. The first literature review was focused on studies investigating the analyzable times obtained in patch recordings. Only a few studies were found to address this important area. One study states that they obtained a median analyzable time of 99% (interquartile range: 94% to 99%) and that 87.1% of the patients obtained an analyzable time equivalent to ≥22 hours/day using a patch-type ECG recorder [2]. A recently published study furthermore showed that 69% of data recorded by another patch-type ECG recorder during different activities were of at least moderate quality [41]. Both these studies indicate the potential for clinically acceptable analyzable times in patch recordings, but the literature review definitely leaves room for new knowledge gained from the analysis of the analyzable time obtained by the ePatch recorder.

The other part of the literature review was focused on the design of algorithms for the automatic estimation of ECG quality. Many of the published papers in the field of automatic ECG quality assessment are related to the Physionet Challenge from 2011. In this challenge, 10-second 12-lead ECG recordings should be classified as "acceptable" or "non-acceptable." The original challenge obtained a high number of participants of which nine groups achieved an accuracy of 90–93.2% on unknown test data [42]. Generally, the existing quality assessment algorithms can be divided into two steps: The feature extraction step and the classification step. The underlying assumptions in the feature design step can be further divided into three different paradigms. The first paradigm aims at designing individual features for the detection of specific artifact types. This could include features designed for the detection of missing leads or flat lines [43]–[47], detection of peak or spike artifacts [46], [47], detection of power line interference [43], [46], detection of baseline wandering [43], [45], [46], or detection of muscle artifacts [43], [46]. The second paradigm includes features designed to capture general statistical differences between clean and noisy ECG segments. Examples of these features include skewness [45], kurtosis [45], [48], Shannon entropy [49], mean value [49], and variance [49]. The third paradigm includes features designed to recognize the

characteristic appearance of a clean ECG segment. This includes features like the comparison of multiple automatic beat detection algorithms [45], [48], beat detection comparison in different leads [45], [48], regularity of detected QRS complexes [47], and the relative spectral power in the region of the QRS complexes (5-14 Hz) [44], [45], [48]. For the classification step, some studies applied empirically found thresholds compared to each feature individually [46], [47], [49], whereas other studies apply more sophisticated classification schemes, e.g., the matrix of regularity defined in [44] or the support vector machine (SVM) and the multi-layer perceptron neural network investigated in [45]. It is not surprising that the highest accuracies were found for algorithms with the more advanced classification schemes.

5.1.3   Description of Project Workflow

In the beginning of this part of the project, our approach reflected a quite traditional engineering mind-set. This approach was highly inspired from the literature review. Our original paradigm was to detect artifacts as undesired events occurring in the long-term ECG recordings. Our goal was therefore to design automatic algorithms that could detect these artifact events. We therefore sought to define and characterize the appearance of the most dominant ECG artifacts: power line interference, interference from muscle activation, baseline wandering, and electrode-motion artifacts. We then attempted to design features for the automatic identification of each of these artifact types in an "event detection" scheme. This is somehow similar to the first feature extraction paradigm described in the literature overview. This paradigm can be characterized as a "shutdown" approach that could ensure the exclusion of potentially noisy segments. As discussed in chapter 4, this could, for instance, be applied to "protect" subsequent automatic algorithms from false detections and incorrect adaptation to extremely noisy segments. Furthermore, we expected that this paradigm might be able to provide new knowledge about the distribution of different artifact types in ePatch recordings. However, using this approach, the performance of the algorithm is naturally limited by the types of artifacts that are accounted for in the feature design phase. We found that the generalization of such an algorithm therefore highly depends on the representation of sufficient amounts of all likely artifacts in the training database. Furthermore, it soon became clear to us that ECG quality is highly subjective and dependent on the desired application of the recorded signals. Therefore, it became important to think more carefully about our definition of ECG signal quality. To accomplish this, we sought information from a number of sources:

- We went through relevant literature to obtain an overview of how other research papers define quality.
- We gained information from our own work with automatic heartbeat detection as described in chapter 4. This experience provided valuable information about where automatic algorithms might fail.
- We visually investigated a high number of long-term ePatch recordings to obtain experience and knowledge about the general quality and the common artifact types.
- We had fruitful discussions with cardiologists and other medical doctors regarding their evaluation of specific ECG segments and hereby learned how they visually analyze each segment. This provided immeasurable information about the specific ECG patterns that should be visible for reliable heart rhythm analysis and, hereby, the correct diagnosis of the patients.
- We watched experienced ECG technicians analyze traditional Holter recordings and create analysis reports. This process again provided us with immeasurable information about the types, amounts, and duration of artifacts that makes clinical interpretation difficult.

We learned that, during clinical ECG interpretation, the human experts (e.g. ECG technicians and cardiologists) are accustomed to recognize artifacts and conduct the interpretations based on periods with diagnostic ECG. This includes "looking through" short periods of data with even pronounced amounts of artifacts and still being able to interpret the underlying heart rhythm with certainty. This is possible due to contextual information provided from periods of diagnostic ECG surrounding the artifact event. This implies that short periods of even very pronounced amounts of artifacts might not interfere with the clinical interpretation of the ECG. This is illustrated in Figure 5.2. It is observed how short-duration artifacts do not interfere with the clinical interpretation, whereas similar long-lasting artifacts preclude clinical interpretation. This illustrates the issue with considering the quality estimation process as an "event detection" problem: It is very difficult from

an engineering point of view to define and reproduce the exact amount and duration of any type of artifact that affects the clinical interpretation of the ECGs. Furthermore, the ECG is often affected by small amounts of several different types of artifacts. This might also go unnoticed by a "noise detection algorithm." We therefore decided to change our understanding of the problem and consider it from a more clinical point of view. This learning process led to the formulation of two different definitions of acceptable signal quality:

1. The quality of an ECG segment is acceptable when no significant artifacts are present.
2. The quality of an ECG segment is acceptable when the heart rhythm can be analyzed with certainty.

The first definition is highly related to the "artifact event" detection approach. In our study, we found the second definition more clinically relevant, and we therefore adopted this definition in our work. As described above, we furthermore learned that it is important to include adequate contextual information and consider each potential artifact event together with information about the quality of the surrounding ECG segments. This also implied that we became more interested in features from the second and third paradigm described in the literature overview. This type of features attempts to characterize the known characteristics of a clinically useful ECG segment rather than specific artifact types. The original work where we attempted to apply a "noise event detection" approach according to the first definition of ECG quality is not further described in this thesis.
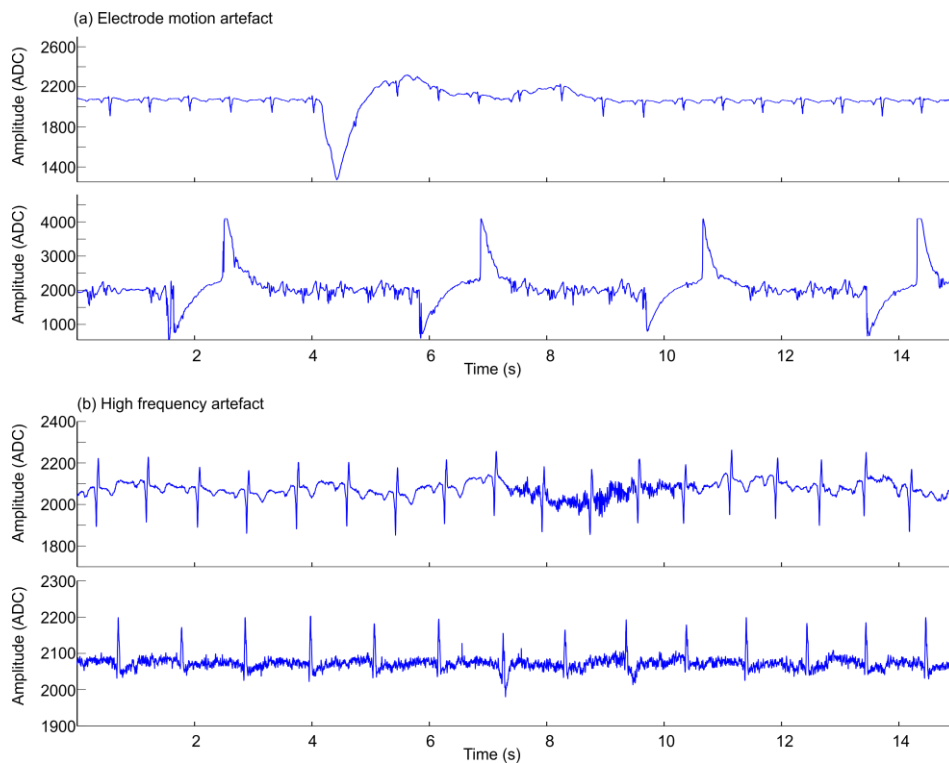

Figure 5.2: Illustration of the influence of different types of artifacts. (a) illustrates two different electrode-motion artifacts. The artifact in the top plot is surrounded by high-quality ECG, and the rhythm is observed to be NSR. This artifact does not interfere with rhythm analysis. In the lower plot, the artifact is repeated. This renders the segment useless for both rhythm analysis and reliable estimation of the HR. (b) illustrates two different high frequency artifacts. The artifact in the top plot is surrounded by high-quality ECG, and the rhythm is observed to be NSR. Thus, this artifact does not interfere with the clinical interpretation. In the lower plot, the artifact lasts throughout the duration of the segment. This implies that it is impossible to decipher the presence/absence of P-waves with certainty. Rhythm analysis is therefore not possible in this segment, but reliable HR estimation is.

We found that it was crucial to ensure that we conducted our analysis on a database with realistic amounts of abnormal beat morphologies as well as a high number of expected normal daily life activities. We furthermore found that some of our real-life ePatch recordings were of poor quality throughout the recording period. This would completely prevent clinical

interpretation and is thus highly undesirable. This would especially be problematic for long-term recordings without telemetry feedback. We therefore found it relevant to keep in mind that future applications of our designed algorithms might serve as "red flags" that could be turned on during a recording if the quality remained poor for extended periods of time. This could be obtained by the embedded implementation of a quality assessment algorithm. We therefore defined the following requirements for our final quality estimation algorithm:

1. The algorithm should obtain high performance with respect to the correct estimation of the percentage of analyzable time (PAT) in ePatch recordings. This feature is applied to gain new knowledge about the general quality obtained in patch recordings.
2. The algorithm should be able to point out specific areas of high and low qualities. This could be used to save time during manual analysis by only investigating periods with analyzable data.
3. The algorithm should be designed using computationally efficient features that might be embedded in future versions of the ePatch. This could allow a "red flag" or warning system against poor quality during the recording.

5.1.4 Chapter Overview

As described above, the research presented in this chapter was characterized by an important learning process that led to a clinically relevant understanding of ECG quality. Furthermore, it should be noted that this research field is much less described in the literature than the field of automatic heartbeat detection presented in chapter 4. The research in this field is thus not pushed forward and helped along by a number of available standard databases that facilitate easier understanding of the important aspects of the field and definitions for the evaluation and comparison of algorithm performances. It was therefore natural that we initiated the project by the design of a preliminary algorithm based on the ePatch databases available in the beginning of the project. We then refined this algorithm based on a new manually annotated ePatch database later in the project. The preliminary algorithm is briefly presented in section 5.3, and the refined algorithm is presented in detail in section 5.4. The refined algorithm was then applied to investigate the overall PAT obtained in a high number of ePatch recordings. This is described in section 5.5. As mentioned, a major part of this project was to extract relevant databases that can provide a reliable investigation of the diagnostic quality obtained in the ePatch recordings. This topic is therefore described first.

5.2 Description of Databases

For this project, we applied 250 long-term ECG recordings from four different existing databases. An overview of the four databases is provided in Table 5.1. All patients from the Stroke Database (STRDB) were admitted after an episode of stroke, the Telemetry Database (TDB) contains recordings from patients who were admitted and selected for regular telemetry monitoring, the patients from the Cardio-Respiratory Monitoring Database (CRMDB) were monitored ambulant as a part of diagnosing potential obstructive sleep apnea, and the Fitness Database (FDB) contains ambulatory recordings from subjects recruited in a fitness study [50]. The patients from the first two databases are thus considered a high-risk population with respect to the presence of abnormal heart rhythms, especially atrial fibrillation, whereas the recordings from the last two databases are expected to represent patients with a high prevalence of physical activity during the recording period. This database selection is thus expected to ensure a small overrepresentation of both arrhythmia events and episodes of artifacts arising from everyday activities. This ensures a very realistic investigation of the diagnostic quality obtained in 24-hour ePatch recordings.

It should be mentioned that the ePatch Training Database (eTDB) described in section 4.2.3 was extracted from the CRMDB and the STRDB. Each ECG recording in these two databases was associated with a full ECG analysis report (similar to a traditional Holter analysis report). These reports were created by experienced ECG technicians, and they were applied during the diagnosis of the patients. As mentioned, these highly trained ECG technicians are accustomed to recognize disturbances as noise and conduct the interpretation on clean data segments. However, when the general signal quality of a recording is decreased enough to interfere with the clinical interpretation, thus inducing uncertainty about the analysis, the nurses write remarks of this in the analysis reports. These subjective and spontaneous comments on potentially low signal

quality were therefore available for these two databases. Furthermore, a grading of each recording according to the following scheme became available during the project:

- Grade 0: Useless recording, no diagnosis was possible
- Grade 1: Almost useless recording, only possible to identify HR from QRS complexes
- Grade 2: Generally too much noise to allow full diagnosis
- Grade 3: Periods with too much noise or noise that, in general, disturb the diagnosis
- Grade 4: A few episodes of noise that disturb the ECG morphology
- Grade 5: Noise-free recording or recording with only movement artifacts

The ECG analysis reports were available from the beginning together with the ECG recordings, but the quality assessments described above were provided to us later. No additional information was available about the quality in the recordings from the TDB and the FDB. The length of each recording was found by visual inspection of the relevant data file.

Table 5.1: Patient demographics for each of the four original databases.

	STRDB	CRMDB	TDB [e]	FDB	Total
Patients [a]	84	84	50	32	250
Length (hours) [b]	20.3±6.7	18.3±3.6	23.2±3.4	23.8±1.9	20.7±5.1
Gender [c]	M: 64	M: 46	M: 27	M: 3	M: 140
	F: 20	F: 38	F: 22	F: 29	F: 109
Age (years) [d]	49.7±13.4	65.5±16.2	72.6±13.1	61.4±9.2	61.0±16.4

[a] Number of patients

[b] Recording length stated as mean ± standard deviation

[c] Gender: M = males; F = females

[d] Age stated as mean ± standard deviation

[e] Information about gender and age is missing for one subject

5.3 Preliminary Algorithm for ECG Quality Estimation

The first preliminary version of our quality estimation algorithm was designed to classify entire long-term ECG recordings into two groups: "good" and "bad" recordings. We defined a "bad" recording as a recording where the experienced ECG technician made comments on bad quality in either one or both channels in the analysis report. On the other hand, a "good" recording was defined as a recording without comments on quality or positive comments regarding high quality. This algorithm was thus intended to mimic these subjective spontaneous comments on noise levels. This choice reflected both the available manual annotations in the beginning of the project (the analysis reports were provided from the beginning) and the above discussed requirement for contextual information when defining ECG quality. To our best knowledge, this is the first study investigating the possibility of an automatic method for the determination of the overall signal quality in entire long-term ECG recordings. The clinical applications of such an algorithm might include a fast and robust possibility to compare the quality of different recording techniques and a possibility to avoid wasting time on the manual analysis of a useless recording. Furthermore, the design of this algorithm was used to gain inspiration and knowledge for the design of our final proposed quality estimation algorithm. A brief summary of the results obtained in this study is provided in the next sections, whereas a detailed description is provided in Paper VI.

5.3.1 Description of Database

We randomly extracted 20 "bad" and 20 "good" recordings from the CRMDB. We chose recordings from the CRMDB to ensure a high frequency of normal daily life activities in the recordings. Furthermore, to ensure inclusion of both very clean and normal recordings, the 20 clean recordings were extracted as five random recordings with remarks on good quality and 15 random recordings without remarks on quality.

5.3.2 Description of Algorithm

An overview of the algorithm is provided in Figure 5.3. The input is a two-channel ePatch ECG signal, and the output is a classification of the entire recording as being either "good" or "bad." The first feature, F_1, was based on the percentage of saturated samples in the recording. Saturation is never intended in an ECG signal, and it is therefore expected that the signal would always be noisy when this feature was high. However, this feature proved redundant when the other features were optimized, and it was therefore excluded from the final algorithm described in section 5.4. The second feature, F_2, is a measure of how often the mean value of the scaled rectified ECG signal exceeds a pre-defined threshold. The third feature, F_3, is a measure of how often the number of significant signal peaks exceeds a pre-defined threshold. Both these features were optimized and included in the final version of the algorithm. The optimized versions of these features are therefore further described in section 5.4. For the classification task in this pilot study, we applied a simple Bayes classifier.
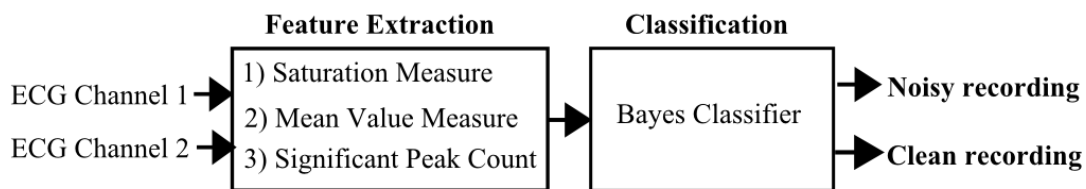
Figure 5.3: Schematic overview of the first preliminary quality estimation algorithm. The input to the classification scheme is three feature vectors describing the overall amount of noise based on contextual information from the entire recording.

5.3.3 Results

The algorithm performance was evaluated in terms of the sensitivity (*Se*), specificity (*Sp*), and accuracy (*Acc*) as defined in (5.1) – (5.3), where TP is the number of clean recordings correctly classified as clean (true positive), TN is the number of noisy recordings correctly classified as noisy (true negative), FN is the number of clean recordings wrongly classified as noisy (false negative), and FP is the number of noisy recordings wrongly classified as clean (false positive). Due to the intermediate number of recordings in this pilot study, the performance was evaluated by a five-fold cross validation. Each fold consists of training the classifier on 32 recordings (16 from each class) and testing the performance of the obtained classifier on the remaining eight recordings. The training and test performances for each fold, as well as the average performances, are provided in Table 5.2.

.

$$Se = \frac{TP}{TP+FN} \cdot 100\% \tag{5.1}$$

$$Sp = \frac{TN}{TN+FP} \cdot 100\% \tag{5.2}$$

$$Acc = \frac{TP+TN}{TP+TN+FP+FN} \cdot 100\% \tag{5.3}$$

Table 5.2: Performance Evaluation of the preliminary quality estimation algorithm. Training data: *. Test data: ¤.

	Se*	Sp*	Acc*	Se¤	Sp¤	Acc¤
Fold 1	93.8%	81.3%	87.5%	100%	75%	87.5%
Fold 2	93.8%	87.5%	90.6%	75%	100%	87.5%
Fold 3	93.8%	87.5%	90.6%	100%	75%	87.5%
Fold 4	93.8%	93.8%	93.8%	100%	75%	87.5%
Fold 5	93.8%	75.0%	84.4%	100%	100%	100%
Average	93.8%	85.0%	89.4%	95%	85%	90%

5.3.4 Discussion

The proposed novel algorithm is capable of obtaining an average accuracy of 90% on the test data. This is considered a high clinical performance. It should be stated that this high performance is obtained on clinically relevant ambulatory ECG recordings acquired from real patients in their homes. This was chosen to ensure a realistic amount of abnormal heart rhythms and beat morphologies. It is, of course, very important to ensure that automatic noise classification algorithms will not classify a recording with a high number of abnormal beat morphologies as noisy. However, it should be noted that no specific test was conducted to ensure this, and this should be conducted in future studies. In general, it should be mentioned that the findings should be validated on a larger database to ensure the applicability in the general population or in specific high-risk patient groups. However, due to the apparently high clinical performance of the algorithm, this novel approach to the quantification of noise levels in entire ECG recordings is expected to be useful in many different applications. As mentioned, it is extremely important to gain solid knowledge related to the benefits and drawbacks of the new technologies for long-term ambulatory ECG monitoring in different situations. Choosing the right device in each application can increase the diagnostic yield and decrease the burden on the patients and the health care facilities. An automatic classification of entire ECG recordings provides the possibility of an objective and fast assessment of the clinical quality of a high number of ECG recordings acquired using the different technologies. This could provide important information to answers related to the benefits and drawbacks of the new technologies. Another application scenario is related to the pre-screening of recordings before the manual analysis. If a specific recording is classified as being very noisy, it might be beneficial to exclude the recording from manual analysis to increase the efficiency of the health care facilities. From this study, we thus learned that it is possible to achieve a high clinical classification performance using a relatively simple automatic algorithm and contextual information from entire ECG recordings. This strengthened our assumption regarding the inclusion of contextual information instead of the originally investigated "artifact event detection" paradigm. It furthermore inspired us to improve the algorithm further. We found that it would be interesting to investigate the possibilities of providing continuous quality indexes instead of only a classification into either a "bad" or a "good" recording. This would also render the algorithm even more applicable with respect to the above mentioned application scenarios. We furthermore learned that two of the designed features (F_2 and F_3) were very promising, and we therefore decided to explore them further in the new algorithm. Not surprisingly, these features both belong to the second feature extraction paradigm described in the literature review. The design and validation of the finally proposed quality assessment algorithm is described in detail in the next section.

5.4   Design of Automatic Algorithm for Estimation of Percentage of Analyzable Time

This algorithm was designed to allow an investigation of the overall percentage of analyzable time (PAT) obtained in the ePatch recordings. This investigation is highly important to gain new knowledge about the practical usability of the technology in a clinical setting. The algorithm was designed based on the earlier described assumption about the requirements regarding adequate contextual information and knowledge from the design of the preliminary algorithm. Furthermore, we kept the algorithm requirements formulated in section 5.1.3 in mind. The algorithm design and performance is described in detail in the next sections. This work is also presented in Paper VII.

5.4.1   Description of Algorithm

To allow the estimation of the overall PAT, we divided the long-term recordings into several smaller non-overlapping segments and automatically assigned each of these segments to one of the two classes: "analyzable" (class I) or "non-analyzable" (class II). As illustrated in Figure 5.4, this procedure facilitates the easy evaluation of the overall PAT. As discussed in section 5.1.3 and learned from the high classification performance obtained by the preliminary algorithm, we found that the diagnostic quality of any ECG segment is best characterized when enough contextual information is included. The selection of segment length was therefore a compromise between including adequate contextual information (longer segment lengths) and keeping a high "resolution" of the overall estimated PAT (shorter segment lengths). Furthermore, it is our experience that the types of activities that would often cause artifacts that could significantly impair clinical interpretations occur on the scale of several minutes. This could, for instance, include running on stairs, carrying shopping baskets, or exercising. We therefore subjectively decided to apply segments of 10 minutes. We found this segment length to provide a good compromise. The proposed quality assessment algorithm is based on three carefully designed features and an SVM classifier. The algorithm design is described in detail in the next sections.
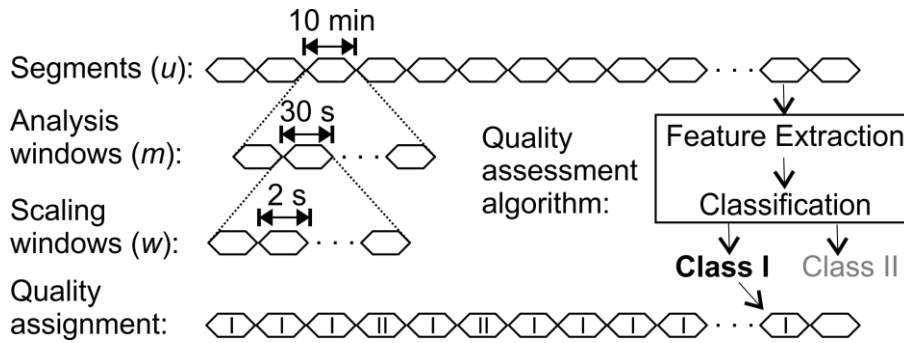

Figure 5.4: The long-term recordings were divided into smaller non-overlapping segments, u. Each segment was then classified as being either analyzable (class I) or non-analyzable (class II) using our proposed quality assessment algorithm. The algorithm is based on three features and an SVM classifier. The input to the quality assessment algorithm is a two-channel ECG segment, and the output is an assignment to one of the two classes. For the calculation of F_1 and F_2, each segment was further divided into smaller analysis windows, m. For the calculation of F_2, each analysis window was also divided into even smaller scaling windows, w. This segment division is further described later.

5.4.1.1   Feature Extraction

All three features were designed to obtain small values (close to 0) for the analyzable ECG segments and high values (close to 1) for the non-analyzable ECG segments. The first two features, F_1 and F_2, were designed to measure the quality of the important isoelectric line. These features thus fall in the second feature extraction paradigm described earlier. Simpler variations of these features were applied in the preliminary algorithm. The third feature, F_3, was based on the assumption that the performance of an automatic QRS complex detection algorithm depends on the quality of the ECGs. This feature thus belongs to the third feature extraction paradigm. Variations of this feature were also investigated in [43], [45], [48]. In our implementation, an automatic QRS complex detection algorithm was applied to estimate R peak positions in each channel individually, and the similarity obtained between the two channels was applied for the calculation of F_3. Figure 5.5

contains ECG snippets from three different ECG segments. The final and temporary feature values obtained for each segment are furthermore provided in Table 5.3. The calculation of each of the stated features is described in detail in the following sections. It should be noted that the stated feature values are based on the entire 10-minute duration of each segment and not only the illustrated snippet. This is especially observed from segment C, where channel II apparently seems more noisy than channel I in the illustrated snippet, but it is observed from Table 5.3 that, based on the entire 10-minute segment, $F_{1,2} < F_{1,1}$ and $F_{2,2} < F_{2,1}$.

Table 5.3: Calculation of the feature values for each of the three ECG segments illustrated in Figure 5.5. The calculation of the features is described in the next sections.

Segment	$F_{1,1}$	$F_{1,2}$	F_1	$F_{2,1}$	$F_{2,2}$	F_2	FD/TP	η	F_3
A	0.00	1.00	**0.00**	0.00	1.00	**0.00**	0.41	0.28	**0.11**
B	0.00	0.00	**0.00**	0.00	0.00	**0.00**	0.00	0.92	**0.00**
C	0.45	0.20	**0.20**	1.00	0.90	**0.90**	0.60	0.99	**0.60**
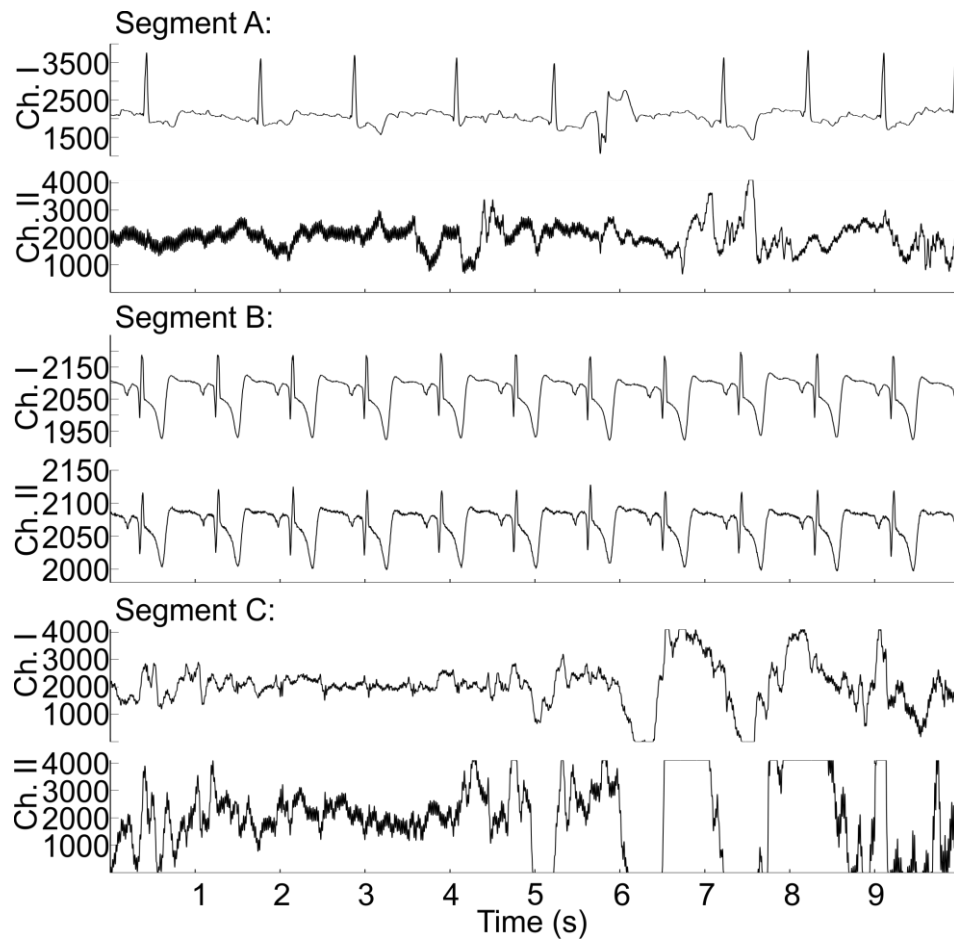
Figure 5.5: Illustration of three ECG snippets with different quality characteristics. The amplitudes are illustrated in ADC counts. Segments A and B were manually annotated to class I (analyzable), whereas segment C was manually annotated to class II (non-analyzable). It is noted that the rhythm in segment A is AF with a single VEB beat and segment B displays an example of NSR. The temporary and final feature values for each segment are provided in Table 5.3.

The first feature, F_1, provides a measure of the number of significant signal peaks observed in the current analysis window. It is expected that a noisy non-analyzable ECG segment obtains significantly more signal peaks than a clean segment. The 10-minute ECG segment was divided into smaller analysis windows, *m* (see Figure 5.4). The length of each analysis window was again a compromise between including adequate contextual information and obtaining a high "resolution" on the possible feature values. We therefore decided to apply analysis windows of 30 seconds, yielding a total of 20 windows (*M* = 20). For each analysis window, the number of significant signal peaks, $P_j(m)$, was estimated for each channel *j*. A significant signal peak was defined as any sample obtaining a higher value than the three previous and the three subsequent samples. For each channel, $F_{1,j}$ was calculated according to (5.4), where *logical{}* obtains the value 1 when the expression is true and 0 if otherwise. The threshold, T_1, was optimized using a parameter grid search described later. The final value of F_1 for each segment was defined as the minimum value obtained from the two channels (see (5.5)). This prevents the final feature value from being wrongly increased in cases where only one of the two channels obtains poor quality. An example of this is illustrated as segment A in Figure 5.5.

$$F_{1,j} = \frac{1}{M}\sum_{m=1}^{M} logical\ \{P_j(m) > T_1\} \tag{5.4}$$

$$F_1 = Min\{[F_{1,1}\ \ F_{1,2}]\} \tag{5.5}$$

The calculation of F_1 for a clean and a noisy ECG segment is visualized in Figure 5.6. It is observed how the noisy ECG segment contains a much higher density of significant signal peaks. This causes the value of F_1 to increase for the noisy segment compared to the clean segment.

5.4.1.1.2   Calculation of F_2

The second feature, F_2, was designed as a measure of the mean value of the baseline-corrected, rectified, and scaled ECG signal. This mean value is expected to be higher for noisy ECG segments than for an analyzable segment. The calculation of F_2 for a clean and a noisy ECG segment is illustrated in Figure 5.6. The baseline was removed to avoid the influence of high P- and T-waves and non-disturbing amounts of baseline wandering and electrode-motion artifacts. The baseline was estimated using a 32-point average filter. The baseline-corrected ECG signal, $ECG_{filt,j}$ was obtained by subtracting the estimated baseline from the raw ECG signal. Then, $ECG_{filt,j}$ was rectified. The baseline-corrected rectified ECG segment was termed $|ECG_{filt,j}|$. It is important to account for the known differences in the general amplitude in ECG recordings. A scaling parameter, $s_j(m)$, was therefore calculated for $|ECG_{filt,j}|$ in each analysis window. We decided to design the scaling parameter to theoretically obtain a value close to 1 in the R peak positions after the scaling of $|ECG_{filt,j}|$. This ensures that the mean value estimates the noise level relative to the R peak amplitudes. To achieve this, each analysis window was divided into even smaller scaling windows, *w* (see Figure 5.4). The length of each scaling window was chosen to be two seconds. This implies that at least one QRS complex is expected in each scaling window. In most scaling windows, the maximum value of $|ECG_{filt,j}|$ is thus expected to represent the amplitude of a QRS complex. The scaling parameter in the *m*'th analysis window was therefore calculated as the median value of the maximum value of $|ECG_{filt,j}|$ obtained from each of the 15 scaling windows. This calculation of $s_j(m)$ thus provides a reliable estimate of the general R peak amplitude in the *m*'th analysis window. The mean value of the scaled, rectified, and baseline-corrected ECG signal was calculated for each analysis window. This is defined in (5.6), where *N* is the total number of samples in each analysis window. For each channel, $F_{2,j}$ was then calculated according to (5.7). The threshold, T_2, was optimized by a parameter grid search described later. As for F_1, the final value of F_2 for each segment was defined as the minimum value obtained from the two channels (see (5.8)).

$$\mu_j(m) = \frac{1}{s_j(m)\cdot N}\sum_{n=1}^{N}|ECG_{filt,j}(n)| \tag{5.6}$$

$$F_{2,j} = \frac{1}{M}\sum_{m=1}^{M} logical\ \{\mu_j(m) > T_2\} \tag{5.7}$$
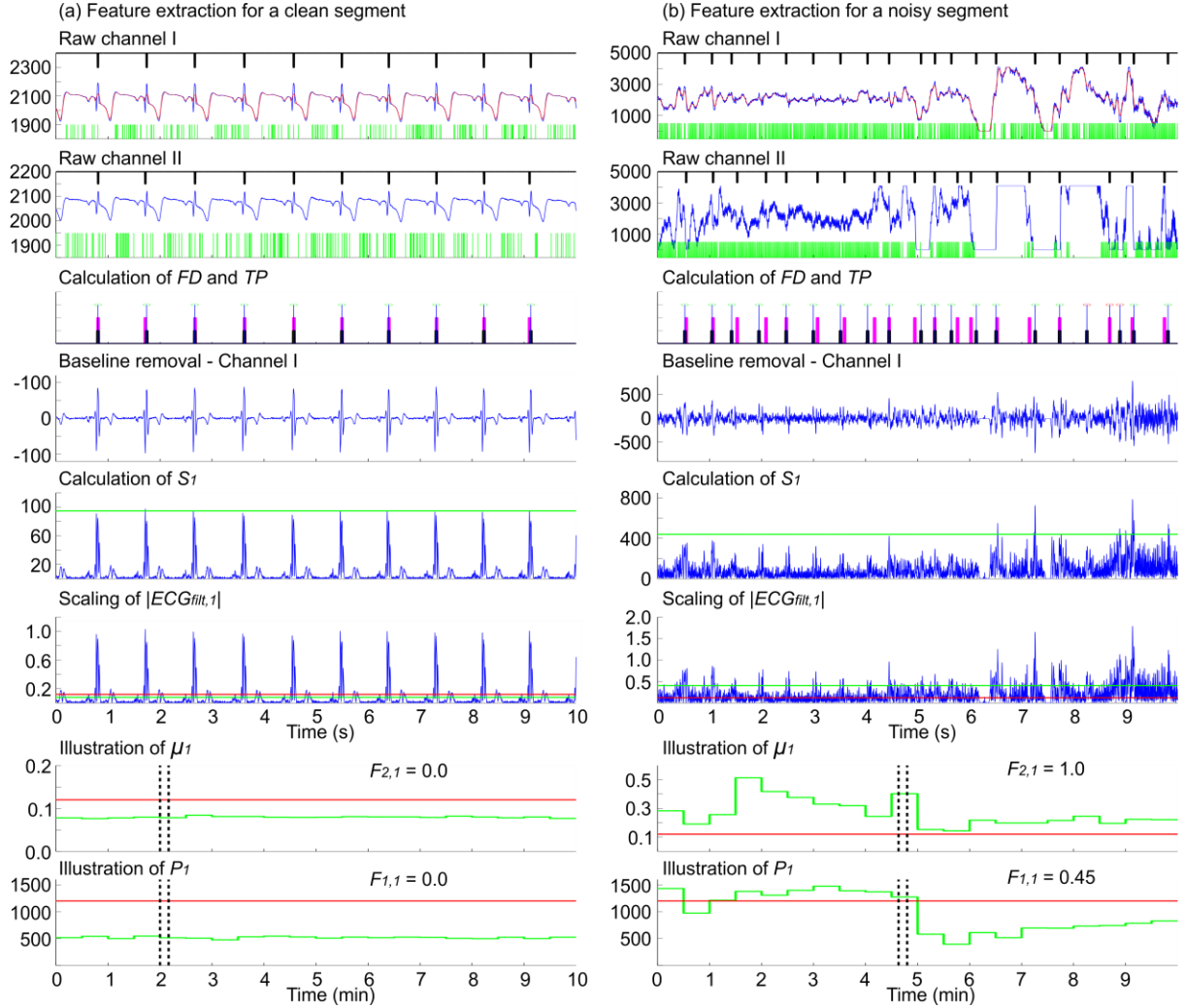
$$F_2 = Min\{[F_{2,1} \quad F_{2,2}]\}$$ (5.8)

Figure 5.6: Illustration of the feature extraction for a clean ECG segment (a) and a noisy ECG segment (b). It is noted that these are segments B and C from Figure 5.5, respectively. The top plots contain the raw ECG signals from channel I and channel II (blue lines), the estimated baseline for channel I (red lines), the positions of the QRS complexes detected in each channel individually (vertical black lines), and the positions of the significant signal peaks detected in each channel individually (vertical green lines). The green and black vertical lines are applied for the calculation of F_1 and F_3, respectively. The third plot illustrates the calculation of FD and TP. The black and magenta vertical lines indicate the detected positions of QRS complexes using channel I and channel II, respectively. The vertical blue lines indicate the common QRS positions obtained from the two channels. The green marks indicate QRS complexes detected simultaneously by both channels (counted in TP), whereas the red marks indicate non-simultaneous QRS detections (counted in FD). The influence of the 150-ms match window in the pairing step is observed in (b). The feature values obtained by the entire 10-minute segments were $F_3 = 0.0$ and $F_3 = 0.60$, respectively. The next three plots illustrate the calculation of μ_1. The first plot illustrates the baseline removal. It is observed how the influence of pronounced T-waves is also reduced. The next plot illustrates the absolute value of the baseline-corrected ECG signal, $|ECG_{filt,1}|$, (blue lines) and the scaling parameter, s_1 (green lines). The sixth plot illustrates the scaling of $|ECG_{filt,1}|$ (blue lines), the temporary feature signal, μ_1, representing the mean value of the current window (green lines), and the threshold, T_2 (red lines). It is observed that μ_1 is below T_2 for the clean segment and above T_2 for the noisy segment. It is furthermore observed how the scaling parameter achieves to scale both signals to the same range and hereby allow noise estimation relative to the QRS amplitudes in each segment. The two bottom plots illustrate the calculation of P_1 and μ_1 for the entire duration of each segment (green lines) and the thresholds, T_1 and T_2, respectively (red lines). The dashed black lines indicate the time instance illustrated in the top plots. All amplitudes are in ADC values. The feature values obtained by channel I are stated in the figure. However, since the final feature values are defined as the minimum between the two channels (see (5.5) and (5.8)), the final values were $F_1 = 0.0$ and $F_2 = 0.0$ for the clean segment and $F_1 = 0.2$ and $F_2 = 0.90$ for the noisy segment. This is also stated in Table 5.3.

5.4.1.1.3 Calculation of F_3

For the calculation of F_3, the segment was not divided into the previously described analysis windows. The input to this feature is an array of R peak positions estimated from each ECG channel individually. We applied the single-channel BP filter-based algorithm described in chapter 4. For each segment, we calculated the number of true positive detections (TP) and the number of false detections (FD). We defined TP as the number of QRS complexes simultaneously detected in both channels and FD as the number of QRS complexes only detected in one channel. In compliance with [24], we used a match window of 150 ms. This implies that the absolute distance between the QRS complexes detected in channel I and channel II should not exceed 150 ms in order for the pair of QRS complexes to be counted in TP. This is illustrated in Figure 5.6. The third feature was then based on the relation between FD and TP (see (5.10)). However, this relation is expected to be high when either one or both channels obtain poor quality. This is not intended (see segment A in Figure 5.5). To account for this, we designed a novel scaling parameter, η, defined by (5.9), where $\sigma(RR_j)$ is the variance of the elements in the RR interval vector for channel j. If both channels display the same quality (either good or poor), the variation between the detected RR intervals is expected to be similar in both channels. In this case, η will obtain a value close to 1, and the relation between FD and TP will not be modulated significantly. On the other hand, when the quality is different for the two channels, η is expected to decrease and, hereby, reduce the influence of a potentially high relation between FD and TP caused by poor quality in only one channel. The performance of η is observed from Table 5.3.

$$\eta = \frac{Min\{[\sigma(RR_1)\ \sigma(RR_2)]\}}{Max\{[\sigma(RR_1)\ \sigma(RR_2)]\}} \tag{5.9}$$

$$F_3 = \frac{FD}{TP} \cdot \eta \tag{5.10}$$

5.4.1.1.4 The Final Feature vector

The final feature vector was then defined by (5.11). The discriminative capability of the final feature vector is observed from Figure 5.7. This difference provides the foundation for an automatic classifier to obtain high performance in differentiating between the two classes.

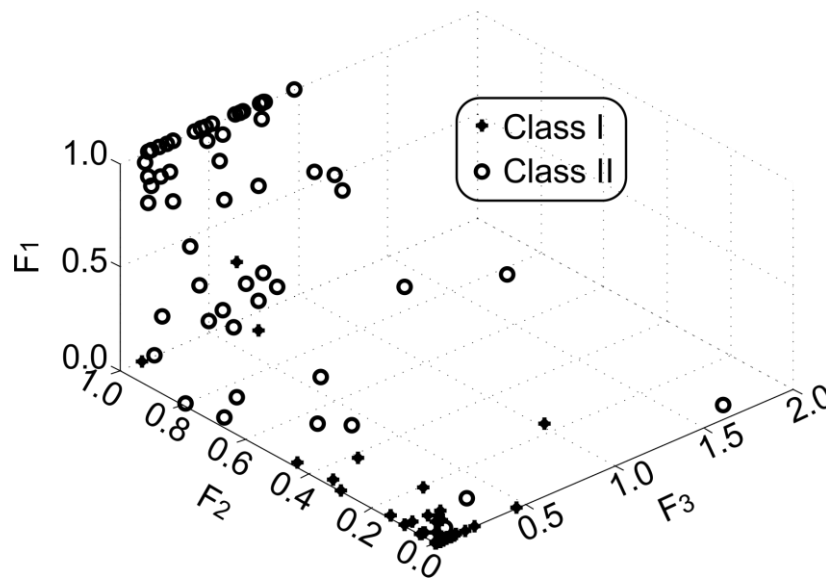$$\mathbf{F} = [F_1\ F_2\ F_3] \tag{5.11}$$

Figure 5.7: Illustration of the three dimensional feature space for the ECG segments from the training database. The plot is thus based on feature values obtained from 292 diagnostic ECG segments (class I) and 58 non-analyzable ECG segments (class II). It is observed that most feature vectors from the analyzable class are located in a very small area in the three-dimensional feature space. This is very promising for subsequent automatic classification between the two classes.

5.4.1.2   Classification

The feature vector for each ECG segment was fed to an automatic classifier that separates the two classes and labels each of the ECG segments as being analyzable or non-analyzable. We decided to apply a soft margin SVM with a radial basis function kernel. This was also applied with success in [45]. The SVM classifier applies a hyperplane to distinguish between the two classes. This hyperplane can be defined by (5.12), where w and w_0 indicate the direction and the exact position in space of the separating hyperplane, respectively [51]. Each feature vector, F_u, is assigned to one of the two classes according to its location relative to the separating hyperplane. This is illustrated in Figure 5.8.

$$g(F_u) = w^T F_u + w_0 = 0 \qquad (5.12)$$

Based on a given training database, a high number of separating hyperplanes can be drawn with equal classification accuracies on the training database. In many classification schemes, the applied hyperplane is therefore somehow arbitrary. The high generalization performance of the SVM classifier arises from the calculation of the separating hyperplane based on the maximization of the margin indicated as the distance between the dashed hyperplanes in Figure 5.8 [51]. These hyperplanes are described by (5.13), and they are defined by the support vectors from the two classes [51]. The support vectors are thus the feature vectors with the highest importance with respect to separating the two classes. In the linearly separable case, the support vectors will be the feature vectors closest to the separating hyperplane, and no feature vectors will be placed inside the margin. This is termed a hard margin SVM. This implies that the separating hyperplane is located as far away from both classes as possible, thus yielding optimal separability for unseen data points that can be expected to fluctuate with some radius from the feature vectors in the training database. In our case, we use the soft margin SVM that is applied in the nonseparable case. To account for classification errors in the nonseparable training database, a slack variable, ξ_u, is introduced. This is defined in (5.14), where y_u = 1 for the feature vectors from class I and -1 for the feature vectors from class II [51]. For feature vectors correctly classified and located outside the margin, ξ_u = 0, for feature vectors correctly classified but located inside the margin, $0 < \xi_u \leq 1$, and for feature vectors in the training database that were wrongly classified, $\xi_u > 1$. The slack variable can thus be interpreted as a "punishment" for classifying training vectors wrongly.

$$w^T F_u + w_0 = \pm 1 \qquad (5.13)$$

$$y_u[w^T F_u + w_0] \geq 1 - \xi_u \qquad (5.14)$$

The process of finding the optimal separating hyperplane can then be interpreted as finding w and w_0 such that the margin is maximized while the number of data points in the training database that are misclassified or placed on the wrong side of the margin boundaries is minimized [51]. This can be shown to correspond to the optimization of the cost function defined in (5.15) [51], where C is implemented to control the relative influence of the two terms in the optimization.

$$min\left\{\frac{1}{2}\|w\|^2 + C\sum_{n=1}^{N}\xi_u\right\} \text{ subject to } y_u[w^T F_u + w_0] \geq 1 - \xi_u \text{ and } \xi_u \geq 0 \quad (5.15)$$

For the implementation, we applied the *svmtrain* and *svmclassify* functions in *MATLAB R2013b*. In this SVM implementation, C is implemented so that the misclassification of feature vectors that belong to a potentially underrepresented class in the training data is "punished" harder than the misclassification of the overrepresented class [52]. This is obtained by rescaling C with $G/(2·G_1)$ for data points from class I and with $G/(2·G_2)$ for data points from class II, where G_1 and G_2 are the number of segments in class I and class II, respectively, and $G = G_1 + G_2$ [52]. The optimal value of C was found by a parameter grid search described later.
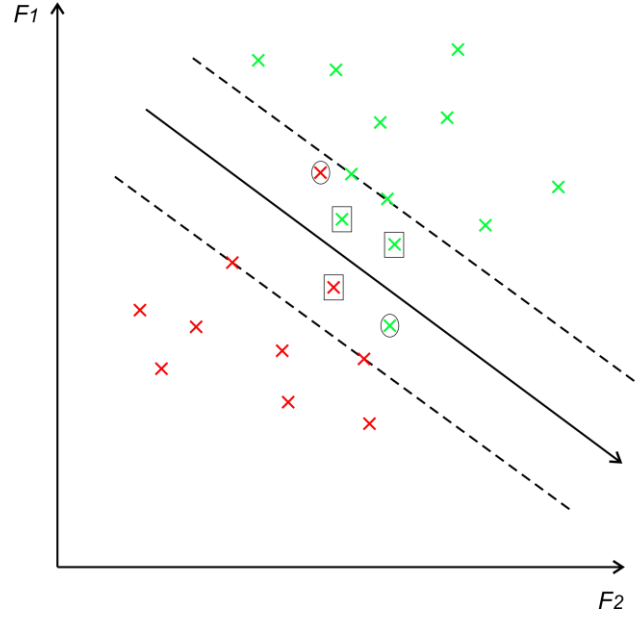
Figure 5.8: Schematic illustration of the functionality of the SVM classifier using two features. The two classes are indicated by the red and green marks, respectively. The separating hyperplane is illustrated as the solid line, and the margin is illustrated as the distance between the two dashed parallel hyperplanes. The support vectors are located on the dashed hyperplanes. The squares indicate feature vectors with $0 < \xi_u \leq 1$, and the circles indicate feature vectors with $\xi_u > 1$ (wrongly classified).

It is observed that the SVM classifier, in general, is linear. In cases where the separation of the feature vectors is not linear, the *kernel trick* is applied [51]. The *kernel trick* is based on mapping the original features into a higher dimensional feature space, where they are linearly separable. As described in [51], this can be accomplished by the use of a kernel function, $K(\mathbf{F_{u1}}, \mathbf{F_{u2}})$. As mentioned, we applied the radial basis function kernel defined in (5.16), where $|\mathbf{F_{u1}} - \mathbf{F_{u2}}|^2$ is the squared Euclidian distance between the two feature vectors $\mathbf{F_{u1}}$ and $\mathbf{F_{u2}}$ in the original feature space. The radial basis function kernel parameter, γ, was optimized using the parameter grid search described later. Since the feature values were designed to be approximately in the range [0; 1], no additional scaling was conducted prior to the SVM classification.

$$K(\mathbf{F_{u1}}, \mathbf{F_{u2}}) = e^{\left(-\frac{|\mathbf{F_{u1}} - \mathbf{F_{u2}}|^2}{2\gamma^2}\right)} \tag{5.16}$$

5.4.2   Description of Algorithm Design Database

For the algorithm design and validation, we decided to randomly select two ECG segments of 10 minutes from each of the patients from the four original databases described in section 5.2. This yields a total of 500 ECG segments. The random selection of segments from each patient ensures a realistic amount of artifacts, a realistic distribution of the types of artifacts (e.g. power line interference, muscle artifacts, and electrode-motion artifacts), a representation of normal sinus rhythm with different ventricular frequencies, and a realistic amount of abnormal heart rhythms and different beat morphologies. Each of the 500 ECG segments were manually annotated and assigned to one of the two classes. The annotation was conducted in two steps. The first step was designed to point out challenging segments and provide the final annotation of non-challenging segments. This was accomplished by asking three engineers with experience in ECG interpretation to provide an independent assessment of the quality of each of the 500 ECG segments. For all ECG segments where the three engineers agreed on the quality, this consensus was considered appropriate for the final annotation. Of the 500 segments, agreement between the engineers was obtained for 402 segments. The annotation of the remaining 98 segments was considered more challenging. These segments were therefore also annotated independently by a set of doctors. All 98 segments were annotated by two different cardiologists and one of two medical doctors. The final annotation for the 98 segments was based on majority voting between the three medical annotations for each segment. Table 5.4 contains information about the total

number of segments, the number of challenging segments, and the number of analyzable segments obtained from each of the four original databases.

Table 5.4: Information about the algorithm training and validation database.

Database	STRDB	CRMDB	TDB	FDB	Total
Patients	84	84	50	32	250
Segments	168	168	100	64	500
Training [a]	59	59	35	22	175
Validation [a]	25	25	15	10	75
Simple [b]	82.7%	87.5%	69.0%	73.4%	80.4%
Analyzable [c]	85.1%	76.2%	91.0%	92.2%	84.2%

[a] The number of patients from each database that were randomly selected for the training and validation phase, respectively. The training and validation phases are further described in the section 5.4.3.1.

[b] Percentage of segments with agreement between the three engineers.

[c] Percentage of analyzable segments (class I).

5.4.3   Results

To ensure the thorough evaluation of the algorithm performance, we applied five different performance measures: sensitivity (*Se*), specificity (*Sp*), accuracy (*Acc*), negative predictive value (*P*⁻), and positive predictive value (*P*⁺) defined in (5.1) – (5.3), (5.17), and (5.18). Positive refers to the clean segments, whereas negative refers to the noisy segments. Each of the five performance measures and their mutual relations contain important information regarding the ability to correctly classify each segment and, hereby, the algorithm's ability to provide a reliable estimate of the overall PAT.

$$P^+ = \frac{TP}{TP+FP} \cdot 100\% \qquad\qquad (5.17)$$

$$P^- = \frac{TN}{TN+FN} \cdot 100\% \qquad\qquad (5.18)$$

5.4.3.1   Algorithm Parameter Optimization

As mentioned, four algorithm parameters (T_1, T_2, C, and γ) were optimized using a grid search. The optimal value of each parameter depends on the value of the other parameters. We therefore optimized all four parameters simultaneously. To ensure the possibility of estimating the performance on unseen data, we randomly selected 30% of the patients as a validation group. The parameter optimization was only based on ECG segments from the remaining 70% of the patients (the training database). For each cross validation fold, 80% of the patients in the training database were applied to train the classifier, and the performance was evaluated on the data from the remaining 20%. The performance might depend on the random selection of the training and test data in the training database. To obtain a reliable estimate of the average performance as well as performance variations for each parameter combination, we therefore conducted 100 folds with random division of the training database. For each parameter combination, the average and standard deviation of *Se*, *Sp*, *P*⁻, and *P*⁺ over the 100 folds were calculated. These results are provided in Figure 5.9. The *Acc* was not applied for optimization since this performance measure might result in a biased optimization when the classes are unbalanced. We selected the parameter combination with the best compromise between the four performance measures. The performance of this parameter combination is indicated with a black circle in Figure 5.9. This combination was T_1 = 1200, T_2 = 0.12, C = 0.7, and γ = 2. The performance of this parameter combination was *Se* = 98.5±1.3, *Sp* = 95.0±6.5, *P*⁺ = 99.1±1.1, *P*⁻ = 92.6±7.0, and *Acc* = 98.0±1.5.
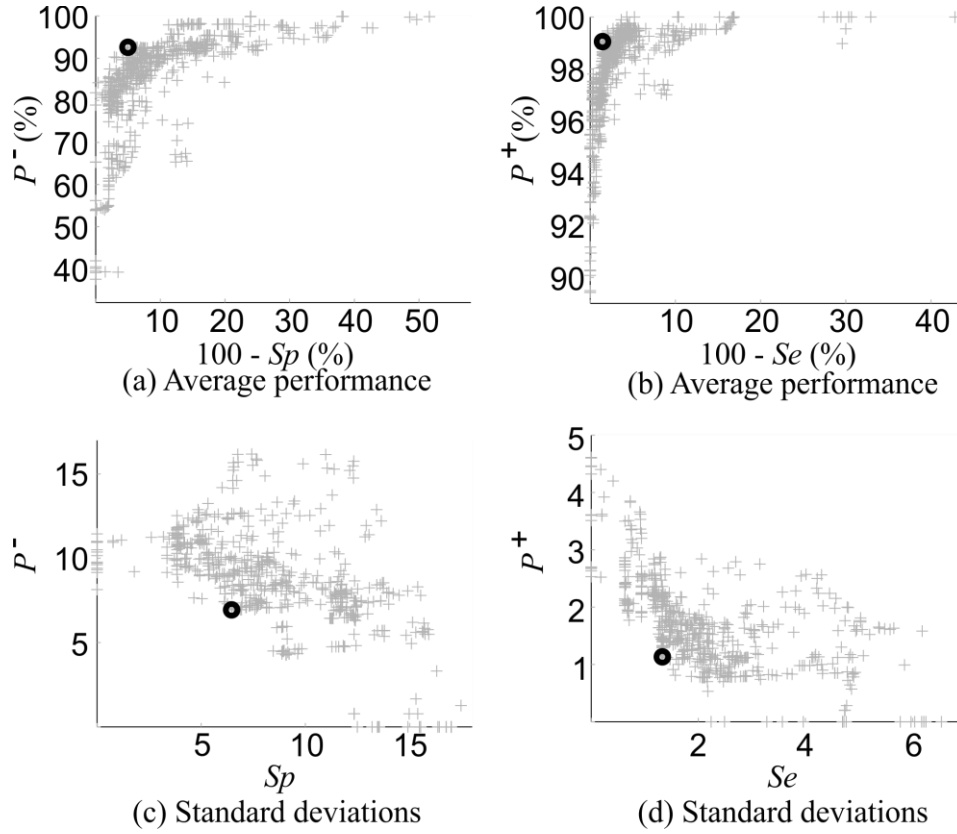
Figure 5.9: Each gray point indicates the performance obtained by one of the 750 different parameter combinations investigated. (a) Relation between average *Sp* and average *P⁻* obtained from the 100 random folds. (b) Relation between average *Se* and average *P⁺* obtained from the 100 folds. (c) Relation between the standard deviation of *Sp* and *P⁻* obtained from the 100 folds. (d) Relation between the standard deviation of *Se* and *P⁺* obtained from the 100 folds. The black circle indicates the performance of the selected parameter combination.

5.4.3.2   Performance of the Final Algorithm

The algorithm was then retrained using all the segments in the training database and the selected parameter combination. The performance of this final algorithm on the training database is provided in Table 5.5. The final algorithm was then applied to the unseen validation database. These results are also provided in Table 5.5 together with the performance of each human expert annotator with respect to the final manual annotations.

Table 5.5: Performance of the final algorithm and the human experts with respect to the final manual reference annotation.

Annotator	N^a	Se (%)	Sp (%)	P- (%)	P+ (%)	Acc (%)
Engineer I	500	96.9	98.7	85.7	99.8	97.2
Engineer II	500	81.0	92.4	47.7	98.3	82.8
Engineer II	500	99.5	82.3	97.0	96.7	96.8
Medical doctor I	64	100.0	100.0	100.0	100.0	100.0
Medical doctor II	34	93.3	100.0	66.7	100.0	94.1
Cardiologist I	98	90.0	100.0	69.2	100.0	91.8
Cardiologist II	98	93.7	66.7	70.6	92.5	88.7
Training [b]	350	98.6	96.6	93.3	99.3	98.3
Validation [c]	150	98.4	95.2	90.9	99.2	98.0

[a] N indicates the number of segments analyzed by each annotator.

[b] Performance on the entire training database when all segments from the training database were applied to train the final algorithm classifier.

[c] Performance on the unseen validation database when the final algorithm trained on the entire training database was applied.

5.4.4   Discussion

We have designed a novel algorithm for the estimation of the overall PAT in ECG recordings. The reliability of this algorithm highly depends on the ability to correctly classify each segment in the recordings as being either analyzable or non-analyzable. The performance of our novel algorithm on the unseen validation data was Se = 98.4%, Sp = 95.2%, P^+ = 99.2%, P^- = 90.9%, and Acc = 98.0%. For comparison, the highest Acc obtained on test data in the original Physionet challenge was 93.2% [42]. Our algorithm thus obtains much better Acc. However, care should be taken when comparing Acc on different unbalanced databases. Furthermore, the Acc does not provide any information about the relative performance in the detection of the two classes. The authors of [45] extended their Physionet entry by relabeling the database and balancing it by adding artificially generated noisy segments. Using this database and an algorithm based on five features and an MLP classifier, they obtained Acc = 95.9%, Sp = 96.0%, and Se = 95.8% on their test data. In [49], the achieved performance on a private database of unseen data was Acc = 95.36%, Se = 94.73%, and Sp = 96.63%. Comparing to the literature, our obtained performance is thus very satisfactory. The high performance obtained both during the cross validation and validation on unseen data is expected to be achieved from the design of appropriate features with high discriminative capabilities and the choice of an SVM classifier. Furthermore, it is observed that the standard deviations obtained from the cross validation are relatively low. This furthermore indicates the stability of the designed algorithm.

The selection of the optimal parameter combination depends on the requirements for each application. In some applications, it is crucial that only noisy segments are detected for exclusion. In this case, the high performance of Se and P^- should be valued at the expense of Sp and P^+. In other applications, it might be more important to ensure that a selected data segment is, in fact, clean and therefore useful for rhythm analysis. In this case, the compromise between the four performance measures should be opposite. Since our goal was to estimate the overall PAT, we decided to allow each of the four performance measures equal weights during the parameter selection phase. However, it is observed that Sp is higher than P^- and Se is slightly lower than P^+. Looking at (5.1), (5.2), (5.17), and (5.18), this indicates an overrepresentation of FNs compared to FPs. This implies that more clean segments are wrongly classified than noisy segments, and thus, the algorithm might have a small tendency to overestimate the overall noise level. However, the mean analyzable time obtained from all 250 recordings was 83.4% (see section 5.5). This number is very comparable to the number of randomly selected segments that were manually annotated as analyzable (84.2%; see Table 5.4). The high similarity between these numbers

might suggest that the novel designed ECG quality estimation algorithm still provides a fairly reliable estimate of the overall PAT. Furthermore, the algorithm performance is well within the performance obtained by each human expert annotator (see Table 5.5). This does not necessarily indicate a higher performance of the algorithm. The difference in the human expert annotations might originate from different experience levels with respect to ECG interpretation. Furthermore, each individual annotator might look for different ECG characteristics to judge whether each segment is diagnostic or not. However, the high algorithm performance compared to that of the human expert annotators does indicate that the algorithm provides a more reproducible estimate of the overall PAT than would be possible to achieve using human expert annotations. The results might also indicate that the automatic estimation of the overall PAT provides a good compromise between potential disagreements between the human experts.

It should, of course, be mentioned that the possibilities of improving the quality estimation algorithm are not exhausted. Improvements might include adding noisy segments to obtain a better balance between the classes. Improvements might also include the investigation of new and more advanced features. However, with the potential future embedded functionality in mind, we found it relevant to apply as simple features as possible. It should furthermore be noted that the most appropriate design choices (the definition of analyzability, the segment length, and the combination of the two channels) depend on the intended application of the algorithm. It could also be interesting to test the algorithm performance in the presence of specific arrhythmia events. In this study, the ability to correctly classify abnormal ECG segments as being analyzable or non-analyzable was based on a random selection from ECG recordings in a high-risk population, but it was not investigated specifically. It is important to keep these algorithm limitations in mind when analyzing the overall PAT. However, our overall impression is still that the designed algorithm provides a useful estimate that can provide important new knowledge about the general signal quality obtained in patch ECG recordings. The high classification accuracy also makes it possible to apply the algorithm to point out areas of high and low quality. This could be an important feature that might help save time during the manual analysis of the recorded ECGs.

5.5   Investigation of Analyzable Time in 24-hour ePatch Recordings

After the definition of our interpretation of signal quality and the design of an automatic algorithm for the reliable estimation of the overall PAT in ePatch recordings, we finally investigated the last research question. The final version of the algorithm described in section 5.4 was applied to estimate the overall PAT for each of the 250 patients described in 5.2. These results are provided in Figure 5.10. The x-axis indicates the recording numbers sorted according to their overall PAT.
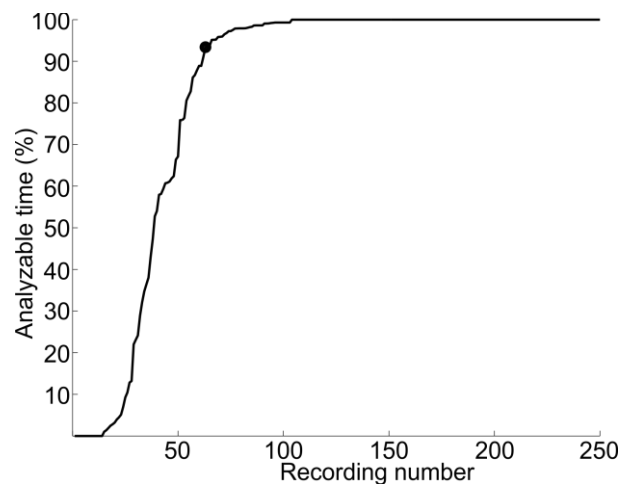

Figure 5.10: Illustration of the overall analyzable time obtained in each recording. The analyzable time was estimated by the novel proposed automatic algorithm described in section 5.4. As observed from the curve, 25 recordings (10%) obtained less than 10% analyzable time. The recordings to the right of the black circle obtained an overall analyzable time equivalent to ≥22 hours/day.

It is observed from Figure 5.10 that 147 of the recordings obtain an analyzable time of 100%. It should be noted that this does not imply that we claim that these recordings display no artifacts or noisy episodes. The algorithm is designed to detect periods of the recording where diagnostic interpretation is possible. This does not imply that no artifacts can be present. It implies that, using contextual information, it is possible with certainty to recognize the heart rhythm. On the other end of the scale, 25 recordings obtained an analyzable time of <10%. These recordings were considered to be incorrect measurements, and they would not be useful for diagnostic purposes. A new recording should therefore be obtained if any diagnostic information was to be extracted. These recordings were therefore treated separately, and they were not included in the calculation of the mean and median analyzable times. It is worth noting that this number is relatively high. When the recordings possess poor quality throughout the recording period, we expect that the poor quality is caused by improper mounting or disconnected electrodes. This high number might therefore suggest difficulties in the mounting procedure. With reference to the design choices, this finding was surprising. However, it is not known how often this actually happens for Holter recordings, and it is therefore difficult to know whether this is, in fact, an issue related to the new technology. Furthermore, it must be expected that there is a certain running-in period for clinical applications of new devices where the clinical staff learn how to use the new technologies correctly. We therefore don't find these results to be concerning, but it is something that could be investigated further. Furthermore, this illustrates the future benefits that could be obtained by an embedded algorithm for real-time estimation of the obtained recording quality. Using such an algorithm, these long-lasting useless recordings might be avoided.

For the remaining 225 recordings, the median analyzable time was 100% (interquartile range: 97.9% to 100%), and the mean analyzable time was 92.4±18.8%. Our estimated median analyzable time thus corresponds well with the findings in [2]. Furthermore, the analyzable time is higher than that found in [41]. This is also expected since the data analyzed in [41] were obtained during different kinds of physical activities (walking, running, Nordic walking, and biking), whereas the ePatch recordings were obtained during normal daily life. Physical activity is therefore not expected to be present constantly in our recordings. The percentage of ePatch recordings obtaining analyzable data equivalent to at least 22 hours/day was 83.6%. Comparing to [2], this number is slightly lower but still comparable. We thus believe that our findings correspond well with the limited available literature. Furthermore, it should be noted that the authors of [2] don't disclose the methodology behind their proprietary algorithm applied for the estimation of the percentage of analyzable time. We aimed at a high reproducibility by applying a fully disclosed algorithm for the estimation of the overall PAT. Furthermore, the shape of the curve presented in Figure 5.10 imposes a new interesting question:

- How much analyzable time is required to ensure a sufficient clinical interpretation of the recording?

This question is highly relevant to understand the clinical impact of the estimated PATs. To investigate this area and hereby obtain a deeper understanding of the concept of ECG signal quality from a clinical point of view, we compared the PATs estimated by our algorithm and the manual quality indexes provided with the STRDB and the CRMDB (see section 5.2). This investigation is described in the next section.

5.5.1 Comparison with Manual Quality Indexes

The purpose of this investigation was to gain knowledge about the level of PAT that provides sufficient quality for the clinical interpretation of the entire recording. To investigate this, we applied the manual quality indexes from the CRMDB and the STRDB. The original indexes were divided into six categories. To simplify the analysis and provide a better overview, we applied three categories based on merging the original indexes as described below:

- Bad recordings: Recordings with original grade 0 (useless recording, no diagnosis was possible) or original grade 1 (almost useless recording, only possible to identify HR from QRS complexes).
- Intermediate recordings: Recordings with original grade 2 (generally too much noise to allow full diagnosis) or original grade 3 (periods with too much noise or noise that, in general, disturbs the diagnosis)

- Good recordings: Recordings with original grade 4 (a few episodes of noise that disturb the ECG morphology) or original grade 5 (noise-free recording or recording with only movement artifacts).

For each of the two databases, we illustrated the obtained PAT with an indication of the manual quality index for each recording. This is provided in Figure 5.11. A high relation between the manual grades and the automatically estimated PAT is generally observed. The "bad" recordings are located in the bottom of the curve with low PATs, and the "good" recordings are generally located at the high end of the curve. Together with the high classification performance described in section 5.4.3.2, this creates the foundation for "trusting" the estimated PATs. It is furthermore observed that one "bad" recording in the STRDB obtains a PAT of 100%. The conclusion in the Holter analysis report for this recording was as follows: "*There is noise in most of the recording. The impression is that the patient suffers from AF during the entire recording*" and the quality grade was 1. A short ECG segment from this patient is provided in Figure 5.12. It is observed that the atrial activity is very pronounced. This appearance is sometimes present during AF in the ePatch recordings. This looks quite similar to ECG recordings with AF obtained from the esophagus. This appearance is thus expected to be caused by the location of the ePatch on the sternum. The low quality grade for this recording might therefore be an expression of the need to get used to the ePatch recordings rather than actually bad quality.
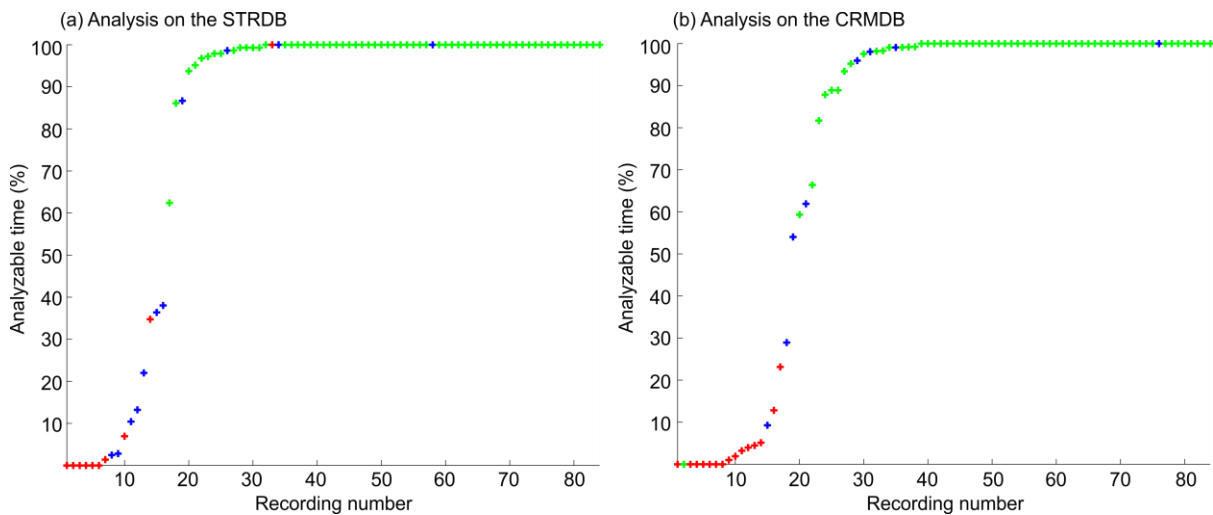
Figure 5.11: Illustration of the PAT obtained on all recordings from the STRDB (a) and the CRMDB (b). The PAT was estimated using the final version of the quality assessment algorithm. The red marks indicate "bad" recordings, the blue marks indicate "intermediate" recordings, and the green marks indicate "good" recordings.

The lack of recordings obtaining PATs between approximately 30% and 85% makes it impossible to provide a definitive clinical requirement for PAT. However, it is observed that most recordings obtaining more than approximately 85% analyzable time were manually annotated as a "good" recording. This might suggest that this is the level that is required to obtain easy clinical interpretation. There is, of course, always a risk of missing a single important arrhythmia event experienced by a patient during an episode of non-analyzable data. However, this unfortunate situation might also occur using the traditional Holter recorders. It is not possible to completely remove this risk, and it is not known with certainty whether this occurs more frequently in patch-type ECG recorders than the traditional Holter recorders. It is furthermore difficult to find literature describing the actual analyzable time in Holter recorders, and therefore, a direct comparison with the traditional devices was not possible. As mentioned, it is furthermore expected that some of the artifacts observed in patch recordings originate from the increased possibility of continuing normal daily life activities throughout the monitoring period compared to traditional Holter recorders. The recording conditions might therefore be considered quite different for the patch recorders and the traditional recorders. Overall, we find that the PAT obtained in the ePatch recordings is high, and this is very promising for the application of this technology in the future health care system. As mentioned earlier, it has furthermore been shown that the extended monitoring period facilitated by the novel patch recorders can result in an overall higher diagnostic yield, the detection of more significant arrhythmias, and a higher degree of definitive diagnosis compared

to traditional Holter recordings [2], [7], [9]. This indicates that a potential increase in the amount of artifacts recorded with the patch recorders is outbalanced by the advantages of the increased monitoring period.
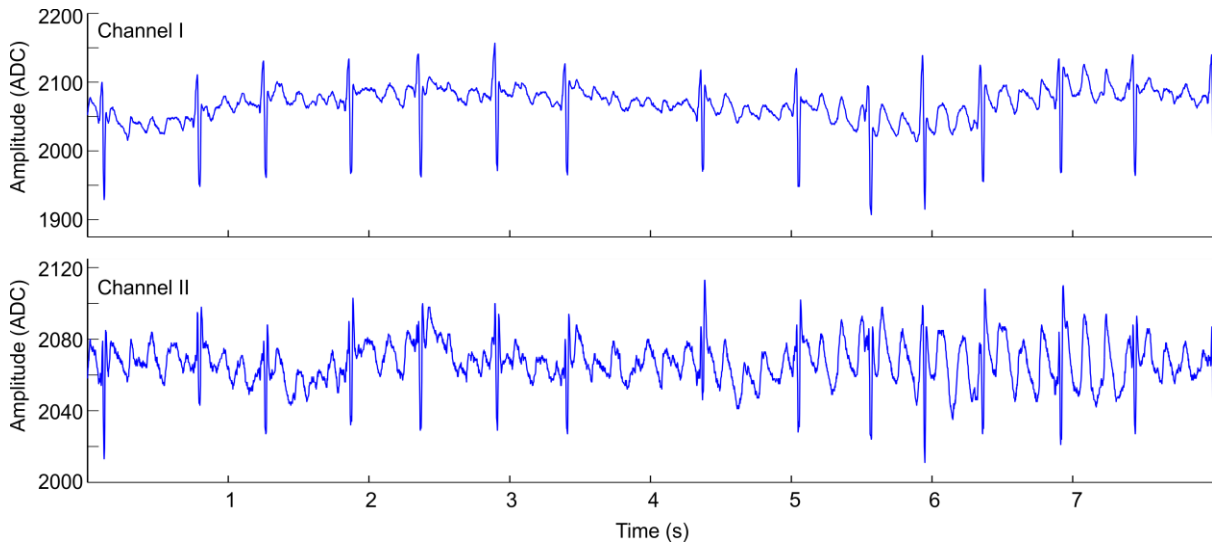

Figure 5.12: Illustration of a segment with AF from patient 4 from the STRDB. The patient obtained the manual score 1 which indicates a signal of very poor quality. The segment scored an analyzable time of 100% by the automatic algorithm. This segment is the "wrongly placed" red mark in Figure 5.11(a). However, the typical appearance of the signal in this recording is similar to the segment illustrated here. The patient suffers from AF, and this is sometimes characterized like this in ePatch recordings (due to the electrode placement). However, it might require some experience with ePatch analysis to acknowledge this, and maybe, this is the reason for the poor manual quality score. The automatic algorithm dos not consider this as artifacts (the illustrated segment is extracted from segment 233 from the algorithm design database, and it was manually annotated as analyzable).

5.5.2   Relation Between the Two Algorithms

After comparing the estimated PATs with the manual quality indexes, we also found it interesting to compare with the preliminary version of the algorithm. We therefore retrained the preliminary version of the algorithm on all 40 subjects from the database described in section 5.3.1. This algorithm was then applied to classify all 168 recordings from the STRDB and CRMDB as either "good" or "bad" recordings. The results are provided in Figure 5.13. It is observed that most recordings that obtain more than approximately 60% analyzable time by the final algorithm are classified as "good" recordings by the preliminary algorithm. Only four recordings from the STRDB and three recordings from the CRMDB are classified differently. We therefore looked closer at these recordings to investigate what caused the differences between the two algorithms for these recordings. Five recordings were "wrongly" classified as "bad" according to a threshold of an analyzable time of 60%. One of the recordings was found to obtain very poor quality of channel I and high quality of channel II. The difference for this recording is therefore probably caused by the difference in the combination of information from the two channels. In the preliminary version, we included all recordings with comments on bad quality in either one or both channels in the "bad" group. This paradigm was changed for the final version of the algorithm. One other recording (see Figure 5.12) was found to possess very pronounced atrial activity. The other recordings were generally characterized by periods of data with very pronounced T-waves or movement artifacts. The difference for these recordings is also expected based on the improvements of the mean value feature. In the preliminary version of the algorithm, the baseline correction step was not included. It is therefore expected that recordings with pronounced atrial activity, high T-waves, or many episodes of pronounced movement artifacts are misclassified as "bad" recordings. If the preliminary version of the algorithm was updated with the baseline correction, it is therefore likely that it would provide a very reliable estimation of the quality relative to the 60% threshold. As discussed above, most recordings obtain either a quite high or quite low PAT, and it is therefore difficult to decide a specific threshold for a clinically acceptable PAT based on Figure 5.11. This is also the case with the somehow arbitrarily selected 60% threshold, and the results in Figure 5.13 actually correspond quite well with the green marks (high-quality recordings) in Figure 5.11. This indicates that the preliminary version of the algorithm actually provides a

quite reliable estimation of the possibility to conduct a clinical interpretation of the recording. For this application, it might therefore be sufficient with an algorithm that provides the overall assessment of "good" or "bad." This strengthens our impression of the importance of including adequate contextual information when evaluating ECG signal quality. In many clinical applications, the final version of the algorithm is still appreciated over a single indication describing the entire recording:

- The final version of the algorithm allows for the exclusion of specific periods of the recording and not the entire recording. This might be highly relevant when clinical interpretation is required for an outpatient recording with a duration of several days. This is an acknowledgment of the second algorithm requirement formulated in section 5.1.3.
- The features applied in the algorithm are computationally quite simple. The biggest computational load in the feature extraction is the automatic QRS detection in both channels. It can, for instance, be imagined that this algorithm could be "turned on" once every hour during a recording to provide a warning if the quality suddenly decreases. This meets the third algorithm requirement formulated in section 5.1.3.
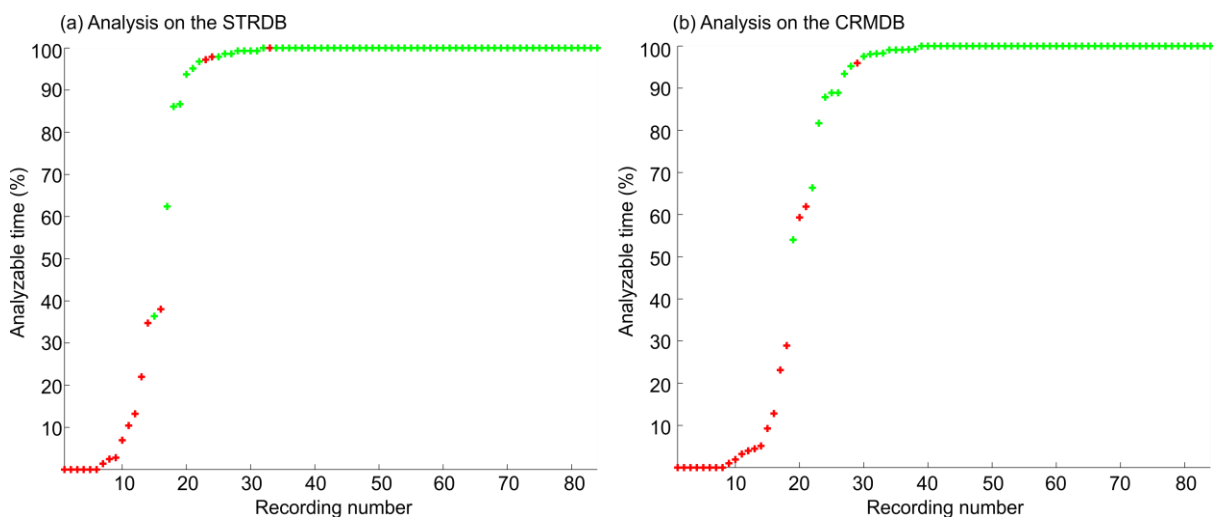
Figure 5.13: Illustration of the PAT obtained on all recordings from the STRDB (a) and the CRMDB (b). The PAT was estimated using the final version of the quality assessment algorithm. The red marks indicate recordings that were classified as "bad" by the preliminary version of the algorithm, whereas the green marks indicate recordings that were classified as "good" by the preliminary version of the algorithm.

It is interesting that the overall signal quality can be obtained both by applying the entire recording at once (the preliminary algorithm) and by considering the recording segment by segment (the final algorithm). This might suggest that it could be investigated to apply even smaller segments. It would be interesting to investigate how small the segments could be and still include enough contextual information to provide a reliable clinical assessment of the overall quality of the entire recording. Furthermore, it is, of course, possible that even very small segments could be applied to investigate the presence/absence of specific artifact types. As discussed earlier, this type of "shutdown" algorithm might be interesting to "protect" subsequent automatic arrhythmia classification algorithms. However, it should be noted that, even though smaller segments might also provide high classification results, we still advocate against the "artifact event detection" paradigm as the only source of information about the clinical quality of an ECG recording. As discussed in section 5.1.3, this approach might not be sensitive enough for prolonged periods of time with apparently minor artifacts that still might interfere with the clinical interpretation (see Figure 5.2).

5.6   Conclusions

In this chapter, we have discussed the concept and understanding of ECG signal quality. We have investigated different ways of defining ECG signal quality, and we decided to use an approach that is highly related to the clinical interpretation of ECGs. We were therefore focused on the ability to conduct clinical interpretation with certainty (i.e. diagnosis of the patient) rather than the presence/absence of specific types of artifacts. This requires the application of contextual information when the influence of a potential artifact event is investigated. We thus defined the acceptable quality of an ECG segment based on the ability to conduct heart rhythm analysis. We furthermore learned that an ECG recording is generally considered of sufficient diagnostic quality when at least 85% of the recording is found to be analyzable according to our definition.

We have designed a novel algorithm for the automatic estimation of the overall PAT obtained in ECG recordings. The algorithm divides the long-term recording into smaller segments and classifies each segment as being either "analyzable" or non-analyzable." This allows an easy estimation of the overall PAT. The algorithm was based on three computationally simple features that were designed to provide an accurate characterization of the difference between an analyzable ECG segment and a non-analyzable segment. The algorithm obtained a very high performance with respect to the correct classification of clinically relevant manually annotated ePatch ECG segments (Se = 98.4%, Sp = 95.2%, P^- = 90.9%, P^+ = 99.2%, and Acc = 98.0%). Furthermore, the estimated overall PATs obtained a high correlation with manually provided quality indexes. We therefore find that it is possible to design biomedical signal processing algorithms for the reliable estimation of ECG quality in the ePatch recordings.

We then applied the designed algorithm to gain knowledge about the overall PAT in ePatch recordings obtained from 250 different patients. We found that 10% of the 250 recordings obtained less than 10% analyzable time. These recordings were considered as recording errors. For the remaining recordings, we found a median and a mean analyzable time of 100% (interquartile range: 97.9% to 100%) and 92.4±18.8%, respectively. We consider these PATs to be high, and we furthermore expect that sufficient training of hospital staff can decrease the number of recording errors. We thus find that it is possible to obtain sufficient signal quality for clinical applications of the ECGs recorded with the ePatch system. However, it should, of course, be mentioned that the findings are based on the performance of the designed quality assessment algorithm, and the validity is therefore strongly connected to the performance of the designed algorithm. Overall, we consider the analyzable times obtained in the patch recordings to be high and hereby relevant for clinical applications. This is promising for the application of the ePatch technology in a high number of different clinical settings both as a substitute for the traditional Holter recorders and in clinically relevant applications where the traditional Holter recordings fall short.

6 Conclusions

The main focuses in this project were to increase the currently limited amount of knowledge about the clinical applicability of the novel ePatch recorder and to initiate the design of new low-power algorithms that are optimized for embedded analysis in the ePatch sensor. We have pursued this through three different research areas that each contribute to the overall understanding of the future possibilities with the novel patch recorder. These investigations were guided by the three main objectives stated in chapter 1. The findings related to each of these objectives are separately discussed below.

Objective I: To conduct a preliminary investigation of the clinical usability of ECGs recorded with the novel ePatch technology

This research area provided important information about the clinical usability of ePatch ECG for heart rhythm analysis. This has not previously been investigated for the ePatch recorder. In our first pilot study, we found that two different medical doctors indicated that more than 98% of the selected ePatch ECG segments were useful for heart rhythm analysis, and in our second pilot study, a cardiologist found that there was no difference in the clinically relevant information that could be extracted from simultaneous recordings obtained with the ePatch recorder and traditional telemetry equipment from 11 admitted patients. These pilot studies thus provided a fundamental confidence in the reliability of the recorded ECGs. They furthermore indicate the clinical potential for this novel patch device for the monitoring and management of different heart diseases in the future. This research area thus formed the basis for the applicability of the remaining investigations described in this dissertation.

Objective II: To conduct a preliminary investigation of the ability to obtain sufficient diagnostic quality of ECG recordings obtained with the ePatch technology

In this research area, we gained valuable information about the signal quality obtained using the ePatch recorder. First, we found it necessary to develop a clinically relevant definition of signal quality. This definition was then applied to design a novel algorithm for the automatic estimation of the overall PAT obtained in an ECG recording. The algorithm was designed using three computationally efficient features that were carefully designed to describe some of the characteristic differences between an analyzable and a non-analyzable ECG segment. This choice was made to ensure the potential for the future embedded implementation of the feature extraction procedure in the ePatch sensor. The algorithm achieved a very high classification performance on manually annotated ECG segments (Se = 98.4%, Sp = 95.2%, Acc = 98.0%, P^- = 90.9%, and P^+ = 99.2%). We then applied the designed algorithm to 250 recordings obtained with the ePatch recorder. We found that 10% of the recordings obtained less than 10% analyzable time. These recordings were considered as recording errors, and it is not expected that any clinically relevant information could be extracted from these. These erroneous recordings are undesired, and this relatively high number thus illustrates the future potential for embedded quality assurance. On the other hand, we found very high mean and median analyzable times in the remaining recordings. In agreement with published studies treating the signal quality obtained by other patch devices, we thus found the overall PAT in the ePatch recordings to be high. This indicates that the many advantages of the patch ECG recorders are not counterbalanced by low signal quality. Overall, we thus find that, in most cases, it is possible to obtain sufficient diagnostic quality in ECGs obtained with the ePatch technology.

- *Objective III: To design and validate a novel embedded QRS complex detection algorithm with high clinical performance in real-life ePatch ECGs and low computational load*

Many new application areas of the ePatch technology might highly benefit from real-time embedded interpretation of the recorded ECGs. With the practical applications and the required flexibility of the ePatch technology platform in mind, we defined an acceptable power consumption based on the ability to perform embedded analysis without significant loss in the total recording time of the current version of the ePatch sensor. The first important step in any automatic ECG interpretation

is the reliable detection of each individual heartbeat. We therefore focused our research on the design of a novel QRS complex detection algorithm that was optimized for high clinical performance in real-life ePatch recordings with low computational costs. We achieved this by designing a novel cascade of computationally simple FIR filters that obtains adequate enhancement of the QRS complexes as well as high artifact attenuation. Furthermore, we implemented a refined search back scheme and two computationally simple adaptive thresholds. Using this novel algorithm, we achieved a very high clinical detection performance (average detection performance on 952,632 beats obtained from 198 different patients from five different databases: Se = 99.86% and P^+ = 99.74%). We furthermore found that the embedded implementation of the algorithm only increases the energy consumption by theoretically up to 5.5% of the normal energy consumption in the ePatch sensor. This implies that a total recording time of 80 hours reduces to as much as 75.8 hours. We thus find this algorithm very applicable for real-time embedded heartbeat detection within the ePatch sensor. The design of this algorithm thus opens completely new possibilities for the embedded processing of the recorded ECGs. Based on this research area, we thus conclude that it has been possible to design a novel automatic QRS complex detection algorithm with high clinical performance and adequately low computational costs.

Overall, the research described in this thesis has covered previously unanswered questions related to this novel outpatient recording technique. Of course, large-scale clinical studies on much larger patient populations are required to confirm the findings, but we believe that our findings generally indicate a high potential for the ePatch recorder in many different clinical applications in the future. These applications include both known areas where ambulatory ECG recordings are already applied as a clinical tool today and completely new areas where ambulatory ECG monitoring has not been feasible with the older technologies. We thus believe that the implementation of these recorders might help initiate a completely new way of looking at ambulatory ECG monitoring.

6.1   Future Perspectives

The potential future application areas of the ePatch recorder are quite extensive. As discussed above, this thesis serves to increase the knowledge about the clinical applicability of the ePatch recorder. It should, of course, be mentioned that the work described here is not exhaustive, and future research could be conducted to further investigate the potentials for the new technology. Some of the interesting directions for future work could therefore be the following:

- An extensive comparison between the diagnostic yields obtained from simultaneous recordings obtained with the ePatch system and the traditional Holter recorders. It is recommended that this comparison would be conducted using the final analysis reports created by the ECG technicians and hereby investigate the potential differences in the diagnosis and treatment prescribed by the referring physician. Inspiration to the study design protocol might be gained from [9] and [7].
- One of the advantages of the novel patch recorders is the possibility of prolonged monitoring. In our investigation, however, only 24-hour recordings were available. It was therefore not possible to investigate the diagnostic quality obtained beyond the initial 24 hours. The quality is not expected to decrease during the recording period, but an investigation of this might be an important future study. This investigation could be conducted quite easily using the designed quality assessment algorithm as soon as sufficient amounts of long-term recordings become available. However, it is recommended that the designed algorithm is first validated with respect to correct quality assessment in the presence of specific arrhythmia events.
- Today, it is not known whether the quality of the ePatch recordings are affected by different factors, e.g. patient demographics (age, gender, BMI, activity level, and ethnicity), the experience level of the nurse attaching the device, and the experience level of the ECG technician analyzing the recording. This investigation might also be interesting in the future.
- In this project, we have investigated the possibilities for the embedded real-time detection of individual heartbeats in the recorded ECGs. It should be noted that the designed algorithm should be validated in the presence of different types and amounts of artifacts. This could be conducted by a well-designed noise stress test.

Furthermore, it should be noted that the designed novel cascade of filters, and hereby the entire algorithm, is dependent on the sampling frequency. In future versions of the ePatch, the sampling frequency is user defined (128 Hz, 256 Hz, 512 Hz, or 1024 Hz). For future clinical application of the designed algorithm, it should therefore be updated to handle different sampling frequencies. In the next generation of the ePatch, additional recording modalities, e.g. accelerometers, are furthermore available. It might therefore also be very interesting to explore the possibilities of the "shutdown" approach using an automatic multi-modal algorithm that could detect segments with profound amounts of artifacts that could hinder the proper functionality of the algorithm.

- The design of an automatic algorithm for heartbeat detection also opens a world of opportunities for the design of algorithms for the automatic detection of other relevant clinical markers. These future algorithms might again be based on information from both the ECG signal and the accelerometers. This could include the automatic estimation of, for instance, posture, activity level, and sleep quality, the signal real-time estimation of signal quality indexes, and the detection of potential arrhythmia events. The design of such algorithms could highly extend the potential application areas of the ePatch technology.

- Finally, it is recommended to conduct large-scale clinical studies to explore new areas where cardiac monitoring might be highly beneficial for the management of different conditions but is omitted today due to the difficulties with the current Holter and event recorders. This could exponentially increase the market potential for the novel patch technologies.

Bibliography

[1] S. Mittal, C. Movsowitz, and J. S. Steinberg, "Ambulatory external electrocardiographic monitoring: Focus on atrial fibrillation.," *J. Am. Coll. Cardiol.*, vol. 58, no. 17, pp. 1741–9, Oct. 2011.

[2] M. P. Turakhia, D. D. Hoang, P. Zimetbaum, J. D. Miller, V. F. Froelicher, U. N. Kumar, X. Xu, F. Yang, and P. A. Heidenreich, "Diagnostic utility of a novel leadless arrhythmia monitoring device," *Am. J. Cardiol.*, vol. 112, no. 4, pp. 520–4, Aug. 2013.

[3] M. E. Lemmert, A. Janata, P. Erkens, J. K. Russell, S. Gehman, K. Nammi, H. J. G. M. Crijns, F. Sterz, and A. P. M. Gorgels, "Detection of ventricular ectopy by a novel miniature electrocardiogram recorder.," *J. Electrocardiol.*, vol. 44, no. 2, pp. 222–8, 2011.

[4] A. Janata, M. E. Lemmert, J. K. Russell, S. Gehman, R. Fleischhackl, O. Robak, E. Pernicka, F. Sterz, and A. P. M. Gorgels, "Quality of ECG monitoring with a miniature ECG recorder.," *Pacing Clin. Electrophysiol.*, vol. 31, no. 6, pp. 676–84, Jun. 2008.

[5] J. Malmivuo and R. Plonsey, *Bioelectromagnetism - Principles and applications og bioelectric and biomagnetic fields*. Oxford University Press (web version), 1995.

[6] A. J. Camm, P. Kirchhof, G. Y. H. Lip, U. Schotten, I. Savelieva, S. Ernst, I. C. Van Gelder, N. Al-Attar, G. Hindricks, B. Prendergast, H. Heidbuchel, O. Alfieri, A. Angelini, D. Atar, P. Colonna, R. De Caterina, J. De Sutter, A. Goette, B. Gorenek, M. Heldal, S. H. Hohloser, P. Kolh, J.-Y. Le Heuzey, P. Ponikowski, and F. H. Rutten, "Guidelines for the management of atrial fibrillation: the Task Force for the Management of Atrial Fibrillation of the European Society of Cardiology (ESC).," *Eur. Heart J.*, vol. 31, no. 19, pp. 2369–429, Oct. 2010.

[7] M. A. Rosenberg, M. Samuel, A. Thosani, and P. J. Zimetbaum, "Use of a noninvasive continuous monitoring device in the management of atrial fibrillation: A pilot study.," *Pacing Clin. Electrophysiol.*, vol. 36, no. 3, pp. 328–33, Mar. 2013.

[8] P. Zimetbaum and A. Goldman, "Ambulatory arrhythmia monitoring: choosing the right device.," *Circulation*, vol. 122, no. 16, pp. 1629–36, Oct. 2010.

[9] P. M. Barrett, R. Komatireddy, S. Haaser, S. Topol, J. Sheard, J. Encinas, A. J. Fought, and E. J. Topol, "Comparison of 24-hour Holter monitoring with 14-day novel adhesive patch electrocardiographic monitoring.," *Am. J. Med.*, vol. 127, no. 1, pp. 95.e11–7, Jan. 2014.

[10] IEC60601-2-47:2012, *Medical electrical equipment - Part 2-47: Particular requirements for the basic safety and essential performance of ambulatory electrocardiographic systems*. International Electrotechnical Commision (IEC), 2012.

[11] "Corventis." [Online]. Available: http://www.corventis.com/int/. [Accessed: 20-Jan-2015].

[12] J. S. Shinbane, M. Merkert, R. Fogoros, V. Mehta, M. Cao, and L. A. Saxon, "Wearable Wireless Arrhythmia Detection Patches : Diagnostic Arrhythmia Yield , Time to First Arrhythmia , and Patient Compliance," *Heart Rhythm Society (Poster #9813)*, 2015. [Online]. Available: http://www.corventis.com//wp-content/uploads/2013/09/Shinbane-poster-5-5-Final.pdf. [Accessed: 20-Jan-2015].

[13] N. Chakravarthy, J. M. Engel, A. Chavan, B. Finlay, and G. Nosbush, "A study of activity and body posture with the PiiX mobile body- adherent device," in *36th Annual International Conference of the IEEE Engineering in Meidicine and Biology Society (EMBC)*, 2014, pp. 2714–7.

[14] J. M. Engel, N. Chakravarthy, G. Nosbush, M. Merkert, M. D. Fogoros, and A. Chavan, "Comparison of Arrhythmia Prevalence in NUVANT Mobile Cardiac Telemetry System Patients in the US and India," in *36th Annual International Conference of the IEEE Engineering in Meidicine and Biology Society (EMBC)*, 2014, pp. 2730–3.

[15] "IRhythm." [Online]. Available: http://www.irhythmtech.com/index.php. [Accessed: 20-Jan-2015].

[16] "Johns Hopkins Medicine." [Online]. Available: http://www.hopkinsmedicine.org/healthlibrary/test_procedures/cardiovascular/holter_monitor_92,P07976/. [Accessed: 08-Dec-2014].

[17] "medilog Darwin Liberty Online Holter Analysis," *HASIBA Medical GmbH*. [Online]. Available: http://hasimed.com/. [Accessed: 04-Jun-2014].

[18] "myPatch® Interface Software Utility," *DMS-Service llc*. [Online]. Available: http://dms-service.com/. [Accessed: 06-Aug-2014].

[19] "Medical Expo - The Online Medical Devices Exhibition." [Online]. Available: http://www.medicalexpo.com/prod/bionet/fetal-central-monitoring-stations-67832-624185.html. [Accessed: 28-Sep-2014].

[20] G. Moody, W. Muldrow, and R. Mark, "A noise stress test for arrhythmia detectors," *Comput. Cardiol.*, pp. 381–4, 1984.

[21] G. B. Moody and R. G. Mark, "The impact of the MIT-BIH arrhythmia database.," *IEEE Eng. Med. Biol. Mag.*, vol. 20, no. 3, pp. 45–50, 2001.

[22] A. Taddei, G. Distante, M. Emdin, P. Pisani, G. B. Moody, C. Zeelenberg, and C. Marchesi, "The European ST-T database: standard for evaluating systems for the analysis of ST-T changes in ambulatory electrocardiography.," *Eur. Heart J.*, vol. 13, no. 9, pp. 1164–72, Sep. 1992.

[23] A. L. Goldberger, L. A. N. Amaral, L. Glass, J. M. Hausdorff, P. C. Ivanov, R. G. Mark, J. E. Mietus, G. B. Moody, C.-K. Peng, and H. E. Stanley, "PhysioBank, PhysioToolkit, and PhysioNet : Components of a new research resource for complex physiologic signals," *Circulation*, vol. 101, no. 23, pp. e215–e220, Jun. 2000.

[24] AAMI, *ANSI/AAMI EC57: 1998/(R) 2003: Testing and reporting performance results of cardiac rhythm and ST-segment measurement algorithms*. Association for the Advancement of Medical Instrumentation, 2003.

[25] B.-U. Köhler, C. Hennig, and R. Orglmeister, "The principles of software QRS detection.," *IEEE Eng. Med. Biol. Mag.*, vol. 21, no. 1, pp. 42–57, 2002.

[26] J. Pan and W. Tompkins, "A real-time QRS detection algorithm," *IEEE Trans. Biomed. Eng.*, vol. 32, no. 3, pp. 230–6, Mar. 1985.

[27] L. Y. Di Marco and L. Chiari, "A wavelet-based ECG delineation algorithm for 32-bit integer online processing.," *Biomed. Eng. Online*, vol. 10, p. 23, Jan. 2011.

[28] Z. Zidelmal, A. Amirou, M. Adnane, and A. Belouchrani, "QRS detection based on wavelet coefficients.," *Comput. Methods Programs Biomed.*, vol. 107, no. 3, pp. 490–6, Sep. 2012.

[29] X. Liu, Y. Zheng, M. W. Phyu, B. Zhao, M. Je, and X. Yuan, "Multiple functional ECG signal is processing for wearable applications of long-term cardiac monitoring," *IEEE Trans. Biomed. Eng.*, vol. 58, no. 2, pp. 380–9, Feb. 2011.

[30] C. Li, C. Zheng, and C. Tai, "Detection of ECG characteristic points using wavelet transforms," *IEEE Trans. Biomed. Eng.*, vol. 42, no. 1, 1995.

[31] J. P. Martínez, R. Almeida, S. Olmos, A. P. Rocha, and P. Laguna, "A wavelet-based ECG delineator: evaluation on standard databases.," *IEEE Trans. Biomed. Eng.*, vol. 51, no. 4, pp. 570–81, Apr. 2004.

[32] A. Ghaffari, M. R. Homaeinezhad, M. Akraminia, M. Atarod, and M. Daevaeiha, "A robust wavelet-based multi-lead Electrocardiogram delineation algorithm.," *Med. Eng. Phys.*, vol. 31, no. 10, pp. 1219–27, Dec. 2009.

[33] A. Ghaffari, M. R. Homaeinezhad, and M. M. Daevaeiha, "High resolution ambulatory holter ECG events detection-delineation via modified multi-lead wavelet-based features analysis: Detection and quantification of heart rate turbulence," *Expert Syst. Appl.*, vol. 38, no. 5, pp. 5299–5310, May 2011.

[34] C. F. Zhang and T.-W. Bae, "VLSI friendly ECG QRS complex detector for body sensor networks," *IEEE J. Emerg. Sel. Top. Circuits Syst.*, vol. 2, no. 1, pp. 52–59, Mar. 2012.

[35] M. Cvikl, F. Jager, and A. Zemva, "Hardware Implementation of a Modified Delay-Coordinate Mapping-Based QRS Complex Detection Algorithm," *EURASIP J. Adv. Signal Process.*, vol. 2007, no. 1, p. 057286, 2007.

[36] A. Martínez, R. Alcaraz, and J. J. Rieta, "Application of the phasor transform for automatic delineation of single-lead ECG fiducial points.," *Physiol. Meas.*, vol. 31, no. 11, pp. 1467–85, Nov. 2010.

[37] F. Chiarugi, V. Sakkalis, D. Emmanouilidou, T. Krontiris, M. Varanini, and T. I, "Adaptive Threshold QRS Detector with Best Channel Selection Based on a Noise Rating System," in *Computers in Cardiology*, 2007, pp. 157–160.

[38] H. Boqiang and W. Yuanyuan, "Detecting QRS Complexes of Two-Channel ECG Signals by Using Combined Wavelet Entropy," in *2009 3rd International Conference on Bioinformatics and Biomedical Engineering*, 2009, no. 1, pp. 2439–42.

[39] "Visual Photos." [Online]. Available: http://www.visualphotos.com/image/2x2647763/old_man_sitting_with_dog. [Accessed: 19-Jan-2015].

[40] "London Evening Standard." [Online]. Available: http://www.standard.co.uk/news/103yearold-gardener-is-britains-oldest-worker-7082694.html. [Accessed: 19-Jan-2015].

[41] T. Takalokastari, E. Alasaarela, M. Kinnunen, and T. Jämsä, "Quality of the wireless electrocardiogram signal during physical exercise in different age groups," *IEEE J Biomed Heal. Inf.*, vol. 18, no. 3, pp. 1058–64, 2014.

[42] I. Silva, G. B. Moody, and L. Celi, "Improving the quality of ECGs collected using mobile phones : The PhysioNet / computing in cardiology challenge 2011," in *Computing in Cardiology 2011*, 2011, pp. 273–6.

[43] L. Johannesen and L. Galeotti, "Automatic ECG quality scoring methodology: mimicking human annotators.," *Physiol. Meas.*, vol. 33, no. 9, pp. 1479–89, Sep. 2012.

[44] H. Xia, G. A. Garcia, J. Bains, D. C. Wortham, and X. Zhao, "Matrix of regularity for improving the quality of ECGs.," *Physiol. Meas.*, vol. 33, no. 9, pp. 1535–48, Sep. 2012.

[45] G. D. Clifford, J. Behar, Q. Li, and I. Rezek, "Signal quality indices and data fusion for determining clinical acceptability of electrocardiograms.," *Physiol. Meas.*, vol. 33, no. 9, pp. 1419–33, Sep. 2012.

[46] I. Jekova, V. Krasteva, I. Christov, and R. Abächerli, "Threshold-based system for noise detection in multilead ECG recordings.," *Physiol. Meas.*, vol. 33, no. 9, pp. 1463–77, Sep. 2012.

[47] D. Hayn, B. Jammerbund, and G. Schreier, "QRS detection based ECG quality assessment.," *Physiol. Meas.*, vol. 33, no. 9, pp. 1449–61, Sep. 2012.

[48] Q. Li, R. G. Mark, and G. D. Clifford, "Robust heart rate estimation from multiple asynchronous noisy sources using signal quality indices and a Kalman filter.," *Physiol. Meas.*, vol. 29, no. 1, pp. 15–32, Jan. 2008.

[49] J. Lee, D. D. McManus, S. Merchant, and K. H. Chon, "Automatic motion and noise artifact detection in Holter ECG data using empirical mode decomposition and statistical approaches," *IEEE Trans. Biomed. Eng.*, vol. 59, no. 6, pp. 1499–1506, 2012.

[50] J. R. Thorpe, T. Saida, J. Mehlsen, A.-B. Mehlsen, H. Langberg, K. Hoppe, and H. B. D. Sorensen, "Comparative study of T-amplitude features for fitness monitoring using the ePatch ECG recorder," in *36th Annual International Conference of the IEEE Engineering in Meidicine and Biology Society (EMBC)*, 2014, pp. 4172–5.

[51]   S. Theodoridis and K. Koutroumbas, *Pattern Rcognition*, 4th ed. Elsevier, 2009.

[52]   "svmtrain," *The MathWorks, Inc.* [Online]. Available: http://www.mathworks.se/help/stats/svmtrain.html. [Accessed: 06-Nov-2014].

Appendix A

Description: This appendix contains a detailed description of the pre-processing of the ePatch ECG recordings applied for the comparison between clinically relevant information extracted from simultaneous recordings obtained with the ePatch ECG recorder and the traditional telemetry equipment. The study is further described in section 3.3.

During this pre-processing of ECGs it is important to attenuate the influence of different types of artifacts. The most common artifacts in ECG signals include electrode motion artifacts, baseline wandering, muscle artifacts, and noise from the power line (50 Hz in Denmark). However, it is also important not to change the appearance of the ECG signal in a way that could lead to misinterpretation. This could for instance occur, if the ST segment was changed due to removal of baseline wandering and electrode motion artifacts using a regular HP filter with too high cut-off frequency. The pre-processing was therefore conducted as illustrated in Figure A.1. The sampling frequency of the raw ECGs was 512 Hz.
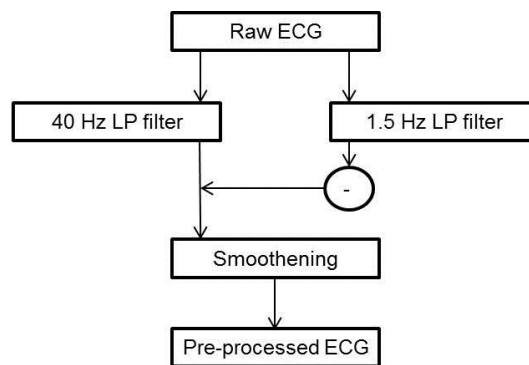
Figure A.1: Block diagram of the pre-processing. The input is a raw ECG signal. The output is the pre-processed ECG signal that was provided to the cardiologist.

First, the steady DC value of 2048 ADC counts was subtracted to obtain a signal located around 0 ADC counts. Then the raw ECG signal was filtered using a LP filter at 1.5 Hz. This result in an estimation of the baseline wandering that also includes some episodes of electrode motion artifacts with low frequencies. This baseline estimation is illustrated as the dashed red line in Figure A.2(b). This filtering step was conducted using a FIR equiripple filter with stop frequency at 1.5 Hz and pass frequency at 0.75 Hz. As observed from Figure A.1, the raw ECG signal was also filtered using a LP filter at 40 Hz. This filter provides a high attenuation of power line interference and some attenuation of muscle artifacts. The output from this filtering step is illustrated as the solid blue line in Figure A.2(b). This filtering step was conducted using a FIR filter with a Hamming window. The cut-off frequency was set to 40 Hz, and a filter order of N = 259 was applied. To obtain zero-phase distortion of the signal, forward and backward filtering was conducted (the "filtfilt" function in MATLAB). This filtering technique is applicable for offline analysis. The outputs from these two filtering steps were then subtracted to obtain a signal with attenuation of baseline wandering and high frequency noise. This is illustrated in Figure A.2(c). The last pre-processing step was smoothening of the signal. This was obtained using a FIR filter with a Bartlett window with cut-off frequency at 40 Hz, and order N = 10. All digital filters were designed using the "fdatool" in MATLAB. An example of the final pre-processed ePatch ECG signal is provided in Figure A.2(d). It is observed that the baseline wandering is completely removed, and the muscle artifacts are attenuated.
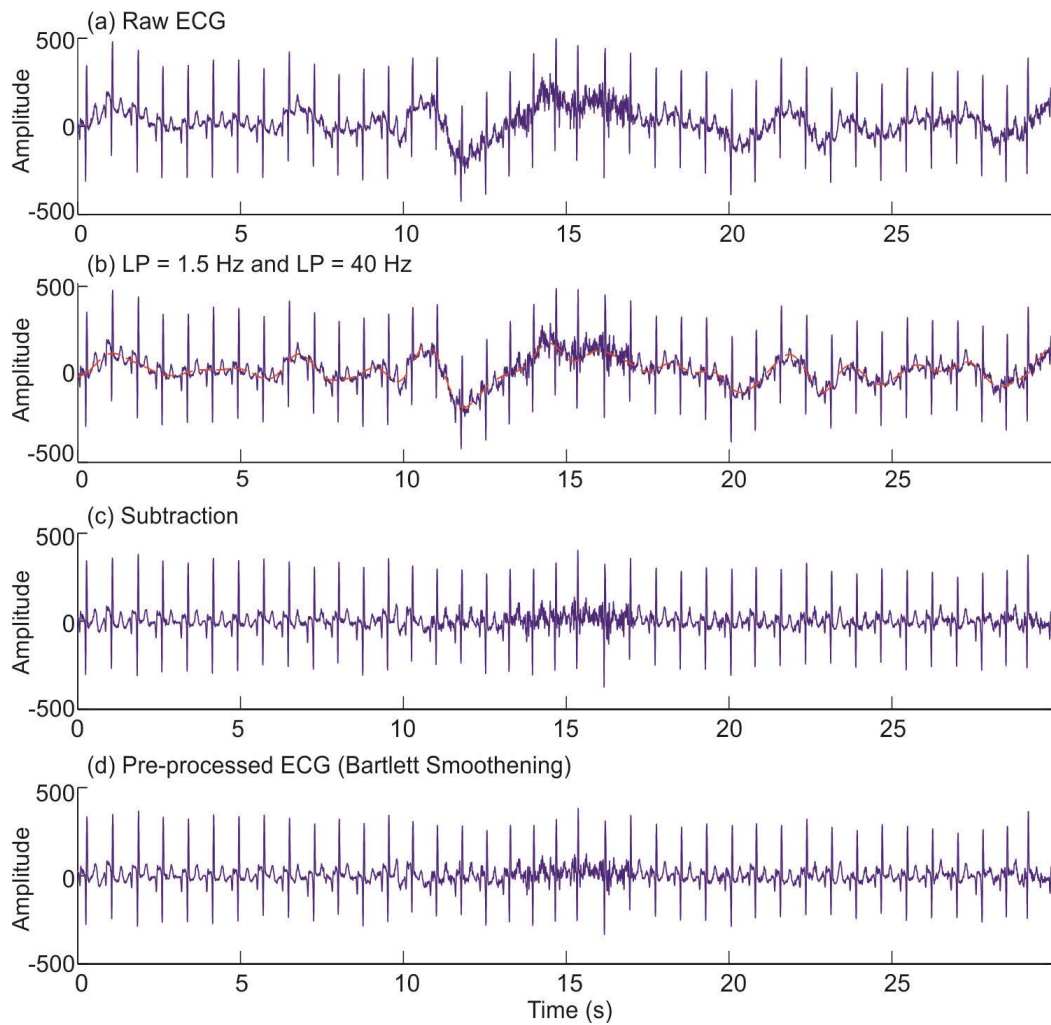
Figure A.2: Illustration of the pre-processing of the raw ePatch ECG signal: (a) Illustrates a segment of raw ECG recorded with the ePatch technology, (b) illustrates the 40 Hz LP filtered ECG signal (blue solid line), and the 1.5 Hz LP filtered ECG signal (red dashed line), (c) illustrates the subtraction of the blue and red curves in (b), and (d) is the final pre-processed ECG signal after Bartlett smoothening of the signal obtained in (c). The amplitudes are in ADC counts.

Appendix B

Description: *This appendix contains a detailed description and reasoning for the correction of the performance obtained on record e0614 from the EDB in the "corrected" overall QRS detection performances stated in Table 4.8 in section 4.5.*

This correction originates from a problematic reference annotation for record e0614. This is illustrated in Figure B.1. It is observed that the reference annotations for many VEB beats are placed right before the actual position of the QRS complex. In spite of the applied 150ms match window [24], this sometimes causes an actual true detection of a VEB beat to be classified as a pair of a missed VEB beat and a false detection (a false positive). This is especially pronounced when channel II from this record is applied. The performance for record e0614 was therefore manually corrected according to Table B.1. The gross average performance for the database with this correction is provided in Table 4.8 on page 52. It is observed how this correction significantly improves the sensitivity with respect to VEB beats.
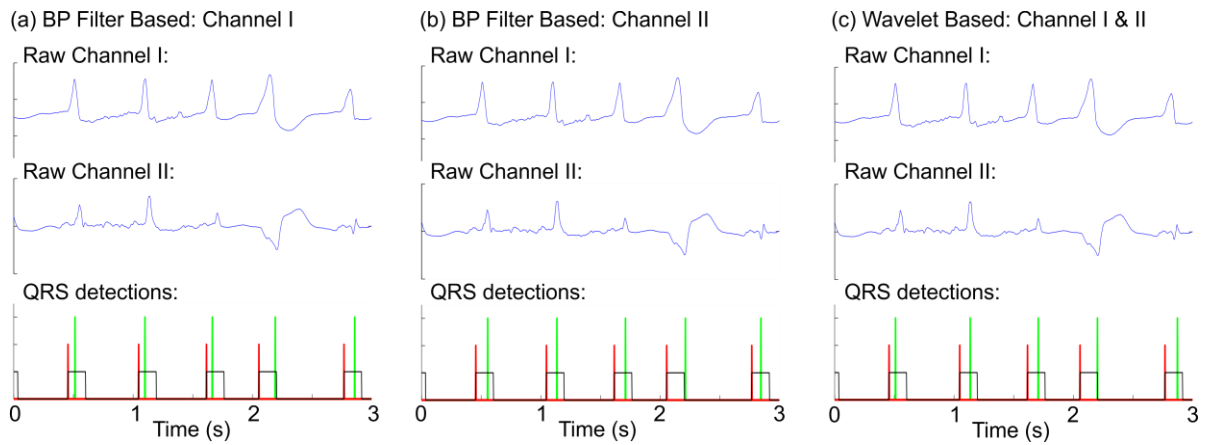
Figure B.1: Illustration of performance correction for record e0614 from the EDB: (a) QRS detection using the BP filter based algorithm applied to channel I, (b) QRS detection using the PB filter based algorithm applied to channel II, and (c) QRS detection using the multi-channel wavelet based algorithm. The green vertical lines indicate the detected QRS positions for each algorithm. The red vertical lines indicate the QRS positions from the reference database. The black squares indicate the right side of the 150ms match window defined in [24]. It is observed that the reference QRS positions are positioned a little left for each QRS complex. This implies that even though the detections for all algorithms are within the duration of the QRS complexes, the VEB beat is detected outside the match window in (b). This implies that the BP filter based algorithm applied to channel II will be wrongly "punished" with both a missed VEB beat and a false positive detection. This was manually corrected as stated in Table B.1.

Table B.1: Correction of performance for record e0614 from the EDB. Only pairs of missed VEBs and false positive detections as illustrated in Figure B.1 were corrected.

Method	Performance measure	Original	After correction
Wavelet based: Channel I & Channel II	FP	97	7
	FN VEB	164	74
BP filter based: Channel I	FP	45	3
	FN VEB	44	2
BP filter based: Channel II	FP	223	10
	FN VEB	228	15

Paper I

TITLE: ePatch ® - A clinical Overview

AUTHORS: Dorthe B. Saadi, Helge B. D. Sorensen, I. H. Hansen, K. Egstrup, P. Jennum, and K. Hoppe

JOURNAL: Not applicable (white paper format)

STATUS: Available online (http://orbit.dtu.dk/en/publications/epatch--a-clinical-overview(5a3e37a2-76a8-4240-aae6-781269a8ca2a).html)

ePatch® - A Clinical Overview

Dorthe Bodholt Saadi [a,b]

Helge Bjarup Dissing Sørensen [b]

Ingeborg Helbech Hansen [b]

Kenneth Egstrup [c]

Poul Jørgen Jennum [d]

Karsten Hoppe [a]

[a] DELTA Danish Electronics, Light & Acoustics, Venlighedsvej 4, 2970 Hørsholm, Denmark. Phone: +45 72 19 40 00, Fax: +45 72 19 40 01, e-mail: ePatch@delta.dk.

[b] Department of Electrical Engineering, Technical University of Denmark, Ørsteds Plads, Bldg. 349, 2800 Kgs. Lyngby, Denmark.

[c] Department of Medical Research, OUH Svendborg Hospital, Valdemarsgade 53, 5700 Svendborg, Denmark.

[d] Danish Center for Sleep Medicine, Department of Clinical Neurophysiology, University of Copenhagen, Glostrup Hospital, 2600 Glostrup, Denmark.

We help ideas meet the real world

ePatch® - A Clinical Overview

ePatch Research Unit*

I. WHY DELTA DESIGNED THE EPATCH

Since the first Holter recorders were invented in the 1940s there has been a tremendous development in the capabilities for ambulatory ElectroCardioGraphic (ECG) monitoring. A detailed overview of the different monitoring techniques is provided in [1] and [2]. Many applications of the older technologies induce significant issues related to patient comfort, duration of the monitoring period, and the integrity of the recorded data. The event and loop recorders only store ECG data when either a patient trigger system or an automatic event detection system is activated. This prevents full disclosure and investigation of potential dangerous but asymptomatic events which were not correctly detected by the automatic algorithms. This situation is overcome by the continuous Holter and telemetry systems. However, the nature of these systems induces significant issues related to patient comfort and compliance with wearing the systems for extended periods of time. The selection of monitoring technique in each situation was thus a compromise between sufficient diagnostic information from adequate continuous monitoring on one hand, and patient comfort and compliance on the other. The DELTA ePatch system was created to fit right in the middle of this compromise: The ePatch was designed to provide reliable high quality continuous ECG monitoring for long periods of time without any patient discomfort or impairment of normal daily life activities.

The results of a patient satisfaction survey based on ePatch recordings from 169 different patients clearly illustrate how the comfort and daily activity level is not altered by wearing the ePatch system (see Fig. 1). This is achieved due to the "wear and forget" principle that was a key factor during the design phase. As illustrated in Fig. 2, the ePatch system is placed on the chest and consists of two parts: 1) The single-use ePatch electrode, and 2) the reusable ePatch sensor. To increase the comfort, the two

How did the ePatch recording affect your daily activities?

- No impact (75%)
- Slight inconvenience (16.4%)
- Some inconvenience (4.7%)
- Normal activities were hindered (3.9%)
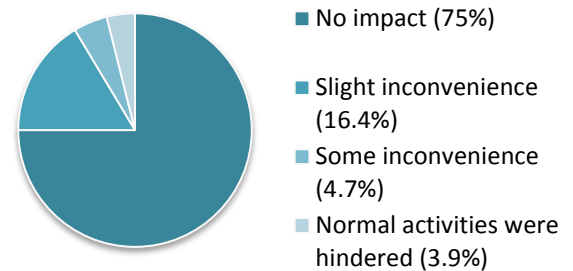
Figure 1. Results from a patient satisfaction survey on 169 different patients undergoing up to 24 hours of continuous ePatch recording. Approximately half of the patients were hospitalized, and the other half were wearing the ePatch system ambulant in their own homes.

parts are connected directly without any cables. The ePatch is thus capable of providing the same clinical information as regular Holter or telemetry equipment. However, this information is gained in a much less intrusive way. This reveals an opportunity to monitor new patient populations, deploy large-scale screening programs, intensified follow-up on known cardiac patients as well as post-operative monitoring, possibilities of close cardiac surveillance of patients in their own homes, and improved surveillance and guidance in rehabilitation and exercise programs.

(a) ePatch placement
(b) ePatch electrode and ePatch sensor
ePatch sensor
ePatch electrode

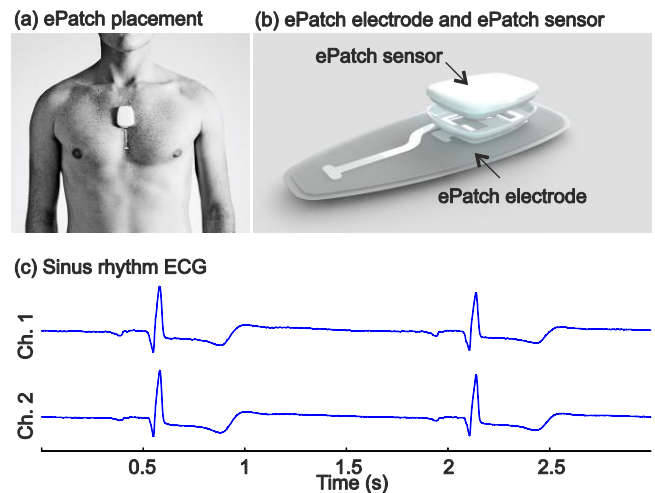(c) Sinus rhythm ECG
Ch. 1
Ch. 2
0.5 1 1.5 2 2.5
Time (s)

Figure 2. (a) Illustration of the CE marked and FDA approved ePatch system placed on the chest. (b) The ePatch sensor and the ePatch electrode before assembly. The ePatch will automatically start recording after mounting of the system. (c) Illustration of normal sinus rhythm ECG recorded with the ePatch system.

*This paper was written by the ePatch research unit in collaboration with Professor, chief physician (cardiology), Dr. Med. Kenneth Egstrup (Department of Medical Research, OUH Svendborg Hospital, Denmark) and Professor, chief physician, Dr. Med. Poul Jennum (Danish Center of Sleep Medicine, Department of Clinical Neurophysiology, Glostrup Hospital, Denmark).

Contact information: DELTA Danish Electronics, Light & Acoustics, Venlighedsvej 4, 2970 Hørsholm, Denmark. Phone: +45 72 19 40 00, Fax: +45 72 19 40 01, e-mail: ePatch@delta.dk.

This white paper was released in August 2014.

II. CLINICAL INTERPRETATION OF ePATCH ECGs

Reliable interpretation and high quality of the recorded ECG signals are the primary conditions for a successful diagnosis and treatment of the patients. The ePatch ECGs can be visualized and analysed in the exact same ways as ECGs recorded with traditional equipment. Several commercially CE marked and FDA approved Holter analysis software systems are available for regular rhythm analysis of ECG recorded with the ePatch system, e.g. [3] and [4]. An example of a Heart Rate (HR) trend curve, and two ECG strips from a healthy test subject is provided in Fig. 3. This test subject is recruited from a fitness study [5], and the high HR observed in the last hours of the recording is due to high intensity exercise in a fitness centre. It is clearly observed how the HR drops during the night. The relatively low mean HR indicates the fitness level of this test subject. The different stages of sleep are also observed as short peaks in the HR trend curve during the night. The recording illustrates a case of Normal Sinus Rhythm (NSR) with only a few SupraVentricular Ectopic Beats (SVEBs). An example of NSR is illustrated in the first ECG strip and an episode of two SVEBs is illustrated in the second ECG strip. Additional examples of clinical ECGs recorded with the ePatch system are provided in section IV.

The user-friendly design of the ePatch implies that the placement of the electrodes is different from the standard Holter/telemetry electrode locations. In addition, the distance between the recording sites is slightly shorter. This induces small changes in the appearance of the recorded ECGs. However, a variety of clinical studies have demonstrated the possibility of recording of diagnostic relevant ECG using prototype patch devices [6], [7], [8], [9]. To further confirm the clinical quality, diagnostic yield and recognizable appearance of clinically relevant heart rhythms, a number of different clinical studies were conducted with the novel ePatch system. The purpose of the first study was to confirm that individual ECG strips extracted from long-term recordings obtained with the ePatch system can be used for heart rhythm analysis. This application scenario is similar to the traditional Holter analysis applied today, where selected ECG strips are extracted by an experienced ECG technician and provided to the referring medical doctor together with a general description of the findings in the recording. Two medical doctors conducted an individual assessment of seven-second ECG strips which were selected by an experienced ECG technician from 25 randomly selected admitted patients. As illustrated in Fig. 4, the result was that the two medical doctors found as much as 98.5% and 99.5% of the
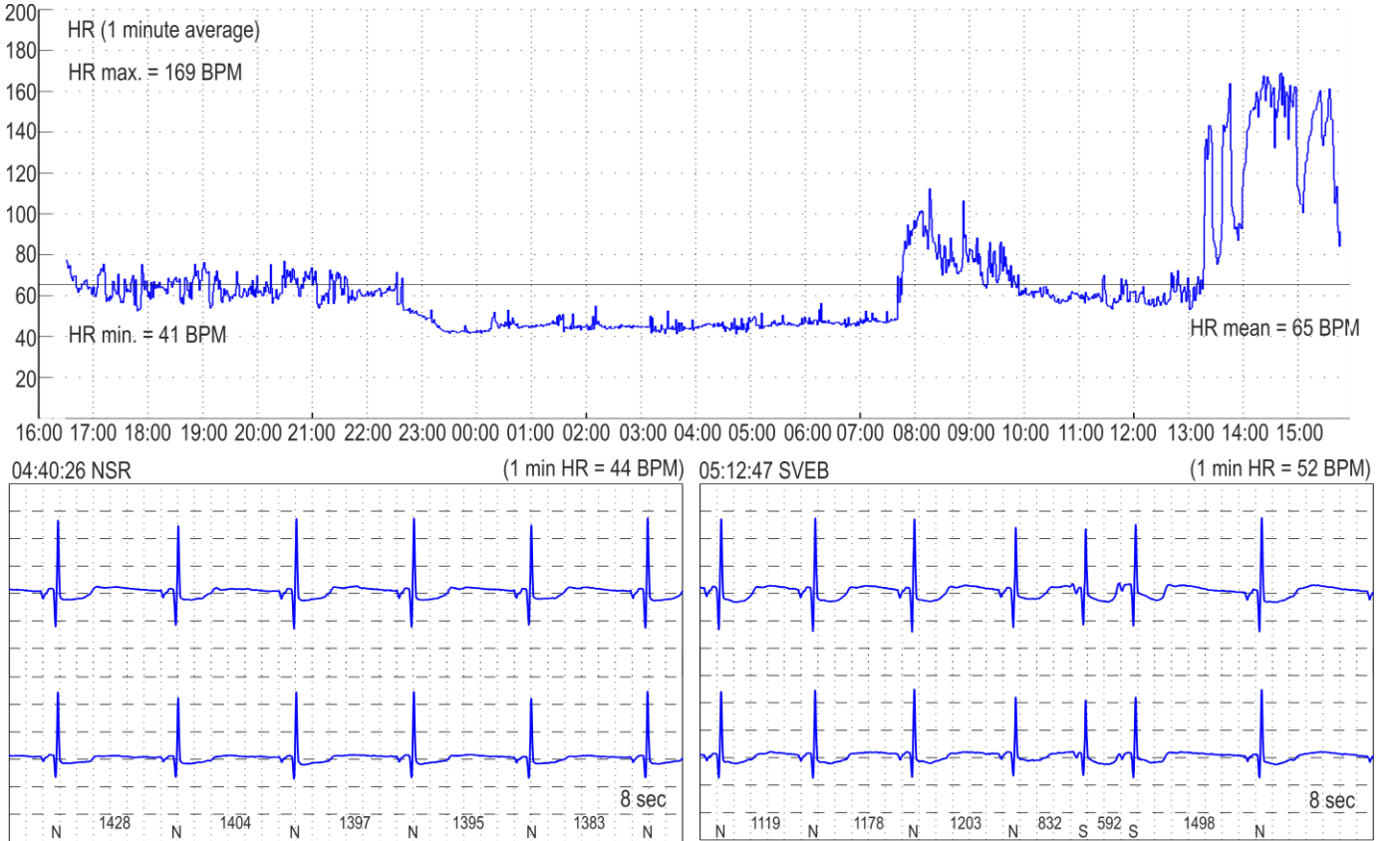
Figure 3. Example of a HR trend curve from a healthy test subject recruited from a fitness study [5]. The HR clearly drops during the night, and increases rapidly in the morning. The different stages of sleep are observed from the short HR peaks during the night. The last couple of hours with relatively high HR were recorded during heavy exercise. The lower plot illustrates two ECG strips extracted from the recording. The first strip illustrates NSR during the night, and the second ECG strip illustrates two SVEB beats.
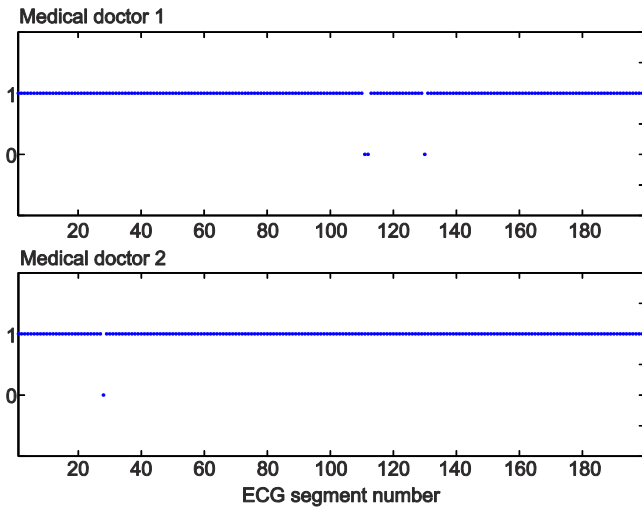
Figure 4. Result from a clinical study investigating the usefulness of two channel ePatch ECG for heart rhythm analysis. Eight segments were selected from 25 different patients, yielding a total of 200 ECG segments. Each of the 200 segments was independently evaluated by two medical doctors. The score 1 indicates that the medical doctor found the segment useful for heart rhythm analysis, whereas the score 0 indicates that he did not find the segment useful for rhythm analysis [10].

segments useful for rhythm analysis [10].

In another clinical study, the overall diagnostic information from a 24-hour ePatch recording was compared with the diagnostic information from simultaneous monitoring with regular telemetry equipment [11]. This comparison was conducted by a cardiologist using 11 randomly selected admitted patients. The cardiologist selected relevant alarm events from the telemetry recording, and these were compared with the same time period of the ePatch recordings to confirm the presence of the arrhythmia event in the ePatch recordings. An example of these comparisons is provided in Fig. 5. The general heart rhythm and HR trend curves were compared as well. For all patients, the same diagnostic information was extracted from the two monitoring techniques. The clinically relevant

TABLE 1. SUMMARY OF CLINICAL FINDINGS USING EPATCH ECG RECORDED ON 169 DIFFERENT PATIENTS. THE RIGHT COLUMN INDICATES THE NUMBER OF PATIENTS THAT DISPLAYED EACH ARRHYTHMIA TYPE.

Arrhythmia type	Number
Atrial flutter (AFL)	5
Atrial fibrillation (AF)	14
Atrio-ventricular block (AV block)	4
Sino-atrial block (SA block)	3
Supraventricular tachycardia (ST)	2
Supraventricular ectopic beats (SVEBs)	50
Ventricular ectopic beats (VEBs)	44

heart rhythms and beats observed in this investigation included NSR, Atrial Fibrillation (AF), paroxysmal AF, pauses, Ventricular Ectopic Beats (VEBs), and SVEBs. Furthermore, ventricular frequencies up to 150 Beats Per Minute (BPM) were represented. This study indicates that ECGs recorded with the ePatch system contain the same diagnostic information as traditional telemetry systems.

In a third clinical study, data from the CE marked ePatch was applied as the primary ECG source. The ECG data was analysed by experienced ECG technicians using the CE marked MyDarwin software [4]. This implies that solely the ECG recorded with the ePatch was analysed in order to gain information about the patients. The study enrolled 169 patients from two different patient groups: 1) 84 patients admitted after apoplexy, and 2) 85 patients that were monitored in their homes as a part of an ambulant PolySomnoGraphy (PSG) recording. A total summary of the overall arrhythmia findings is provided in Table 1. Overall, 17 significant findings were reported (12 in the apoplexy group and five in the ambulant group).
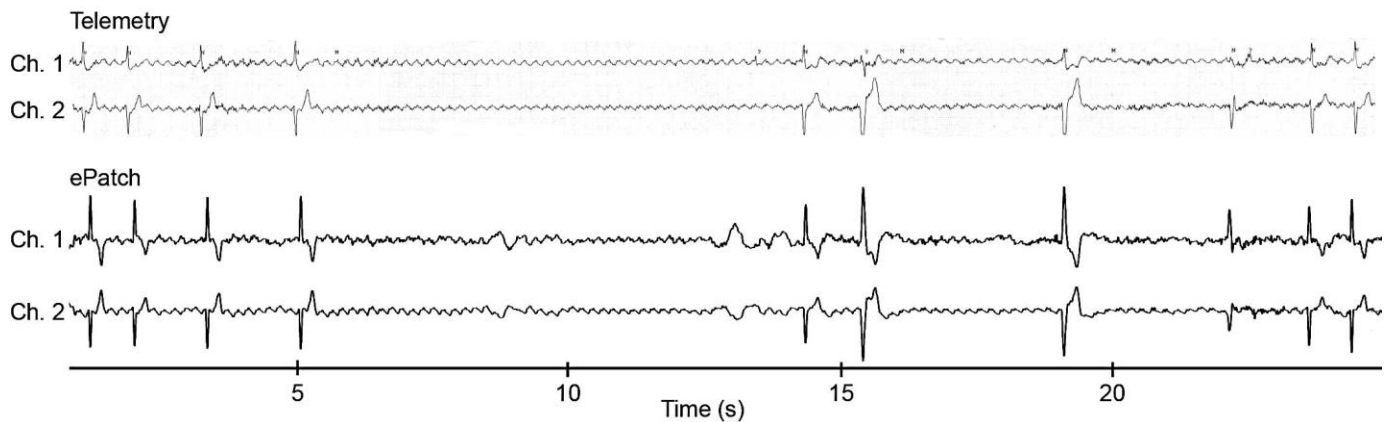
Figure 5. Example of comparison between an alarm event from the traditional telemetry equipment and the corresponding time in the ePatch recording. This case illustrates an episode with 9 seconds pause. The two telemetry ECG channels are provided in the upper traces. The two ePatch ECG channels are provided in the lower traces.

III. Clinical Usability of the ePatch

As mentioned earlier, the key design goals of the ePatch system were to develop a reliable, safe, comfortable ECG recording system which is easy to use for both the patients and the healthcare providers. This has been accomplished both by the easy handling and mounting of the system, and the cable free design.

A. Mounting of the ePatch

The simple mounting of the ePatch system is illustrated in Fig. 6. The mounting consists of six easy steps: 1) The ePatch sensor and the ePatch electrode are easily attached by clicking the two parts together; 2) The protective plastic back liner is removed from the electrode to expose the adhesive part; 3) The electrode is attached to the skin in the correct position; 4) The assistive front liner is removed from the electrode; 5) The corners of the electrode are carefully pressed to ensure firm adhesion to the skin; and 6) The patient can wear normal clothing immediately after the mounting and throughout the entire recording period. The simple mounting procedure even facilitates the possibility for patients to mount the ePatch and conduct an ambulatory recording themselves, for instance before a follow-up consultation. After the mounting, the ePatch sensor will automatically start recording. Of course, the skin should be

How long time did you spend on mounting the ePatch?

- 0-2 minutes (75.8%)
- 2-5 minutes (23.6%)
- > 5 minutes (0.6%)
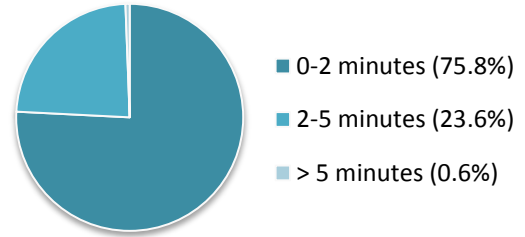
Figure 7. Results from a survey on the mounting time for the ePatch system. The nurses from this survey conducted a total of 169 ePatch recordings during a period of approximately six months.

prepared before mounting. This preparation follows the known procedure from other ECG equipment. The results from a clinical study including a total of 169 patients and three different hospital units show that more than 75% of the recordings were mounted in less than two minutes, and more than 99% were mounted in less than five minutes (see Fig. 7). After the recording, the ePatch system is easily removed from the chest. The ePatch sensor and the ePatch electrode are separated, and the data is extracted from the sensor using a standard USB cable. Studies show that the removal of the ePatch system is conducted in less than two minutes in more than 99% of the recordings.
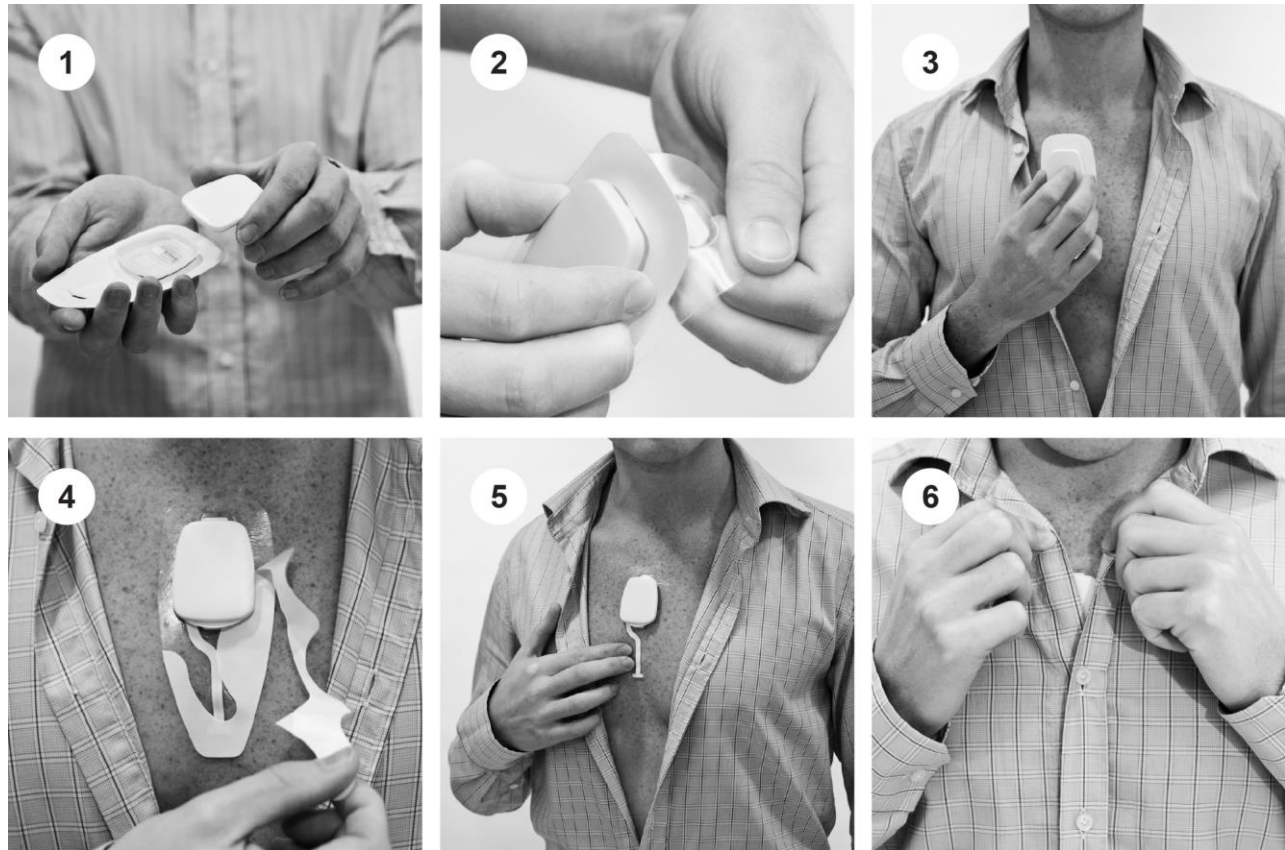
Figure 6. Mounting of the ePatch is carried out in six easy steps: 1) Attach the ePatch sensor to the ePatch electrode by clicking them together; 2) Remove the back liner from the electrode to expose the adhesive part; 3) Place the adhesive electrode in the correct position; 4) Remove the assistive front liner from the electrode; 5) Press carefully around the corners of the electrode to ensure firm adhesion to the skin; and 6) The patient wears normal clothing immediately after mounting and throughout the entire duration of the recording.

B. Patient and Healthcare Provider Satisfaction

The results from a user satisfaction survey based on the 169 ePatch recordings clearly show how the design goals are reached by the ePatch system: 83.6% of the nurses indicated that the ePatch was simpler than the traditional ECG equipment (see Fig. 8). It was also indicated by 75% of the patients that they experienced no impact on their ability to perform normal daily life activities during the recording period (see Fig. 1). Only 3.9% of the patients experienced to be hindered in normal daily activities. Furthermore, another clinical study enrolling 50 patients admitted for cardiac surveillance shows that 92.5% of the patients answering the questionnaire regarding their satisfaction with wearing the ePatch system answered to be "very satisfied". The remainder patients indicated to be "satisfied". None of the patients were "dissatisfied" or "very dissatisfied". Fourteen patients also made additional comments regarding either their non-awareness of wearing the ePatch system or that they preferred the ePatch over the traditional telemetry equipment which was worn simultaneously. These results demonstrate the simplicity of the system and the satisfaction with using the system – from both a patient and healthcare provider point-of-view.

IV. EXAMPLES OF CLINICAL ECGs

This section contains some interesting cases of clinical ECGs recorded with the ePatch system. Each example is illustrated by use of raw unfiltered ECG data recorded with a CE marked ePatch system. Each heart beat is automatically detected with DELTA's proprietary embedded algorithm. The ECG strips are visualized with standardized square sizes to indicate time and amplitude (two vertical squares indicate 1mV and five horizontal squares indicate 1s). The HR trend curves contain one minute HR averages. Each Lorenz plot indicates the relationship between the current RR interval (time between two subsequent heart beats) and the subsequent RR interval for one hour of the recordings.

How did you find the application of the ePatch compared to traditional ECG equipment?

- Simpler (83.6%)
- Equal (14.5%)
- Harder (0%)
- Don't know (1.9%)
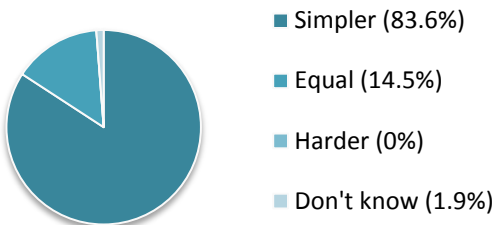
Figure 8. Results from a clinical study regarding the nurse evaluation of the ePatch system compared to traditional ECG equipment: 83.6% of the nurses from three different regular hospital units found the ePatch system simpler than the traditional ECG equipment. A total of 169 ePatch recordings were evaluated for this survey.
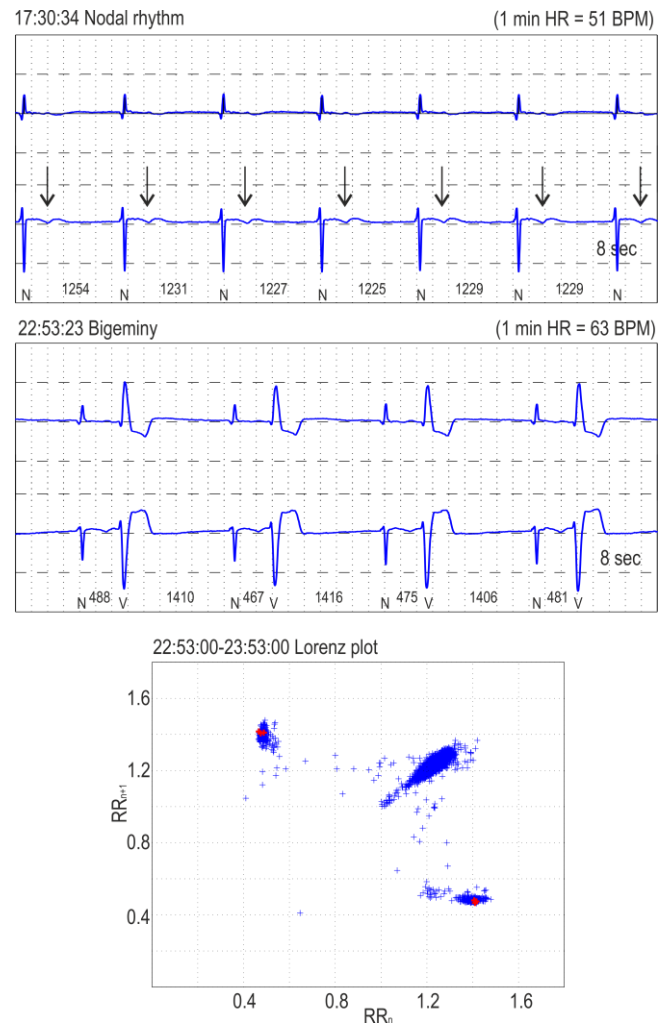
Figure 9. Clinical ECG strips from a patient with nodal rhythm. The retrograde P-waves positioned after the QRS complex are marked with black arrows in the first ECG strip. The lower ECG strip illustrates a case of bigeminy for the same patient. The bigeminy present during this hour is also observed from the Lorenz plot where the red marks indicate the heart beats from the second ECG strip.

Fig. 9 illustrates ECG strips and a Lorenz plot recorded from a patient with nodal rhythm. The nodal rhythm is clearly observed from the first ECG strip. The recording is furthermore described by a high number of VEBs which often are present as bigeminy. This is illustrated in the second ECG strip. The bigeminy is also observed from the Lorenz plot. The red marks in the Lorenz plot indicate the heart beats that are illustrated in the second ECG strip.

Fig. 10 illustrates an overview of a recording on a patient that suffers from paroxysmal AF. The irregular heart rhythm is clearly observed from the first ECG strip, and a case of AF termination, including the sinus recovery period, is represented in the second ECG strip. During the first hour of the recording, there are three shifts from AF to NSR. This is also observed from the sudden drops in the HR trend curve.
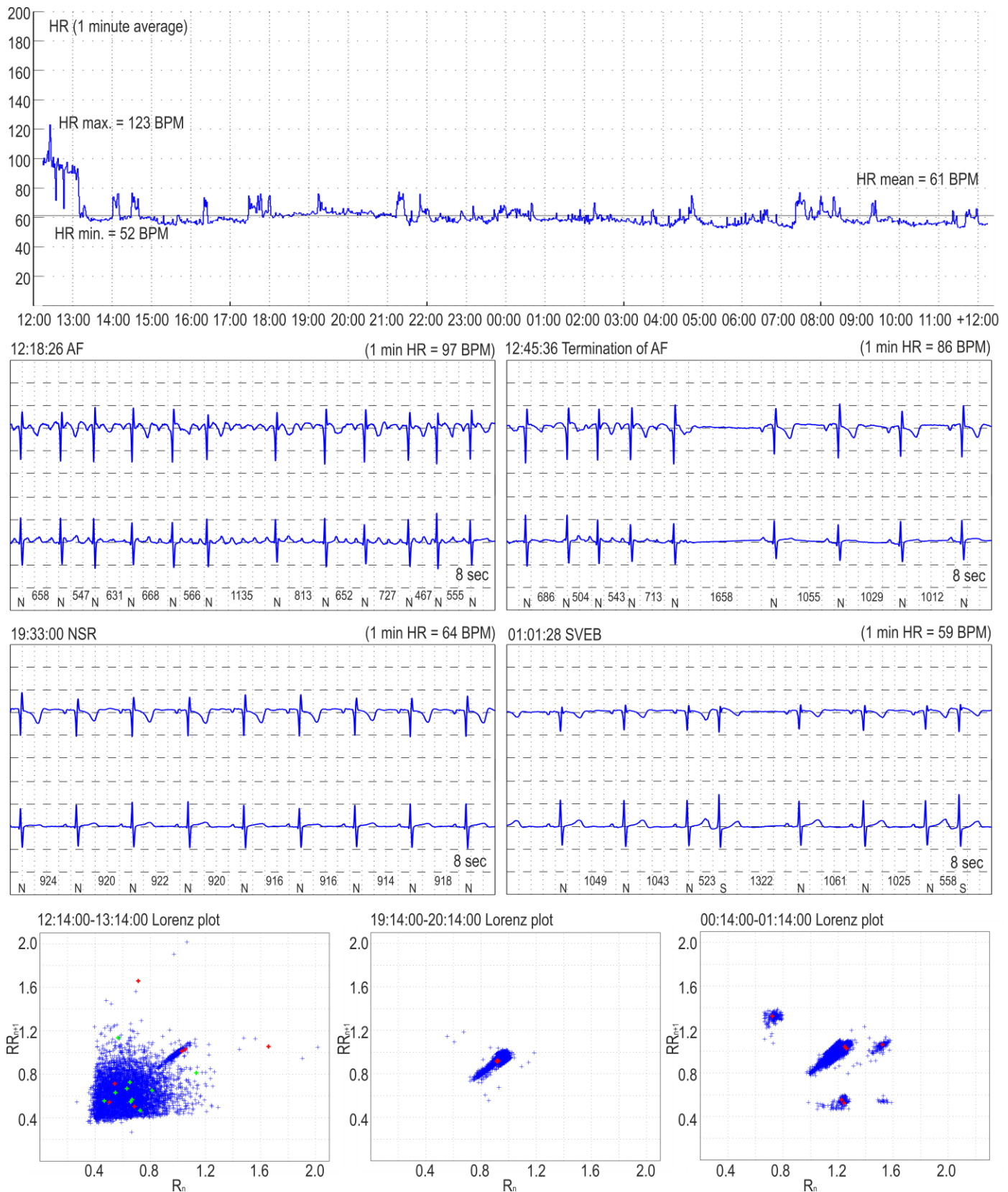
Figure 10. Overview of a clinical ECG recording from a patient with paroxysmal AF. The HR trend curve indicates a high HR in the first hour with a few drops. This part of the recording represents episodes of paroxysmal AF, and the drops in the HR curve represent episodes of NSR. The first ECG strip illustrates a period with AF. The heart beats in this strip are illustrated with green marks in the left Lorenz plot. The red marks in the left Lorenz plot indicate the beats from the second ECG strip that illustrates a case of AF termination. It is observed that the first beats from this ECG strip are placed in the "chaotic AF region" of the Lorenz plot. The sinus recovery period causes two beats to be located away from most other beats, and the last 3 beats are located in the "cigar shaped" area of the Lorenz plot that represents periods of NSR. The third ECG strip illustrates a period of NSR. These beats are indicated by red marks in the middle Lorenz plot. The last ECG strip illustrates a period with two SVEBs. The red marks on the right Lorenz plot illustrate the beats from this ECG strip. The right Lorenz plot generally illustrates that this hour of data contains a very high number of SVEBs.

The first Lorenz plot in Fig. 10 represents both the irregular nature of RR intervals during episodes of AF as well as a "cigar shaped" group of RR intervals which represent the episodes of NSR. The green marks in the first Lorenz plot indicate the heart beats that are illustrated in the first strip. The red marks in the first Lorenz plot indicate the heart beats from the second ECG strip (AF termination episode). The combination from AF to sinus recovery to NSR is observed from the red marks in the first Lorenz plot. The second Lorenz plot is taken from one hour of the recording with primarily NSR and only a few SVEBs. The ECG strip with NSR is marked with red in the second Lorenz plot. The third Lorenz plot is from one hour with a very high number of SVEBs. This is observed from the four distinct areas in the Lorenz plot. Again, the red marks indicate the heart beats represented in the fourth ECG strip.

An overview of a recording with primarily NSR is illustrated in Fig. 11. The recording contains scattered VEBs as illustrated in the first ECG strip. The second ECG strip illustrates a period of NSR. The patient also has two episodes of 2nd degree AV block during the night. An example of this is illustrated in the third ECG strip. At the end of the recording there is an episode of sinus tachycardia. An ECG segment from the one minute with the highest average HR is presented in the fourth strip. A slight decrease in the HR is observed during the night.
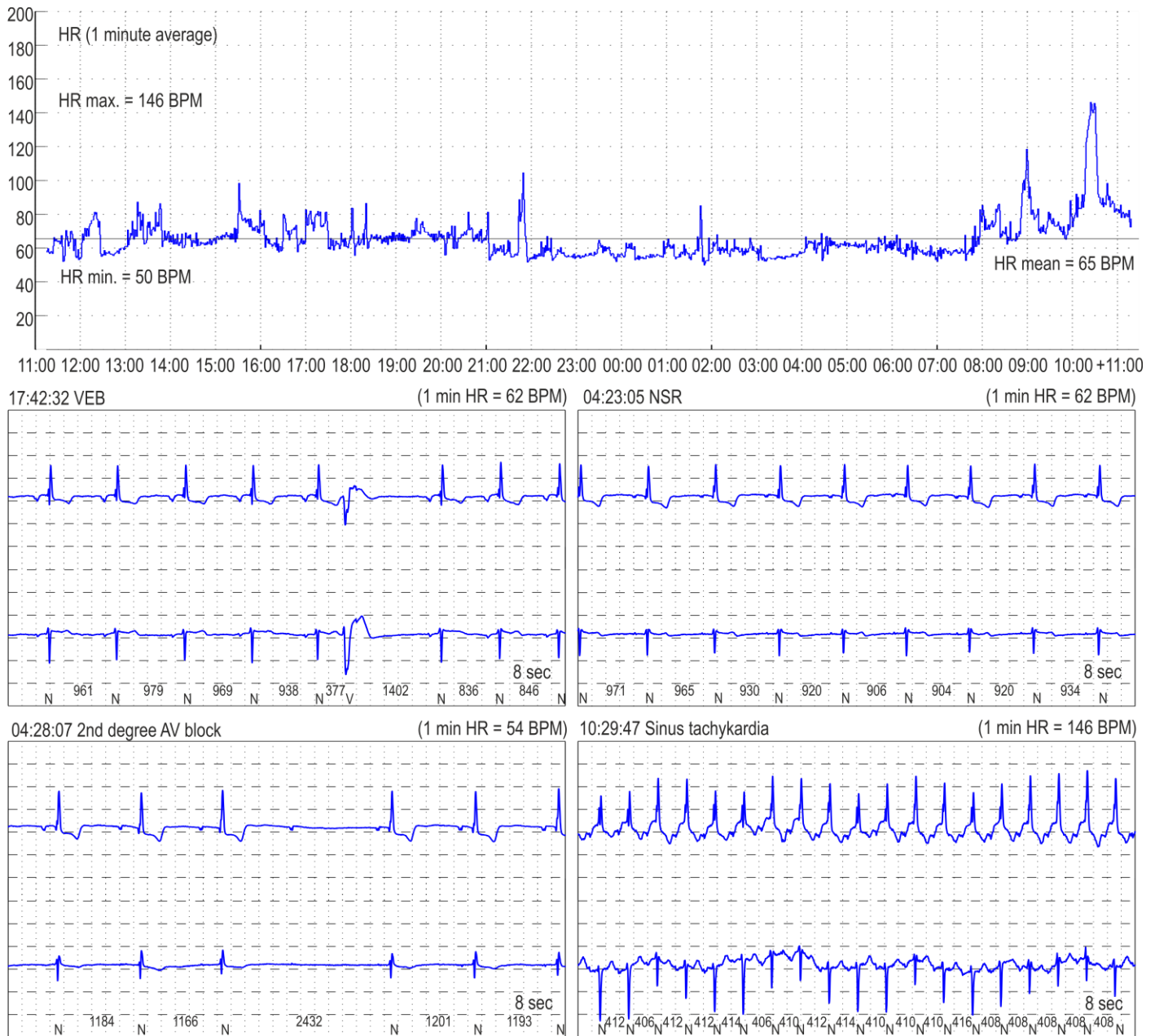
Figure 11. Overview of a clinical ECG recording from a patient with primarily NSR. The recording has scattered VEBs, as illustrated in the first ECG strip, and two cases of 2nd degree AV block, as illustrated in the third ECG strip. The second strip illustrates a period of NSR, and the fourth strip illustrates a data segment from the period with the highest one minute HR.

Another interesting clinical example is illustrated in Fig. 12. This patient suffers from AF during the entire duration of the recording. It is observed from the three Lorenz plots that the nature of the irregularity of the RR intervals differs from the one observed for the patient in Fig. 10. The two ECG strips illustrate examples of AF with different ventricular frequencies. The first strip has a relatively low frequency. The heart beats from this strip are illustrated by red marks in the second Lorenz plot. The second ECG strip illustrates a period of relatively high ventricular frequency. The heart beats from this strip are illustrated by red marks in the third Lorenz plot. It is observed how the different ventricular frequencies are located in different regions of the Lorenz plots.

The last clinical example is provided in Fig. 13. This patient suffers from AF with a high number of VEBs that are often present as bigeminy.

These clinical examples illustrate how ECG recorded with the ePatch system can be applied to diagnose and monitor patients with different kinds of rhythm disorders. Together with the described results from the clinical studies regarding the ePatch interpretability, this demonstrates that the ePatch system is easily used as a substitute for traditional ECG equipment (e.g. Holter or telemetry recorders). Moreover, the high patient satisfaction facilitates the possibility of very long-term monitoring, and
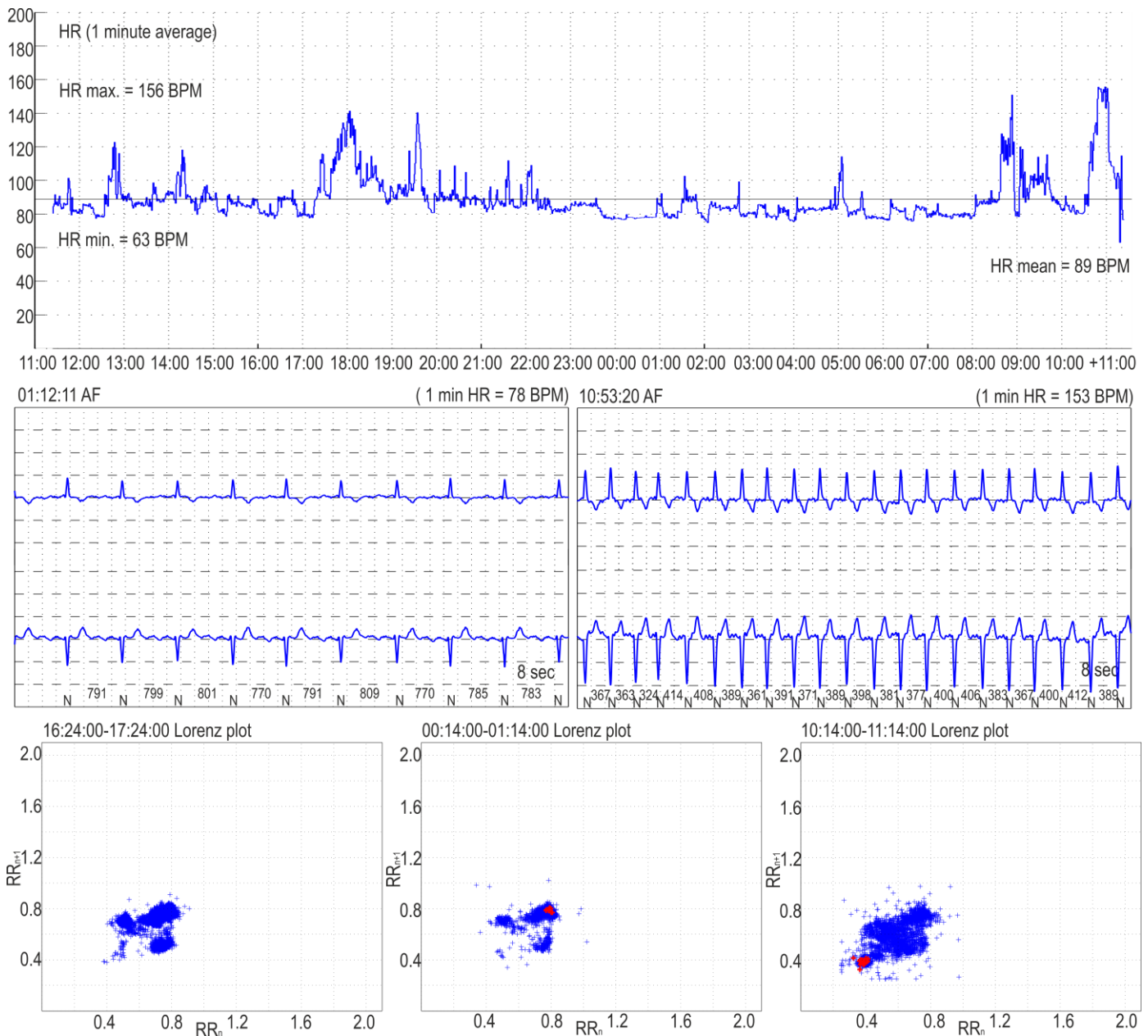
Figure 12. This patient suffers from AF, and the irregularity of the QRS complexes is observed in the three Lorenz plots. The two ECG strips illustrate AF with different ventricular frequencies. The red marks in the second and third Lorenz plots correspond to the heart beats illustrated in the two ECG strips.

consequently improved diagnosis and treatment for a high number of patients where ECG monitoring is not conducted today, or is limited by patient compliance or other obstacles related to the healthcare system.

V. TECHNICAL SPECIFICATIONS OF THE EPATCH

The adhesive ePatch electrode is bio-compatible and contains the skin contact points that allow the recording of bio-potentials. The ePatch sensor contains all the electronic parts, a rechargeable battery, data storage module, a signal processing module, and equipment for wireless data transmission. The ePatch is placed on the chest of the patient, and the recording of high quality ECG starts automatically after the mounting of the system.

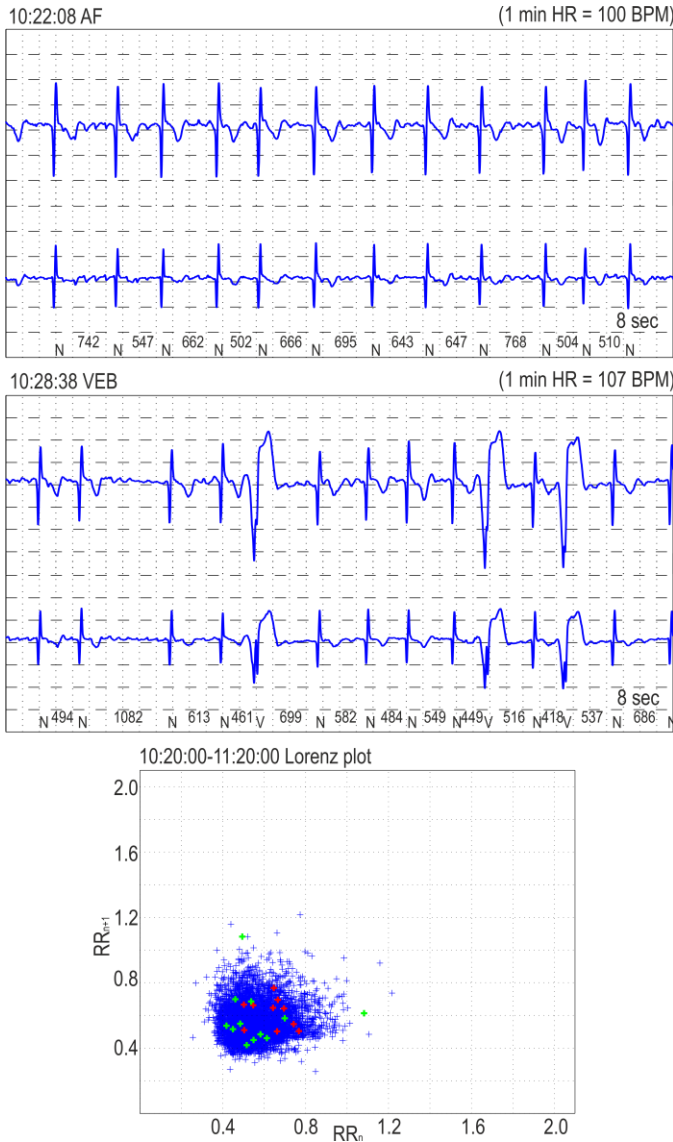The ePatch is shower proof, it is easily worn under

Figure 13. Clinical ECG strips from a patient with AF and a high number of VEBs. The irregular nature of the RR intervals is observed from the Lorenz plot. The red marks in the Lorenz plot represent the heart beats included in the upper ECG strip, whereas the green marks represent the heart beats included in the lower ECG strip.

normal clothing, and it can thus be applied during most normal daily life activities. The unique modular design of the ePatch system allows easy adaptation and customization to match the specific needs in every monitoring situation. The current standard EU version of the ePatch is CE approved for 24-hour ambulatory ECG recording. It is able to record two ECG channels with a sampling frequency of 512 Hz, and a bit resolution of 12 bits. The current US version is FDA approved for ambulatory recording of two ECG channels for 72 hours with a sampling frequency of 256 Hz. One of the major advantages of the ePatch system is the possibility of continuous ECG recording for long periods of time. All ECG data can be stored, and full disclosure of the recorded data is therefore possible. This ensures that no critical events are lost. After the recording, the data is transferred to a computer with fast data transmission using a USB cable. The ECG can then be analysed offline.

The next generation of the ePatch will be available during the fall 2014. This generation can record a varying number of channels (one to three) for multiple days with a bit resolution of up to 16 bits, and a user-defined sampling frequency from 128 Hz to 1024 Hz. Furthermore, the next generation is born with additional recording modalities, e.g. accelerometers for activity estimation and adaptive quality assurance. There is also possibility of real-time embedded signal processing and real-time transmission of e.g. ECG strips, events or HR trend curves. The data can either be analysed offline after the recording, or it can be wirelessly transmitted to for instance a central monitoring station (e.g. regular hospital telemetry equipment, monitoring of cardiac patients in their own homes). This transmission is secure and follows standard protocols for transmission of private information. Each ECG file is stored in the proprietary ePatch File System (EFS) format, and can be converted to other formats to allow analysis with commercial software, e.g. [3] and [4].

VI. OTHER RESEARCH ACTIVITIES

Research activities related to the ePatch platform have been carried out and are still ongoing. Some of them have already been presented in this paper. These studies were primarily related to the usefulness of two ECG channels recorded on the sternum with the novel ePatch ECG recorder. Research is also conducted to investigate the correlation between ECG recorded with the ePatch placed in different chest locations and the standard 12-lead ECG. This particular investigation will provide knowledge about the morphological content of ECGs recorded with the ePatch in various chest locations. A schematic overview of the experimental set-up is provided in Fig. 14. The ePatch is placed in three different locations: X, Y and Z. Each ePatch sensor records two ECG channels (X1, X2, Y1, Y2, Z1, and Z2). Simultaneous recordings were conducted using standard 12-lead ECG equipment. An example of the recorded ECGs is provided in Fig. 15. The experiment was conducted on 10 healthy volunteers. As observed from Fig.

15, the similarity is highest between Y1 and V2. This may indicate that the morphological information from V2 could also be extracted from the ePatch lead Y1. The mean correlation between Y1 and V2 for the 10 test subjects was found to be 0.8715 with a standard deviation of 0.1232. Further research is conducted to explore the potential for reconstruction of some of the standard leads in the 12-lead ECG system based on information from ePatch sensors placed in different chest locations.

Besides these studies, a number of research projects have already obtained benefits from the advantages gained from this technology. One study includes the application of the ePatch system for automatic classification of acute stress [12]. Another study is related to automatic assessment of the overall quality of long-term ECG recordings obtained using patch type ECG recorders [13]. A third study applies different features based on the T-wave amplitude to estimate fitness level of the test subjects [5]. A fourth study investigated the relation between heart rate variability obtained with photoplethysmography (PPG) and ECG on the sternum [14]. Furthermore, DELTA has participated in a number of larger projects where the possibilities with the ePatch platform were investigated. One of these studies include the European REACTION project that aimed at finding solutions for online diabetes management and therapy in different healthcare settings [15]. During this project, the ePatch was successfully tested in the primary care setting. The ePatch was applied to monitor high risk patients for heart rhythm abnormalities. Other ongoing

Figure 15. Illustration of ECG example from the three ePatch ECG recorders and the standard 12-lead ECG equipment. The top six traces illustrate the two channels from each of the three ePatch sensors, and the lower 12 traces illustrate the traditional 12-lead ECG. A high similarity is observed between Y1 and V2.

research activities are related to areas like design of automatic algorithms for real-time analysis of the ePatch ECG signals, implementation of new sensor modalities, and investigation of new potential areas where all the advantages of the ePatch system provide benefits and possibilities that were not present with the older technologies.

VII. SUMMARY AND CONCLUSIONS

The novel CE marked and FDA approved ePatch ECG monitor was designed to overcome the disadvantages with older ambulatory ECG recorders. The ePatch system thus allows continuous recording of high quality ECG for extended periods of time without patient discomfort and impairment of normal daily life activities. The usability of the ePatch system has been evaluated in a number of clinical studies. These studies include both investigations of the clinical usefulness of the ECG signals recorded with the system and the user satisfaction. The studies clearly indicate the potential for the application of this system for

Figure 14. Illustration of the experimental set-up. Three ePatch recorders were placed in various chest locations, and simultaneous recordings from the three ePatch sensors and the standard 12-lead ECG equipment were obtained from 10 healthy test subjects. Modified from [16].

future ECG monitoring. This opens the possibilities of applying the ePatch for a wide range of situations, e.g. tele-monitoring of patients at home, rehabilitation programs, large-scale screening programs, and follow-up on known cardiac or high risk patients.

REFERENCES

[1] P. Zimetbaum and A. Goldman, "Ambulatory arrhythmia monitoring: choosing the right device.," *Circulation*, vol. 122, no. 16, pp. 1629–36, Oct. 2010.

[2] S. Mittal, C. Movsowitz, and J. S. Steinberg, "Ambulatory external electrocardiographic monitoring: Focus on atrial fibrillation.," *J. Am. Coll. Cardiol.*, vol. 58, no. 17, pp. 1741–9, Oct. 2011.

[3] "myPatch® Interface Software Utility," *DMS-Service llc*. [Online]. Available: http://dms-service.com/. [Accessed: 06-Aug-2014].

[4] [4] "medilog Darwin Liberty Online Holter Analysis," *HASIBA Medical GmbH*. [Online]. Available: http://hasimed.com/. [Accessed: 04-Jun-2014].

[5] J. R. Thorpe, T. Saida, J. Mehlsen, A.-B. Mehlsen, H. Langberg, K. Hoppe, and H. B. D. Sorensen, "Comparative study of T-amplitude features for fitness monitoring using the ePatch ECG recorder," in *36th Annual International Conference of the IEEE Engineering in Meidicine and Biology Society (EMBC)*, 2014, pp. 4172–5.

[6] M. Puurtinen, J. Viik, and J. Hyttinen, "Best electrode locations for a small bipolar ECG device: signal strength analysis of clinical data.," *Ann. Biomed. Eng.*, vol. 37, no. 2, pp. 331–6, Feb. 2009.

[7] M. E. Lemmert, A. Janata, P. Erkens, J. K. Russell, S. Gehman, K. Nammi, H. J. G. M. Crijns, F. Sterz, and A. P. M. Gorgels, "Detection of ventricular ectopy by a novel miniature electrocardiogram recorder.," *J. Electrocardiol.*, vol. 44, no. 2, pp. 222–8, 2011.

[8] A. Janata, M. E. Lemmert, J. K. Russell, S. Gehman, R. Fleischhackl, O. Robak, E. Pernicka, F. Sterz, and A. P. M. Gorgels, "Quality of ECG monitoring with a miniature ECG recorder.," *Pacing Clin. Electrophysiol.*, vol. 31, no. 6, pp. 676–84, Jun. 2008.

[9] P. A. J. Ackermans, T. A. Solosko, E. C. Spencer, S. E. Gehman, K. Nammi, J. Engel, and J. K. Russell, "A user-friendly integrated monitor-adhesive patch for long-term ambulatory electrocardiogram monitoring.," *J. Electrocardiol.*, vol. 45, no. 2, pp. 148–53, Mar. 2012.

[10] D. B. Saadi, I. Fauerskov, A. Osmanagic, H. M. Sheta, H. B. D. Sorensen, K. Egstrup, and K. Hoppe, "Heart rhythm analysis using ECG recorded with a novel sternum based patch technology - A pilot study," in *Cardiotechnix 2013: Proc. of the International Congress on Cardiovasular Technologies*, 2013, pp. 15–21.

[11] D. B. Saadi, K. Egstrup, K. Hoppe, and H. B. D. Sorensen, "Comparison of diagnostic information from regular telemetry equipment and a novel patch type electrocardiogram recorder," in *Presented as a late breaking research poster at the 36th Annual International Conference of the IEEE Engineering in Medicine and Biology Society*, 2014.

[12] G. Tanev, D. B. Saadi, K. Hoppe, and H. B. D. Sorensen, "Classification of acute stress using linear and non-linear heart rate variability analysis derived from sternal ECG," in *36th Annual International Conference of the IEEE Engineering in Medicine and Biology Society (EMBC)*, 2014, pp. 3386–9.

[13] D. B. Saadi, K. Hoppe, K. Egstrup, P. Jennum, H. K. Iversen, J. L. Jeppesen, and H. B. D. Sorensen, "Automatic quality classification of entire electrocardiographic recordings obtained with a novel patch type recorder," in *36th Annual International Conference of the IEEE Engineering in Medicine and Biology Society (EMBC)*, 2014, pp. 5639–42.

[14] S. S. Chreiteh, B. Belhage, K. Hoppe, J. Branebjerg, and E. V. Thomsen, "Sternal pulse rate variability compared with heart rate variability on healthy subjects," in *36th Annual International Conference of the IEEE Engineering in Meidicine and Biology Society (EMBC)*, 2014, pp. 3394–7.

[15] "The European REACTION Project," 2014. [Online]. Available: http://www.reactionproject.eu. [Accessed: 25-Jun-2014].

[16] "Wikipedia." [Online]. Available: http://en.wikipedia.org/wiki/Electrocardiography. [Accessed: 09-Jul-2014].

Paper II

Heart Rhythm Analysis using ECG Recorded with a Novel Sternum based Patch Technology
A Pilot Study

Dorthe B. Saadi[1,2], Inge Fauerskov[3], Armin Osmanagic[3], Hussam M. Sheta[3], Helge B. D. Sorensen[2], Kenneth Egstrup[3] and Karsten Hoppe[1]

[1]*DELTA Dansk Elektronik, Lys & Akustik, Venlighedsvej 4, 2970 Hørsholm, Denmark*
[2]*Electrical Engineering, Technical University of Denmark, Ørsteds Plads, Bldg. 349, 2800 Kgs. Lyngby, Denmark*
[3]*Department of Medical Research, OUH Svendborg Hospital, Valdemarsgade 53, 5700 Svendborg, Denmark*
{dbs, kh}@delta.dk, hbs@elektro.dtu.dk, {inge.fauerskov, armin.osmanagic, hussam.m.sheta, kenneth.egstrup}@rsyd.dk

Abstract: According to the World Health Organization, cardiovascular diseases are the number one cause of death globally. Early diagnosis and treatment of many of these patients depend on ambulatory electrocardiography recordings. Therefore a novel wireless patch technology has been designed for easy, reliable long-term ECG recordings. The device is designed for high compliance and low patient burden. This novel patch technology is CE approved for ambulatory ECG recording of two ECG channels on the sternum. This paper describes a clinical pilot study regarding the usefulness of these ECG signals for heart rhythm analysis. A clinical technician with experience in ECG interpretation selected 200 noise-free 7 seconds ECG segments from 25 different patients. These 200 ECG segments were evaluated by two medical doctors according to their usefulness for heart rhythm analysis. The first doctor considered 98.5% of the segments useful for rhythm analysis, whereas the second doctor considered 99.5% of the segments useful for rhythm analysis. The conclusion of this pilot study indicates that two channel ECG recorded on the sternum is useful for rhythm analysis and could be used as input to diagnosis together with other clinical tests and medical history.

1 INTRODUCTION

According to the World Health Organization (2013), cardiovascular diseases (CVDs) are the number one cause of death globally. They state that CVDs were responsible for 30% of all deaths in 2008.

CVDs are not only lethal, but they are also associated with a high economic burden on the healthcare system. Furthermore, diseases like ischemic stroke can have high human costs and decrease significantly the quality of life. Early diagnosis and treatment of cardiac related diseases is therefore crucial. For more than hundred years, the 12-lead electrocardiogram (ECG) has served as the "gold standard" for diagnosis of different heart conditions, including arrhythmias (Mittal et al., 2011). The well-chosen and standardized selection of electrode positions allows a full investigation of different projections of the electrical activity of the heart. This allows a careful investigation of the heart in different "spatial plans".

However, for some conditions, it is more important to obtain long-term information about the general rhythm of the heart from a rhythm analysis. In this case, an ambulatory long-term ECG recording is desired. Some examples of conditions that are not sufficiently managed by baseline 12-lead ECG recordings are paroxysmal atrial fibrillation (AF), non-sustained ventricular tachycardia, unexplained episodes of syncope, and diagnosis of other cardiac symptoms not explained by a baseline 12-lead resting ECG (Mittal et al., 2011), (Zimetbaum and Goldman, 2010). It is, however, important to notice the different possibilities with a standard 12-lead ECG and an ambulatory recording. Some of the main advantages of ambulatory ECG recordings are long monitoring period, detection of paroxysmal and asymptomatic arrhythmias, remote monitoring of the patient and correlation between specific symptoms and the ECG signals.

It is however still important that the ambulatory long-term ECG recordings have a sufficient quality for analysis of specific ECG patterns. Some of the

15

key features in rhythm analysis include the depolarization of the atria (the P-wave) and the depolarization of the ventricles (the QRS complex). An example of a short unfiltered ECG segment recorded with the ePatch is provided in Figure 1.
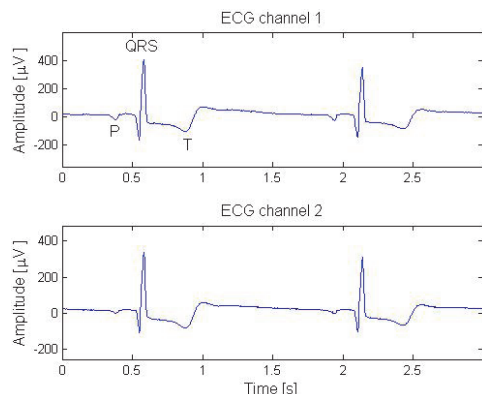

Figure 1: Illustration of a normal sinus rhythm ECG recorded with the novel ePatch technology. The important ECG markers are indicated in channel 1 for one heart cycle. The ECG is raw without any digital filtering.

A number of different long-term ambulatory monitoring techniques are accepted today. One of the most commonly applied ambulatory ECG recorders is the HOLTER monitor.

1.1 Traditional Holter Analysis

The HOLTER monitor typically records 2 – 3 ECG leads continuously for 24 – 48 hours (Zimetbaum and Goldman, 2010). During a traditional HOLTER recording, a medical technician attaches the electrodes and the HOLTER recorder to the patient. The electrodes are attached to the recorder through wires. After the monitoring period, the recorder with the ECG data is returned to the hospital or healthcare facility. At the hospital, a specially trained nurse looks through the recorded data using automatic software and generates a report for the referring medical doctor. This report contains a general description of the rhythm during the recording, any special findings, and a number of descriptive ECG "snippets" displaying the different rhythms found during the recording. The report serves as input to the diagnosis together with other clinical tests and the medical history of the patient. If the recording is of sufficient quality, the following parameters may be determined based on a traditional HOLTER recording: Average heart rate and heart rate range, quantification of atrial and ventricular ectopic beats, and determination of whether AF is present – including information about pattern of AF initiation

and termination, shortest and longest duration of AF, heart rate during AF and AF burden (Mittal et al., 2011).

However, this monitoring technique possesses a number of disadvantages including cables that affect the ability to perform some daily activities during the recording and the lack of real-time data transmission and analysis. Furthermore, the relatively short monitoring duration might not be sufficient for investigation of infrequent arrhythmias (Zimetbaum and Goldman, 2010), (Rosenberg et al., 2013). To account for some of these disadvantages, a novel wireless ECG patch technology was designed.

1.2 The ePatch Technology Platform

The ePatch heart monitoring platform is designed according to a "wear and forget" principle. Thus, the device is designed to be reliable, safe, comfortable and easy to use for both the patient and the healthcare professionals. The ePatch is designed as a technology platform that can be customised to account for the needs in a high variety of situations. Some of the advantages and possibilities with this novel technology platform are listed below:

- Possibility of multi-sensor design with e.g. accelerometer recordings for activity estimation.
- Splash proof design: Patients can shower while wearing the ePatch.
- No cables are needed to connect the electrodes to the recording device. This highly increases the patient comfort and decreases the patient burden.
- Possibility of wireless data transmission and/or local data storage. The platform can be adapted to any desired communication protocol.
- Home monitoring of cardiac patients that might reduce hospitalizations.
- Possibility of long-term monitoring due to the expected higher patient comfort and compliance with wearing the device.
- Module design allows easy adaptation to different applications.
- Real-time embedded signal processing, e.g. automatic detection of cardiac events.

In this pilot study, the focus is to investigate the application of the ePatch for heart rhythm analysis. The ePatch version applied in this study is CE approved for 24 hour ambulatory ECG recordings, and the ECG signals are stored locally on an internal memory. An illustration of the applied ePatch is provided in Figure 2. As observed from Figure 2, the ePatch is placed at the sternum.

Figure 2: Illustration of the placement of the ePatch electrode and sensor on the sternum.

The ePatch system consists of two parts: 1) A bio-compatible, single-use adhesive electrode with multiple skin contact points that is attached directly to the skin surface (this part is termed the ePatch electrode) and 2) A reusable device that contains a rechargeable battery, electronic parts, data storage module, equipment for wireless data transmission, and a signal processing module (this part is termed the ePatch sensor). The ePatch sensor is attached directly on the ePatch electrode. This makes the system completely free of cables. This is designed so that patients can perform normal daily activities during the recording. Furthermore, the ePatch is easily worn under normal clothing and the cable free design makes it possible for the patient to easily change clothes during the recording. This patch design also facilitates a very small and light weight construction that minimizes the awareness of the system while wearing it. The two ECG channels are measured as bipolar derivations from the multiple skin contact points, cf. Figure 3.
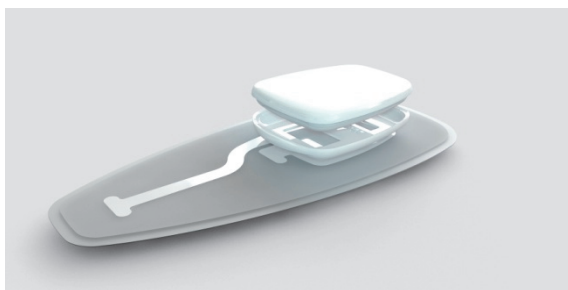
Figure 3: Illustration of the ePatch electrode and sensor before assembly. The ePatch version applied in this study records two ECG channels using bipolar derivations from the multiple skin contact points in the ePatch electrode.

The placement of the ePatch electrode results in a shorter distance between the bipolar recording electrodes. This might influence the quality of the ECG signal. This reservation toward the quality of ECG signals recorded using patch technologies with near-field recording electrodes was also stated by Mittal et al., (2011). However, Rosenberg et al., (2013) compared the ability of a patch type ECG recorder to recognize episodes of AF with a traditional 24-hours HOLTER recording. They found an excellent agreement between the patch recorder and the HOLTER recorder for both AF episode detection and AF burden estimation during a 24 hour recording in 74 consecutive patients.

The selected electrode placement furthermore changes the different projections of the cardiac vector, and hereby changes the appearance of the ECG slightly. This might induce issues regarding the medical professional's ability to recognize different heart rhythms and hereby reduce the practicability of the system. On the other hand, the advantages of this placement are expected to include the benefits of reduced artefacts from large muscles and large movements of electrodes and wires. Furthermore, several studies have shown promising results with experimental ECG recorders placed at a midsternal location. Two research groups, (Janata et al., 2008) and (Lemmert et al., 2011), conducted studies where 7 seconds noise free HOLTER recordings were visually compared with 7 seconds noise free ECG recordings from a prototype device developed by Phillips Healthcare. Janata et al., (2008) investigated different placements of the experimental device and compared the ability to recognize the presence of P waves, PR time, ventricular morphology (QRS width $\leq$ 0.12 seconds or prolonged), and rhythm diagnosis. They found that for the presence of P waves, PR time and general rhythm diagnosis, the device location had a significant influence, and that a midtsternal location was optimal. They generally obtain a good agreement between the two devices. Lemmert et al., (2011) investigated the ability to visually recognize ventricular ectopic beats (VEBs) and ventricular fibrillation (VF) with ECGs recorded with the prototype device and EASI lead. The authors found a very high accuracy between the two devices for recognition of VEBs and VEB configuration counts. The results furthermore showed a perfect agreement between the two devices for the recognition of VF. The recognition of pace spikes was better on the standard device. Furthermore, studies conducted by Puurtinen et al., (2009), indicate that, with respect to P-wave amplitude, the optimal placement of closely spaced

bipolar electrodes is diagonally above the standard 12-lead precordial leads V1 and V2.

A review of the literature thus indicates a strong potential for the recording of relevant ECG signals on the sternum. However, the described systems are not completely comparable to the ePatch system and it is therefore desirable to investigate the practical usefulness of two ECG channels recorded with the novel ePatch technology placed at the sternum. This investigation is thus the focus of this clinical pilot study. During the study, the analysis of the recorded ECG signals is performed in a setting fairly similar to the setting for the traditional HOLTER or telemetry recordings.

2 METHODS AND DESIGN

This study includes ECG data segments from 25 different hospitalized patients. The choice of hospitalized patients ensures a realistic amount of abnormal beat morphologies and abnormal heart rhythms. Each of the patients was monitored with an ePatch for approximately 24 hours. All patients were simultaneously monitored with the regular telemetry equipment at the hospital department. The ePatch ECG signals were recorded using a sampling frequency of 512 Hz and a resolution of 12 bits. In compliance with IEC 60601-2-47, the ePatch front end had an analog bandpass filter between 0.67 and 40 Hz. The study was conducted in accordance with the principles of Good Clinical Practice (GCP) (Research Ethics Committee ID: S-20120132). All patients were informed about the study and signed a written consent form before their inclusion in the study. The patients were furthermore questioned about any discomfort and their general satisfaction with wearing the system. They were asked regarding their level of satisfaction on an analog scale from "very satisfied" to "very dissatisfied". The study included 15 males and 10 females. The mean Body Mass Index (BMI) was 27.5 with a standard deviation of 6.3. The mean age was 71.7 years with a standard deviation of 13.0 years.

As mentioned, the purpose of the study was to investigate whether two channel ECG signals recorded with the ePatch placed at the sternum is useful for heart rhythm analysis. In a realistic setting, a medical technician with speciality in HOLTER or telemetry analysis extracts relevant ECG segments that are provided to the referring medical doctor. This step was also performed in this study. An experienced nurse was asked to extract 7 seconds ECG segments where the interpretation of

the ECG signal was not hindered by noise, in other words, the data should be of sufficient signal quality. The definition of sufficient signal quality was thus based on a subjective judgement by an experienced ECG analyzer. This is somehow similar to the extraction of ECG snippets during a traditional HOLTER analysis. The ECG segments were provided to both the nurse and the medical doctors without any form of digital filtering, that is, the analysis was based on raw ECG signals. A total of 8 segments were extracted from each patient according to the scheme illustrated in Figure 4.
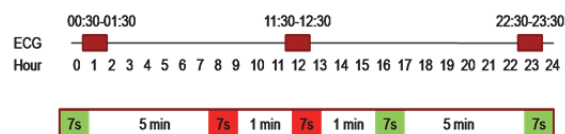

Figure 4: Illustration of the data extraction and selection process. The red marks on the top panel indicate the three one hour segments that were extracted for the study for a recording of exactly 24 hours. The bottom panel illustrates the process of selection of 7 seconds segments from the extracted data. Green segments are selected for the study, whereas red segments are excluded.

For each patient, three hours of data was considered. The three hours were extracted as 1 hour in the beginning, 1 hour in the middle, and 1 hour at the end of the recording. The first and last 30 minutes were, however, not considered to ensure that artefacts from mounting and removal of electrodes did not affect the extracted data. The three hours of extracted data for a recording of exactly 24 hours is illustrated by red colour marks in Figure 4. This ensures that a patient is only excluded from the analysis if the general signal quality is insufficient throughout the recording.

The 7 seconds ECG segments are extracted from these three hours of data according to the following scheme: 1) If the current 7 seconds data segment is considered noise free, it is selected for the study, and a new 7 seconds segment is investigated 5 minutes later. 2) If the current 7 seconds data segment is not considered noise free, it is excluded from the study, and a new 7 seconds segment is investigated 1 minute later. 3) If it is not possible to extract 8 segments of sufficient signal quality within these three hours of data, the patient is excluded from the study.

The data was selected with a custom designed Graphical User Interface (GUI) using MATLAB R2012B. The GUI provided an illustration of 7 seconds of two channel ECG data, and the nurse was asked to use two check boxes to choose between

"noise free segment" and "noise disturbed segment". The study included a total of 200 two channel ECG segments.

After selection of the 200 ECG segments, two medical doctors with experience in ECG interpretation performed an independent individual evaluation of each of the ECG segments according to the usefulness for heart rhythm analysis.

The medical evaluation of each segment was conducted using another GUI designed in MATLAB R2012B. This GUI is illustrated in Figure 5. The two channel ECG signal is visualized and the medical doctor was asked to choose between two check boxes, indicating the usefulness of the ECG segment for rhythm analysis.

3   RESULTS

Each ECG segment was evaluated according to the usefulness for heart rhythm analysis. The score "good" indicates that the ECG segment was found useful for heart rhythm analysis, whereas the score "bad" indicates that the ECG segment was not considered useful for rhythm analysis. The

evaluation from both medical doctors is illustrated in Figure 6.

Table 1: Results from the evaluation for ECG segment relevance for rhythm analysis from the two medical doctors.

Segments marked as "good"	Number	Percentage
Medical doctor 1	197	98.5%
Medical doctor 2	199	99.5%
Both medical doctors	196	98%
At least one medical doctor	200	100%

As observed from Figure 6, the doctors did not agree on the segments that were not useful for rhythm analysis. This is also illustrated in Table 1 that contains the percentage of "good" ECG segments for each doctor, the percentage of ECG segments considered as "good" by both doctors and the percentage of segments considered as "good" by at least one of the doctors.

Of the 25 patients, 22 indicated that they were very satisfied with wearing the device, 1 indicated to be satisfied, and 2 did not answer the question. Furthermore, several patients mentioned that they did not even notice that they were wearing it.
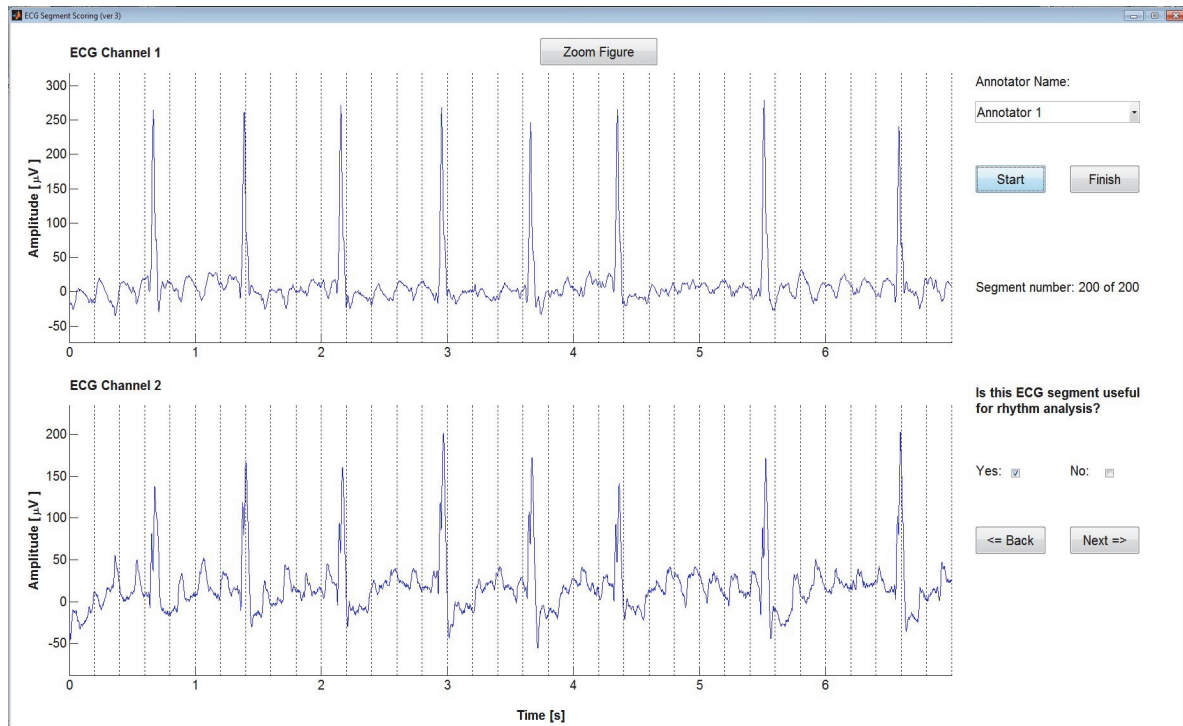
Figure 5: Illustration of the designed GUI used for the medical doctor evaluation of each 7 seconds ECG segment. The two channel ECG segment was visualized on a computer screen, and the medical doctor was asked to check one of the check boxes dependent on his evaluation of the relevance of the current ECG segment for rhythm analysis. Note, that this segment illustrates a case of AF.
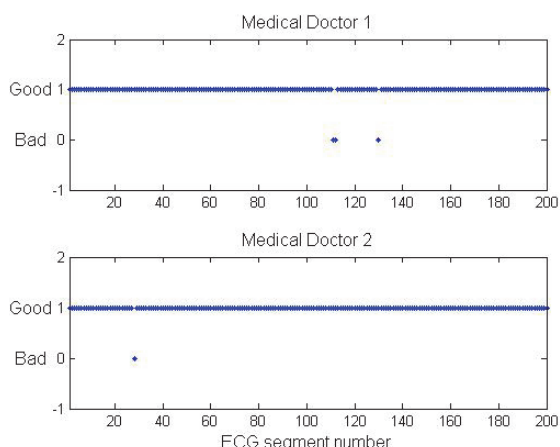
Figure 6: Illustration of the evaluation from both medical doctors for each of the 200 ECG segments. The score "1" is "good" and indicates that the ECG segment was considered useful, whereas the score "0" indicates that the ECG segment was not considered useful for rhythm analysis.

4 DISCUSSION

Both medical doctors indicated that more than 98% of the selected ECG segments were diagnostically meaningful to them, and that the ECG could help toward a rhythm analysis and diagnosis of the patient. It should, of course, be stated that the diagnosis of the patient would contain results from other relevant clinical tests, medical history, review of the entire long-term ECG recording, and general comments from the nurse preparing the ECG report for the referring medical doctor. The diagnosis is not imagined to be based solely on the 7 seconds ECG segments investigated in this study. However, the results from this pilot study are very promising and indicate the potential for this novel device for ambulatory cardiac monitoring.

The fact that the "bad" segments were not the same for both medical doctors, could indicate a certain degree of inter reader variability. The number of doctors could be increased in a future study to investigate the true inter reader variability. For the purpose of this pilot study, it is, however, considered sufficient with the evaluation by two medical doctors. It should also be stated that even using the "worst case" of judging all segments evaluated as "bad" by at least one of the doctors as a "bad" segment, still results in 98% of the segments being useful. Furthermore, a traditional HOLTER recording might also contain segments of data that is not useful for rhythm analysis. In a real life situation, cases of doubt about a diagnosis are solved by discussion and consensus with other doctors. This is also expected to be the case when ePatch ECG signals are applied for rhythm analysis.

Another interesting finding is the generally high patient satisfaction with wearing the system. This is one of the expected advantages of this novel technology. The high patient comfort is expected to allow very long-term monitoring in the future. This could increase the likelihood of detecting paroxysmal and infrequent arrhythmias. The higher patient comfort is also expected to increase the compliance with wearing the system, and a high patient compliance is necessary for reliable monitoring results (Ackermans, Solosko, Spencer, Gehman, Nammi, Engel and Russell, 2012).

The focus of this pilot study was to obtain preliminary knowledge about the overall applicability of ECG signals recorded with the ePatch on the sternum. Future studies might include more direct comparisons between ECG signals recorded synchronously with the ePatch and traditional HOLTER recordings. Future studies might also investigate the ability to correctly detect specific ECG features, e.g. the presence of the P-wave.

The future possibilities of this type of long-term ambulatory ECG recorders seem to be very high in areas like home monitoring, screenings, and follow-up consultations. However, the knowledge about the practical application of these new technologies is still relatively limited due to the lack of large-scale applications of the technology in everyday clinical situations. This study contributes to the currently limited amount of knowledge about the usability of these patch type ECG recorders. Further investigations could be conducted to investigate the usefulness for specific cardiac conditions on a larger database. Furthermore, in this study, only noise free ECG segments were presented to the medical doctors. This mimics the everyday selection of representative ECG "snippets" for the referring medical doctor and serves the purpose of this study. However, large-scale studies should be conducted to investigate the general level of artefacts and signal quality with this new patch technology.

5 CONCLUSIONS

This clinical pilot study indicates the medical usefulness of two channel ECG signals recorded at the sternum using the novel ePatch technology for heart rhythm analysis. Furthermore, the 25 included patients provided positive declarations regarding

their experience with the device. Further studies should be conducted to establish possible new application areas for this new technology and to determine the general quality of the signal and the vulnerability to different types of artefacts.

ACKNOWLEDGEMENTS

REFERENCES

Ackermans, P. A. J., Solosko, T. A., Spencer, E. C., Gehman, S. E., Nammi, K., Engel, J. & Russell, J. K. (2012). A user-friendly integrated monitor-adhesive patch for long-term ambulatory electrocardiogram monitoring. *Journal of Electrocardiology,* 45(2), 148-153. doi:10.1016/j.jelectrocard.2011.10.007.

IEC 60601-2-47:2012 Medical electrical equipment – Part 2-47: Particular requirements for the basic safety and essential performance of ambulatory electrocardiographic systems.

Janata, A., Lemmert, M. E., Russell, J. K., Gehman, S., Fleischhackl, R., Robak, O., Pernicka, E., Sterz, F. & Gorgels, A. P. M. (2008). Quality of ECG Monitoring with a Miniature ECG Recorder. *Pacing and Clinical Electrophysiology,* 31(6), 676-684. doi: 10.1111/j.1540-8159.2008.01070.x.

Lemmert, M. E., Janata, A., Erkens, P., Russell, J. K., Gehman, S., Nammi, K., Crijns, H. J. G. M., Sterz, F. & Gorgels, A. P. M. (2011). Detection of ventricular ectopy by a novel miniature electrocardiogram recorder. *Journal of Electrocardiology,* 44(2), 222-228. doi: 10.1016/j.jelectrocard.2010.10.028

Mittal, S., Movsowitz, C. & Steinberg, J. S. (2011). Ambulatory External Electrocardiographic Monitoring Focus on Atrial Fibrillation. *Journal of American College of Cardiolog,* 58(17), 1741-1749. doi: 10.1016/j.jacc.2011.07.026.

Puurtinen, M., Viik, J. & Hyttinen, J. (2009). Best Electrode Locations for a Small Bipolar ECG Device: Signal Strength Analysis on Clinical Data. *Annals of Biomedical Engineering,* 37(2), 331-336. doi: 10.1007/s10439-008-9604-y.

Rosenberg, M. A., Samuel, M., Thosani, A. & Zimetbaum, P. J. (2013). Use of a Noninvasive Continuous Monitoring Device in the Management of Atrial Fibrillation: A Pilot Study. *Pacing and Clinical Electrophysiology,* 36(3), 328-333. doi: 10.1111/pace.12053.

World Health Organization (March 2013). *Cardiovascular diseases (CVDs).* Retrieved June 6, 2013, from http://www.who.int/mediacentre/factsheets/fs317/en/

Zimetbaum, P. & Goldman, A. (2010). Ambulatory Arrhythmia Monitoring: Choosing the Right Device. *Circulation,* 122(16), 1629-1636. doi: 10.1161/CIRCULATIONAHA.109.925610.

Paper III

TITLE: Comparison of diagnostic information from regular telemetry equipment and a novel patch type electrocardiogram recorder

AUTHORS: Dorthe B. Saadi, Kenneth Egstrup, Karsten Hoppe, and Helge B. D. Sorensen

JOURNAL: 36th Annual International Conference of the IEEE Engineering in Medicine and Biology Society (EMBC), 2014.

STATUS: Presented as a late breaking research poster

Comparison of Diagnostic Information from Regular Telemetry Equipment and a Novel Patch Type Electrocardiogram Recorder*

Dorthe B. Saadi[¤§], Kenneth Egstrup[#], Karsten Hoppe[¤], and Helge B. D. Sorensen[§]

Abstract—**The purpose of this pilot study is to compare the diagnostic information obtained using regular telemetry equipment and the novel ePatch heart monitor. The comparison was conducted by a cardiologist on 24-hour recordings from 11 admitted patients. For all 11 recordings, the same diagnostic information was found using the two recording techniques.**

I. INTRODUCTION

The diagnosis and treatment of many life threatening cardiovascular diseases depend on analysis of long-term electrocardiogram (ECG) recordings. The nature of traditional equipment is characterized by high patient burden and low compliance. To overcome this, the ePatch heart monitor was designed. The wireless ePatch is CE marked for ambulatory recording of two ECG channels, see Fig. 1(a). The location of the ePatch and the small distance between the bipolar recording electrodes cause the projection of the cardiac vector to be slightly different from the regular equipment. This might induce changes in the appearance of the ECG signals. It is therefore highly relevant to compare the diagnostic information obtained using the ePatch recordings and simultaneous recordings with standardized equipment. This investigation is exactly the purpose of this pilot study.

II. METHODS

To obtain a meaningful investigation, it is important to ensure representation of a realistic amount of abnormal beat morphologies. We therefore decided to use ECG data from 11 different patients that were admitted and selected for regular telemetry monitoring. The ePatch system was attached to obtain simultaneous recordings with the two systems. After each recording, information from the telemetry reports was extracted from the telemetry software. This included ECG segments of automatically generated alarms indicating potential arrhythmias, arrhythmia event overviews, and heart rate (HR) trend curves. Furthermore, information and potential notes from the electronic patient journal was available. This information was compared to the information that could be extracted by visual inspection and analysis of the 24-hour ePatch recordings. The comparison was conducted by a cardiologist. This investigation thus allows for a high level comparison of the clinically relevant information available using the two recording techniques.

III. RESULTS

An example of a HR trend curve from an ePatch recording is provided in Fig. 1(b). The overall HR observed from the 11 recordings was up to 150 beats per minute (BPM). A high number of relevant heart rhythms and abnormal beat morphologies were correctly found in the ePatch recordings and confirmed by the telemetry alarms and/or the patient journal. Examples of this include the nine seconds pause illustrated in Fig. 1(c), and a case of termination of atrial fibrillation (AF) illustrated in Fig. 1(d). Overall, the cardiologist found that the same clinically relevant information could be extracted from the two monitoring techniques for all 11 patients. Furthermore, the cardiologist judged the signal quality of the ePatch recording to be excellent for ten of the 11 patients. In these recordings, the clinically relevant ECG fiducial points were clearly observed. The last ePatch recording contained several episodes of very noisy data, but the telemetry alarms from this patient also contained a high number of false detections due to noise.

IV. DISCUSSIONS

This pilot study clearly indicates the clinical usefulness of ECG recorded with the ePatch system, and facilitates the possibility of applying the ePatch system for cardiac monitoring instead of the regular telemetry or Holter recorders. Future studies might include a validation of the findings on a larger database with representation of a higher number of different abnormal beat morphologies and more relevant abnormal heart rhythms.
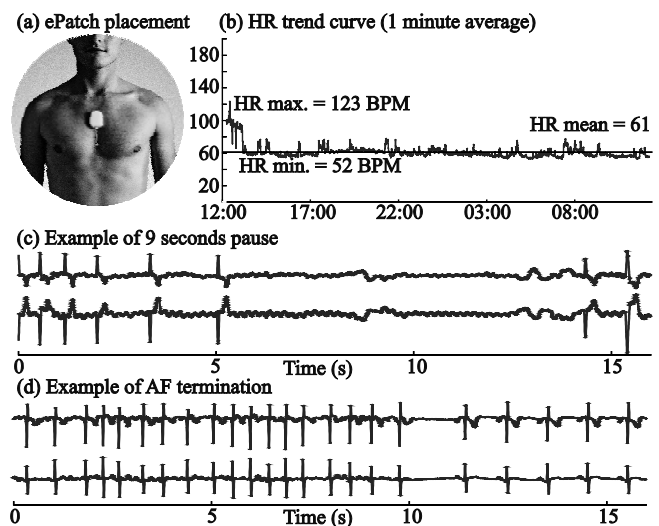

Figure 1. (a) Illustration of the ePatch system. (b) HR trend curve for an ePatch recording. (c) Example of a nine seconds pause. (d) Example of termination of AF from the same ePatch recording used in (b). The alternating pattern between AF and sinus rhythm is observed in the first hour.

Paper IV

Automatic QRS Complex Detection Algorithm Designed for a Novel Wearable, Wireless Electrocardiogram Recording Device*

Dorthe B. Nielsen[ab], Kenneth Egstrup[c], Jens Branebjerg[b], Gunnar B. Andersen[b] and Helge B.D. Sorensen[a]

Abstract— We have designed and optimized an automatic QRS complex detection algorithm for electrocardiogram (ECG) signals recorded with the DELTA ePatch platform. The algorithm is able to automatically switch between single-channel and multi-channel analysis mode. This preliminary study includes data from 11 patients measured with the DELTA ePatch platform and the algorithm achieves an average QRS sensitivity and positive predictivity of 99.57% and 99.57%, respectively. The algorithm was also evaluated on all 48 records from the MIT-BIH Arrhythmia Database (MITDB) with an average sensitivity and positive predictivity of 99.63% and 99.63%, respectively.

I. INTRODUCTION

The advantages of a small, wireless electrocardiogram (ECG) recording device for ambulatory ECG monitoring are numerous. Therefore, DELTA has developed the ePatch. This is a small wireless prototype ECG recorder that measures two ECG channels on the sternum. These channels do not correspond to any standard HOLTER leads. The projections of the electrical activity of the heart, and hereby the recorded ECG signals, are thus slightly different from standard HOLTER leads. This requires special attention in the design of new algorithms that are specialized for analysis of these signals. The basis for being able to perform ECG analysis is a robust, reliable and automatic QRS detection algorithm. Therefore this study is aimed at the design of a novel QRS detection algorithm that is optimized for the special ePatch ECG signals.

Many QRS detection algorithms described in the literature are designed for one channel analysis only [9], [8]. However, several different approaches have also been proposed for two or three channel QRS detection [1], [2], [3]. The motivation for including more channels arise from the assumption that the signal quality of one channel might occasionally or permanently decrease during a long term ambulatory recording. Noise is often only contaminating one of the channels. Therefore, the inclusion of clean ECG from addition channels is expected to improve detection performance. In [3], information from three different ECG channels is constantly applied for QRS detection. This approach may have some

limitations: High amounts of noise in one channel might deteriote otherwise good performance obtained from analysis of the other channel [1]. Furthermore, the application of more channels, introduces more computational complexity. This is especially important when designing algorithms for a small wearable device. Another important aspect of automatic QRS detection is the ability to correctly detect QRS complexes with abnormal morphologies. The appearance of abnormal beats may be different in two different ECG channels. Therefore, the inclusion of an addition channel might increase the QRS detection performance of anormal beats. This study is thus focosed on the design of an automatic, intelligent algorithm that is able to apply information from both available ECG channels. To overcome some of the mentioned limitations, the proposed QRS detection algorithm can be applied in two different modes: Single-channel and multi-channel mode. The multi-channel mode applies information from both available channels. The single-channel mode is derived from the multi-channel mode, but with the exclusion of information from one channel. The algorithm can automatically switch between the two modes when predefined artefacts are present in one channel. If these artefacts are present in both channels, a complete shutdown occurs. The idea of generally applying both channels and then exclude a potentially noisy channel was also investigated by the authors of [1]. A slightly different approach was introduced by the authors of [2]. In this study, the QRS detection is generally based on channel I of the MIT-BIH Arrhythmia Database (MITDB), and then a combination of the two channels is applyed if the current RR interval exceeds a predefined interval.

II. METHODOLOGY

A. Data

The applied ePatch database contains data recorded from 11 different patients. The patients were hospitalized at Svendborg Hospital for diagnostic monitoring during the recordings and they were simultaneously monitored with conventionel telemetry equipment. The 2 ECG channels were recorded with a sampling frequency of 500 Hz and a resolution of 13 bits. The electrode placement is illustrated in Fig. 1. Records with 30 minutes of data were extracted from each measurement. For all patients, the 30 minutes were extracted one hour after the beginning of the recording. The patients were allowed to move around in the monitoring unit during the recordings. This ensures a fair amount of realistic in-hospital artefacts in each record. A reference annotation

file was created for each record, cf. Fig 1. During the first three steps, all beats were annotated as "normal". During the final manual scoring by the cardiologist (KE), the beats were divided into different beat types, cf. Fig 1.
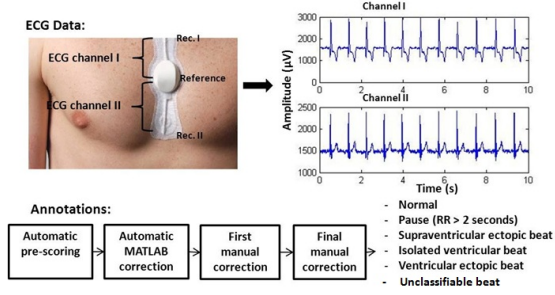

Fig. 1. Illustration of the DELTA ECG ePatch platform and the electrode placements. The annotation file was created in several steps: Automatic pre-scoring using the "sqrs" program available from [4], automatic placement correction with a maximum algorithm in MATLAB, manual correction by one of the authours (using "WAVE" - available from [4]), and finally manual correction by the cardiologist (KE) (using "WAVE"). Noise annotations were also included as well as indication of atrial fibrillation (AF).

To further evaluate the algorithm and allow comparison with other studies, all 48 records from the MITDB were applied [5]. Each record contains 2 ECG channels digitalized with a sampling frequency of 360 Hz. In compliance with [6], each record was re-sampled to 500 Hz using the "xform" program available from [4]. The automatic QRS complex detection algorithm was implemented in MATLAB R2010b. The WFDB Toolbox for MATLAB [4] was applied to convert the data files between WFDB readable files and mat-files.

B. Automatic QRS Complex Detection Algorithm

An overview of the algorithm is provided in Fig. 2. The channel exclusion block marks the point of separation of the single-channel and multi-channel modes. The channel exlusion, high maximum removal, adaptive threshold calcuation, and decision fusion blocks were executed in 1 second non-overlapping analysis windows.
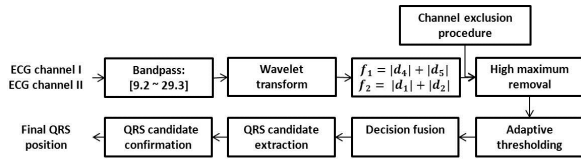

Fig. 2. Schematic overview of the QRS complex detection algorithm.

1) Channel Exclusion Criteria: Saturation of the raw ECG signals produces false detections and disturbs the adaptive algorithm parameters. The channel was therefore excluded if the raw ADC counts of 15 consecutive samples in the current analysis window obtained the maximum or minimum possible value. Furthermore, it was expected that the feature signals might be disturbed immediately after a saturation. The channel was therefore also shutdown in the first "clean" analysis window after saturation. The threshold of 15 samples was found by visual and experimental analysis of challenging ECG examples.

2) Bandpass Filtering: The raw ECG signals were bandpassed filtered to reduce baseline wandering, power line interference and high frequency muscle artifacts. A simple FIR bandpass filter with integer coefficients and passband between 9.2 and 29.3 Hz was designed in line with [7]. After correction for the filter delay, the bandpass filtered signal will ideally have a zero-crossing at the R peak position in the raw ECG signal.

3) Wavelet Transform: The non-downsampling *a trous algorithm* has been widely applied for wavelet transformation (WT) of ECG signals [8], [3]. Some advantages of the WT are a good balance between detection performance and efficient hardware implementation [8], and the possibililty of dividing the ECG signal into different relevant frequency subbands [3]. The WT consists of a cascade of lowpass (LP) and highpass (HP) filters. The WT output of level m was implemented as [8]:

$$a_m(n) = \sum_l h_{LP,m}(l) \cdot a_{m-1}(n-l) \qquad (1)$$

$$d_m(n) = \sum_l h_{HP,m}(l) \cdot a_{m-1}(n-l) \qquad (2)$$

where a_m is the LP output and d_m is the HP output. The impulse responses were implemented as described in [8]. In each filtering step throughout the algorithm, the input signal was padded with the last value of the signal, and the filter delay was corrected to ensure correct location of the QRS complexes relative to the original signal.

The frequency content of the QRS complex is mainly in the interval 5-15 Hz [9]. With a sampling frequency of $f_s = 500$ Hz, this correpsonds approximately to d_4 and d_5 of the WT. Therefore the first feature was calculated from eq. 3. The absolute value was used to ensure equal detection of QRS complexes with positive and negative polarity. However, in some cases this feature signal obtained high values at the P and T wave locations. Therefore an additional feature signal representing the higher frequency components was computed using eq. 4. Both features were calculated for both channels.

$$f_1 = |d_4| + |d_5| \qquad (3)$$

$$f_2 = |d_1| + |d_2| \qquad (4)$$

It is thus expected that f_1 obtains high values during QRS complexes as well as during high P and T waves, whereas f_2 should obtain high values during QRS complexes and high frequency noise. Periods where both feature signals obtain high values are thus expected to correspond to the location of QRS complexes.

4) Detection of QRS Candidates: To detect QRS candidates, an adaptive threshold was calculated for each of the feature signals in eq. 3 and 4 in each analysis window:

$$T_k = \lambda \cdot T_{k-1} + (1 - \lambda) \cdot (\mu_k + c \cdot \sigma_k), \qquad (5)$$

where $0 < \lambda < 1$ is a forgetting factor, c is a scaling parameter, T_k is the final threshold in the current window,

T_{k-1} is the threshold value in the previous window, σ_k and μ_k are the mean and standard deviation of the feature signal in the current window. This threshold calculation ensures a smooth adaptation to changes in the feature signal. Based on simulations on the ePatch database $\lambda = 0.4$ and $c = 0.8$ was chosen. In cases with abnormal beat morphologies, the threshold might be increased to a level that hinder detection of subsequent QRS complexes. To avoid this, a high maximum removal was applied before the threshold calculation. This block contains information about the maximum value in the 8 previous analysis windows. Application of the 8 most recent beats (approximately corresponding to the 8 previously 1 second analysis windows) has also been applied for tracking the "normal" behaviour of an ECG signal in other studies [9]. Any samples in the current analysis window excedding the median value of this maximum register were set to the median value before the threshold calculation. The adaptive threshold and the maximum register were not updated for channel j when it was excluded from the analysis. Based on the adaptive thresholds, binary feature signals were created from:

$$f_{bin} = \{1 \text{ if } f > T_k, \ 0 \text{ otherwise}\} \qquad (6)$$

These binary signals were then combined in a decision fusion scheme to detect QRS candidates: If both channels were selected for analysis, at least three of the four binary features should be asserted to indicate a QRS candidate. If one channel was excluded from the analysis, both binary features from the other channel should be asserted. The new binary feature signal was denoted f_{final} and it contained the QRS candidates. To the best knowledge of authors, this combintation of wavelet based features is novel. As is the later described confirmation block.

5) QRS Localization and Confirmation Block : The temporary duration of the QRS candidate was defined from the rising edge of f_{final} and 100 ms forward. The bandpass filtered signal was investigated for zero crossings in this time interval. The QRS candidate was confirmed if at least one active channel possessed at least one zero crossing during this period. This zero-crossing corresponds to a peak in the original signal. The first zero-crossing in this interval might correspond to the position of the Q peak. It was therefore decided to apply the location of the second zero-crossing if more than one zero-crossing occurred in the bandpass filtered signal during this time interval. The position of the selected zero-crossing was extracted for each active channel. In multi-channel mode, the final QRS position was estimated as the minimum sample number suggested by the two active channels. This location was saved as the new position of the QRS candidate. To further decrease the number of false detections, an additional confirmation block with three possible outputs was implemented: *Case 1:* Accept both the previously detected QRS complex and the current QRS candidate, *Case 2:* Delete the previously detected QRS complex, and accpet the current QRS candidate, and *Case 3:* Accept the previously detected QRS complex, but reject the current QRS candidate. This block was initiated if the current RR interval was less than half the median of the 8 previous RR intervals. The assumption in this block was that the feature values of two closely located QRS complexes should not vary significantly. This was measured with the maximum amplitude value in both feature signals (f_1 and f_2) in all active channels. For each of the included feature signals, the maximum value was calcluated in a 100 ms interval around the position of the previously detected QRS complex (F_{old}) and the current QRS candidate (F_{new}). The decision rule depends on the algorithm mode, cf. Table I. This block was developed based on experiments and visual inspection of different challenging ECG examples. After confirmation of a QRS candidate, a refractory period of 200 ms was implemented in line with [9].

TABLE I

DECISION RULE IN THE FINAL QRS CONFIRMATION BLOCK.

Case	Multi-channel	Single-channel
1	At least 3 of 4 maximun values should satisfy the requirement: $\frac{F_{old}}{2} < F_{new} < 2 \cdot F_{old}$	Both maximun values should satisfy the requirement: $\frac{F_{old}}{2} < F_{new} < 2 \cdot F_{old}$
2	At least 3 of 4 maximun values should satisfy the requirement: $F_{new} \geq 2 \cdot F_{old}$	Both maximun values should satisfy the requirement: $F_{new} \geq 2 \cdot F_{old}$
3	Otherwise	Otherwise

III. RESULTS

In compliance with [6], the beat detection accuracy was evaluated using the QRS sensitivity, Se, and positive predictivity, $+P$. The mean QRS detection performance on the ePatch database is stated with both the gross and the average statistics [6], see Table II. The statistics was calculated with the default settings of the "bxb" and "sumstats" programs available in the WFDB Software Package [4] (match window = 150 ms, 5 minutes initiation time). The performance was evaluated using only channel I, only channel II (single-channel modes) and both channels (multi-channel mode). The QRS detection sensitivity in multi-channel mode was 100% with respect to both supraventricular ectopic beats (SVEBs) and ventricular ectopic beats (VEBs).

The detection performance on the 48 records of the MITDB using the ePatch optimized algorithm is provided in Table III. In compliance with [6], episodes of ventricular flutter or fibrillation were excluded from the performance evaluation. Table III also contains detection accuracy for three other studies using multi-channel QRS detection. However, the authors of [3] evaluated their multi-channel approach using only channel I of the MITDB.

IV. DISCUSSION

The multi-channel detection performance on the 11 records from the ePatch database is acceptable, but not excellent. The poorer performance originates from 2 records with considarable amounts of artefacts: Record 11 contains approximately 2.5 minutes with very poor data quality, and

Pt. #	# of beats	Channel I		Channel II		Both channels	
		Se(%)	+P(%)	Se(%)	+P(%)	Se(%)	+P(%)
1	1450	99.52	98.97	99.52	99.31	99.93	99.52
2	1617	100	100	100	100	100	100
3	1594	99.69	99.94	99.94	100	99.87	100
4	1727	99.94	100	99.07	92.69	100	100
5	1465	99.66	99.59	98.98	99.72	99.86	99.80
6	3049	99.97	100	99.93	100	100	100
7	1762	99.72	100	99.89	100	100	100
8	1984	99.80	100	99.55	99.95	99.95	100
9	2562	99.49	94.69	99.88	96.46	99.88	96.75
10	1651	99.94	99.94	100	100	99.94	99.94
11	3219	92.58	92.00	97.20	99.36	95.84	99.26
μ_1	22080	99.12	98.65	99.45	98.86	99.57	99.57
μ_2	22080	98.73	98.09	99.34	98.81	99.35	99.46

Algorithm	Number of beats	Overall QRS		SVEB	VEB
		Se(%)	+P(%)	Se(%)	Se(%)
TW, channel I & II	91285	99.63	99.63	98.80	98.71
TW, channel I	91285	99.63	99.43	98.25	98.52
TW, channel II,	91285	99.03	95.22	98.43	97.95
Ghaffari et al. [3],	109428	99.94	99.91	NA	NA
Boqiang et al. [2],	109496	99.91	99.93	NA	NA
Chiarugi et al. [1],	109494	99.76	99.81	NA	NA

record 9 contains a number of episodes with high frequency noise. The average Se and $+P$ on the remaining 9 patients in the multi-channel mode were 99.95% and 99.92%, respectively, which is an excellent performance. Furthermore, the sensitivity for detection of abnormal beats is considered to be very high.

Even though the algorithm was designed and optimized for the ePatch data, the performance on the MITDB is only slightly lower than [1]. The lower performance might be caused by the optimization to the ePatch database or the very simple channel exclusion criteria. The performance is lower than obtained in [2]. However, this study used a different approach, where channel I was used for analysis unless no R peak was detected in a predefined interval. Since the general appearance of QRS complexes is better in channel I of the MITDB [4], it might be uncertain whether this approach will provide a reliable result in a real-life situation with no prior knowledge about the optimal channel. The performance difference between the two individual channels on the MITDB is clearly observed from Table III. As with the ePatch database, the sensitivity to detection of abnormal beat morphologies is considered fairly high. However, it is difficult to compare these results with other studies since these sensitivities are rarely stated in spite of their importance for subsequent arrhythmia analysis. This study shows that the sensitivity regarding detection of these beats increases with the inclusion of an additional channel. Furthermore, it is observed for the ePatch database that both single-

channel modes obtains a considerably lower performance than the multi-channel mode. This furthermore indicates the importance of applying both channels in the analysis. During a real-life recording, it would probably be impossible to know the optimal channel on before hand and the optimal channel might even change during the recording. The overall detection performance is furthermore not decreased by the inclusion of the addition channel on the MITDB, and this method is thus considered "safer" than a single-channel appraoch using an abitrary channel. It should, of course, be mentioned that the channel I performance on the MITDB is slightly lower than other studies using only channel I [8]. However, their approaches are developed for single-channel use, and it would be interesting to know the performance on channel II of the database to clarify how the performance would be if this channel was arbitrary selected for the single-channel analysis.

The overall conclusion of this preliminary study is that the proposed algorithm achieves good performance. The algorithm might be further improved by implementation of more sophisticated channel exclusion criterias. This might be able to lower the false detections. However, the potential decrease in false detections should not be achieved at the expense of the high detection sensitivity to abnormal beats. The benefits from more sophisticated channel exclusion criterias should therefore be carefully investigated and the algorithm should generally be evaluated on a larger ePatch dataset.

REFERENCES

[1] F. Chiarugi, V. Sakkalis, D. Emmanouilidou, T. Krontiris, M. Varanini, and I. Tollis, Adaptive threshold QRS detector with best channel selection based on a noise rating system, Comput. Cardiol., pp. 157160, 2007.

[2] H. Boqiang and W. Yuanyuan, Detecting QRS complexes of two-channel ECG signals by using combined wavelet entropy, 3rd International Conference on Bioinformatics and Biomedical Engineering, vols. 1-11, pp. 24392442, 2009.

[3] A. Ghaffari, M. R. Homaeinezhad, and M. M. Daevaeiha, High resolution ambulatory holter ECG events detection-delineation via modified multi-lead wavelet-based features analysis: Detection and quantification of heart rate turbulence, Expert Syst. Appl., vol. 38, no. 5, pp. 52995310, 2011.

[4] A. L. Goldberger, L. A. Amaral, L. Glass, J. M. Hausdorff, P. C. Ivanov, R. G. Mark, J. E. Mietus, G. B. Moody, C. K. Peng, and H. E. Stanley, PhysioBank, PhysioToolkit and PhysioNet: Components of a new research resource for complex physiologic signals, Circulation, vol. 101, no. 23, pp. e215220, June 2000.

[5] G. B. Moody and R. G Mark, The impact of the MIT-BIH arrhythmia database, IEEE Eng. Med. Bio. Mag., vol. 20, no. 3, pp. 4550, May-June 2001.

[6] Association for the Advancement of Medical Instrumentation (AAMI), ANSI/AAMI EC57:1998/(R)2003: Testing and reporting performance results of cardiac rhythm and ST-segment measurement algorithms, 1999.

[7] M. Cvikl, F. Jager, and A. Zemva, Hardware implementation of a modified delay-coordinate mapping-based QRS complex detection algorithm, EURASIP Journal on Advances in Signal Processing, vol. 2007, pp. 57286, 2007.

[8] X. Liu, Y. Zheng, M. W. Phyu, B. Zhao, M. Je, and X. Yuan, Multiple functional ECG signal is processing for wearable applications of long-term cardiac monitoring, IEEE Trans. Biomed. Eng., vol. 58, no. 2, pp. 380389, Feb. 2011.

[9] J. Pan and W. J. Tompkins, A real-time QRS detection algorithm, IEEE Trans. Biomed. Eng., vol. 32, no. 3, pp. 230236, Mar. 1985.

Paper V

Automatic Real-time Embedded QRS Complex Detection for a Novel Patch-Type Electrocardiogram Recorder

D.B. Saadi, G. Tanev, M. Flintrup, A. Osmanagic, K. Egstrup, K. Hoppe, P. Jennum, J. Jeppesen, H.K. Iversen, and H.B.D. Sorensen

Abstract Cardiovascular diseases are projected to remain the single leading cause of death globally. Timely diagnosis and treatment of these diseases are crucial to prevent death and dangerous complications. One of the important tools in early diagnosis of arrhythmias is analysis of electrocardiograms (ECGs) obtained from ambulatory long-term recordings. The design of novel patch type ECG recorders has increased the accessibility of these long-term recordings. In many applications, it is furthermore an advantage for these devices that the recorded ECGs can be analyzed automatically in real-time. The purpose of this study was therefore to design a novel algorithm for automatic heart beat detection, and embed the algorithm in the CE marked ePatch heart monitor. The algorithm is based on a novel cascade of computational efficient filters, optimized adaptive thresholding, and a refined search back mechanism. The design and optimization of the algorithm was performed on two different databases: The MIT-BIH Arrhythmia Database (Se=99.90%, P^+=99.87) and a private ePatch Training Database (Se=99.88%, P^+=99.37%). The offline validation was conducted on the European ST-T Database (Se=99.84%, P^+=99.71%). Finally, a double-blinded validation of the embedded algorithm was conducted on a private ePatch Validation Database (Se=99.91%, P^+=99.79%). The algorithm was thus validated with high clinical performance on more than 300 ECG records from 189 different subjects with a high number of different abnormal beat morphologies. This demonstrates the strengths of the algorithm, and the potential for this embedded algorithm to improve the possibilities of early diagnosis and treatment of cardiovascular diseases.

Index Terms—automatic QRS complex detection, embedded ECG analysis, ePatch ECG recorder, patch type ECG recorder, real-time ECG analysis

I. INTRODUCTION

Cardiovascular diseases (CVDs) are projected to remain the single leading cause of death globally, and according to the World Health Organization (WHO), as much as 30% of all deaths in 2008 were caused by CVDs [1]. These diseases

D.B. Saadi is with the Department of Electrical Engineering, Technical University of Denmark, Ørsteds Plads, Bldg. 349, 2800 Kgs. Lyngby, Denmark and DELTA, Venlighedsvej 4, 2970 Hørsholm, Denmark (e-mail: dorthe_bodholt@hotmail.com).

G. Tanev, M. Flintrup, and K. Hoppe are with DELTA, Venlighedsvej 4, 2970 Hørsholm, Denmark (e-mail: gtdevel@gmail.com, mf@delta.dk, and kh@delta.dk).

A. Osmanagic and K. Egstrup are with the Department of Medical Research, OUH Svendborg Hospital, Valdemarsgade 53, 5700 Svendborg, Denmark (e-mail:Kenneth.Egstrup@rsyd.dk, Armin.Osmanagic@rsyd.dk).

P. Jennum is with the Danish Center for Sleep Medicine, Department of Clinical Neurophysiology, University of Copenhagen, Glostrup Hospital, 2600 Glostrup, Denmark (e-mail: poul.joergen.jennum@regionh.dk).

J. Jeppesen is with the Department of Medicine, Glostrup Hospital, 2600 Glostrup, Denmark (e-mail: joergen.lykke.jeppesen@regionh.dk).

H. K. Iversen is with the Department of Neurology, Glostrup Hospital, 2600 Glostrup, Denmark (e-mail: helle.klingenberg.iversen@regionh.dk).

H.B.D. Sorensen is with the Department of Electrical Engineering, Technical University of Denmark, Ørsteds Plads, Bldg. 349, 2800 Kgs. Lyngby, Denmark (e-mail: hbs@elektro.dtu.dk).

are also a major economic burden to the World's healthcare facilities. One of the important diagnostic tools for timely detection and diagnosis of heart arrhythmias is ambulatory electrocardiography (ECG) recordings. The standard equipment for this has for many years been the Holter recorder. However, the traditional Holter system possesses a number of issues that prevents prolonged monitoring. To overcome this, a number of patch type ECG recorders have recently reached the market [2], [3]. We have chosen to apply the ePatch ECG recorder designed by DELTA [3]. The ePatch is illustrated in Fig. 1 together with a short two-channel ECG snippet. These type of recorders provide a possibility of an extended monitoring period, and studies have shown how this can ensure detection of more significant arrhythmias and lead to a definitive diagnosis for more patients [2], [4], [5]. Furthermore, some patches possess the possibility of wireless data transmission and automatic real-time embedded processing of the recorded signals. This might allow real-time transmission of e.g. arrhythmia events to a central monitoring station. The first step in this analysis is automatic detection of QRS complexes. This field has been investigated in the literature for at least 30 years [6]. Generally, the automatic QRS complex detection can be divided into two steps: 1) The feature extraction step, where the QRS complexes are enhanced, and 2) the detection step, where the position of

the QRS complexes are found based on the feature signal and a classification procedure. Two of the commonly applied techniques for feature extraction include different variations of digital bandpass (BP) filtering [6] and wavelet decomposition [7]–[14], but several other techniques have also been proposed, e.g. morphological operators [15] or the phasor transform method [16]. For the detection step, a well-known and accepted method is different variations of adaptive thresholding [6]–[10], [13]–[15]. This method has proven robust with respect to both secure detection of abnormal beat morphologies and varying signal to noise ratios (SNRs). An extensive review of methods for software QRS detection can be found in [17]. However, many of the traditional algorithms applied in ECG analysis software today are not optimized for real-time embedded analysis. Furthermore, the location of the ePatch and the short distance between the bipolar recording sites imply that the morphology of the recorded ECGs is slightly different. The focus of this study is therefore to design, implement, and validate a novel algorithm which is optimized for automatic embedded detection of QRS complexes in patch ECGs. The requirements of the algorithm are thus high clinical performance and low computational costs.
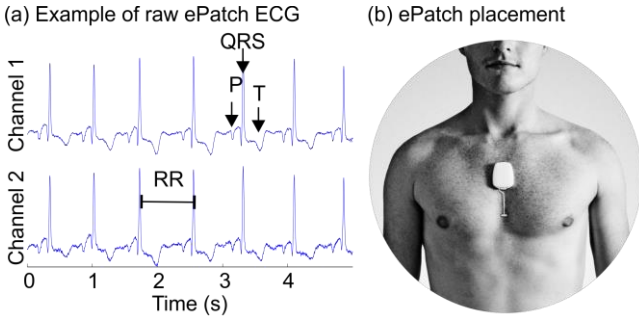

Fig. 1. (a) Example of two channel raw ePatch ECG. The most relevant ECG fiducial points are indicated. (b) Illustration of the ePatch ECG recorder correctly placed on the chest. Each recording contains two ECG channels sampled at 512 Hz with a resolution of 12 bits. In compliance with [18], the ePatch sensor has an analog BP filter between 0.67 Hz and 40 Hz. Modified from [3].

II. METHODS AND PROCEDURES

An overview of the study is provided in Fig. 2. In the first step, we designed and optimized the algorithm using MATLAB R2013b (The MathWorks Inc., Massachusetts, USA). In the second step, we conducted an offline validation to ensure that the clinical performance on unseen data was satisfactory. The third step was to implement the algorithm in ANSI C and embed it in the ePatch sensor to allow real-time QRS detection. During the design and validation, it is important to apply ECGs with a high number of different beat morphologies from many different patients. As indicated in Fig. 2, we therefore decided to apply four different databases according to the following scheme: The design and optimization phase was based on the MIT-BIH Arrhythmia Database (MITDB) [19] and a private ePatch Training Database (eTDB). The offline validation was conducted using the European ST-T Database (EDB) [20]. And finally, the double blinded embedded validation was conducted using the private ePatch Validation Database (eVDB). An overview of the characteristics of each database is provided in Table I, and a detailed description is provided in the section "Data Description". This database selection ensures both a solid impression of the performance on ECGs recorded with the ePatch and allows for comparison with other published work. The algorithm is designed with special attention to overcome some of the difficulties related to the placement of the recording sites applied in the ePatch. Some of the challenges include relatively large changes in signal amplitude related to changes in patient posture (including changes in QRS polarity), and cases of very pronounced P-, Q- and/or S-waves. During the design and optimization phase, priority was therefore given to improve detection performance on challenging ePatch ECGs. However, consideration for these issues during the design phase is not expected to necessarily decrease the performance on ECGs recorded with traditional equipment represented by the MITDB and the EDB.
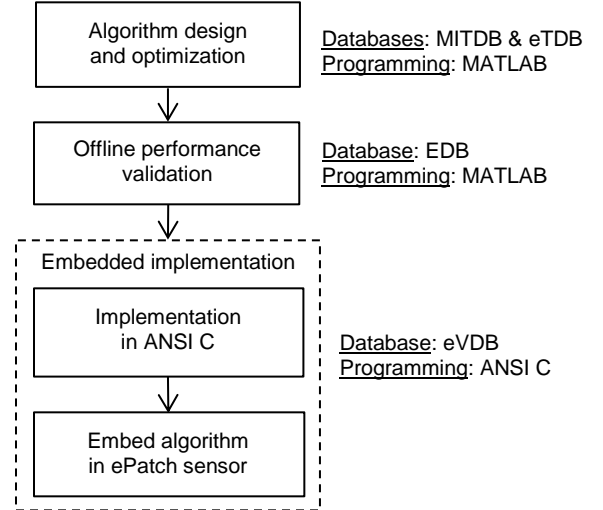

Fig. 2. Overview of the study design. The algorithm was designed and optimized in MATLAB using the MIT-BIH Arrhythmia Database (MITDB) and the private ePatch Training Database (eTDB). The performance of the algorithm was then tested offline in MATLAB using the European ST-T Database (EDB). Finally, the algorithm was implemented in ANSI C and embedded in the ePatch sensor. The performance of the embedded algorithm was tested in a double-blinded validation scheme using the ePatch Validation Database (eVDB).

TABLE I
SUMMARY OF DATABASE CHARACTERISTICS.

Database	Fs (Hz)[a]	Records[b]	Length (min)[c]	Beats[d]
MITDB	360	48	30	91,285
EDB	250	90	120	759,878
eTDB	512	120	10	45,248
eVDB	512	61	15	38,429

[a] The original database sampling frequency (fs).
[b] Total number of records in the database.
[c] Entire duration of each record. Note that the first five minutes of each record is allowed as initialization time and is not included in the evaluation.
[d] The total number of beats in the evaluation period of the database.

A. Algorithm Overview

An overview of the algorithm is provided in Fig. 3. The feature extraction and detection steps are indicated by the dashed green and blue squares, respectively. The output of the feature extraction is a feature signal (*Feature*) that is directly applied as input to the detection step. We designed the algorithm for real-time embedded functionality in a clinical setting. This was achieved by the design of a novel cascade of simple finite impulse response (FIR) filters that allow efficient enhancement of the QRS complexes and artefact attenuation. For the detection step, we applied two adaptive thresholds in a search back scheme. This is a well-known procedure [6]. However, we have simplified the calculation of the adaptive thresholds to decrease the computational load, and we have refined the adaptation of the search back procedure in cases of irregular heart rhythms.
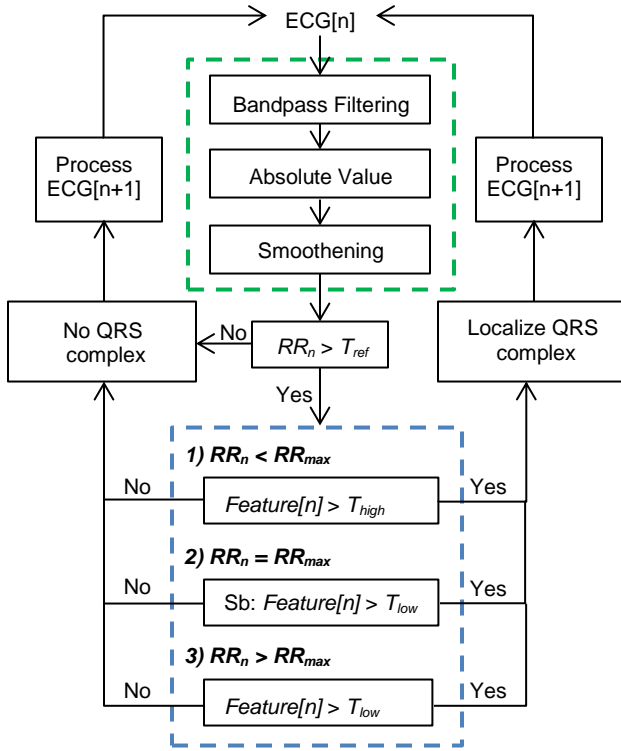
Fig. 3. Schematic overview of the designed QRS complex detection algorithm. The algorithm processes the ECG signal sample by sample, indicated by *n*. The input to the algorithm is one channel raw ECG. The feature extraction is indicated by the dashed green square. It consists of BP filtering, removal of signs, and smoothening. The output of the feature extraction block is a feature signal (*Feature*) that is directly applied in the detection block (indicated by the dashed blue square). RR_n indicates the current RR interval, if a QRS complex is detected at the current sample, *n*. If the refractory period (T_{ref}) is exceeded, the algorithm is allowed to continue to the detection block. This block can operate in three different modes dependent on the distance to the previously detected QRS complex (RR_n). This implies that only one of the three modes is applied for each sample. The second mode includes the search back (Sb) procedure. The expected maximum distance between two subsequent QRS complexes is termed RR_{max}. If the relevant threshold is exceeded, a QRS complex is detected, and the localization block is initiated.

As observed from the dashed blue square in Fig. 3, the QRS detection block can function in three different modes. The first mode applies the high threshold, T_{high}, and is active when the distance from the previous QRS detection is within the expected maximum RR interval (RR_{max}). If RR_{max} is exceeded, a search back is performed using the low threshold value, T_{low}. If several samples exceed T_{low} in the search back interval, the sample with the highest feature value is selected as the preliminary QRS position. This search back procedure is the second mode. If no QRS complex is detected during the search back, T_{low} is applied until a new QRS complex is detected. This is the third mode. When a QRS complex is detected, a delineation procedure is applied to locate the QRS complex at the correct position, and the detection block switches back to the first mode. The algorithm is designed to analyze the ECGs in a sample-by-sample manner. This enables real-time embedded detection with only minor insignificant delays in the detection of each QRS complex. The following sections contain a detailed description of each part of the algorithm.

B. Bandpass Filtering

The purpose of the BP filtering step is two-fold: 1) Increase the influence of the QRS complexes, and 2) attenuate the influence of different types of noise, as well as pronounced P- and T-waves. However, it is also important to keep in mind that BP filtering might unintentional decrease the influence of abnormal beat morphologies, especially ventricular ectopic beats (VEBs) that are generally recognized by an increase in the width of the QRS complex. The performance of the PB filtering step is a major determinant of the necessary complexity of the remaining parts of the algorithm. It is generally accepted that the frequency components of the QRS complex primarily is between approximately 5 to 22 Hz [6], [9], [14], [15]. As mentioned, we designed a novel cascade of simple FIR filters that obtain a favorable passband in the region of the QRS complex. The cascade of filters consists of two BP filters followed by one lowpass (LP) filter. The impulse responses for the two successive BP filters are defined by (1) and (2).

$$h_{BP1}[n] = \{-\delta[n+10] - \delta[n+9] + \delta[n+2] + \delta[n+1] + \delta[n] + \delta[n-1] - \delta[n-8] - \delta[n-9]\} \quad (1)$$

$$h_{BP2}[n] = \{-\delta[n+14] - \delta[n+13] + \delta[n+2] + \delta[n+1] + \delta[n] + \delta[n-1] - \delta[n-12] - \delta[n-13]\} \quad (2)$$

The LP filter, with impulse response defined by h_{LP} is an average filter with 16 points. This cascade of filters corresponds to an equivalent BP filter with impulse response *h* defined by (3), where $*$ is the convolution operation. The amplitude characteristics of the three individual filters, and the equivalent BP filter is provided in Fig. 4.

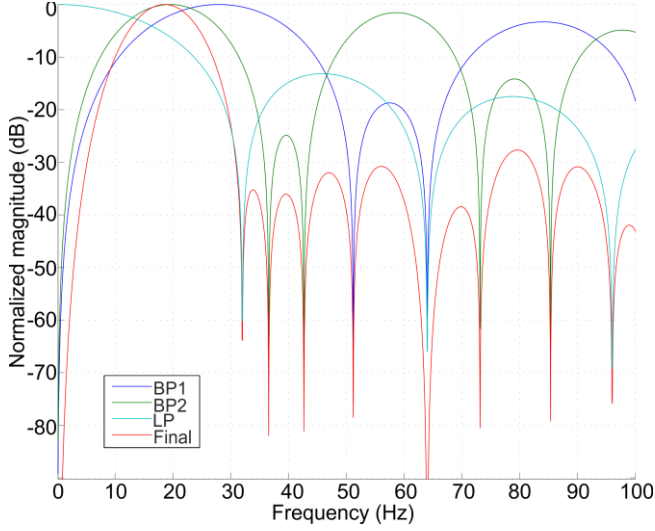$$h[n] = h_{BP1}[n] * h_{BP2}[n] * h_{LP}[n] \qquad (3)$$

Fig. 4. The amplitude characteristics of the three individual filters (the dark blue line represents BP1, the green line represents PB2, and the light blue line represents LP), and the resulting equivalent BP filter (red line) using a sampling frequency of 512 Hz. For frequencies above 100 Hz, the final equivalent BP filter has attenuation of at least -30 dB.

A. Final Feature Extraction

The final feature signal, *Feature*, is obtained by smoothening the absolute value of the output from the BP filtered ECG signal using an 8 point FIR average filter. The absolute value is applied to ensure equal detection of QRS complexes with positive and negative polarity. As mentioned, this is especially important for ECGs recorded with the ePatch technology. An illustration of the feature extraction is provided in Fig. 5. It is observed how muscle artefacts, electrode motion artefacts, and P- and T-waves are attenuated. The total delay of all four cascaded filters is 34 samples. Using a sampling frequency of 512 Hz, this corresponds to 66.4ms, which we considered to be within the acceptable limit for clinical applications.

B. The QRS Detection Block

As mentioned, the QRS detection block consists of two adaptive thresholds that are applied in a search back manner. One of the important components in such an algorithm is timely initiation of the search back procedure. This initiation is decided by the maximum expected RR interval between two subsequent QRS complexes, RR_{max}. The assumption in this study was that RR_{max} should vary with the general variation of the RR intervals. The timely initiation of the search back procedure is especially important in the presence of abnormal beats that might not be detected using T_{high}. In many cases, it is therefore advantageous to initiate the search back procedure earlier in a recording with high variability in the RR intervals. The algorithm was therefore designed to function in two different variability modes (low variability and high variability) described below.
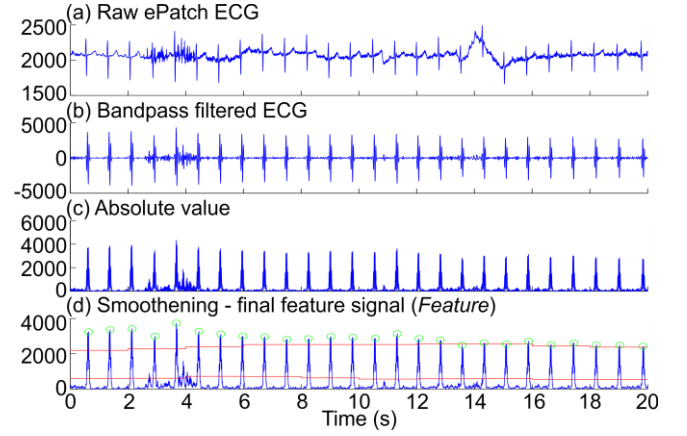

Fig. 5. Illustration of each step in the feature extraction block: (a) Example of raw ECG signal recorded with the ePatch sensor. The amplitude is illustrated in analog-to-digital count (ADC) values for all plots. Note the presence of both muscle artefacts and electrode motion artefacts. (b) The ECG signal after BP filtering using the novel cascade of simple filters. (c) Absolute value of the BP filtered ECG signal. (d) Smoothening of the feature signal. The red lines indicate T_{high} and T_{low}. The green circles indicate the detected positions of the QRS complexes.

Estimation of the Optimal Variability Mode

To estimate the optimal variability mode and RR_{max}, three different set of previous RR intervals are saved:

1) RR_{long}: This contains the 34 previously detected RR intervals, disregarding the detection mode used for detection. The number of RR intervals is chosen to obtain enough RR intervals to provide a reliable estimate of the variability, but without losing the adaptive capability if the heart rhythm suddenly changes.

2) RR_{short}: This contains the 8 previously detected RR intervals, disregarding the detection mode. This can be derived directly from RR_{long}, but it contains a shorter history, and is thus faster adapted to changes in the heart rhythm.

3) $RR_{searchback}$: This contains the 8 previously detected RR intervals that were detected during search back. This implies that information about the general RR intervals during previous episodes of search back is saved, even though the search back procedure might not have been initiated during the previous 34 RR intervals.

The current variability parameter, θ, is then estimated as:

1) Calculate the median of RR_{long}.
2) Calculate the absolute deviation between each RR interval in RR_{long} and the median. The deviation vector is termed ε.
3) Remove the two largest values from ε.
4) θ is then defined as the mean value of the remaining 32 entries in ε.

The third step is included to prevent a single ectopic beat detection, a single missed detection, or a single false positive from pushing the algorithm in the high variability mode. This mode is only intended to be activated for records with many ectopic beats or generally high variation

in the RR intervals, e.g. cases of AF. In these records, it is expected that the risk of missing a beat is increased, and to prevent this, the "sensitivity" of the search back is increased. The high and low variability modes are defined based on θ being above or below a threshold, T_θ. The threshold was set to $T_\theta = 35$ samples. This was obtained by visual inspection of the time course of θ calculated from the reference annotations from the MITDB relative to the heart rhythms that are intended to initiate the high variability mode.

Estimation of the Expected Maximum RR Interval (RR$_{max}$)
RR_{max} is calculated according to (4) and (5).

$$RR_{temp} = \begin{cases} \widetilde{RR_{long}} & if\ \theta \leq T_\theta \\ Min(\widetilde{RR_{short}}, \widetilde{RR_{searchback}}) & if\ \theta > T_\theta \end{cases} \quad (4)$$

$$RR_{max} = RR_{temp} \cdot RR_{scale}. \quad (5)$$

In (4) and (5) $\tilde{x}$ is the median value of the elements in *x*, *Min(x)* is the minimum value of the elements in *x*, and *RR$_{scale}$* is a scaling parameter. The median value is applied to avoid high influence of a single false high or low RR interval. In the low variability mode, *RR$_{long}$* provides a good estimate of the expected RR interval. In the high variability mode, the minimum of the two more sensitive RR variables is used to increase the search back sensitivity. *RR$_{max}$* and θ are updated every two seconds together with the adaptive thresholds.

Adaptive Thresholding
The purpose of adaptive thresholding is to obtain thresholds that follow the changes in the signal. This is especially important for analysis of ePatch ECG signals. The goal is to obtain smooth adaptation to changes in both ECG signal amplitude and changes in the amount and types of artefacts. We decided to update the threshold parameters in non-overlapping windows of two seconds. This ensures the presence of at least one QRS complex in each window within the normal heart rate range. The high threshold, *T$_{high}$*, is based on the median of the maximum feature value in the eight previous windows:

$$T_{high}[m] = (\widetilde{max_{F[m-8]}, \ldots max_{F[m-1]}}) \cdot \alpha. \quad (6)$$

In (6) *m* indicates the window number, *F[m]* represents the final feature signal in window *m*, max_x is the maximum value of the elements in *x,* and α is a scaling factor slightly lower than 1. It most cases, the maximum value of a two second ECG segment is expected to represent the amplitude of a QRS complex. *T$_{high}$* is thus designed to float right below the expected amplitude of the QRS complexes.

The low threshold, *T$_{low}$*, is intended to adjust faster to rapid changes in the amount of artefacts. This threshold is therefore based on information about the mean value of the final feature signal in the two previous windows. It is known that an increase in heart rate induces an increase in the mean value of the feature signal. *T$_{low}$* is not intended to increase as a consequence of increased heart rate. Therefore, *T$_{low}$* is scaled according to the number of QRS detections obtained in the two successive windows applied for the threshold calculation. This modification is termed *s$_1$*. The *s$_1$* parameter is furthermore bounded as follows:
1) If no QRS complexes were detected, set $s_1 = 1$.
2) If > 8 QRS complexes were detected, set $s_1 = 8$.

It is furthermore important to note that episodes of very noisy data might disturb the QRS detection and produce a number of false positive detections that might induce RR variability similar to e.g. episodes of AF. To prevent the increased sensitivity of the search back procedure from exacerbating the number of false positive detections in noisy data, a modification of *T$_{low}$* is also needed in the high variability mode. Therefore the *s$_2$* parameter is defined as:

$$s_2 = \begin{cases} 10 & if\ \theta \leq T_\theta \\ 12 & if\ \theta > T_\theta \end{cases}. \quad (7)$$

These values were obtained by visual inspection of different challenging ECG snippets from the training data (MITDB and eTDB). The temporary low threshold, *T$_{low,temp}$*, is thus calculated by (8), where μ_x is the mean value of the elements in *x*.

$$T_{low,temp}[m] = (\widetilde{\mu_{F[m-2]}, \mu_{F[m-1]}}) \cdot \frac{s_2}{s_1}. \quad (8)$$

Finally, *T$_{low}$* is furthermore bounded by a percentage, *β,* of *T$_{high}$*. This is defined in (9). This ensures a proper functionality of *T$_{low}$* to detect beats missed by *T$_{high}$*:

$$T_{low} = \begin{cases} T_{low,temp} & if\ T_{low,temp} \leq T_{high} \cdot \beta \\ T_{high} \cdot \beta & if\ T_{low,temp} > T_{high} \cdot \beta \end{cases} \quad (9)$$

QRS Localization and Refractory Blanking
The preliminary QRS location is the first sample where the feature signal exceeds the relevant threshold. However, this point is probably not the location of the R peak. To allow better delineation, a search is performed for the maximum point in the feature signal for a period of time after the exceedance of the threshold. The sample point that obtains the maximum feature value during this time interval was selected as the QRS position. The search period is chosen to be equal to the refractory period (*T$_{ref}$*), in which detection of a new QRS complex is not allowed.

C. Data Description
As mentioned, we applied four different databases to ensure thorough evaluation of the algorithm performance. An overview of the different databases is provided in Table I, whereas this section contains a detailed description. For all four databases, only the first ECG channel was applied.

The eTDB was generated by extracting 10 minute ECG

segments from two large existing ePatch databases. The first original database contains recordings from patients admitted to the stroke unit at Glostrup Hospital. The second original database contains ECG recordings from patients undergoing ambulatory diagnosis for obstructive sleep apnea at Glostrup Hospital. Each ECG recording in the two databases was associated with an ECG analysis report (similar to a traditional Holter analysis report). It was important to include ECG recordings from many different patients. We therefore selected 30 patients from the stroke unit database and 30 patients from the ambulatory database. It was furthermore important to ensure representation of many different abnormal beat morphologies as well as normal sinus rhythm with different ventricular frequencies. To ensure this, we selected the 60 patients based on the summaries in the associated ECG analysis reports. From the selected patients, we extracted a total of 120 ECG segments of which 40% were selected randomly and the remaining 60% were selected based on markings of interesting data segments in the analysis reports. This segment extraction ensures a database with realistic amounts of artefacts as well as representation of many different types of abnormal beat morphologies. Some examples of included arrhythmia events are: Atrial fibrillation (AF), episodes of supraventricular tachycardia (SVT) with different frequencies, supraventricular ectopic beats (SVEBs), runs of SVEBs, VEBs, ventricular bigeminy (B), ventricular trigeminy (T), bradycardia, and AV blocks.

The eVDB was generated from three ECG recordings obtained from three different healthy volunteers. The volunteers continued normal daily life activities throughout the recordings. The embedded algorithm output was calculated in real-time during the recordings, and saved in a special channel in the data file. The algorithm output was not investigated before the manual annotation of the eVDB. For each subject, a 15 minute segment was automatically extracted from minute 30 to 45 in each hour of the recording. The mean recording time was 21.0 hours, yielding a total of 20-21 segments for each subject. This ensures representation of realistic amounts of normal daily life activities and provides an overview of a potential change in performance during the recording period.

The ePatch reference annotations were created based on manual corrections of the output from the "sqrs" function from the WFDB Toolbox [21]. The manual corrections were conducted by a biomedical engineer with experience in ECG interpretation. All beats were labelled as normal. To validate the annotation performance of the biomedical engineer, 12 randomly selected records from the eTDB (10%) were also annotated by a medical doctor. The medical doctor did not find any errors in the manual annotations conducted by the biomedical engineer. The manual corrections were conducted using the WAVE program from the WFDB Toolbox [21].

The MITDB and EDB were downloaded from Phyisonet [21]. To obtain similar sampling frequencies for all databases, the recordings from the MITDB and EDB were resampled to 512 Hz using the "xform" function from the WFDB Toolbox [21], and they were converted to mat-files using the WFDB Toolbox for MATLAB [21]. All beats in both databases are manually labelled according to the beat type. This allows evaluation of the detection performance with respect to VEBs and SVEBs.

D. Evaluation of QRS Detection Performance

The QRS detection performance was evaluated as the QRS sensitivity ($Se = TP/(TP+FN)$) and positive predictivity ($P^+ = TP/(TP+FP)$), where TP is the number of true positive detections, FP is the number of false positive detections, and FN is the number of false negative detections (missed QRS complexes). In compliance with [22], TP, FP, and FN for each record, were calculated using the default settings of the "bxb" function from the WFDB toolbox. This implies that the first five minutes of each record is allowed as a training period and episodes of ventricular flutter or fibrillation (VF) were excluded [21]. The performance for each database is stated as gross statistics [22]. No records were excluded in the performance evaluation.

E. Evaluation of Embedded Algorithm Processing Time

After the offline validation, the algorithm was implemented in ANSI C, compiled and embedded in the ePatch sensor. The sensor has a 32 bit micro controller based on the ARM Cortex-M3 processor from Energy Micro (now acquired by Silicon Labs). A low processing time for each sample allows the processor to enter "sleep" mode and hereby save energy. Furthermore, it is important that the processing time of each sample will never exceed the time between two samples. The processing time for each sample will among other things depend on the algorithm mode applied for that specific sample and whether a QRS complex is detected or not. Furthermore, every two seconds the thresholds and other adaptive parameters are updated. This will clearly require more processor time than processing a non-boundary ECG sample between two QRS complexes. We therefore decided to investigate the processing time using a histogram. The histogram was created with a clock cycle counter that counted how many clock cycles the algorithm spends on processing each sample in a real-life recording. The duration of the recording was approximately 2.3 hours, yielding a total of 4,271,185 samples.

III. RESULTS

A. Algorithm Parameter Optimization

Four of the algorithm parameters were chosen based on a parameter grid search on the training databases (MITDB and eTDB). The four parameters were the refractory blanking period ($T_{ref} = 0.2$ms, 0.25ms, or 0.3ms), the scaling of the expected RR interval ($RR_{scale}= 1$, 1.2, or 1.3), the boundary for T_{low} ($\beta = 0.4$, 0.5, or 0.6), and the scaling parameter for T_{high} ($\alpha = 0.8$, 0.9, or 0.99). The investigated

values were selected based on clinical relevance, theoretical sense, and experience from the literature. The parameters are mutually dependent on each other. Therefore, the performances of all 81 different combinations of parameter values were investigated. The relationship between *Se* and P^+ for all 81 combinations is provided in Fig. 6. Fig. 6(a) illustrates the performance on the MITDB. The blue marks indicate the performance on the entire database, the green marks indicate *Se* on SVEB beats only, and the red marks indicate *Se* of VEB beats only. The black circles indicate the parameter combination selected for further embedded implementation. Fig. 6(b) illustrates the performance on the eTDB. The selected parameter combination was $T_{ref} = 0.25$ms, $RR_{scale} = 1.2$, $\alpha = 0.8$, and $\beta = 0.4$.
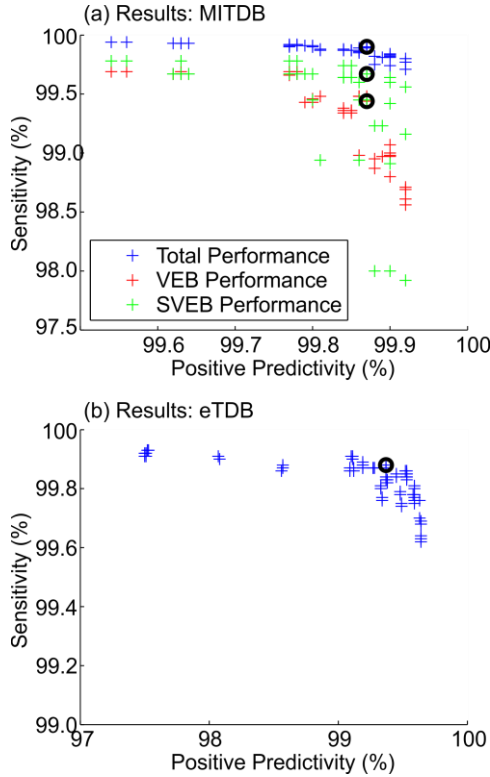
Fig. 6. Relation between P^+ and *Se* for (a) the MITDB and (b) the eTDB. Each mark indicates the performance for one of the 81 investigated parameter combinations. In (a), the blue marks indicate performance on the entire database, the green marks indicate *Se* on SVEB beats only, and the red marks indicate *Se* on VEB beats only. The black circles indicate the parameter combination that was selected for further embedded implementation. Note, that the axes are zoomed to allow a better view of each point.

TABLE II
QRS DETECTION PERFORMANCE ON THE MITDB AND THE EDB.

Method	MITDB		EDB	
	P^+ (%)	*Se* (%)	P^+ (%)	*Se* (%)
This work [#]	99.87	99.90	99.71	99.84
Di Marco and Chiari [7]	99.86	99.77	99.56	99.81
Ghaffari *et al.* [13]	99.88	99.91	99.55	99.63
Ghaffari *et al.* [14]	99.91	99.94	-	-
Liu *et al.* [10] [$]	99.86	99.80	-	-
Li *et al.* [11] [+]	99.94	99.89	-	-
Martìnez *et al.* [16]	99.97	99.71	99.73	99.67
Martìnez *et al.* [12]	99.86	99.80	99.48	99.61
Zhang and Bae [15] [*]	99.82	99.76	-	-
Pan and Tompkins [6] [+#]	99.54	99.75	-	-
Zidelmal *et al.* [9]	99.82	99.64	-	-

[-] Not stated in paper.
[#] Algorithm is implemented and tested in a microprocessor.
[$] Algorithm is implemented and tested on an ASIC.
[*] Algorithm is implemented and tested on a FPGA.
[+] A discrepancy was found between the stated total number of beats and the record-by-record total number of beats. In this table, the record-by-record numbers are applied.

B. QRS Detection Performance

With the selected parameter combination, the obtained *Se* and P^+ on the eTDB was 99.88% and 99.37%, respectively. The performance obtained on the MITDB and the EDB using this parameter combination is provided in Table II. Table II furthermore contains examples of the performance on these databases reported in the literature. For the MITDB, *Se* with respect to VEBs and SVEBs was 99.44% and 99.67, respectively. For the EDB, *Se* with respect to VEBs and SVEBs was 97.60% and 99.53%, respectively. The results from the double-blinded performance evaluation on the eVDB are provided in Table III. The performance is stated for both the MATLAB code, the offline C code, and the embedded code for comparison between the three implementations of the algorithm.

C. QRS Detection Examples

Fig. 7 illustrates the algorithm performance in different challenging clinically relevant cases from the eTDB. The top plot of each subfigure illustrates one channel of raw ePatch ECG. The bottom plot illustrates the final feature signal (blue line) together with T_{low} and T_{high} (red lines). The green circles indicate QRS complexes detected using T_{high} (mode 1), the black circles indicate QRS complexes detected in search back (mode 2), and the magenta circles indicate QRS complexes detected using T_{low} (mode 3).

TABLE III
PERFORMANCE OF THE DOUBLE-BLINDED VALIDATION OF THE QRS DETECTION ALGORITHM ON THE eVDB.

Subject	Records[a]	Beats[b]	MATLAB		Offline C code		Embedded	
			Se (%)	P^+ (%)	*Se* (%)	P^+ (%)	*Se* (%)	P^+ (%)
Subject1	20	11,510	99.83	99.72	99.83	99.72	99.83	99.72
Subject2	20	12,396	99.99	99.85	100	99.86	100	99.86
Subject3	21	14,523	99.92	99.80	99.91	99.79	99.89	99.80
Total	61	38,429	99.92	99.79	99.92	99.79	99.91	99.79

[a] The number of records extracted from each healthy test subject.
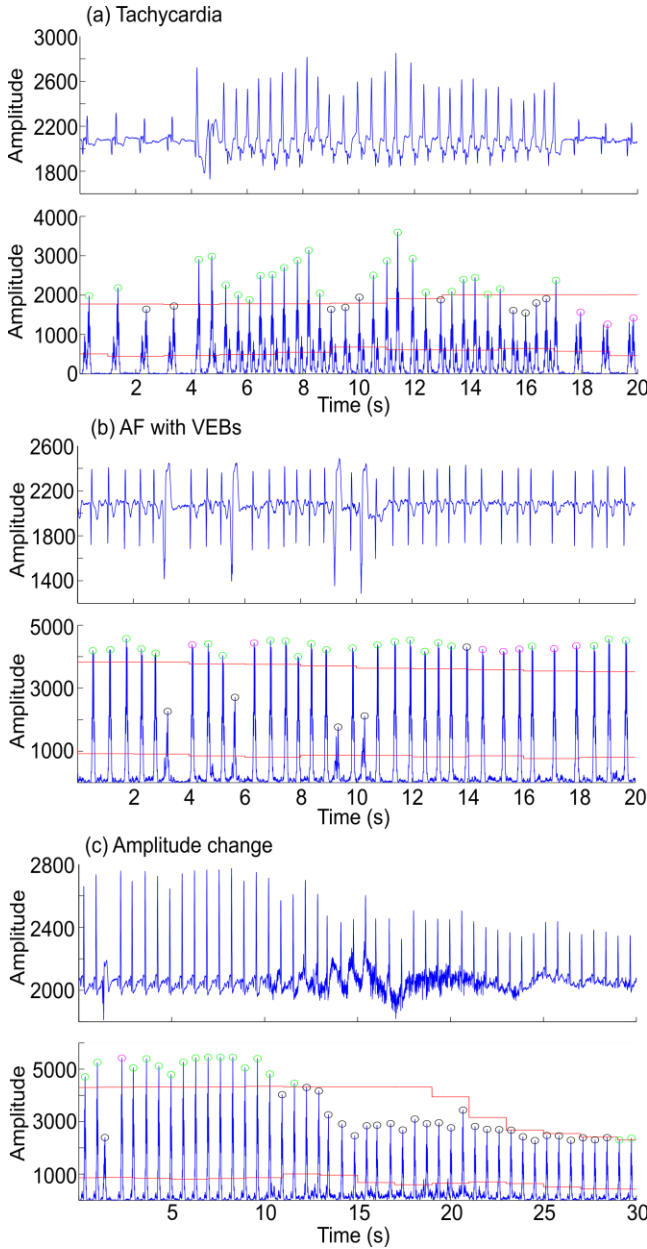[b] The total number of beats in the evaluation period for each test subject.

Fig. 7. Illustration of performance on three challenging cases from the eTDB: (a) Sudden onset of tachycardia, (b) AF with VEBs, and (c) sudden change in amplitude. The top plot in each subfigure is one channel of raw ECG. The amplitude is illustrated in analog-to-digital counts (ADC). The bottom plot in each subfigure is the final feature signal (blue line) together with T_{high} and T_{low} (red lines). The green circles indicate QRS positions detected using T_{high} (mode 1), the black circles indicate QRS positions detected during search back (mode 2), and the magenta circles indicate QRS complexes detected using T_{low} (mode 3).

Fig. 7 (a) illustrates two interesting issues: 1) Very pronounced P-waves with high slopes, and 2) a run of SVEBs/sudden tachycardia onset. It is observed that all QRS complexes are correctly detected by the algorithm. This is obtained through a timely initiation of the search back procedure for all QRS complexes in the SVEB run with amplitude lower than Thigh (indicated by black circles). This illustrates the high adaptability of the search back initiation in this algorithm. It is furthermore observed that the QRS complexes after the SVEB run are detected

using T_{low} in the third algorithm mode (magenta circles). This occurs because it requires some time to adapt to the slower heart rate by decreasing the sensitivity of the search back procedure again. The pronounced P-waves are also observed in the final feature signal. In cases using T_{high}, this is not problematic. In cases using the search back procedure or T_{low}, this could induce false detections of the P-wave when they exceed T_{low}. However, the localization block is observed to correctly prevent false detections of the P-wave for all QRS complexes.

Fig. 7 (b) illustrates a case of AF with VEBs. The VEBs are wider, and therefore less pronounced in the final feature signal. This is, again, not problematic due to timely initiation of the search back procedure in the VEB positions (black circles). It is furthermore observed that the normal beats after two of the VEBs are detected in the third algorithm mode (magenta circles). In these two cases, the algorithm thus proves to function exactly as intended. At fourteen seconds, one QRS complex is detected using the search back mode even though the amplitude exceeds T_{high}. This is due to a very sensitive search back that is initiated on the rising slope of the QRS complex. The localization block is then initiated from the search back procedure and ensures correct localization of the QRS complex. The high search back sensitivity for this recording is caused by the characteristic irregularity of the RR intervals that is observed during episodes of AF.

Fig. 7 (c) illustrates the performance during a sudden change in amplitude. It is observed how T_{high} is quickly adapted to the new level of the QRS complexes. Even in the meantime, no QRS complexes are missed due to the correct functionality of the search back procedure. This feature of the algorithm is very important in real-life clinical applications where patients would wear the ePatch during normal daily life activities for extended periods of time. Furthermore, it is observed that the minor muscle and motion artefacts present in Fig. 7 (c) does not disturb the automatic QRS detection.

D. Embedded Processing Time

The histogram of the processing times for a real-life recording is provided in Fig. 8. Two distinct peaks are observed from the histogram. The first peak represents samples with a processing time between 30μs and 90μs. This peak corresponds to processing of a non-boundary sample. The smaller peak represents samples with processing times between 120μs and 240μs. This corresponds to samples lying on a two second boundary where all the adaptive parameters are updated. It is furthermore observed that no sample has a processing time of more than 240μs. Furthermore, 99.82% of the recorded samples belong to the second histogram bin. To provide a theoretical estimate of the worst case energy consumption, we therefore apply the upper limit of this bin corresponding to a processing time of 60μs. This implies that we expect the algorithm to be active in less than 3.07% of the time with a sampling frequency of 512Hz. This allows the

processor to enter sleep mode or perform other activities for almost 97% of the time. The typical energy consumption of the processor is 5.62mA. Theoretically, the algorithm thus uses up to 0.1726mA. During normal operation (recording, sampling, storage etc.) the ePatch sensor uses 3.125mA. This implies that the algorithm causes a theoretical worst case increase in the energy consumption compared to the normal ePatch sensor activity of 5.5%. This corresponds to a decrease from a maximum recording time of 80 hours to a maximum recording time of 75.8 hours using a 250mAh battery.
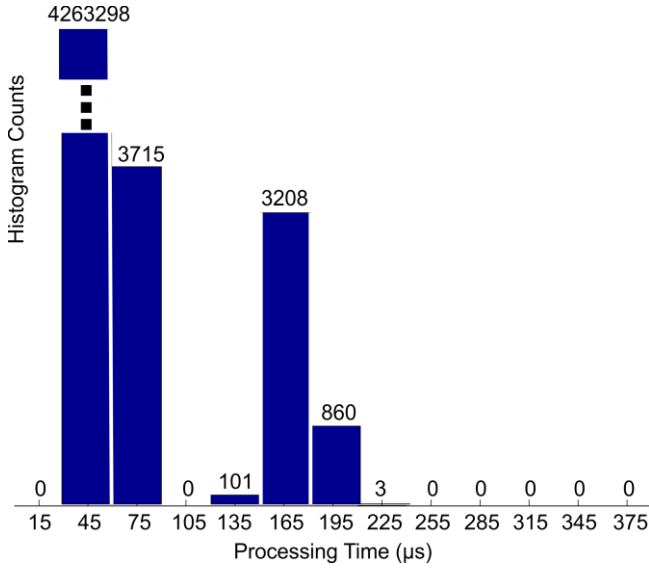
Fig. 8. Histogram of the embedded algorithm processing time for each sample in a real-life recording of 2.3 hours. The x-axis indicates the center value of each histogram bin. This implies that the first bin contains samples with a processing time of 0-30μs, the second bin contains samples with a processing time of 30-60μs etc.

IV. Discussion

On the MITDB, we obtained a sensitivity and positive predictivity of 99.90% and 99.87%, respectively. This performance is definitely comparable to the best results obtained in the literature (see Table II). These results [13], [14] are, however, not obtained by an embedded algorithm that have been tested in real-life situations. When compared to other embedded algorithms [6], [10], [15] the performance obtained by our novel algorithm is slightly superior. The sensitivity with respect to detection of abnormal beat morphologies was unfortunately not stated by the other authors, which makes comparison impossible. However, we consider our detection sensitivity with respect to VEBs and SVEBs to be very high. This is especially relevant if the algorithm is intended to be applied in a clinical setting. In a clinical setting, it can be imagined that the automatic QRS complex detection algorithm works as a pre-processor or initiator of a beat or event classification procedure. This could be highly relevant in applications like tele-monitoring, "admission" of patients in their own home, or rehabilitation programs. Reliable products that can manage tasks like these could highly increase the diagnosis

and treatment of many different groups of patients.

On the EDB, we obtained a sensitivity and positive predictivity of 99.84% and 99.71%, respectively. As observed from Table II, this performance is slightly superior to the other algorithms from the literature. It should furthermore be noted that this database was used only as a validation database. This implies that the algorithm design and parameter selection was not changed prior to the processing of this database. This result can thus provide a relatively realistic impression of the performance on unseen ECG signals with different types of abnormal beat morphologies from a large number of different patients.

The sensitivity (Se = 99.88%) on the eTDB is also considered to be very high. The positive predictivity (P^+ = 99.37%) is, however, slightly lower than for the other databases. This is primarily caused by low P^+ in two records from the same patient. These records contain ECG data of relatively poor quality. The rhythm is AF, and the fibrillating "P-waves" are very pronounced compared to the QRS complexes. These records were, however, included in the study to ensure that the parameter optimization would be more realistic.

Furthermore, the performance in the double-blinded validation of the embedded algorithm is also considered superior (Se = 99.91% and P^+ = 99.79%). This demonstrates how the algorithm can obtain a high performance throughout a long-term recording with artefacts from normal daily life activities. Furthermore, there is no significant difference between the performances of the three implementations of the algorithm.

From the literature it is observed that especially the wavelet decomposition method has been investigated with good performance in a high number of studies. The difference equations for implementation of the commonly applied *a trous* wavelet scheme can be found in [10]. The computational complexity of the proposed novel cascade of filters is similar to the traditional *a trous* wavelet decomposition. However, using the wavelet decomposition, the relevant frequencies of the QRS complex is often divided across several wavelet detail sub-bands. Therefore, a combination of the information in several different sub-bands is usually required when applying the wavelet technique [7]–[14]. This combination of information requires additional computations. Furthermore, the application of the wavelet transform often requires additional blocks after the wavelet decomposition to obtain satisfactory enhancement of the QRS complexes or to confirm a QRS candidate. This includes for instance calculation of maximum-minimum-difference [7], confirmation of zero-crossings [8], multiplication of detail coefficients from selected scales [9], [10], denoising of wavelet output [10], detection of modulus-maxima exceeding thresholds in several detail bands [11], [12], calculation of area-curve length [13], [14], normalization using standard deviation [14], and non-linear exponential amplification of the feature signal [14]. These additional

algorithm steps decrease the computational efficiency of the algorithms. The desired low computational burden associated with our algorithm is obtained partly by the novel cascade of simple FIR filters. The output from these filters is a feature signal that is smooth enough to allow direct detection of QRS complexes using only two adaptive thresholds. However, it should be noted that many studies have also obtained high performance in P- and T-wave delineation using the wavelet transform. If the intended application requires this delineation, it should therefore be investigated whether the decreased computational load in our QRS complex detection algorithm might be out weighted when P- and T-wave delineation is included. However, the influence of this depends highly on the intended application of the QRS complex detection algorithm and the features selected for subsequent potential arrhythmia and event classification.

The application of two adaptive thresholds and timely initiation of the search back procedure is another advantage of our algorithm. This design decreases algorithm sensitivity with respect to detection of noise events without decreasing the sensitivity with respect to detection of abnormal beats. The idea of increasing algorithm sensitivity when irregular RR intervals is observed was already suggested by [6]. However, we propose a different solution where the algorithm sensitivity is increased directly by fast adjustments of RR_{max} instead of decreasing the detection thresholds. This method increases the likelihood of detecting premature beats. Using this method, it is possible to obtain high clinical detection performance without application of computationally costly thresholds.

The superior performance of the algorithm observed from the challenging, but clinically very relevant cases in Fig. 7 is promising. Furthermore, the performance in the double-blinded validation and on the standard databases is considered very high. This high clinical performance is obtained using an algorithm that is simple enough for embedded real-time implementation in the ePatch sensor. This is also illustrated in Fig. 8: 99.82% of the samples are processed in less than 60µs. Even every two seconds when a boundary is reached and the adaptive algorithm parameters are updated, the maximum processing time is 240µs. This feature is very attractive since it allows the processor to enter "sleep" mode and hereby save energy. Furthermore, it leaves valuable overhead for the recording functionality and processing of other potential embedded algorithms in future applications.

It should be noted that future work could include specific noise stress tests of the algorithm. In our study, we include artefacts from normal daily life activities (especially in the eVDB), but the investigation of algorithm performance during specific types and amounts of artefacts could be further investigated. In extremely noisy data segments there is always a risk of obtaining a high number of FP or FN detections. In extreme cases, this might disturb the adaptive parts of the algorithm. This might in extreme cases, exacerbate a poor performance. This could be accounted for in future versions of the algorithm. This improvement could for instance include a pre-qualification of the signal quality that could decide whether the adaptive parameters should be updated, or it could include hard boundaries on the adaptive parameters. A compensation for this could furthermore include a possibility of resetting the adaptive parameters when it is detected that the previous data segment was very noisy. However, the amount of noise needs to be very pronounced for a longer period of time before this becomes problematic.

It should also be noted that the algorithm can produce some FP detections during episodes of AF if the baseline is very influenced by the unorganized electrical activity of the atria. Due to the placement of the ePatch, this atrial activity during episodes of AF is sometimes very pronounced on ECG recorded with the ePatch. This is actually expected to be an advantage for heart rhythm analysis, but it might increase the difficulty of automatic QRS complex detection. However, a few false detections during episodes of AF are not expected to disturb subsequent automatic rhythm analysis and automatic classification of AF versus other heart rhythms. The characteristic irregularity of the RR intervals during AF is still expected to be clearly observed in case of a few false positive detections.

Our overall impression is that this novel algorithm is very relevant in clinical applications. The high performance on both normal and abnormal beat morphologies and the possibility of embedded implementation opens possibilities of real-time monitoring of clinically relevant parameters like heart rate, rhythm analysis, and detection of cardiac events on patients outside the hospital.

V. Conclusion

We have designed a computationally efficient algorithm for real-time automatic QRS complex detection. The performance of the algorithm has been validated on ECG signals from two large standard databases and two private ePatch databases (MITDB: Se=99.90%, P^+=99.87, EDB: Se=99.84%, P^+=99.71%, eTDB: Se=99.88%, P^+=99.37%, and eVDB: Se=99.91%, P^+=99.79%). Together, these four databases contain a high number of abnormal beat morphologies, normal sinus rhythm with different ventricular frequencies, and different amount of artefacts originating from daily life activities. The performance of the algorithm is thus considered high enough for clinical application of the embedded algorithm in the ePatch ECG recorder. The implementation of automatic ECG analysis functionality in small wearable patch type ECG recorders is expected to highly increase the possibilities of early diagnosis, timely treatment, and regular follow-up on patients with life threatening heart diseases like AF.

selection of the database.

References

[1] WHO, "Cardiovascular diseases (CVDs)," *World Health Organization*, 2013. [Online]. Available: http://www.who.int/mediacentre/factsheets/fs317/en/. [Accessed: 24-Jan-2014].

[2] M. P. Turakhia, D. D. Hoang, P. Zimetbaum, J. D. Miller, V. F. Froelicher, U. N. Kumar, X. Xu, F. Yang, and P. A. Heidenreich, "Diagnostic utility of a novel leadless arrhythmia monitoring device," *Am. J. Cardiol.*, vol. 112, no. 4, pp. 520–4, Aug. 2013.

[3] D. B. Saadi, I. Fauerskov, A. Osmanagic, H. M. Sheta, H. B. D. Sorensen, K. Egstrup, and K. Hoppe, "Heart rhythm analysis using ECG recorded with a novel sternum based patch technology - A pilot study," in *Cardiotechnix 2013: Proc. of the International Congress on Cardiovasular Technologies*, 2013, pp. 15–21.

[4] M. A. Rosenberg, M. Samuel, A. Thosani, and P. J. Zimetbaum, "Use of a noninvasive continuous monitoring device in the management of atrial fibrillation: A pilot study.," *Pacing Clin. Electrophysiol.*, vol. 36, no. 3, pp. 328–33, Mar. 2013.

[5] P. M. Barrett, R. Komatireddy, S. Haaser, S. Topol, J. Sheard, J. Encinas, A. J. Fought, and E. J. Topol, "Comparison of 24-hour Holter monitoring with 14-day novel adhesive patch electrocardiographic monitoring.," *Am. J. Med.*, vol. 127, no. 1, pp. 95.e11–7, Jan. 2014.

[6] J. Pan and W. Tompkins, "A real-time QRS detection algorithm," *IEEE Trans. Biomed. Eng.*, vol. BME-32, no. 3, pp. 230–236, Mar. 1985.

[7] L. Y. Di Marco and L. Chiari, "A wavelet-based ECG delineation algorithm for 32-bit integer online processing.," *Biomed. Eng. Online*, vol. 10, p. 23, Jan. 2011.

[8] D. B. Nielsen, K. Egstrup, J. Branebjerg, G. B. Andersen, and H. B. D. Sorensen, "Automatic QRS complex detection algorithm designed for a novel wearable, wireless electrocardiogram recording device.," *Conf. Proc. IEEE Eng. Med. Biol. Soc.*, vol. 2012, pp. 2913–6, Aug. 2012.

[9] Z. Zidelmal, A. Amirou, M. Adnane, and A. Belouchrani, "QRS detection based on wavelet coefficients.," *Comput. Methods Programs Biomed.*, vol. 107, no. 3, pp. 490–6, Sep. 2012.

[10] X. Liu, Y. Zheng, M. W. Phyu, B. Zhao, M. Je, and X. Yuan, "Multiple functional ECG signal is processing for wearable applications of long-term cardiac monitoring," *IEEE Trans. Biomed. Eng.*, vol. 58, no. 2, pp. 380–9, Feb. 2011.

[11] C. Li, C. Zheng, and C. Tai, "Detection of ECG characteristic points using wavelet transforms," *IEEE Trans. Biomed. Eng.*, vol. 42, no. 1, 1995.

[12] J. P. Martínez, R. Almeida, S. Olmos, A. P. Rocha, and P. Laguna, "A wavelet-based ECG delineator: evaluation on standard databases.," *IEEE Trans. Biomed. Eng.*, vol. 51, no. 4, pp. 570–81, Apr. 2004.

[13] A. Ghaffari, M. R. Homaeinezhad, M. Akraminia, M. Atarod, and M. Daevaeiha, "A robust wavelet-based multi-lead Electrocardiogram delineation algorithm.," *Med. Eng. Phys.*, vol. 31, no. 10, pp. 1219–27, Dec. 2009.

[14] A. Ghaffari, M. R. Homaeinezhad, and M. M. Daevaeiha, "High resolution ambulatory holter ECG events detection-delineation via modified multi-lead wavelet-based features analysis: Detection and quantification of heart rate turbulence," *Expert Syst. Appl.*, vol. 38, no. 5, pp. 5299–5310, May 2011.

[15] C. F. Zhang and T.-W. Bae, "VLSI friendly ECG QRS complex detector for body sensor networks," *IEEE J. Emerg. Sel. Top. Circuits Syst.*, vol. 2, no. 1, pp. 52–59, Mar. 2012.

[16] A. Martínez, R. Alcaraz, and J. J. Rieta, "Application of the phasor transform for automatic delineation of single-lead ECG fiducial points.," *Physiol. Meas.*, vol. 31, no. 11, pp. 1467–85, Nov. 2010.

[17] B.-U. Köhler, C. Hennig, and R. Orglmeister, "The principles of software QRS detection.," *IEEE Eng. Med. Biol. Mag.*, vol. 21, no. 1, pp. 42–57, 2002.

[18] IEC60601-2-47:2012, *Medical electrical equipment - Part 2-47: Particular requirements for the basic safety and essential performance of ambulatory electrocardiographic systems*. International Electrotechnical Commision (IEC), 2012.

[19] G. B. Moody and R. G. Mark, "The impact of the MIT-BIH arrhythmia database.," *IEEE Eng. Med. Biol. Mag.*, vol. 20, no. 3, pp. 45–50, 2001.

[20] A. Taddei, G. Distante, M. Emdin, P. Pisani, G. B. Moody, C. Zeelenberg, and C. Marchesi, "The European ST-T database: standard for evaluating systems for the analysis of ST-T changes in ambulatory electrocardiography.," *Eur. Heart J.*, vol. 13, no. 9, pp. 1164–72, Sep. 1992.

[21] A. L. Goldberger, L. A. N. Amaral, L. Glass, J. M. Hausdorff, P. C. Ivanov, R. G. Mark, J. E. Mietus, G. B. Moody, C.-K. Peng, and H. E. Stanley, "PhysioBank, PhysioToolkit, and PhysioNet: Components of a new research resource for complex physiologic signals," *Circulation*, vol. 101, no. 23, pp. e215–e220, Jun. 2000.

[22] AAMI, *ANSI/AAMI EC57: 1998/(R) 2003: Testing and reporting performance results of cardiac rhythm and ST-segment measurement algorithms*. Association for the Advancement of Medical Instrumentation, 2003.

Dorthe B. Saadi received the M.Sc. degree in Biomedical Engineering from the Technical University of Denmark and the University of Copenhagen, Denmark, in 2011. She is currently pursuing a Ph.D. degree at the Department of Electrical Engineering, Technical University of Denmark. Her Ph.D. project is carried out in a close corporation with DELTA and Svendborg Hospital. Her research interests include automatic biomedical signal processing, heart arrhythmias, algorithm design, and clinical validations.

George Tanev received the M.Sc. degree Biomedical Engineering from the Technical University of Denmark and the University of Copenhagen, Denmark, in 2014. His Master's thesis is based on developing a measurement methodology for non-invasive blood pressure. His Master's thesis was carried out in close collaboration with DELTA. He also holds his B.Eng. in Biomedical Engineering from Carleton University, Ottawa, Canada, in 2008. His research interests include biomedical signal processing, heart rate variability, pulse transit time, portable medical technologies and real-time embedded systems.

Karsten Hoppe received the M.Sc. degree in Electrical Engineering from the Technical University of Denmark in 1995. He is currently working as Research Manager in the ePatch group at DELTA. His main interest is ePatch based medical device design.

Jørgen L. Jeppesen received his medical degree and his doctor of medical science degree from the University of Copenhagen in 1989 and 2004, respectively. Jørgen Jeppesen is currently working as a consultant cardiologist and professor in the Department of Medicine, Glostrup Hospital, University of Copenhagen.

Helge B. D. Sorensen (M'90) received his M.Sc.E.E. degree in Electrical Engineering and the Ph.D. degree in Electrical Engineering from Institute of Electronic Systems, Ålborg University, in 1985 and 1992, respectively. He was initially research assistant here and from 1989-1993, he was Assistant Professor at Institute of Electronic Engineering, Ålborg University. From 1993-1995, he was Associate Professor at Engineering Academy Denmark. Currently (since 1995) he is Associate Professor and Head of the Biomedical Signal Processing research group at the Department of Electrical Engineering, Technical University of Denmark.

Paper VI

Automatic Quality Classification of Entire Electrocardiographic Recordings Obtained with a Novel Patch Type Recorder

Dorthe B. Saadi, Karsten Hoppe, Kenneth Egstrup, Poul Jennum, Helle K. Iversen,
Jørgen L. Jeppesen, and Helge B.D. Sorensen

Abstract—Recently, new patch type electrocardiogram (ECG) recorders have reached the market. These new devices possess a number of advantages compared to the traditional Holter recorders. This forms the basis of questions related to benefits and drawbacks of different ambulatory ECG recording techniques. One of the important questions is the ability to obtain high clinical quality of the recordings during the entire monitoring period. It is thus desirable to be able to obtain an automatic estimate of the global quality of entire ECG recordings. The purpose of this pilot study is therefore to design an algorithm for automatic classification of entire ECG recordings into the groups "noisy" and "clean" recordings. This novel algorithm is based on three features and a simple Bayes classifier. The algorithm was tested on 40 ECG recordings in a five-fold cross validation scheme and it obtained an average accuracy of 90% on the test data.

I. INTRODUCTION

Realistic long-term electrocardiogram (ECG) recordings will always contain certain amounts of artifacts including muscle artifacts, baseline wandering, electrode motions, and power line interference. This has been an unavoidable premise since the development of the first Holter recorders in the 1940s. The artifacts arise partly from normal daily life activities that neither can nor shall be avoided during the long-term recordings. The levels of noise in long-term Holter recordings have been silently tolerated, and automatic assessment of the general signal quality of Holter recordings has only obtained limited research efforts. This acceptance of the quality level is partly related to the previous lack of competitive devices. Recently, new cable-less patch type ECG recorders have reached the market [1], [2], [3]. These new devices possess a number of advantages compared to the traditional Holter recorders. These advantages include much higher patient comfort and compliance with wearing the system for extended periods of time. The extended monitoring period (up to 14 days for one device) has shown to result in the detection of more significant arrhythmias, an overall higher diagnostic yield, and a higher degree of definitive diagnosis based on the ambulatory recordings [1], [2]. However, questions concerning the long-term stability of the obtained signal quality using closely spaced recording electrodes have also been raised in the literature [4]. These new technologies thus form the basis of questions related to benefits and drawbacks of different ambulatory ECG recording techniques. This highly increases the relevance of research into areas related to automatic quantification of the clinical recording quality obtained using different techniques. Furthermore, the new technologies allow for recording of previously unknown amounts of data that need analysis. If the quality of the increased amount of data is not controlled, it might overwhelm the healthcare facilities and decrease the efficiency. This issue was also addressed by the Physionet Challenge from 2011, where participants should classify 10 seconds 12-lead ECG signals into the two groups acceptable and unacceptable [5]. In Denmark, long-term ECG recordings are analyzed by highly experienced nurses. They create the analysis reports for the referring medical doctor. These highly trained ECG technicians are accustomed to recognize disturbances as noise, and conduct the interpretation on clean data segments. However, when the general signal quality of a recording is decreased enough to interfere with the clinical interpretation and thus induces uncertainty about the analysis, the nurses write remarks of this in the analysis reports. It is highly relevant to design automatic algorithms that can mimic these subjective comments on noise levels in entire ECG recordings. The purpose of this pilot study is thus to design an algorithm that can distinguish between entire ECG recordings that are essentially noisy or essentially clean. To the best knowledge of the authors, this is the first study investigating automatic noise classification of entire ECG recordings.

II. METHODOLOGY

A. Data Description

We decided to use ECG data from an existing database recorded with the CE marked DELTA ePatch system that records two ECG channels with a sampling frequency of 512 Hz and an analog-to-digital converter (ADC) resolution of 12 bits [3]. The ePatch system is illustrated in Fig. 1. This pilot study includes 20 noisy recordings and 20 clean recordings. The data was extracted from a database of patients that underwent an ambulatory polysomnography at Glostrup Hospital as a part of diagnosing potential obstructive sleep

D. B. Saadi is with the Department of Electrical Engineering, Technical University of Denmark, Ørsteds Plads, Bldg. 349, 2800 Kgs. Lyngby, Denmark and DELTA Danish Electronics, Light & Acoustics, Venlighedsvej 4, 2970 Hørsholm, Denmark (Phone: +45 72 19 40 00; fax: +45 72 19 40 01; e-mail: dbs@delta.dk / dorthe_bodholt@hotmail.com).

K. Hoppe is with DELTA Danish Electronics, Light & Acoustics, Venlighedsvej 4, 2970 Hørsholm, Denmark (e-mail: kh@delta.dk).

K. Egstrup is with the Department of Medical Research, OUH Svendborg Hospital, Valdemarsgade 53, 5700 Svendborg, Denmark (e-mail:Kenneth.Egstrup@rsyd.dk).

P. Jennum, H. K. Iversen and J. L. Jeppesen are with the Danish Center for Sleep Medicine, Department of Neurology, Department of Medicine, University of Copenhagen, Glostrup Hospital, 2600 Glostrup, Denmark (poul.joergen.jennum@regionh.dk, helle.klingenberg.iversen@regionh.dk, joergen.lykke.jeppesen@regionh.dk).

H.B.D. Sorensen is with the Department of Electrical Engineering, Technical University of Denmark, Ørsteds Plads, Bldg. 349, 2800 Kgs. Lyngby, Denmark (e-mail: hbs@elektro.dtu.dk).

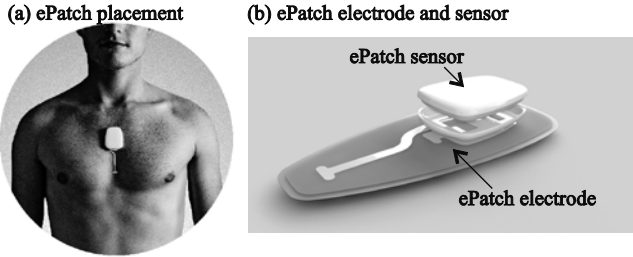(a) ePatch placement (b) ePatch electrode and sensor

Figure 1. (a) Illustration of the ePatch system correctly placed at the sternum. (b) Illustration of the ePatch sensor and the ePatch electrode before assembly. The two ECG channels are recorded as bipolar derivations from the three skin contact points within the ePatch electrode. Modified from [3].

TABLE I. DEMOGRAPHIC INFORMATION FOR EACH GROUP.

	Noisy Recordings	Clean Recordings
Age (mean ± std)	53.6 ± 12.9 years	50.4 ± 13.9 years
Gender	17 males, 3 females	15 males, 5 females
Recording length (mean ± std)	19.3 ± 2.0 hours	19.3 ± 1.5 hours

apnea. The demographic from each group is provided in Table I. Each of the recordings was analyzed by experienced ECG technicians using the automatic myDarwin software [6]. The noisy recordings were extracted as random recordings from the database where the ECG technician conducting the analysis included any comments on bad recording quality in either one or both channels. To ensure inclusion of both very clean and normal recordings, the 20 clean recordings were extracted as five random recordings with remarks on good quality and 15 random recordings without remarks on quality. This database thus allows for a top-level classification of entire recordings that only contains small non-disturbing amounts of noise and recordings that contain noise to an extent where the ECG technician felt enough insecure due to noise to make remarks in the analysis report. In some recordings, the system was obviously detached from the patient before the end of the data file. This is especially pronounced in the clean recordings, whereas it is difficult to judge in many of the noisy recordings. The length of all clean recordings was therefore defined by visual inspection of the recorded data.

B. Algorithm Overview

The algorithm consists of two steps: Feature extraction and classification. The algorithm output is a classification of entire two-channel ECG recordings into one of the two groups "noisy" and "clean" recordings. The algorithm applies three different features that are designed to describe some of the characteristic differences between a clean and a noisy ECG signal. The features are generally based on measuring the amount of time where the recording is noisy based on simultaneous information from both ECG channels.

C. Feature Extraction

The first feature, F_1, describes the amount of saturation in the signal. Saturation is not intended in a clean ECG signal. The feature is defined by (1), where j indicates the channel number, N is the total length of the recording in samples, x_j is the j'th ECG channel, "logical" is the value 1, when the expression is true, and 0 otherwise, "|" is the or operator, α is the maximum possible ADC value (12 bit resolution, α = 4095), and β is the minimum possible ADC value (β = 0).

$$F_1 = \frac{1}{N}\sum_{j=1}^{2}\sum_{n=1}^{N} logical\{x_j(n) = \alpha \mid x_j(n) = \beta\} \quad (1)$$

The second feature, F_2, is a measure of the general mean value of the absolute value of the raw ECG signal in non-overlapping one minute windows. In a clean ECG signal, most samples are expected to obtain a low value corresponding to the isoelectric line between the T-waves and

the P-waves. A noisy segment, on the other hand, will typically contain a certain amount of samples that are significantly different from (numerical higher than) the expected isoelectric line. The mean value of a clean ECG signal is thus expected to be lower than the mean value of a noisy ECG signal with the same heart rate (HR). It is extremely important to scale the signal to attenuate the influence of the general amplitude in the recording. The amplitude can vary significantly between recordings, and even within the same recording. A scaling parameter is therefore calculated for each of the non-overlapping one minute windows. The scaling parameter was found by dividing each one minute window into 30 new equally sized non-overlapping windows. The scaling parameter was set to the median value of the maximum value in each of the 30 small windows. This scaling parameter is expected to estimate the general amplitude of the QRS complexes in the current one minute window, and is thus expected to scale the absolute value of the ECG signal between 0 and 1. The scaling is illustrated in Fig. 2(b)-(c). It is observed how this novel scaling technique allows a measurement of the noise level relative to the individual QRS amplitude for each window. For each channel, the temporary feature, $F_{2,temp,j}$ is thus calculated by (2), where m is the one minute window number, s_j is the scaling parameter, Q is the number of samples in each one minute window, and "| |" is the absolute value operator. This corresponds to the mean value of the signal in Fig. 2(c). Fig. 2(d) illustrates $F_{2,temp,1}$ for the entire duration of a noisy and a clean recording.

$$F_{2,temp\ j}(m) = \frac{1}{s_j(m)\cdot Q}\sum_{q=1}^{Q}|x_j(q)| \quad (2)$$

The final feature, F_2, is then calculated as the sum of the percentage of one minute windows from each channel, where $F_{2,temp,j}$ exceeds a predefined threshold, T_2. This is defined in (3), where M is the total number of one minute windows. The threshold value was set to 0.2 by visual inspection of illustrations similar to Fig. 2(d).

$$F_2 = \frac{1}{M}\sum_{j=1}^{2}\sum_{m=1}^{M} logical\{F_{2,temp\ j}(m) > T_2\} \quad (3)$$

The third feature, F_3, is a measure of the number of significant signal peaks in each of the one minute windows. The assumption in this feature is somehow similar to the assumption in F_2: There will be more significant signal peaks in a noisy segment than a clean segment. A significant signal peak is defined as any sample that obtains higher amplitude than the three preceding samples and the three subsequent samples. The detection of significant signal peaks is illustrated for a noisy and a clean ECG segment in Fig. 2(a). The number of peaks in channel 1 in each window is illustrated for the entire duration of the two recordings in Fig.
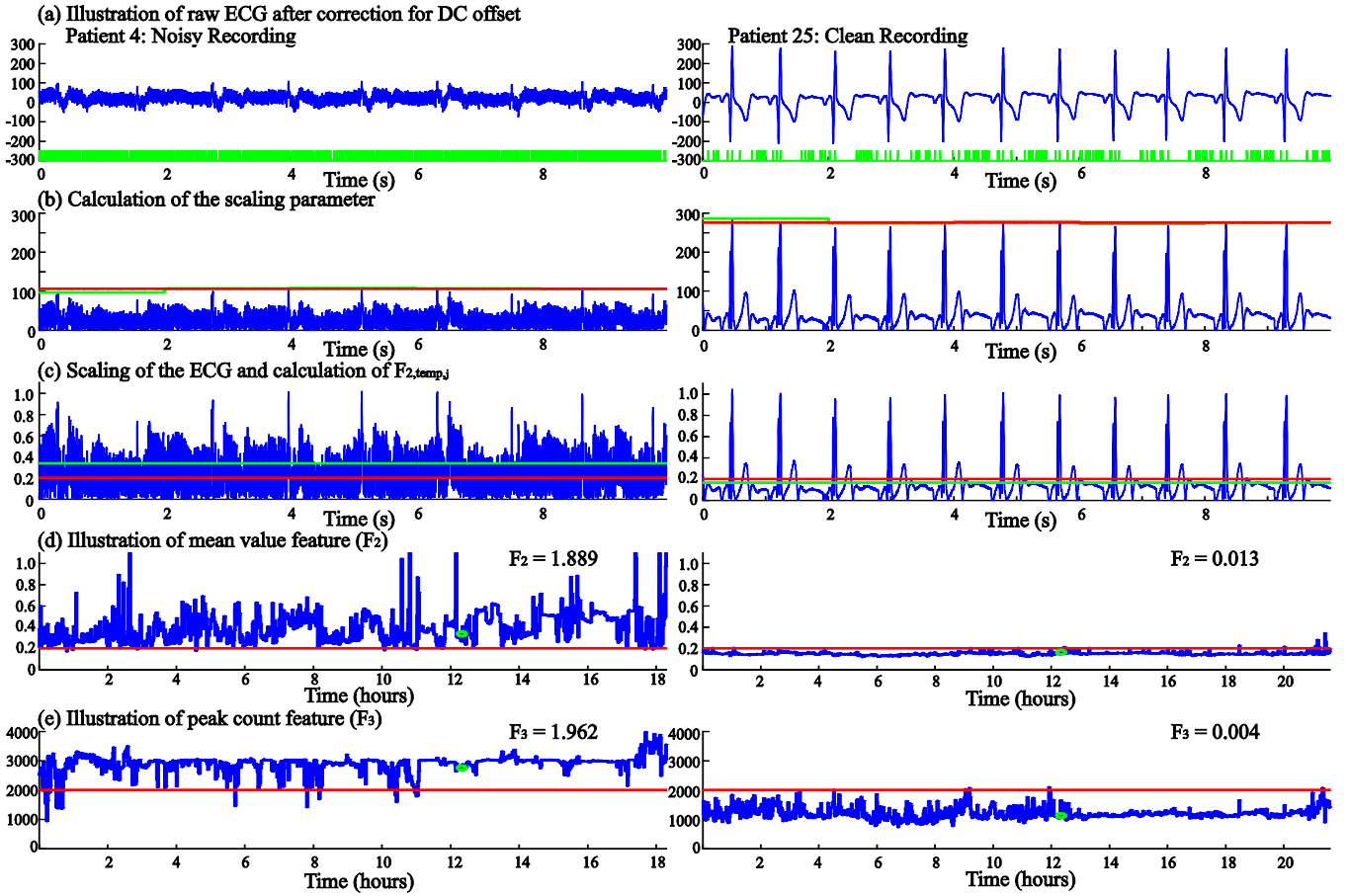
Figure 2. Illustration of feature calculation for a noisy and a clean recording (left and right panel, respectively). (a) Illustration of the raw ECG from channel 1 without any filtering. However, the DC value corresponding to 2^{11} (12 bit resolution) is removed to center the signal on 0. This raw ECG is applied for the calculation of F_2 and F_3. The green lines in the bottom indicate the samples where significant signal peaks were detected for F_3. (b) Calculation of the scaling parameter. The green lines indicate the maximum value in each two second window, and the red lines indicate the resulting scaling parameter for the current one minute window. (c) Scaling of the signal according to the scaling parameter. The green lines indicate the value of $F_{2,temp,j}$ for the current one minute window, and the red lines indicate the threshold, T_2. It is observed that $F_{2,temp,1}$ is above T_2 for the noisy segment and below for the clean segment. (d) The value of $F_{2,temp,j}$ for the entire duration of the signals. The red lines indicate T_2. (e) The number of detected signal peaks in each one minute window throughout the entire recordings. The red lines indicate T_3. The green marks in (d)-(e) indicate the position of the example illustrated in (a)-(c). The calculated feature values for each recording are also provided in (d)-(e). The value of F_1 is 0.015 and 0.000 for the noisy and clean recording, respectively.

2(e). The final feature is calculated from (4), where T_3 is a threshold, and P_j is the number of significant signal peaks in channel j. The threshold was set to 2000 by visual inspection of illustrations similar to Fig 2(e).

$$F_3 = \frac{1}{M}\sum_{j=1}^{2}\sum_{m=1}^{M} logical\{ P_j(m) > T_3 \} \qquad (4)$$

D. Classification

For this pilot study, different types of discriminant functions were investigated for the classification task. We decided to use a simple Bayes classifier that is known to have high performance with low computational costs. A diagonal covariance matrix is applied, corresponding to assuming that the features are non-correlated. The discriminant function, d_i, is thus calculated according to (5), where $\sum_i$ is the covariance matrix of class i, "ln" is the natural logarithm operator, p_i is the prior probability of class i ($p_1 = p_2 = 0.5$), μ_i is the mean vector of the feature vectors from class i in the training data, y is the feature vector to be classified ($y = [F_1, F_2, F_3]$), and c is a constant equal to the natural logarithm of the determinant of the class covariance matrix, $\sum_i$.

$$d_i(y) = -\frac{1}{2}(y - \mu_i)^T \sum_i^{-1}(y - \mu_i) + \ln(p_i) + c \qquad (5)$$

The feature vector under classification, y, is then classified to the class obtaining the highest value of d_i. The signal processing was conducted in MATLAB R2013b, and the classification was implemented using the build-in function "classify" with the option "diagQuadratic".

III. RESULTS

The algorithm performance was evaluated as the sensitivity (Se=TP/(TP+FN)), specificity (Sp=TN/(TN+FP)), and accuracy (Acc=(TP+TN)/(TP+TN+FP+FN)), where TP is the number of clean recordings correctly classified as clean (true positive), TN is the number of noisy recordings correctly classified as noisy (true negative), FN is the number of clean recordings wrongly classified as noisy (false negative), and FP is the number of noisy recordings wrongly classified as clean (false positive). Due to the intermediate number of recordings in this pilot study, the performance was evaluated by a five-fold cross validation. Each fold consists of training the classifier on 32 recordings (16 from each class), and testing the performance of the obtained classifier

on the remaining eight recordings. The training and test performances for each fold, as well as the average performances are provided in Table II.

IV. DISCUSSION

The proposed novel algorithm is capable of obtaining an average accuracy of 90% on the test data. This is considered a high clinical performance. It should be stated that this high performance is obtained on clinically relevant ambulatory ECG recordings acquired from real patients in their homes. This was chosen to ensure a realistic amount of abnormal heart rhythms and beat morphologies. It is, of course, very important to ensure that automatic noise classification algorithms will not classify a recording with a high number of abnormal beat morphologies as noisy. The general HR, non-disturbing baseline wandering, and different P- and T-wave morphologies might affect the values of F_2 and F_3. This was not accounted for in the calculation of the features in this pilot study. Further improvements of the algorithm might include adjustments to account for these issues. The values of T_2 and T_3 were furthermore found by visual inspection. The overall performance of the algorithm depends on the performance of these thresholds, and the overall performance might therefore be increased, if the threshold values were corrected using a proper parameter optimization method, e.g. Receiver Operator Curves (ROCs). Furthermore, some of the algorithm parameters (e.g. α and β), should be adjusted to different recording devices with different front-end specifications. However, the novel adaptive scaling of the ECG signal before calculation of F_2 ensures the possibility of a global T_2 value that is not neither patient nor device dependent. Due to the high clinical performance of the algorithm, this novel approach to quantification of noise levels in entire ECG recordings is expected to be very useful in many different applications in the future. It is extremely important to gain solid knowledge related to the benefits and drawbacks of the new technologies for long-term ambulatory ECG monitoring in different situations. Choosing the right device in each application can increase the diagnostic yield and decrease the burden on the patients and the healthcare facilities. An automatic classification of entire ECG recordings provides the possibility of an objective and fast assessment of the clinical quality of a high number of ECG recordings acquired using the different technologies. This could provide important information to answers related to the benefits and drawbacks of the new technologies. Another application scenario is related to pre-screening of recordings before the manual analysis. If a specific recording is classified as being very noisy, it might be beneficial to exclude the recording from manual analysis to increase the efficiency of the healthcare facilities. Furthermore, the algorithm is designed using very simple features that can be efficiently calculated in real-time. This could allow for future embedded implementation of the algorithm in the patch type ECG recorders. This could be imagined to provide a real-time estimate of the recorded signal quality, and allow prober actions to increase the quality if the recording quality is generally too low, or if the quality suddenly decreases during a recording. Another approach to noise estimation is using a shut-down algorithm. The shut-down approach might provide a percentage of analyzable data, but this does not necessarily directly translate to an estimate of the general quality of the

TABLE II. PERFORMANCE EVALUATION. TRAINING: *. TEST: ¤.

	Se*	Sp*	Acc*	Se¤	Sp¤	Acc¤
Fold 1	93.8%	81.3%	87.5%	100%	75%	87.5%
Fold 2	93.8%	87.5%	90.6%	75%	100%	87.5%
Fold 3	93.8%	87.5%	90.6%	100%	75%	87.5%
Fold 4	93.8%	93.8%	93.8%	100%	75%	87.5%
Fold 5	93.8%	75.0%	84.4%	100%	100%	100%
Average	93.8%	85.0%	89.4%	95%	85%	90%

entire recording: It is extremely difficult from an engineering point of view to determine the specific types, amounts, and duration of artifacts that might interfere with the clinical interpretation of a signal. The shut-down approach might be less sensitive to long periods of data with relatively poor quality that would not trigger the detection of an artifact event, but that would still impose difficulties in the interpretation of the recorded ECG signal. We therefore find it highly relevant, not only to attempt to detect the noise events, but also to provide an overall estimate of the quality of entire ECG recordings. Future work might include dividing the recording into smaller segments, and for instance disregard data based on an hour basis instead of the entire recording. It should, of course, also be stated that the algorithm performance might be further improved by exploring new features, adaptive thresholds, and more advanced classification schemes. Furthermore, the algorithm should be tested on a larger database to confirm the performance in the general population and in ECG signals with a higher variety of abnormal beat morphologies.

REFERENCES

[1] P. M. Barrett, R. Komatireddy, S. Haaser, S. Topol, J. Sheard, J. Encinas, A. J. Fought, and E. J. Topol, "Comparison of 24-hour Holter Monitoring with 14-day Novel Adhesive Patch Electrocardiographic Monitoring.," *Am. J. Med.*, vol. 127, no. 1, pp. 95.e11–7, Jan. 2014.

[2] M. P. Turakhia, D. D. Hoang, P. Zimetbaum, J. D. Miller, V. F. Froelicher, U. N. Kumar, X. Xu, F. Yang, and P. A. Heidenreich, "Diagnostic utility of a novel leadless arrhythmia monitoring device," *Am. J. Cardiol.*, vol. 112, no. 4, pp. 520–4, Aug. 2013.

[3] D. B. Saadi, I. Fauerskov, A. Osmanagic, H. M. Sheta, H. B. D. Sorensen, K. Egstrup, and K. Hoppe, "Heart rhythm analysis using ECG recorded with a novel sternum based patch technology - A pilot study," in *Cardiotechnix 2013: Proc. of the International Congress on Cardiovasular Technologies*, 2013, pp. 15–21.

[4] S. Mittal, C. Movsowitz, and J. S. Steinberg, "Ambulatory external electrocardiographic monitoring: focus on atrial fibrillation.," *J. Am. Coll. Cardiol.*, vol. 58, no. 17, pp. 1741–9, Oct. 2011.

[5] I. Silva, G. B. Moody, and L. Celi, "Improving the Quality of ECGs Collected Using Mobile PhonesThe PhysioNet / Computing in Cardiology Challenge 2011," in Computing in Cardiology 2011, 2011, pp. 273–276.

[6] "medilog Darwin Liberty Online Holter Analysis," *HASIBA Medical GmbH*. [Online]. Available: http://hasimed.com/. [Accessed: 04-Jun-2014].

Paper VII

Investigation of Analyzable Time in 24-hour Patch Electrocardiogram Recordings

Dorthe B. Saadi, Armin Osmanagic, Hussam M. Sheta, Kenneth Egstrup, Lasse Bay, Karsten Hoppe, Jorgen L. Jeppesen, Helle K. Iversen, Poul Jennum, and Helge B. D. Sorensen

Abstract— Objective: **The advantages of novel patch type electrocardiogram (ECG) recorders are irresolvable conditioned by the assurance of the ability to obtain high-quality diagnostic ECGs throughout the recording period. The purpose of this study was therefore to investigate the percentage of analyzable time achieved in ECG recordings obtained with a novel patch type recorder.** *Methods:* **First, we designed a novel algorithm for automatic estimation of the percentage of analyzable time in ECG recordings. This algorithm was then applied to a large database with patch ECG recordings obtained from 250 different patients. The patient population was selected to ensure a high representation of both arrhythmia events and normal daily life activities.** *Results:* **We found that 10% of the 250 recordings obtained <10% analyzable time. These recordings where considered as incorrect measurements. The median and mean analyzable time of the remaining 225 recordings were found to be 100% (interquartile range: 97.9% - 100%) and 92.4±18.8%, respectively. Furthermore, 83.6% of the 225 recordings obtained an analyzable time equivalent to ≥22 hours/day.** *Conclusion:* **We found the analyzable time in the patch recordings to be high. This indicates that the many advantages of the patch ECG recorders are not counterbalanced by low signal quality.** *Significance:* **Our findings add to the limited knowledge about the diagnostic quality obtained in clinical long-term patch ECG recordings.**

Index Terms— **analyzable time in patch ECG recordings, automatic ECG quality estimation, ePatch ECG recorder, quality of patch ECG recordings.**

I. INTRODUCTION

THE implementation of patch type electrocardiogram (ECG) recorders is expected to revolutionize the field of ambulatory ECG monitoring. However, outpatient ECG monitoring remains to be sensitive to artefacts arising from daily life activities that neither can nor shall be avoided during long-term recordings. It has been questioned whether the short inter-electrode distance necessary in patch designs can resist the influence of these artefacts and record satisfactory high quality ECG signals throughout the entire monitoring period [1]. It is therefore highly important to investigate the actual analyzable time in patch ECG recordings. Only few studies in the literature have addressed this important area. One study states that they obtained a median analyzable time of 99% (interquartile range: 94% to 99%) and that 87.1% of the patients obtained an analyzable time equivalent to ≥22 hours/day using a patch type ECG recorder [2]. Another recently published study showed that 69% of data recorded by another patch type ECG recorder during different activities were of at least moderate quality [3]. The purpose of this study was to add to the limited knowledge about the signal quality obtained using patch type ECG recorders. In order to achieve this, we have designed a novel algorithm for automatic estimation of the percentage of analyzable time (PAT) in ECG recordings. The first part of this paper thus describes the design and validation of our novel quality estimation algorithm, whereas the second part describes the application of the algorithm to gain knowledge about the overall PAT for a high number of ECG recordings acquired with the DELTA ePatch ECG recorder illustrated in Fig. 1.
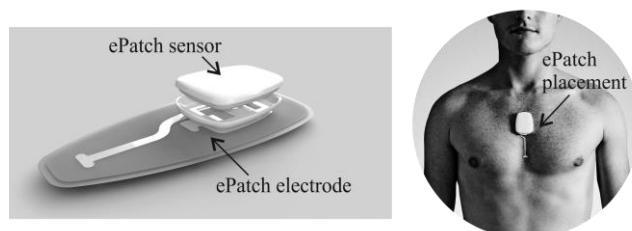

Fig. 1. Illustration of the ePatch sensor, the ePatch electrode, and the correct placement of the ePatch on the sternum. Modified from [4] and [5]. The CE marked ePatch applied in this study records two ECG channels with a sampling frequency of 512 Hz and a resolution of 12 bits. The ePatch system is further described in [5].

A. Literature on Automatic ECG Quality Assessment

Our group recently suggested an approach to classification

of entire long-term patch ECG recordings into the two groups "bad" (defined as recordings were the analyzing ECG technician made comments on poor quality) and "good" (defined as recordings with comments on high quality or no comments on quality) [4]. However, to our knowledge, this is the first paper describing an algorithm designed specifically for estimation of the overall PAT in ambulatory ECG recordings, and hereby providing a continuous score of the obtained signal quality. Many of the published papers in the field of automatic ECG quality assessment are related to the Physionet Challenge from 2011. In this challenge, 10 second 12-lead ECG recordings should be classified as "acceptable" or "non-acceptable". The original challenge obtained a high number of participants of which nine groups achieved an accuracy of 90–93.2% on unknown test data [6]. Generally, the existing quality assessment algorithms can be divided into two steps: The feature extraction step and the classification step. The underlying assumptions in the feature design step can be further divided into three different paradigms. The first paradigm aims at designing individual features for detection of specific artefact types. This could include features designed for detection of missing leads or flat lines [7]–[11], detection of peak or spike artefacts [10], [11], detection of power line interference [7], [10], detection of baseline wandering [7], [9], [10], or detection of muscle artefacts [7], [10]. The second paradigm includes features designed to capture general statistical differences between clean and noisy ECG segments. Examples of these features include skewness [9], kurtosis [9], [12], Shannon entropy [13], mean value [13], and variance [13]. The third paradigm includes features designed to recognize the characteristic appearance of a clean ECG segment. This includes features like comparison of multiple automatic beat detection algorithms [9], [12], beat detection comparison in different leads [9], [12], regularity of detected QRS complexes [11], and the relative spectral power in the region of the QRS complexes (5-14 Hz) [8], [9], [12]. Using the first feature extraction paradigm, the performance of the algorithm is naturally limited by the types of artefacts that are accounted for in the feature design phase. The generalization of the algorithm therefore highly depends on representation of sufficient amounts of all likely artefacts in the training database. This issue might be further increased when the classification is based on empirically found thresholds applied to each feature individually [10], [11], [13]. This methodology excludes information about decreased quality caused by simultaneous influence of small amounts of several different types of artefacts. It is therefore not surprising that some of the highest classification accuracies were obtained by more sophisticated classifications schemes, e.g. the matrix of regularity defined by [8] or the support vector machine (SVM) and the multi-layer perceptron neural network investigated by [9]. We therefore decided to base our algorithm on features extracted using the second and third paradigm and an SVM classifier.

II. Methods and Procedures

To allow estimation of the overall PAT, we divided the

long-term recordings into several smaller non-overlapping segments and automatically assigned each of these segments to one of the two classes "analyzable" (class I) or "non-analyzable" (class II). As illustrated in Fig. 2, this procedure facilitates easy evaluation of the overall PAT.
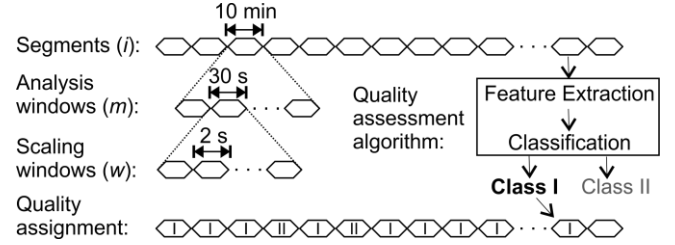

Fig. 2. The long-term recordings were divided into smaller non-overlapping segments, i. Each segment was then classified as being either analyzable (class I) or non-analyzable (class II) using our proposed quality assessment algorithm. The algorithm is based on three features and an SVM classifier. The input to the quality assessment algorithm is a two-channel ECG segment, and the output is an assignment to one of the two classes. For the calculation of F_1 and F_2, each segment was further divided into smaller analysis windows, m. For the calculation of F_2, each analysis window was also divided into even smaller scaling windows, w. This segment division is further described later.

A. Selection of Segment Length

During ECG interpretation, the human experts (e.g. ECG technicians and cardiologists) are accustomed to recognize artefacts and conduct the interpretations based on periods with diagnostic ECG. This includes "looking through" short periods of data with even pronounced amounts of artefacts, and still be able to interpret the underlying heart rhythm with certainty. This is possible due to contextual information provided from periods of diagnostic ECG surrounding the artefact event. This implies that short periods of even very pronounced amounts of artefacts might not interfere with the clinical interpretation of the ECG. On the other hand, prolonged periods with apparently small amounts of artefacts might preclude proper clinical interpretation if the quality of the isoelectric line is affected. This implies that both the duration of a specific artefact event and the quality of the surrounding ECG is highly important when analyzing the potential clinical impact of an artefact event. It is therefore important to include adequate amounts of contextual information in each segment. In our experience, the types of activities that would often cause artefacts that could significantly impair clinical interpretations occur on the scale of several minutes. This could for instance include running on stairs, carrying shopping baskets, or exercising. We therefore subjectively decided to apply segments of 10 minutes. We found this segment length to provide a good compromise between including adequate contextual information (longer segment length) and keeping a high "resolution" of the overall PAT (shorter segment lengths).

B. Feature Extraction

All three features were designed to obtain small values (close to 0) for the analyzable ECG segments and high values

(close to 1) for the non-analyzable ECG segments. The first two features, F_1 and F_2, were designed to measure the quality of the important isoelectric line. These features thus fall in the second feature extraction paradigm described earlier. Simpler variations of these two features were also investigated by our group in [4]. The third feature, F_3, was based on the assumption that the performance of an automatic QRS complex detection algorithm depends on the quality of the ECGs. This feature thus belongs to the third feature extraction paradigm. Variations of this feature was also investigated by [7], [9], [12]. In our implementation, an automatic QRS complex detection algorithm was applied to estimate R peak positions in each channel individually, and the similarity obtained between the two channels was applied for calculation of F_3. Fig. 3 contains ECG snippets from three different ECG segments. The final and temporary feature values obtained for each segment are furthermore provided in Table I. The calculation of each of the stated features is described in details in the following sections. It should be noted that the stated feature values are based on the entire 10 minute duration of each segment and not only the illustrated snippet. This is especially observed from segment C, where channel II apparently seems more noisy than channel I in the illustrated snippet, but it is observed from Table I that based on the entire 10 minute segment $F_{1,2} < F_{1,1}$ and $F_{2,2} < F_{2,1}$.
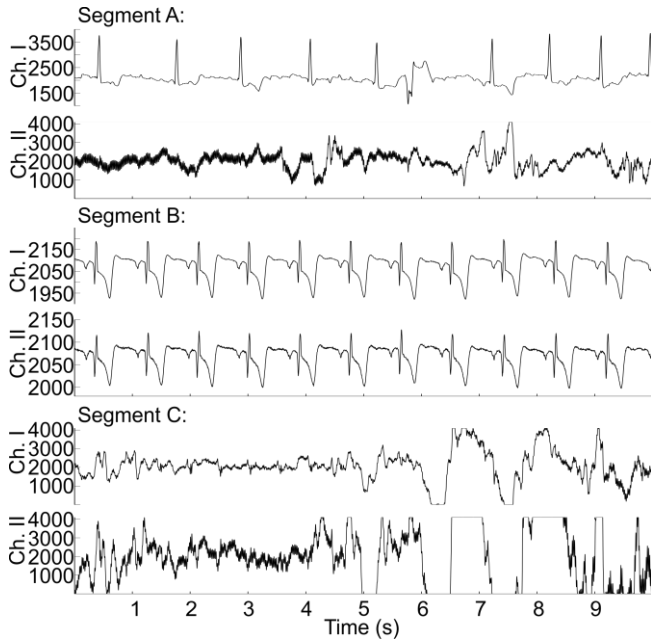

Fig. 3. Illustration of three ECG snippets with different quality characteristics. The amplitudes are illustrated in analog-to-digital counts. Segment A and B were manually annotated to class I (analyzable), whereas segment C was manually annotated to class II (non-analyzable). The temporary and final feature values for each segment are provided in Table I.

TABLE I
CALCULATION OF FEATURE VALUES FOR THE THREE ECG SEGMENTS
ILLUSTRATED IN FIG. 3.

	$F_{1,1}$	$F_{1,2}$	F_1	$F_{2,1}$	$F_{2,2}$	F_2	$\frac{FD}{TP}$	η	F_3
A	0.00	1.00	**0.00**	0.00	1.00	**0.00**	0.41	0.28	**0.11**
B	0.00	0.00	**0.00**	0.00	0.00	**0.00**	0.00	0.92	**0.00**
C	0.45	0.20	**0.20**	1.00	0.90	**0.90**	0.60	0.99	**0.60**

1) Calculation of F_1

The first feature, F_1, provides a measure of the number of significant signal peaks observed in the current segment. It is expected that a noisy non-analyzable ECG segment obtains significantly more signal peaks than a clean segment. The 10 minute ECG segment was divided into smaller analysis windows, m (see Fig. 2). The length of each analysis window was, again, a compromise between including adequate contextual information and obtaining a high "resolution" on the possible feature values. We therefore decided to apply analysis windows of 30 seconds, yielding a total of 20 windows ($M = 20$). For each analysis window, the number of significant signal peaks, $P_j(m)$, was estimated for each channel j. A significant signal peak was defined as any sample obtaining a higher value than the three previous and the three subsequent samples. For each channel, $F_{1,j}$ was calculated according to (1), where $logical\{\}$ obtains the value 1 when the expression is true and 0 otherwise. The threshold, T_1, was optimized using a parameter grid search described later. The final value of F_1 for each segment was defined as the minimum value obtained from the two channels, see (2). This prevents the final feature value from being wrongly increased in cases where only one of the two channels obtains poor quality. An example of this is provided in Fig. 3 (Segment A).

$$F_{1,j} = \frac{1}{M} \sum_{m=1}^{M} logical \{P_j(m) > T_1\} \qquad (1)$$
$$F_1 = Min\{[F_{1,1} \quad F_{1,2}]\} \qquad (2)$$

2) Calculation of F_2

The second feature, F_2, was designed as a measure of the mean value of the baseline-corrected, rectified, and scaled ECG signal. This mean value is expected to be higher for a noisy ECG segments that for an analyzable segment. The baseline was removed to avoid the influence of high P- and T-waves and non-disturbing amounts of baseline wandering and electrode motion artefacts. The baseline was estimated using a 32 point average filter. The baseline corrected ECG signal, $ECG_{filt,j}$ was obtained by subtracting the estimated baseline from the raw ECG signal. Then $ECG_{filt,j}$ was rectified. The baseline-corrected rectified ECG segment was termed $|ECG_{filt,j}|$. It is important to account for the known differences in the general amplitude in ECG recordings. A scaling parameter, $s_j(m)$, was therefore calculated for $|ECG_{filt,j}|$ in each analysis window. We decided to design the scaling parameter to theoretically obtain a value close to 1 in the R peak positions in the scaled $|ECG_{filt,j}|$. This ensures that the mean value estimates the noise level relative to the R peak amplitudes. To achieve this, each analysis window was divided into even smaller scaling windows, w (see Fig. 2). The length of each scaling window was two seconds. This implies that at least one QRS complex is expected in each scaling window. In most scaling windows, the maximum value of $|ECG_{filt,j}|$ is thus expected to represent the amplitude of a QRS complex. The scaling parameter in the m'th analysis window was calculated as the median value of the maximum value of $|ECG_{filt,j}|$ obtained from each of the 15 scaling windows. This

calculation of $s_j(m)$ thus provides a reliable estimate of the general R peak amplitude in the m'th analysis window. The mean value of the scaled, rectified, and baseline-corrected ECG signal was calculated for each analysis window. This is defined in (3), where Q is the total number of samples in each analysis window [4]. For each channel, $F_{2,j}$ was then calculated according to (4). The threshold, T_2, was optimized by a parameter grid search described later. As for F_1, the final value of F_2 for each segment was defined as the minimum value obtained from the two channels, see (5).

$$\mu_j(m) = \frac{1}{s_j(m)\cdot Q}\sum_{q=1}^{Q}\left|ECG_{filt,j}(q)\right| \tag{3}$$

$$F_{2,j} = \frac{1}{M}\sum_{m=1}^{M} logical\left\{\mu_j(m) > T_2\right\} \tag{4}$$

$$F_2 = Min\left\{\left[F_{2,1} \; F_{2,2}\right]\right\} \tag{5}$$

3) Calculation of F_3

For the calculation of F_3, the segment was not divided into the previously described analysis windows. The input to this feature is an array of R peak positions estimated from each ECG channel individually. We applied an automatic QRS complex detection algorithm designed by our group [14]. The algorithm was designed to obtain high performance in the ePatch ECG recordings. For each segment, we calculated the number of true positive detections (*TP*) and the number of false detections (*FD*). *TP* was defined as the number of QRS complexes simultaneously detected in both channels and *FD* as the number of QRS complexes only detected in one channel. In compliance with [15], we used a match window of 150ms. This implies that the absolute distance between QRS complexes detected in channel I and channel II should not exceed 150ms in order for the pair of QRS complexes to be counted in *TP*. The third feature was then based on the relation between *FD* and *TP* (see (7)). However, this relation is expected to be high when either one or both channels obtain poor quality. This is not intended (see Fig. 3, segment A). To account for this, we designed a novel scaling parameter, η, defined by (6), where $\sigma(x)$ is the variance of the elements in x, and RR_j represents the RR interval vector for channel j. If both channels display the same quality (either good or poor), the variation between the detected RR intervals is expected to be similar in both channels. In this case, η will obtain a value close to 1, and the relation between *FD* and *TP* will not be altered significantly. On the other hand, when the quality is different for the two channels, η is expected to decrease, and hereby reduce the influence of a potentially high relation between *FD* and *TP* caused by poor quality in only one channel. The performance of η is observed from Table I.

$$\eta = \frac{Min\{[\sigma(RR_1)\;\sigma(RR_2)]\}}{Max\{[\sigma(RR_1)\;\sigma(RR_2)]\}} \tag{6}$$

$$F_3 = \frac{FD}{TP}\cdot\eta \tag{7}$$

The final feature vector was then defined by (8).

$$\boldsymbol{F} = [F_1 \; F_2 \; F_3] \tag{8}$$

The discriminative capabilities of the three designed features are observed from Fig. 4. This difference provides the foundation for an automatic classifier to obtain high performance in differentiating between the two classes.
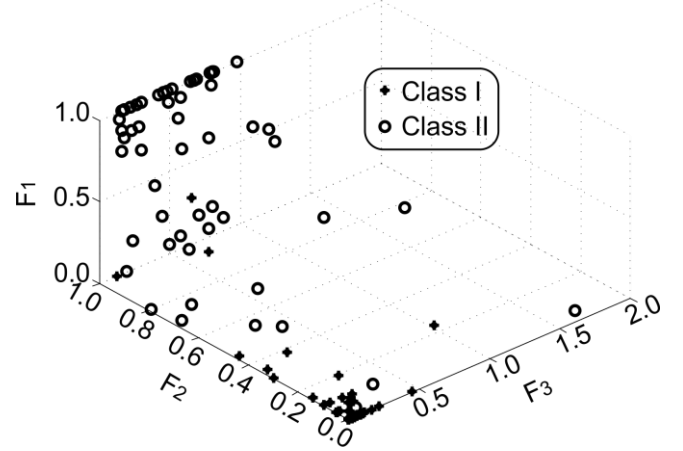

Fig. 4. Illustration of the three dimensional feature space for the ECG segments from the training database. The plot is thus based on feature values obtained from 292 diagnostic ECG segments (class I) and 58 non-analyzable ECG segments (class II). It is observed that most feature vectors from the analyzable class are located in a very small area in the three dimensional feature space. This is very promising for subsequent automatic classification between the two classes.

C. Classification

With inspiration from [9], we decided to apply a soft margin SVM with a radial basis function (RBF) kernel. A detailed description of the SVM classifier and the kernel trick applied for non-linearly separable data is available in [16]. For the implementation, we applied the *svmtrain* and *svmclassify* functions in *MATLAB R2013b* [17]. Since the feature values were designed to be approximately in the range [0; 1], no additional scaling was conducted prior to the classification. The RBF kernel parameter, γ, and the SVM soft margin parameter, C, were optimized using a parameter grid search described later.

D. Algorithm Performance Estimation

To ensure thorough evaluation of the algorithm performance, we applied five different performance measures: Sensitivity (*Se*), specificity (*Sp*), accuracy (*Acc*), negative predictive value (P^-), and positive predictive value (P^+) defined in (9) – (13). Positive refers to the clean segments, whereas negative refers to the noisy segments. Each of the five performance measures and their mutual relations contain important information regarding the ability to correctly classify each segment, and hereby the algorithms ability to provide a reliable estimate of the overall PAT.

$$Se = \frac{TP}{TP+FN}\cdot100\% \tag{9}$$

$$Sp = \frac{TN}{TN+FP}\cdot100\% \tag{10}$$

$$P^+ = \frac{TP}{TP+FP}\cdot100\% \tag{11}$$

$$P^- = \frac{TN}{TN+FN}\cdot100\% \tag{12}$$

$$Acc = \frac{TP+TN}{TP+TN+FP+FN}\cdot100\% \tag{13}$$

E. Database Description

To investigate the overall PAT, we applied 250 long-term ECG recordings extracted from four different existing databases. An overview of the four databases is provided in Table II. All patients from the Stroke Database (STRDB) were admitted after an episode of stroke, the Telemetry Database (TDB) contains recordings from patients who were admitted and selected for regular telemetry monitoring, the patients from the Cardio-Respiratory Monitoring Database (CRMDB) were monitored ambulant as a part of diagnosing potential obstructive sleep apnea, and the Fitness Database (FDB) contains ambulatory recordings from subjects recruited in a fitness study [18]. The patients from the first two databases are thus considered a high risk population with respect to the presence of abnormal heart rhythms, especially atrial fibrillation, whereas the recordings from the last two databases are expected to represent patients with a high prevalence of physical activity during the recording period. This database selection is thus expected to ensure a small overrepresentation of both arrhythmia events and episodes of artefacts arising from everyday activities. This ensures a very realistic investigation of the overall PAT in 24-hour ePatch recordings.

1) Algorithm Design and Validation Database

For the algorithm design and validation, we decided to randomly select two ECG segments of 10 minutes from each patient, yielding a total of 500 ECG segments. The random selection of segments from each patient ensures a realistic amount of artifacts, a realistic distribution of the types of artifacts (e.g. power line interference, muscle artifacts, electrode-motion artifacts), representation of normal sinus rhythm with different ventricular frequencies, and a realistic amount of abnormal heart rhythms and different beat morphologies. Each of the 500 ECG segments were manually annotated and assigned to one of the two classes. The annotation was conducted in two steps. The first step was designed to point out challenging segments and provide the final annotation of non-challenging segments. This was accomplished by asking three engineers with experience in ECG interpretation (D.B.S., L.B., and K.H) to provide an independent assessment of the quality of each of the 500 ECG segments. For all ECG segments where the three engineers agreed on the quality, this consensus was considered appropriate for the final annotation. Of the 500 segments, agreement between the engineers was obtained for 402 segments. The annotation of the remaining 98 segments was considered more challenging. These segments were therefore also annotated independently by a set of doctors. All 98 segments were annotated by two different cardiologists (K.E. and J.L.J.) and one of two medical doctors (A.O. or H.M.S.). The final annotation for the 98 segments was based on majority voting between the three medical annotations for each segment. Table II contains information about the total number of segments, the number of challenging segments, and the number of analyzable segments obtained from each of the four original databases.

TABLE II
DATABASE INFORMATION.

Database	STRDB	CRMDB	TDB	FDB	Total
Patients	84	84	50	32	250
Segments	168	168	100	64	500
Length[a]	20.3±6.7	18.3±3.6	23.2±3.4	23.8±1.9	20.7±5.1
Training[b]	59	59	35	22	175
Validation[b]	25	25	15	10	75
Simple[c]	82.7%	87.5%	69.0%	73.4%	80.4%
Class I[d]	85.1%	76.2%	91.0%	92.2%	84.2%

[a] Length of the recordings in hours, stated as mean ± standard deviation.
[b] The number of patients from each database that were randomly selected for the training and validation phase, respectively. The training and validation phases are further described in the section "Algorithm parameter optimization".
[c] Percentage of segments with agreement between the three engineers.
[d] Percentage of analyzable segments (class I).

III. RESULTS

A. Algorithm Parameter Optimization

As mentioned, four algorithm parameters (T_1, T_2, C, and γ) were optimized using a grid search. The optimal value of each parameter depends on the value of the other parameters. We therefore optimized all four parameters simultaneously. To ensure the possibility of estimating the performance on unseen data, we randomly selected 30% of the patients as a validation group. The parameter optimization was only based on ECG segments from the remaining 70% of the patients (the training database). For each cross validation fold, 80% of the training data was applied to train the classifier and the performance was evaluated on the remaining 20%. The performance might depend on the random selection of the training and test data in the training database. To obtain a reliable estimate of the average performance as well as performance variations for each parameter combination, we therefore conducted 100 folds with random division of the training database. For each parameter combination, the average and standard deviation of Se, Sp, P^-, and P^+ over the 100 folds was calculated. These results are provided in Fig. 5. The Acc was not applied for optimization since this performance measure might result in a biased optimization when the classes are unbalanced. We selected the parameter combination with the best compromise between the four performance measures. The performance of this parameter combination is indicated with a black circle in Fig. 5. This combination was $T_1 = 1200$, $T_2 = 0.12$, $C = 0.7$, and $\gamma = 2$. The performance of this parameter combination was: $Se = 98.5\pm1.3$, $Sp = 95.0\pm6.5$, $P^+ = 99.1\pm1.1$, $P^- = 92.6\pm7.0$, and $Acc = 98.0\pm1.5$.

B. Performance of the Final Algorithm

The algorithm was then retrained using all the segments in the training database and the selected parameter combination. The performance of this final algorithm on the training database is provided in Table III. The final algorithm was then applied to the unseen validation database. These results are also provided in Table III together with the performance of each human expert annotator with respect to the final manual annotations.
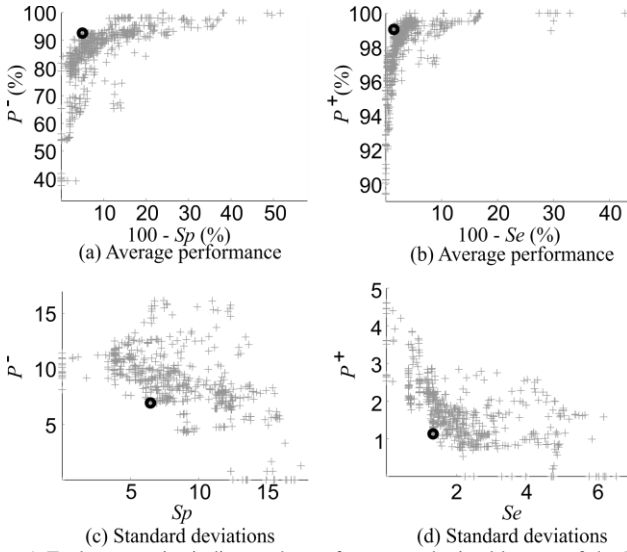
Fig. 5. Each grey point indicates the performance obtained by one of the 750 different parameter combinations investigated. (a) Relation between average Sp and average P^- obtained from the 100 random folds. (b) Relation between average Se and average P^+ obtained from the 100 folds. (c) Relation between the standard deviation of Sp and $^{-+}$ obtained from the 100 folds. (d) Relation between the standard deviation of Se and P^+ obtained from the 100 folds. The black circle indicates the performance of the selected parameter combination.

C. Analyzable Time in ePatch ECG Recordings

The final version of the algorithm was then applied to estimate the overall PAT for each of the 250 patients. These results are provided in Fig. 6. The x-axis indicates the recording numbers sorted according to their overall PAT. It is observed that 25 recordings (10%) obtained less than 10% analyzable time. These recordings were considered incorrect measurements, and were thus not included in the overall statistics for the analyzable time. For the remaining 225 recordings, the median analyzable time was 100% (interquartile range: 97.9% to 100%), and the mean analyzable time was 92.4±18.8%. Furthermore, 83.6% of the 225 recordings obtained more than 91.7% analyzable time (equivalent to ≥22 hours/day). These recordings are located to the right of the black circle in Fig. 6.
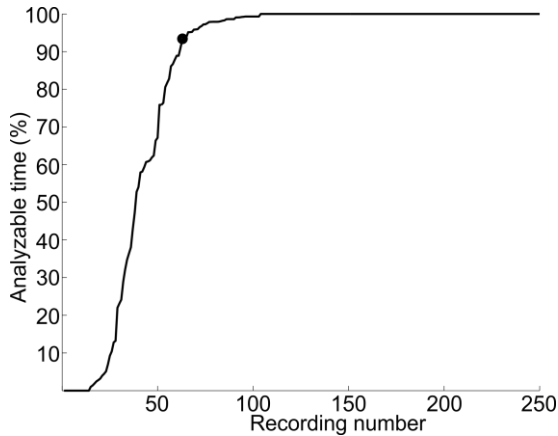

Fig. 6. Illustration of the overall analyzable time obtained in each recording. The analyzable time was estimated by the novel proposed automatic algorithm. As observed from the curve, 25 recordings (10%) obtained less than 10% analyzable time. The recordings to the right of the black circle obtained an overall analyzable time equivalent to ≥22 hours/day.

TABLE III
PERFORMANCE OF FINAL ALGORITHM AND THE HUMAN EXPERTS RELATIVE TO THE FINAL MANUAL REFERENCE ANNOTATION.

Annotator	N^a	Se (%)	Sp (%)	P^- (%)	P^+ (%)	Acc (%)
Eng. I [b]	500	96.9	98.7	85.7	99.8	97.2
Eng. II [b]	500	81.0	92.4	47.7	98.3	82.8
Eng. II [b]	500	99.5	82.3	97.0	96.7	96.8
MD I [c]	64	100.0	100.0	100.0	100.0	100.0
MD II [c]	34	93.3	100.0	66.7	100.0	94.1
Card. I [d]	98	90.0	100.0	69.2	100.0	91.8
Card. II [d]	98	93.7	66.7	70.6	92.5	88.7
Training [e]	350	98.6	96.6	93.3	99.3	98.3
Validation [f]	150	98.4	95.2	90.9	99.2	98.0

[a] N indicates the number of segments analyzed by each annotator.
[b] Eng. = Engineer.
[c] MD = Medical Doctor.
[d] Card. = Cardiologist.
[e] Performance on the entire training database when all segments from the training database was applied to train the final algorithm classifier.
[f] Performance on the unseen validation database when the final algorithm trained on the entire training database was applied.

IV. DISCUSSION

This study is the first study to investigating the overall analyzable time in ECG recordings obtained with the novel DELTA ePatch recorder and compares this to published analyzable times of other similar devices. However, the reliability of the estimated signal quality score highly depends on the performance of the designed algorithm. Therefore the performance of the algorithm is discussed first, and then the general signal quality of the patch recordings is discussed.

A. Algorithm Performance

The performance of our novel algorithm on the unseen validation data was $Se = 98.4\%$, $Sp = 95.2\%$, $P^+ = 99.2\%$, $P^- = 90.9\%$, and $Acc = 98.0\%$. For comparison, the highest Acc obtained on test data in the original Physionet challenge was 93.2% [6]. Our algorithm thus obtains much better Acc. However, care should be taken when comparing Acc on different unbalanced databases. Furthermore, the Acc does not provide any information about the relative performance in detection of the two classes. The authors of [9] extended their Physionet entry by relabeling the database and balancing it by adding artificially generated noisy segments. Using this database and an algorithm based on five features and a MLP classifier, they obtained $Acc = 95.9\%$, $Sp = 96.0\%$, and $Se = 95.8\%$ on their test data. In [13], the achieved performance on a private database of unseen data was $Acc = 95.36\%$, $Se = 94.73\%$, and $Sp = 96.63\%$. Comparing to the literature, our obtained performance is thus very satisfactory. The high performance obtained both during the cross validation and validation on unseen data is expected to be achieved from the design of appropriate features with high discriminative capabilities and the choice of an SVM classifier. Furthermore, it is observed that the standard deviations obtained from the cross-validation are relatively low. This furthermore indicates stability and high reproducibility of the designed algorithm.

The selection of the optimal parameter combination depends on the requirements for each application. In some

applications, it is crucial that only noisy segments are detected for exclusion. In this case, high performance of *Se* and *P⁻* should be valued at the expense of *Sp* and *P⁺*. In other applications, it might be more important to ensure that a selected data segment is in fact clean and therefore useful for rhythm analysis. In this case, the compromise between the four performance measures should be opposite. Since our goal was to estimate the overall PAT, we decided to allow each of the four performance measures equal weights during the parameter selection phase. However, it is observed that *Sp* is higher than *P⁻* and *Se* is slightly lower than *P⁺*. Looking at (9)-(13), this indicates an overrepresentation of *FNs* compared to *FPs*. This implies that more clean segments are wrongly classified than noisy segments, and thus the algorithm might have a small tendency to overestimate the overall noise level. However, the mean analyzable time obtained from all 250 recordings was 83.4%. This number is very comparable to the number of randomly selected segments that were manually annotated as analyzable (84.2%, see Table II). The high similarity between these numbers might suggest that the novel designed ECG quality estimation algorithm still provides a fairly reliable estimate of the overall PAT. Furthermore, the algorithm performance is well within the performance obtained by each human expert annotator (see Table III). This does not necessarily indicate a higher performance of the algorithm. The difference in the human expert annotations might originate from different experience levels with respect to ECG interpretation. Furthermore, each individual annotator might look for different ECG characteristics to judge whether each segment is diagnostic or not. However, the high algorithm performance compared to the human expert annotators does indicate that the algorithm provides a more reproducible estimate of the overall PAT than it would be possible to achieve using human expert annotations. The results might also indicate that the automatic estimation of the overall PAT provides a good compromise between potential disagreements between the human experts.

It should, of course, be mentioned that the possibilities of improving the quality estimation algorithm are not exhausted. Improvements might include adding noisy segments to obtain a better balance between the classes. Improvements might also include investigation of new and more advanced features or different classification schemes. It should furthermore be noted that the most appropriate design choices (the definition of analyzability, the segment length, and the combination of the two channels) depends on the intended application of the algorithm. It could also be interesting to test the algorithm performance in the presence of specific arrhythmia events. In this study, the ability to correctly classify abnormal ECG segments as being analyzable or non-analyzable was based on a random selection from ECG recordings in a high risk population, but it was not investigated specifically. It is important to keep these algorithm limitations in mind when analyzing the overall PAT. However, our overall impression is still that the designed algorithm provides a useful estimate that can provide important new knowledge about the general signal quality obtained in patch ECG recordings.

B. Analyzable Time in Patch ECG Recordings

As observed from Fig. 6, 147 of the recordings obtain an analyzable time of 100%. It should be noted that this does not imply that we claim that these recordings display no artefacts or noisy episodes. The algorithm is designed to detect periods of the recording where diagnostic interpretation is impossible. This does not imply that no artefacts can be present. It implies that using contextual information it is possible with certainty to recognize the heart rhythm. On the other end of the scale, 25 recordings obtained an analyzable time of <10%. As mentioned, these recordings were considered to be incorrect measurements. This could for instance be caused by improper mounting of the device or disconnected electrodes. These recordings would not be useful for diagnostic purposes and a new recording should therefore be obtained if any diagnostic information was to be extracted. These recordings were therefore treated separately, and they were not included in the calculation of the mean and median analyzable times. Our estimated median analyzable time corresponds well with the findings in [2]. Furthermore, the analyzable time is higher than found in [3]. This is also expected since the data analyzed in [3] was obtained during different kinds of physical activities (walking, running, Nordic walking, and biking), whereas the ePatch recordings were obtained during normal daily life. Physical activity is therefore not expected to be present constantly in our recordings. The percentage of ePatch recordings obtaining analyzable data equivalent to at least 22 hours/day was 83.6%. Comparing to [2], this number is slightly lower, but still comparable. We thus believe that our findings correspond well with the limited available literature. Furthermore, it should be noted that the authors of [2] don't disclose the methodology behind their proprietary algorithm applied for estimation of the percentage of analyzable time. We aimed at a high reproducibility by applying a fully disclosed algorithm for estimation of the overall PAT.

There is, of course, always a risk of missing a single important arrhythmia event experienced by a patient during an episode of non-analyzable data. However, this unfortunate situation might also occur using the traditional Holter recorders. It is never possible to completely remove this risk, and it is not known with certainty whether this occurs more frequently in patch type ECG recorders than the traditional Holter recorders. It is furthermore difficult to find literature describing the actual analyzable time in Holter recorders, and therefore direct comparison with the traditional devices was not possible. Furthermore, it is expected that some of the artefacts observed in patch recordings originate from the increased possibility of continuing normal daily life activities throughout the monitoring period compared to traditional Holter recorders. The recording conditions might therefore be considered quite different for the patch recorders and the traditional recorders. Furthermore, it has been shown that the extended monitoring period facilitated by the novel patch recorders can result in an overall higher diagnostic yield, detection of more significant arrhythmias, and a higher degree of definitive diagnosis compared to traditional Holter recordings [2], [19], [20]. This indicates that a potential

increase in the amount of artefacts recorded with the patch recorders is out weighted by the advantages of the increased monitoring period. Overall, we thus consider the analyzable time in the patch recordings to be high. It should, of course, be mentioned that these findings are based on the designed quality assessment algorithm, and their validity is therefore strongly connected to the performance of the designed algorithm.

V. CONCLUSIONS

In this study we have designed a novel algorithm for automatic estimation of the overall PAT in long-term ECG recordings. The algorithm was applied to investigate the general quality of 250 different ePatch recordings. The novel patch ECG recorders possess a high number of advantages compared to the traditional Holter recorders. Some of these advantages include simplicity (the systems are very easy to use), increased patient comfort and compliance, and possibilities of prolonged monitoring. These advantages unveil opportunities to monitor completely new patient populations, initiate large-scale screening programs, monitoring of cardiac patients in their own homes, as well as improved surveillance and guidance in rehabilitation programs. The implementation of these devices is thus expected to revolutionize the field of outpatient ECG monitoring. However, these advantages are irresolvable conditioned by the assurance of the ability to obtain high-quality ECGs throughout the recording period. In agreement with other published work, we found the overall PAT in the ePatch recordings to be high. This indicates that the many advantages of the patch ECG recorders are not counterbalanced by low signal quality. We therefore find the new patch type ECG recorders very promising for future outpatient ECG monitoring. This should, of course, be further confirmed in a larger population to ensure the generalizability to all possible applications of the patch devices.

REFERENCES

[1] S. Mittal et al., "Ambulatory external electrocardiographic monitoring: Focus on atrial fibrillation.," *J. Am. Coll. Cardiol.*, vol. 58, no. 17, pp. 1741–9, Oct. 2011.

[2] M. P. Turakhia et al., "Diagnostic utility of a novel leadless arrhythmia monitoring device," *Am. J. Cardiol.*, vol. 112, no. 4, pp. 520–4, Aug. 2013.

[3] T. Takalokastar et al., "Quality of the wireless electrocardiogram signal during physical exercise in different age groups," *IEEE J Biomed Health. Inform.*, vol. 18, no. 3, pp. 1058–64, 2014.

[4] D. B. Saadi et al., "Automatic quality classification of entire electrocardiographic recordings obtained with a novel patch type

recorder," in *36th Annual International Conference of the IEEE Engineering in Meidicine and Biology Society (EMBC)*, 2014, pp. 5639–42.

[5] D. B. Saadi et al., "Heart rhythm analysis using ECG recorded with a novel sternum based patch technology - A pilot study," in *Cardiotechnix 2013: Proc. of the International Congress on Cardiovasular Technologies*, 2013, pp. 15–21.

[6] I. Silva et al., "Improving the quality of ECGs collected using mobile phones : The PhysioNet / computing in cardiology challenge 2011," in *Computing in Cardiology 2011*, 2011, pp. 273–6.

[7] L. Johannesen and L. Galeotti, "Automatic ECG quality scoring methodology: mimicking human annotators.," *Physiol. Meas.*, vol. 33, no. 9, pp. 1479–89, Sep. 2012.

[8] H. Xia et al., "Matrix of regularity for improving the quality of ECGs.," *Physiol. Meas.*, vol. 33, no. 9, pp. 1535–48, Sep. 2012.

[9] G. D. Clifford et al., "Signal quality indices and data fusion for determining clinical acceptability of electrocardiograms.," *Physiol. Meas.*, vol. 33, no. 9, pp. 1419–33, Sep. 2012.

[10] I. Jekova et al., "Threshold-based system for noise detection in multilead ECG recordings.," *Physiol. Meas.*, vol. 33, no. 9, pp. 1463–77, Sep. 2012.

[11] D. Hayn et al., "QRS detection based ECG quality assessment.," *Physiol. Meas.*, vol. 33, no. 9, pp. 1449–61, Sep. 2012.

[12] Q. Li et al., "Robust heart rate estimation from multiple asynchronous noisy sources using signal quality indices and a Kalman filter.," *Physiol. Meas.*, vol. 29, no. 1, pp. 15–32, Jan. 2008.

[13] J. Lee et al., "Automatic motion and noise artifact detection in Holter ECG data using empirical mode decomposition and statistical approaches," *IEEE Trans. Biomed. Eng.*, vol. 59, no. 6, pp. 1499–1506, 2012.

[14] D. B. Saadi et al., "Automatic real-time embedded QRS complex detection for a novel patch-type electrocardiogram recorder (Periodical style - Submitted for publication)," *IEEE J. Transl. Eng. Helath Med.*

[15] AAMI, *ANSI/AAMI EC57: 1998/(R) 2003: Testing and reporting performance results of cardiac rhythm and ST-segment measurement algorithms*. Association for the Advancement of Medical Instrumentation, 2003.

[16] S. Theodoridis and K. Koutroumbas, *Pattern Rcognition*, 4th ed. Elsevier, 2009.

[17] "svmtrain," *The MathWorks, Inc.* [Online]. Available: http://www.mathworks.se/help/stats/svmtrain.html. [Accessed: 06-Nov-2014].

[18] J. R. Thorpe et al., "Comparative study of T-amplitude features for fitness monitoring using the ePatch ECG recorder," in *36th Annual International Conference of the IEEE Engineering in Meidicine and Biology Society (EMBC)*, 2014, pp. 4172–5.

[19] P. M. Barrett et al., "Comparison of 24-hour Holter monitoring with 14-day novel adhesive patch electrocardiographic monitoring.," *Am. J. Med.*, vol. 127, no. 1, pp. 95.e11–7, Jan. 2014.

[20] M. A. Rosenberg et al., "Use of a noninvasive continuous monitoring device in the management of atrial fibrillation: A pilot study.," *Pacing Clin. Electrophysiol.*, vol. 36, no. 3, pp. 328–33, Mar. 2013.

www.elektro.dtu.dk